Characterisation of Phosphotransferase Systems (PTS) in *Clostridium difficile*

Niall Bollard

Thesis submitted to the University of Nottingham for the degree of Doctor of Philosophy

January 2018

Abstract

Phosphotransferase systems (PTS) represent an important method of sugar uptake in bacteria and have been well described in the past. However, research into PTS within the genus *Clostridium* has been mainly restricted to the non-pathogens. Analysis of the genome of *Clostridium difficile* 630 revealed over 40 intact PTS; this is over three times as many as in other pathogenic *Clostridia,* such as *Clostridium perfringens* and *Clostridium botulinum*. Previously, carbon catabolite repression has been shown to affect toxin production in *C. difficile*. Being capable of utilising different carbohydrates efficiently could be important for *C. difficile* to adapt to, grow, and survive in the human gut. So far, little work has been done to corroborate the role of individual PTS in carbohydrate uptake, sensing of environmental stimuli and regulation of virulence, i.e. toxin expression. A deeper understanding of the PTS in *C. difficile*, and their importance in virulence, could lead to the development of new drug targets.

The aim of this study is to characterise the main PTS of *C. difficile*, determine their role in carbohydrate uptake, and their effect on regulation of virulence. To date, we have chosen the main candidates thought to be involved in mannitol and sorbitol uptake, and have inactivated these PTS using the ClosTron and in-frame deletion methods. Phenotypic characterisation of these mutants was undertaken to prove their role in uptake of the relevant sugar and to determine their role in virulence regulation.

This study has demonstrated, by growth assays and HPLC, that the operons at CD630_0762-8 and CD630_2331-4 respectively encode PTS specific for sorbitol and mannitol uptake. In the case of the mannitol operon, it has been proved

(through the use of cytotoxicity assays, which showed reduced bacterial toxicity in the presence of the sugar) that the suppression of toxin synthesis in the presence of mannitol is dependent upon uptake of the substrate via this operon. With sorbitol, toxin levels are, seemingly, not directly reliant upon uptake of the sugar, resulting in, mainly, an increase of toxin in sorbitol. Presently, it is not possible to say whether these systems have a distinct role or not in the motility of the organism.

List of Figures

Figure 1.1: Map of the PaLoc containing the toxin genes, *tcdA* and *tcdB*, and the accessory genes *tcdR*, *tcdE*, and *tcdC*……..……...……...5

Figure 1.2: Spore structure of *C. difficile* 630 visualised by transmission electron microscopy (TEM)……..……..…...……..……...10

Figure 1.3: Schematic view of the organisation of different transport systems…16

Figure 1.4: The bacterial PEP-dependent phosphotransferase system…...….....19

Figure 1.5: Phylogenetic tree of PTS in *C. difficile* 630 (Mitchell, Heriot-Watt University, unpublished)…….……...…….……...23

Figure 1.6: PTS^{Glu} at loci CD630_2666-7 in *C. difficile* 630 (Artemis)….....….24

Figure 2.1: ClosTron mutagenesis…….……..……..43

Figure 2.2: Map of the ClosTron plasmid pMTL007C-E2……..…..……..…..44

Figure 2.3: Map of the pMK-RQ plasmid containing *mtlA/gutD* knockout cassette (Invitrogen)…….……..…..……47

Figure 2.4: Map of the pMTL-YN3 vector used for allelic exchange manipulation of *C. difficile* 630Δ*erm*Δ*pyrE*……..…….…..……48

Figure 2.5: Schematic representation of gene knock-out by double cross-over (allelic exchange) selecting for an initial single crossover event (University of Nottingham, 2010)…..…….…..……..……..49

Figure 2.6: Schematic representation of gene knock-out by double cross-over (allelic exchange) (University of Nottingham, 2010)……..……..50

Figure 2.7: Map of the pMTL-YN1C plasmid used for complementation of mutants……..……..…..……..…52

Figure 2.8: pMTL-YN1X map of plasmid used to overexpress PTS genes of interest……..……...……..53

Figure 2.9: *pyrE* locus at CD630_0187 within the *C. difficile* 630 genome…..…54

Figure 3.1: Phenotypic appearance of 630Δ*erm*Δ*pyrE* growing on MM +PTS sugar (A-E)…….....…..……..68

Figure 3.2: Constituent genes of PTS^{Mtl} in *C. acetobutylicum* DSM 792.....70

Figure 3.3: Model for the regulation of MtlR……..……..72

Figure 3.4: MtlR protein organisation. Figure of MtlR showing the two-centrally located PRDs and the IIB_bglG_like and IIA_fru-like domains towards the C-terminus (NCBI)……..……..74

Figure 3.5: Alignment of MtlR in pathogenic and non-pathogenic Clostridia illustrating the conserved nature of the MtlR PRDs……..……76

Figure 3.6: Homologue (25%) of *C. difficile* 630 MtlR at locus CD630_2416…78

Figure 3.7: Second putative PTS^{Srl} encoded in *C. difficile* 630 at loci CD630_2414-8 (Artemis)……..…81

Figure 3.8: SrlR protein showing a single PRD (NCBI)……...82

Figure 4.1: Structural diagram illustrating the six-carbon chain mannitol (PubChem)…….……..…..87

Figure 4.2: Constituent genes of the putative PTS^{Mtl} at loci CD630_2331-4 showing genes targeted for CT mutagenesis, indicated by the chosen insertion site, and deletion, marked by a cross (Artemis)…….……88

Figure 4.3: Representative image showing growth of WT (left) and control strain (right) on DMM agar…….…….....91

Figure 4.4: Growth of 630WT vs. 630Δ*erm* in DM with or without mannitol or glucose…….……..92

Figure 4.5: HPLC evaluation of mannitol uptake in DM by 630WT and 630Δ*erm* (control strain)……...…..…….…….…….93

Figure 4.6: HPLC evaluation of glucose uptake in DM by 630WT and 630Δ*erm* (control strain)…….……..……..…94

Figure 4.7: Growth of 630WT vs. 630Δ*erm* in TY with or without mannitol or glucose……..……..……95

Figure 4.8: Cytotoxicity of 630WT and 630Δ*erm* at 24 h in TY…….…….96

Figure 4.9: Cytotoxicity of 630WT and 630Δ*erm* at 48 h in TY…..…….…..…97

Figure 4.10: Cytotoxicity of 630WT and 630Δ*erm* at 72 h in TY……...…….98

Figure 4.11: Representative images of motility assays of 630WT (A) and 630Δ*erm* (control strain) (B) on YTG……..……....99

Figure 4.12: Representative images of motility assays of 630WT (A) and 630Δ*erm* (control strain) (B) on YTM……...……100

Figure 4.13: Representative images of motility assays on BHIS +top agar showing 630WT (A), control strain (B), and negative control (C)……101

Figure 4.14: Representative images of motility assays showing migration of 630WT (A) and control strain (B) through the agar in the tubes. The negative control (C) did not migrate……..……..…….……..102

Figure 4.15: Representative image showing growth of Δ*mtlD* (top left), control strain (top right), complemented mutant (bottom left), and overexpressed mutant (bottom right) on DMM agar……..……..……...103

Figure 4.16: Role of *mtlD* in *C. difficile* 630Δ*erm* growth in DM…..…..…….105

Figure 4.17: Role of *mtlD* in *C. difficile* 630Δ*erm* growth in DM……..107

Figure 4.18: HPLC evaluation of mannitol uptake in DM by 630Δ*erm* (control strain), Δ*mtlD* (mutant), and the complemented mutants (*mtlD* comp and *mtlD* overex)…….....109

Figure 4.19: HPLC evaluation of glucose uptake in DM by 630Δ*erm* (control strain), Δ*mtlD* (mutant), and the complemented mutants (*mtlD* comp and *mtlD* overex)…….……110

Figure 4.20: Role of *mtlD* in *C. difficile* 630Δ*erm* growth in TY...…….…..….112

Figure 4.21: Role of *mtlD* in *C. difficile* 630Δ*erm* growth in TY…...……....113

Figure 4.22: Role of *mtlD* in *C. difficile* 630Δ*erm* toxin production at 24 h in TY…….……..114

Figure 4.23: Role of *mtlD* in *C. difficile* 630Δ*erm* toxin production at 24 h in TY…….……..…….115

Figure 4.24: Role of *mtlD* in *C. difficile* 630Δ*erm* toxin production at 48 h in TY……..……..……....116

Figure 4.25: Role of *mtlD* in *C. difficile* 630Δ*erm* toxin production at 48 h in TY……117

Figure 4.26: Role of *mtlD* in *C. difficile* 630Δ*erm* toxin production at 72 h in TY……118

Figure 4.27: Role of *mtlD* in *C. difficile* 630Δ*erm* toxin production at 72 h in TY……..……..……119

Figure 4.28: Representative images of motility assays showing control strain (A), mutant (B), complemented mutant (C), and overexpressed mutant (D) on YTG…….……120

Figure 4.29: Representative images of motility assays showing control strain (A), mutant (B), complemented mutant (C), and overexpressed mutant (D) on YTM…….……...122

Figure 4.30: Representative images of motility assays on BHIS +top agar showing control strain (A), mutant (B), complemented mutant (C), overexpressed mutant (D), and negative control (E)……...…123

Figure 4.31: Representative images of motility assays showing migration of control strain (A), mutant (B), complemented mutant (C), and overexpressed mutant (D) through the agar in the tubes. The negative control (E) did not migrate…….125

Figure 4.32: Position within the putative PTS^{Mtl} at loci CD630_2331-4 of the gene of interest, *mtlF*, the CT insertion into the gene, and the primers used to screen for the insertion……...……...…….....126

Figure 4.33: PCR screening for CT insertion in CT*mtlF*……127

Figure 4.34: Southern blot showing CT insertion in CT*mtlR* and CT*mtlF*…….128

Figure 4.35: PCR screening for restoration of *mtlF* in CT*mtlF*……...…...129

Figure 4.36: Representative image showing growth of mutant (top left), control strain (top right), complemented mutant (bottom left), and overexpressed mutant (bottom right) on DMM agar……..…….130

Figure 4.37: Role of *mtlF* in the growth of *C. difficile* 630 in DM…….132

Figure 4.38: Role of *mtlF* in the growth of *C. difficile* 630 in DM……..…...133

Figure 4.39: HPLC evaluation of mannitol uptake in DM by 630Δ*erm* (control), CT*mtlF* (mutant), and the complemented mutants (*mtlF* comp and *mtlF* overex)……..…….……..135

Figure 4.40: HPLC evaluation of glucose uptake in DM by 630Δ*erm* (control strain), CT*mtlF* (mutant), and the complemented mutants (*mtlF* comp and *mtlF* overex)…….....136

Figure 4.41: Role of *mtlF* in the growth of *C. difficile* 630 in TY..….....137

Figure 4.42: Role of *mtlF* in the growth of *C. difficile* 630 in TY……..138

Figure 4.43: Role of *mtlF* in *C. difficile* 630 toxin expression at 24 h in TY…..139

Figure 4.44: Role of *mtlF* in *C. difficile* 630Δ*erm* toxin expression at 24 h in TY……..……..140

Figure 4.45: Role of *mtlF* in *C. difficile* 630Δ*erm* toxin expression at 48 h in TY…….……..…..141

Figure 4.46: Role of *mtlF* in *C. difficile* 630Δ*erm* toxin expression at 48 h in TY……....142

Figure 4.47: Role of *mtlF* in *C. difficile* 630Δ*erm* toxin expression at 72 h in TY……143

Figure 4.48: Role of *mtlF* in *C. difficile* 630 toxin expression at 72 h in TY…..144

Figure 4.49: Representative images of motility assays showing control strain (A) and mutant (B) on YTG……...145

Figure 4.50: Representative images of motility assays showing zones of motility of control strain (A), mutant (B), complemented mutant (C), and overexpressed mutant (D) on YTM…….146

Figure 4.51: Representative images showing motility assays on top agar showing control strain (A), mutant (B), and negative control (C)…….……147

Figure 4.52: Representative images of motility assays showing migration of control strain (A) and mutant (B) through the agar in the tubes. The negative control (C) did not migrate……..……148

Figure 4.53: Position within the putative PTS^{Mtl} at loci CD630_2331-4 of the gene of interest, *mtlR*, the CT insertion into the gene, and the primers used to test for the insertion……149

Figure 4.54: PCR screening for CT insertion into CT*mtlR*…….149

Figure 4.55: PCR screening for restoration of *mtlR* and *pyrE*…….151

Figure 4.56: Representative image showing growth of mutant (top left), control strain (top right), complemented mutant (bottom left), and overexpressed mutant (bottom right) on DMM agar……...152

Figure 4.57: Role of *mtlR* in *C. difficile* 630Δ*erm* growth in DM……...153

Figure 4.58: Role of *mtlR* in *C. difficile* 630Δ*erm* growth in DM……...…155

Figure 4.59: HPLC evaluation of mannitol uptake in DM by 630Δ*erm* (control strain), CT*mtlR* (mutant), and the complemented mutants (*mtlR* comp and *mtlR* overex)…….....157

Figure 4.60: HPLC evaluation of glucose uptake in DM by 630Δ*erm* (control strain), CT*mtlR* (mutant), and the complemented mutants (*mtlR* comp and *mtlR* overex)…….158

Figure 4.61: Role of *mtlR* in *C. difficile* 630Δ*erm* growth in TY……159

Figure 4.62: Role of *mtlR* in *C. difficile* 630Δ*erm* growth in TY……161

Figure 4.63: Role of *mtlR* in *C. difficile* 630Δ*erm* toxin production at 24 h in TY…….……...162

Figure 4.64: Role of *mtlR* in *C. difficile* 630Δ*erm* toxin production at 24 h in TY……..……..163

Figure 4.65: Role of *mtlR* in *C. difficile* 630Δ*erm* toxin production at 48 h in TY……164

Figure 4.66: Role of *mtlR* in *C. difficile* 630Δ*erm* toxin production at 48 h in TY……165

Figure 4.67: Role of *mtlR* in *C. difficile* 630Δ*erm* toxin production at 72 h in TY……....166

Figure 4.68: Role of *mtlR* in *C. difficile* 630Δ*erm* toxin production at 72 h in TY……..…....167

Figure 4.69: Representative images of motility assays showing control strain (A) and mutant (B) on YTG……...168

Figure 4.70: Representative images of motility assays showing the control strain (A), mutant (B), complemented mutant (C), and overexpressed mutant (D) on YTM……169

Figure 4.71: Representative images of motility assays showing control strain (A), mutant (B), and negative control (C)…….……..170

Figure 4.72: Representative images of motility assays showing migration of control strain (A) and mutant (B) through the agar in the tubes. The negative control (C) did not migrate……..……171

Figure 4.73: Role of *mtlR* in 630Δ*erm*Δ*pyrE* spore formation…….…...……172

Figure 4.74: Position within the putative PTS^{Mtl} at loci CD630_2331-4 of the gene of interest, *mtlA*, and the primers used to screen for the deletion of *mtlA*……..173

Figure 4.75: PCR screening for deletion of *mtlA*……174

Figure 4.76: PCR screening for restoration of *mtlA* and *pyrE*……175

Figure 4.77: Representative image showing growth of mutant (top left), control strain (top right), and the complemented mutant (bottom left) on DMM agar…….……...….....176

Figure 4.78: Role of *mtlA* in *C. difficile* 630Δ*erm* growth in DM…….……..178

Figure 4.79: Role of *mtlA* in *C. difficile* 630Δ*erm* growth in DM……...179

Figure 4.80: HPLC evaluation of mannitol uptake in DM by 630Δ*erm* (control strain), Δ*mtlA* (mutant), and the complemented mutant (*mtlA* comp)…….……181

Figure 4.81: HPLC evaluation of glucose uptake in DM by 630Δ*erm* (control strain), Δ*mtlA* (mutant), and the complemented mutant (*mtlA* comp)…….182

Figure 4.82: Role of *mtlA* in the growth of *C. difficile* 630 in TY……..183

Figure 4.83: Role of *mtlA* in the growth of *C. difficile* 630Δ*erm* in TY…….....184

Figure 4.84: Role of *mtlA* in *C. difficile* 630Δ*erm* toxin production at 24 h in TY……185

Figure 4.85: Role of *mtlA* in *C. difficile* 630Δ*erm* toxin production at 24 h in TY……186

Figure 4.86: Role of *mtlA* in *C. difficile* 630Δ*erm* toxin production at 48 h in TY……187

Figure 4.87: Role of *mtlA* in *C. difficile* 630Δ*erm* toxin expression at 48 h in TY……188

Figure 4.88: Role of *mtlA* in *C. difficile* 630Δ*erm* toxin production at 72 h in TY……189

Figure 4.89: Role of *mtlA* in *C. difficile* 630Δ*erm* toxin production at 72 h in TY……...190

Figure 4.90: Representative images of motility assays showing control strain (A) and mutant (B) on YTG……..……..……191

Figure 4.91: Representative images of motility assays showing growth of control strain (A), mutant (B), and complemented mutant (C) on YTM…….……192

Figure 4.92: Representative images of motility assays on BHIS +top agar showing control strain (A), mutant (B), and negative control (C)…….……193

Figure 4.93: Representative images of motility assays showing migration of control strain (A), mutant (B) through the agar in the tubes. The negative control (C) did not migrate……...194

Figure 4.94: Role of *mtlA* in *C. difficile* 630Δ*ermΔpyrE* spore formation…....195

Figure 4.95: Constituent genes of PTS^{Mtl} in *B. stearothermophilus*…..……..197

Figure 5.1: Structural diagram illustrating the six-carbon chain sorbitol (PubChem)……..…….218

Figure 5.2: Constituent genes of the putative PTS^{Srl} at loci CD630_0762-8, showing genes targeted for CT mutagenesis, indicated by the chosen insertion site, and deletion, marked by a cross (Artemis)…….……..219

Figure 5.3: CD630_0765-6 encoding the N-terminus (0765) and the C-terminus (0766) of the IIB domain of PTS^{Srl} at loci CD630_0762-8……...……...220

Figure 5.4: Alignment of sequenced CD630_*srlE* fragment with the sequences of *srlE_N* and *srlE_C* available on GenBank…….…….221

Figure 5.5: Representative image showing growth of WT (left) and parent (right) on DMS agar……..…….…….……....222

Figure 5.6: Growth of 630WT vs. 630Δ*ermΔpyrE* (parental strain) in DM…....223

Figure 5.7: HPLC evaluation of sorbitol uptake in DM by 630WT and 630Δ*ermΔpyrE* (parental strain)……..……224

Figure 5.8: HPLC evaluation of glucose uptake in DM by 630WT and 630Δ*ermΔpyrE* (parental strain)……..……225

Figure 5.9: Growth of 630WT vs. 630Δ*ermΔpyrE* (parental strain) in TY...….227

Figure 5.10: Cytotoxicity of 630WT and 630Δ*ermΔpyrE* (parental strain) at 72 h in TY…….……...228

Figure 5.11: Cytotoxicity of 630WT and 630Δ*ermΔpyrE* (parental strain) at 96 h in TY……..……..229

Figure 5.12: Cytotoxicity of 630WT and 630Δ*ermΔpyrE* (parental strain) at 120 h in TY…….……...230

Figure 5.13: Representative images of motility assays showing 630WT (A), parental strain (B), and negative control (C) on YTG…….232

Figure 5.14: Representative images of motility assays showing 630WT (A), parental strain (B), and negative control on YTS……..……..233

Figure 5.15: Representative images of motility assays on BHIS +top agar showing 630WT (A), parental strain (B), and negative control (C)……...……...234

Figure 5.16: Representative images of motility assays showing migration of 630WT (A) and the parental strain (B), through the agar in the tubes. The negative control (C) did not migrate…….……...235

Figure 5.17: PCR screening for deletion of *gutA*…….…….……...236

Figure 5.18: CT insertion in *gutA* (CD630_0764), shown by PCR…….…...….236

Figure 5.19: Representative image showing growth of 630Δ*ermΔpyrE* -parent (left) and CT*gutA* -mutant (right) on DMS agar……..237

Figure 5.20: Role of *gutA* in *C difficile* 630Δ*ermΔpyrE* growth in DM…..…….238

Figure 5.21: HPLC evaluation of sorbitol uptake in DM by 630Δ*ermΔpyrE* (parental strain) and CT*gutA* (mutant)……...……...…….….239

Figure 5.22: HPLC evaluation of glucose uptake by 630Δ*ermΔpyrE* (parental strain) and CT*gutA* (mutant) in DM……240

Figure 5.23: Role of CT*gutA* in *C difficile* 630Δ*ermΔpyrE* growth in TY…….241

Figure 5.24: Role of CT*gutA* in *C. difficile* 630Δ*ermΔpyrE* toxin expression at 72 h in TY…….……242

Figure 5.25: Role of CT*gutA* in *C. difficile* 630Δ*ermΔpyrE* toxin expression at 96 h in TY…….……243

Figure 5.26: Role of CT*gutA* in *C. difficile* 630Δ*ermΔpyrE* toxin expression at 120 h…….……...……....244

Figure 5.27: Representative images showing motility assays with parental strain (A), mutant (B), and negative control (C) on YTG……...……..……245

Figure 5.28: Representative images showing motility assays with parental strain (A), mutant (B), and negative control (C)……...246

Figure 5.29: Representative images showing motility assays with parental strain (A), mutant (B), and negative control (C)……...247

Figure 5.30: Representative images showing motility assays indicating the migration of control strain (A) and mutant (B) through the agar in the tubes. The negative control (C) did not migrate……249

Figure 5.31: Primers used for PCR screening for CT mutagenesis of *srlE_N*…250

Figure 5.32: CT insertion in *srlE_N* (CD630_0765) mutants A and B shown by PCR……..251

Figure 5.33: Southern blot showing CT insertion in CT*srlE_N*……..252

Figure 5.34: Representative image showing growth of 630Δ*ermΔpyrE* -parent (left) and CT*srlE_N* -mutant (right) on DMS agar……..253

Figure 5.35: Role of *srlE_N* in *C difficile* 630Δ*ermΔpyrE* growth in DM……..254

Figure 5.36: HPLC evaluation of sorbitol uptake in DM by 630Δ*ermΔpyrE* (parent) and CT*srlE_N* (mutant)……..……255

Figure 5.37: HPLC evaluation of glucose uptake in DM by 630Δ*ermΔpyrE* (parent) and CT*srlE_N* (mutant)……..……256

Figure 5.38: Role of *srlE_N* in *C difficile* 630Δ*ermΔpyrE* growth in TY…....257

Figure 5.39: Role of *srlE_N* in *C. difficile* 630Δ*ermΔpyrE* toxin production at 72 h in TY…….……258

Figure 5.40: Role of *srlE_N* in *C. difficile* 630Δ*ermΔpyrE* toxin expression at 96 h in TY……259

Figure 5.41: Role of *srlE_N* in *C. difficile* 630Δ*ermΔpyrE* toxin expression at 120 h in TY…….……260

Figure 5.42: Representative images showing motility assays with parental strain (A), mutant (B), and negative control (C) on YTG…….……261

Figure 5.43: Representative images showing motility assays with parental strain (A), mutant (B), and negative control (C) on YTS……..262

Figure 5.44: Representative images showing motility assays on top agar with control strain (A), mutant (B), and negative control…….……...……...263

Figure 5.45: Representative images showing motility assays with the migration of control strain (A), mutant (B), and negative control (C) through the agar in the tubes. The negative control (C) did not migrate……..……264

Figure 5.46: Primers used for PCR screening for CT mutagenesis of *srlE_C*…265

Figure 5.47: CT insertion in *srlE_C* (CD630_0766), shown by PCR…….……265

Figure 5.48: Representative image showing growth of 630Δ*ermΔpyrE* -parent (left) and CT*srlE_C* -mutant (right) on DMS agar……..266

Figure 5.49: Role of *srlE_C* in *C difficile* 630Δ*ermΔpyrE* growth in DM…....268

Figure 5.50: HPLC evaluation of sorbitol uptake in DM by 630Δ*ermΔpyrE* (parent) and CT*srlE_C* (mutant)…….……269

Figure 5.51: HPLC evaluation of glucose uptake in DM by 630Δ*ermΔpyrE* (parent) and CT*srlE_C* (mutant)..……..270

Figure 5.52: Role of *srlE_C* in *C. difficile* 630Δ*ermΔpyrE* growth in TY…....271

Figure 5.53: Role of *srlE_C* in *C. difficile* 630Δ*ermΔpyrE* toxin production at 72 h in TY……..……...272

Figure 5.54: Role of *srlE_C* in *C. difficile* 630Δ*ermΔpyrE* toxin production at 96 h in TY…….……273

Figure 5.55: Role of *srlE_C* in C. difficile 630Δ*ermΔpyrE* toxin production at 120 h in TY…….274

Figure 5.56: Representative images showing motility assays with parental strain (A) and mutant (B) on YTG……..……..275

Figure 5.57: Representative images showing motility assays with parental strain (A), mutant (B), and negative control (C) on YTS……..276

Figure 5.58: Representative images showing motility assays on top agar showing control strain (A), mutant (B), and negative control……277

Figure 5.59: Representative images of motility assays showing migration of control strain (A) and mutant (B) through the agar in the tubes. The negative control (C) did not migrate…….…….278

Figure 5.60: Primers for PCR screening for CT mutagenesis of *srlB*…….279

Figure 5.61: CT insertion shown by PCR in *srlB* (CD630_0767)…….……..279

Figure 5.62: Representative image showing growth of 630Δ*ermΔpyrE* -parent (left) and CT*srlB* -mutant (right) on DMS agar…….……..280

Figure 5.63: Role of *srlB* in *C difficile* 630Δ*ermΔpyrE* growth in DM…...…...281

Figure 5.64: HPLC evaluation of sorbitol uptake in DM by 630Δ*ermΔpyrE* (parent) and CT*srlB* (mutant)..……...282

Figure 5.65: HPLC evaluation of glucose uptake in DM by 630Δ*ermΔpyrE* (parent) and CT*srlB* (mutant)…….…….……283

Figure 5.66: Role of *srlB* in *C. difficile* 630Δ*ermΔpyrE* growth in TY…….....284

Figure 5.67: Role of *srlB* in *C. difficile* 630Δ*ermΔpyrE* toxin production at 72 h in TY……285

Figure 5.68: Role of *srlB* in *C. difficile* 630Δ*ermΔpyrE* toxin production at 96 h in TY…….……...286

Figure 5.69: Role of *srlB* in *C. difficile* 630Δ*ermΔpyrE* toxin production at 120 h in TY…….……...287

Figure 5.70: Representative images of motility assays showing parental strain (A), mutant (B), and negative control (C) on YTG…….288

Figure 5.71: Representative images of motility assays on BHIS +top agar showing control strain (A), mutant (B), and negative control (C)…….289

Figure 5.72: Representative images of motility assays showing migration of control strain (A) mutant (B) through the agar in the tubes. The negative control (C) did not migrate…….……..291

Figure 5.73: Primers for PCR screening for deletion of *gutD*…….292

Figure 5.74: PCR screening for deletion of *gutD*……...292

Figure 5.75: Representative image showing growth of 630Δ*ermΔpyrE* -parent (left) and Δ*gutD* -mutant (right) on DMS agar……..……..293

Figure 5.76: Role of *gutD* in *C difficile* 630Δ*ermΔpyrE* growth in DM…….295

Figure 5.77: HPLC evaluation of sorbitol uptake in DM by 630Δ*ermΔpyrE* (parent) and Δ*gutD* (mutant)..…….……...296

Figure 5.78 HPLC evaluation of glucose uptake in DM by 630Δ*ermΔpyrE* (parent) and Δ*gutD* (mutant)……297

Figure 5.79: Role of *gutD* in *C. difficile* 630Δ*ermΔpyrE* growth in TY…….298

Figure 5.80: Role of *gutD* in *C. difficile* 630Δ*ermΔpyrE* toxin production at 72 h in TY…….……...299

Figure 5.81: Role of *gutD* in *C. difficile* 630Δ*ermΔpyrE* toxin production at 96 h in TY……300

Figure 5.82: Role of *gutD* in *C. difficile* 630Δ*ermΔpyrE* toxin production at 120 h in TY……301

Figure 5.83: Representative images of motility assays showing parental strain (A), mutant (B), and negative control (C) on YTG…….……302

Figure 5.84: Representative images of motility assays showing parental strain (A), mutant (B), and negative control (C) on YTS……..……...303

Figure 5.85: Representative images showing motility assays on BHIS +top agar showing control strain (A), mutant (B), and negative control (C)…..……304

Figure 5.86: Representative images of motility assays showing migration of control strain (A), mutant (B) through the agar in the tubes. The negative control (C) did not migrate……..…….……305

Figure 6.1: Diagram of MtlF showing the presence of histidine residues at AA positions 63 and 106 (NCBI)…….……..322

Figure 6.2: Illustration of *C. difficile* 630 MtlA encoded at locus CD630_2334 showing the IIB and IIC domains of the protein (NCBI)…….……...326

List of Tables

Table 2.1: Bacterial strains used in this study……..…….29

Table 2.2: Plasmids used in this study……..…….30

Table 2.3: Primers used for CT targeting of PTS genes…….……..…….31

Table 2.4: Primers used for cloning…….…….……..…32

Table 2.5: Primers used for complementation……..….33

Table 2.6: Antibiotics used in this study……....……37

Table 2.7: PCR conditions used in this study……..……..41

Table 2.8: Genetic loci and intron position of the PTS genes targeted for CT mutagenesis……44

Table 4.1: Content of each well when showing by PCR the CT insertion in CT*mtlF*……127

Table 4.2: Southern blot confirmation of CT insertion……...128

Table 4.3: Content of each well when showing by PCR the restoration of *mtlF*……..……129

Table 4.4: Content of each well when showing by PCR the CT insertion in CT*mtlR*…….……150

Table 4.5: Content of each well when showing by PCR the restoration of CT*mtlR*……..……...151

Table 4.6: Contents of each well when performing PCR analysis to show deletion of *mtlA*…….……174

Table 4.7: Contents of each well when performing PCR analysis to show complementation of Δ*mtlA*……..175

Table 5.1: Content of each well showing by PCR CT insertion in CT*gutA* mutant vs. parent……..236

Table 5.2: Content of each well showing by PCR CT insertion in CT*srlE_N* mutant vs. parent……..249

Table 5.3: Southern blot confirmation of CT insertion……...252

Table 5.4: Content of each well showing by PCR the CT insertion in CT*srlE_C* mutant vs. parent……..266

Table 5.5: Content of each well when showing by PCR the CT insertion in CT*srlB* mutant vs. parent…….279

Table 5.6: Contents of each well when showing by PCR the deletion of *gutD*……..……...293

Table 6.1: Mutants created indicating the presence of a phenotype following assays…….……...……...318

Table of Contents

Abstract……..……..ii

List of Figures……...……..iv

List of Tables……xvi

Table of Contents……...xviii

List of Abbreviations……xxviii

1.0 Introduction……...……1

1.1 *Clostridia*……...2

1.2 *Clostridium difficile*……...3

1.2.1 *Clostridium difficile* virulence factors……..4

1.2.1.1 The large toxins A and B……..4

1.2.1.2 Binary toxin *Clostridium difficile* transferase (CDT)…….……..8

1.2.1.3 Spores……..…….……9

1.2.1.4 Motility…….……...11

1.2.1.5 Adhesins……..……..……..12

1.2.2 Growth and Adaptation of *C. difficile*…….……...……13

1.2.2.1 Carbohydrate Transport in Prokaryotes……..13

1.2.2.2 Major Facilitator Superfamily (MFS)…….....14

1.2.2.3 ATP-Binding Cassette (ABC) Transporters……..……..……...14

1.2.2.4 Phosphotransferase Systems (PTS)……17

1.3 PTS Families……...21

1.4 Carbon Catabolite Repression (CCR)……...…….21

1.5 PTS in *Clostridium difficile*……22

1.5.1 PTS and Toxin Production…….…..……..….25

1.5.2 PTS, Motility, and Metabolism……..…….……25

1.5.3 PTS and Sporulation/Germination…….…….26

1.6 Aims of the project…….……...…….……....27

2.0 Materials and Methods……...…….....28

2.1.1 Bacterial strains…….……...…….……..29

2.1.2 Plasmids…….……...……..30

2.1.3 Primers…….……...…….……...31

2.2 Media and growth conditions……..…….……..34

2.3 Media supplements……..……...37

2.4 General molecular techniques…….37

2.4.1 Genomic DNA extraction……...37

2.4.2 Plasmid DNA extraction…….38

2.4.3 Restriction digest, dephosphorylation, ligation…...……..…….38

2.4.4 Making electrocompetent cells……...……...38

2.4.5 Electroporation……...…….39

2.4.6 Conjugation……...……..40

2.4.7 DNA sequencing……...……..40

2.4.8 Polymerase Chain Reaction (PCR)……...……..41

2.4.8.1 Primer design...……...41

2.5 ClosTron (CT) mutagenesis……....42

2.5.1 ClosTron targets……...……...44

2.5.2 Isolation of putative CT integrants…….45

2.5.3 Agarose Gel Electrophoresis (AGE)……...……...……45

2.5.4 Southern blotting confirmation of CT mutagenesis……...……46

2.6 In-frame deletion of *mtlA* and *gutD*……...…….46

2.6.1 Knock-out cassette cloning……..……..47

2.6.2 Selecting for single cross-over and double cross-over events……..…….49

2.6.3 Complementation of mutants……...……..50

2.7 Phenotypic assays……54

2.7.1 Growth……...…….……55

2.7.1.1 Growth on Minimal Media (MM) agar…….…...……..55

2.7.1.2 Growth on Defined Media (DM) agar……...……55

2.7.1.3 Growth in Defined Media (DM) broth……...…...……...……55

2.7.1.4 Growth in Enriched Media (EM)……...……...…56

2.7.2 Cytotoxicity assays…….56

2.7.3 High Pressure Liquid Chromatography (HPLC) evaluation of mannitol/sorbitol/glucose consumption…….……59

2.7.4 Motility assays…….……...60

2.7.4.1 Motility assays on YT +glucose/mannitol/sorbitol plates…….60

2.7.4.2 Motility assays on BHIS +top agar plates…….……60

2.7.4.3 Motility assays in tubes…….…….61

2.7.5 Spore assays…….……...61

2.8 Statistical analysis……...……...62

2.9 Bioinformatics……..…….…….63

3.0 Results Chapter I……..……...……64

3.0 Results Chapter I – Preliminary investigations of *C. difficile* 630 PTS……..65

3.1 Culturing of *C. difficile* 630 in the presence of PTS Sugars……...……...67

3.1.1 Culturing of 630Δ*ermΔpyrE* on MM agar plates…….……..…...…..……67

3.2 *In silico* analysis of PTS……...……..69

3.2.1 *In silico* analysis of CD630_2331-4..…….....……..…….....69

3.2.2 *In silico* analysis of CD630_0762-8……...80

4.0 Results Chapter II –Mannitol PTS (CD630_2331-4)……..……86

4.1 Mannitol Operon……..……...87

4.1.1 MtlA –IIBC domain……...…….....88

4.1.2 MtlR –transcriptional regulator……..……..……...…….....89

4.1.3 MtlF – IIA domain……...…..….....90

4.1.4 MtlD – Phosphate Dehydrogenase…….……90

4.2 Growth, sugar uptake, cytotoxicity, and motility of wild-type (WT) and control strains…….90

4.2.1 Growth of 630WT vs. 630Δ*erm* on defined medium (DM) agar……...90

4.2.2 Growth of 630WT vs. 630Δ*erm* in DM, DMM, and DMG broth…….91

4.2.3 HPLC evaluation of mannitol/glucose consumption in DM……..92

4.2.4 Growth of 630WT vs. 630Δ*erm* in TY, TYM, and TYG…….……..94

4.2.5 Cytotoxicity of 630WT and 630Δ*erm*……95

4.2.6 Motility assays……98

4.2.6.1 Motility assays on YT +glucose…….98

4.2.6.2 Motility assays on YT +mannitol……...99

4.2.6.3 Motility assays on BHIS +top agar……...100

4.2.6.4 Motility assays in tubes…….……101

4.3 Investigation and Characterisation of PTS^{Mtl} Phosphate Dehydrogenase –MtlD……...102

4.3.1 Characterisation of 630Δ*ermΔmtlD* (CD630_2331)…….103

4.3.1.1 Growth on DM and DMM agar…….....103

4.3.1.2 Growth in DM, DMM, and DMG broth……...104

4.3.1.3 HPLC evaluation of mannitol/glucose consumption in DM..…..…….107

4.3.1.4 Growth in TY, TYM, and TYG……110

4.3.1.5 Cytotoxicity of 630Δ*erm* and 630Δ*ermΔmtlD*……..114

4.3.1.6 Motility assays…….…….119

4.3.1.6.1 Motility assays on YT +glucose…….…….119

4.3.1.6.2 Motility assays on YT medium +mannitol……...…….…...…...121

4.3.1.6.3 Motility assays on BHIS +top agar……..122

4.3.1.6.4 Motility assays in tubes……124

4.4 Investigation and Characterisation of PTS^{Mtl} IIA domain –MtlF……...…..125

4.4.1 Characterisation of 630Δ*erm*_CT*mtlF* (CD_2332) and complements…..126

4.4.1.1 Growth on DM agar……...130

4.4.1.2 Growth in DM, DMM, and DMG broth…….……...130

4.4.1.3 HPLC evaluation of mannitol/glucose consumption in DM……...…..134

4.4.1.4 Growth in TY, TYM, and TYG……...…..136

4.4.1.5 Cytotoxicity of 630Δ*erm*, 630Δ*erm*_CT*mtlF*, and complements…..…139

4.4.1.6 Motility assays……...144

4.4.1.6.1 Motility assays on YT +glucose……..…….144

4.4.1.6.2 Motility assays on YT +mannitol……...……..145

4.4.1.6.3 Motility assays on BHIS +top agar……...……...…….……..146

4.4.1.6.4 Motility assays in tubes…….…….…...147

4.5 Investigation and Characterisation of PTS^{Mtl} Regulator –MtlR……...…….148

4.5.1 Characterisation of 630Δ*erm*_CT*mtlR* (CD630_2333) and complements……148

4.5.1.1 Growth on DM agar……...151

4.5.1.2 Growth in DM, DMM, and DMG broth……152

4.5.1.3 HPLC evaluation of mannitol/glucose consumption in DM…….155

4.5.1.4 Growth in TY, TYM, and TYG……..……..…….158

4.5.1.5 Cytotoxicity of 630Δ*erm*, 630Δ*erm*_CT*mtlR,* and complements…....161

4.5.1.6 Motility assays.……...…….……..167

4.5.1.6.1 Motility assays on YT +glucose…….…….....167

4.5.1.6.2 Motility assays on YT +mannitol……168

4.5.1.6.3 Motility assays on BHIS +top agar……..…..…….....169

4.5.1.6.4 Motility assays in tubes……...……..……..170

4.5.1.7 Spore assay...….....…….……...……...…….……..172

4.6 Investigation and Characterisation of PTS^{Mtl} IIBC domain –MtlA……..173

4.6.1 Characterisation of 630Δ*erm*Δ*mtlA* (CD630_2334)…….173

4.6.1.1 Growth on DM agar……...……..176

4.6.1.2 Growth in DM, DMM, and DMG broth……..……...…….176

4.6.1.3 HPLC evaluation of mannitol/glucose consumption in DM……...179

4.6.1.4 Growth in TY, TYM, and TYG……..……182

4.6.1.5 Cytotoxicity of 630Δ*erm* and 630Δ*erm*Δ*mtlA*…….184

4.6.1.6 Motility assays…….190

4.6.1.6.1 Motility assays on YT +glucose……..…….…….....190

4.6.1.6.2 Motility assays on YT +mannitol…….……...……...191

4.6.1.6.3 Motility assays on BHIS +top agar……...…….192

4.6.1.6.4 Motility assays in tubes……..……...…….193

4.6.1.7 Spore assay……..……194

4.7 Discussion…….……195

5.0 Results Chapter III -Sorbitol PTS (CD630_0762-8)…….……217

5.1 Sorbitol Operon……..……...218

5.1.1 SrlR –transcriptional regulator…….……..……...219

5.1.2 GutM – operon activator……..…….219

5.1.3 GutA –IIC domain……..……..220

5.1.4 SrlE –IIB domain……..……220

5.1.5 SrlB –IIA domain……...…….221

5.1.6 GutD –Sorbitol Phosphate Dehydrogenase…..……..……...221

5.2 Growth, sugar uptake, cytotoxicity, and motility of wild-type (WT) and parental strains……..……...221

5.2.1 Growth of 630WT vs. 630Δ*ermΔpyrE* on DM agar…...……...…...221

5.2.2 Growth of 630WT vs. 630Δ*ermΔpyrE* in DM, DMS, and DMG broth…….222

5.2.3 HPLC evaluation of sorbitol/glucose consumption in DM…..…..…..224

5.2.4 Growth of 630WT vs. 630Δ*ermΔpyrE* in TY, TYS, and TYG....……....225

5.2.5 Cytotoxicity of 630WT and 630Δ*ermΔpyrE*……..……..227

5.2.6 Motility assays……..……231

5.2.6.1 Motility assays on YT +glucose…….....……231

5.2.6.2 Motility assays on YT +sorbitol……...……232

5.2.6.3 Motility assays on BHIS +top agar……...233

5.2.6.4 Motility assays in tubes…….234

5.3 Investigation and Characterisation of PTS^{Srl} IIB –GutA……...……...235

5.3.1 Characterisation of 630Δ*ermΔpyrE*_CT*gutA* (CD_0764)…..……..……235

5.3.1.1 Growth on DM agar……..……237

5.3.1.2 Growth in DM, DMS, and DMG broth……..…..……237

5.3.1.3 HPLC evaluation of sorbitol/glucose consumption in DM……..239

5.3.1.4 Growth in TY, TYS, and TYG…….240

5.3.1.5 Cytotoxicity of 630Δ*ermΔpyrE* and 630Δ*ermΔpyrE*_CT*gutA*…….242

5.3.1.6 Motility assays……..244

5.3.1.6.1 Motility assays on YT +glucose……...245

5.3.1.6.2 Motility assays on YT +sorbitol……...……246

5.4.1.6.3 Motility assays on BHIS +top agar…….……..247

5.3.1.6.4 Motility assays in tubes…….248

5.4 Investigation and Characterisation of PTS^{Srl} IIB –SrlE……..…….249

5.4.1 Characterisation of 630Δ*ermΔpyrE*_CT*srlE_N* (CD_0765)…….....250

5.4.1.1 Growth on DM agar……..……252

5.4.1.2 Growth in DM, DMS, and DMG broth……253

5.4.1.3 HPLC evaulation of sorbitol/glucose consumption in DM……..…....254

5.4.1.4 Growth in TY, TYS, and TYG…….256

5.4.1.5 Cytotoxicity of 630Δ*ermΔpyrE* and 630Δ*ermΔpyrE*_CT*srlE_N*…….257

5.4.1.6 Motility assays……..…….……...261

5.4.1.6.1 Motility assays on YT +glucose……..……261

5.4.1.6.2 Motility assays on YT +sorbitol……...……...262

5.4.1.6.3 Motility assays on BHIS +top agar……..263

5.4.1.6.4 Motility assays in tubes……...264

5.4.2 Characterisation of 630Δ*ermΔpyrE*_CT*srlE_C* (CD630_0766).....……265

5.4.2.1 Growth on DM agar…...…….……..266

5.4.2.2 Growth in DM, DMS, and DMG broth……..……...…….…..267

5.4.2.3 HPLC evaluation of sorbitol/glucose consumption in DM……...…;...268

5.4.2.4 Growth in TY, TYS, and TYG…….....……...….…….270

5.4.2.5 Cytotoxicity of 630Δ*ermΔpyrE* and 630Δ*ermΔpyrE*_CT*srlE_C*…….271

5.4.2.6 Motility assays……..……274

5.4.2.6.1 Motility assays on YT +glucose……..……..……..274

5.4.2.6.2 Motility assays on YT +sorbitol……..……275

5.4.2.6.3 Motility assays on BHIS +top agar……..276

5.4.2.6.4 Motility assays in tubes……277

5.5 Investigation and Characterisation of PTS^{Srl} IIC –SrlB…….……...…...…278

5.5.1 Characterisation of 630Δ*ermΔpyrE*_CT*srlB* (CD630_0767)…….....…278

5.5.1.1 Growth on DM agar……...…….…….....280

5.5.1.2 Growth in DM, DMS, and DMG broth…….……...280

5.5.1.3 HPLC evaluation of sorbitol/glucose consumption in DM…..……281

5.5.1.4 Growth in TY, TYS, and TYG……...…..283

5.5.1.5 Cytotoxicity of 630Δ*ermΔpyrE* and 630Δ*ermΔpyrE*_CT*srlB*…...…..284

5.5.1.6 Motility assays…….…….…….....287

5.5.1.6.1 Motility assays on YT +glucose……...287

5.5.1.6.2 Motility assays on YT +sorbitol…….…….288

5.5.1.6.3 Motility assays on BHIS +top agar…….....…….…….289

5.5.1.6.4 Motility assays in tubes……..…….…..290

5.6 Investigation and Characterisation of PTS^{Srl} Phosphate Dehydrogenase -GutD…….…….…….291

5.6.1 Characterisation of 630Δ*ermΔpyrEΔgutD* (CD630_0768)…...……..….291

5.6.1.1 Growth on DM Agar……..……293

5.6.1.2 Growth in DM, DMS, and DMG broth……....294

5.6.1.3 HPLC evaluation of sorbitol/glucose in DM…...…...…….…….295

5.6.1.4 Growth in TY, TYS, and TYG…….297

5.6.1.5 Cytotoxicity of 630Δ*ermΔpyrE* and 630Δ*ermΔpyrEΔgutD*……..…298

5.6.1.6 Motility assays……...……301

5.6.1.6.1 Motility assays on YT +glucose……..…….301

5.6.1.6.2 Motility assays on YT +sorbitol……..…….……302

5.6.1.6.3 Motility assays on BHIS +top agar……...303

5.6.1.6.4 Motility assays in tubes…….304

5.7 Discussion……...……..305

6.0 Final Discussion……..…….……..317

7.0 Future Work……...333

7.1 Complementation of Mutants – CT*srlE_N*, CT*srlB*, and CT*mtlF*……334

7.2 Targeting mannitol-specific IIA domains…….……..……..334

7.3 Overexpressing the mannitol-specific PTS IIB and IIC domains…….335

7.4 Investigation and Characterisation of PTS^{Srl} Regulator (CD630_0762)…..335

7.5 Investigation of Sorbitol IIB (CD630_2417)…….…..……..335

7.6 Phosphorylation assays……..……...336

7.7 Spore assays…….…….336

8.0 Acknowledgements……..……..338

9.0 Additional Sources……..……...……340

10.0 References……..……..343

List of Abbreviations

Abs.	Absorbance
A	adenine
ADP	adenosine diphosphate
ATP	adenosine triphosphate
ABC	ATP-binding cassette
AGE	agarose gel electrophoresis
ACE	Allele-couple exchange
AA	amino acid
$(NH_4)_2SO_4$	ammonium sulfate
a	antisense
Asc	ascorbate
B.	*Bacillus*
bp	base pair(s)
BLAST	Basic Local Alignment Search Tool
BD	Becton, Dickson and Company
Bgl	beta-galactosidase
BP	binding protein

BHIS	brain-heart infusion media
C.	*Campylobacter*
CcpA	Carbon catabolite repression protein A
CCR	Carbon Catabolite Repression
crr	carbon repression resistant
CO_2	carbon dioxide
cre	catabolite responsive element
^{O}C	degrees Celsius
cm	centimetre(s)
Chap.	Chapter
CRG	Clostridia Research Group
CbpA	Collagen-binding protein A
C.	*Clostridium*
CD	*Clostridium difficile*
CDI	*Clostridium difficile* infection
cdt	*Clostridum difficile* transferase/binary toxin
Csp	*C. sporogenes*
cm	chloramphenicol
$CoCl_2$	cobalt chloride

CFU	colony-forming unit
comp	complemented
conc.	concentration
CT	ClosTron
CC	cycloserin cefoxitin
C	cytosine
CAAT	cytosine adenosine adenosine thymidine
Δ	Delta
DM	defined media/medium
Deo	deoxyribonucleotide
DNA	Deoxyribonucleic acid
DNP	DNA polymerase
Dha	dihydroxyacetone
H_2SO_4	dihydroxysulphide
dH_2O	distilled water
Dr.	Doctor
EM	enriched media/medium
EI	Enzyme I domain protein
EII	Enzyme II domain protein

Erm	Erythromycin
E.	*Escherichia*
e.g.	for example
EBS	exon binding site
ECM	extra-cellular matrix
ECF	extra-cytoplasmic function
fdx	ferredoxin
FBS	fetal bovine serum
Fig.	Figure
FOA	fluorotic acid
Fru	Fructose
FBP	fructose 1, 6-bisphosphate
F-6-P	fructose-6-phosphate
Gal	galactitol
Gal	galactose
Gut	glucitol
GntP	gluconate: H^+
Glu	glucose
GPH	glycoside-pentoside-hexuronide

g	gram(s)
g	gravity
G	guanine
GTP	guanosine triphosphate
HPr	heat-stable protein
HPLC	high pressure liquid chromatography
h	hour(s)
H	hydrogen
H_2O_2	hydrogen peroxide
i.e.	that is
Km	Kanamycin
kb	kilobases
L.	*Lactobacillus*
Lac	lactose
λ	lambda
LAF	laminar air flow
LHA	Left Homology Arm
lic	lichenin
L.	Listeria

L litre(s)

log logarithemic

LB Lysogeny broth

$MnCl_2$ manganese chloride

Mtl mannitol

M-1-P mannitol-1-phosphate

MPDH mannitol-1-phosphate dehydrogenase

Man mannose

max. maximum

MCP methyl-accepting chemotaxis protein

µg microgram(s)

µL microlitre(s)

mg milligram(s)

mL millilitre(s)

mM millimolar

MEM minimal essential medium

MM minimal media/medium

MIC minimum inhibitory concentrations

min. minute(s)

M	molar
MOPS	3-(N-morpholino) propanesulfonic acid
mut.	mutant(s)
ng	nanogram(s)
nm	nanometre(s)
NCBI	National Center for Biotechnology Information
NEB	New England Biolabs
N_2	nitrogen
No.	number
OD	optical density
orf	open reading frame
pyrE	orotate phosphoribosyl transferase
OM	outer membrane
OMR	outer membrane receptor
overex	overexpressed
PaLoc	Pathogenicity Locus
p	passage
P	phosphate/phosphorylated
PDH	phosphate dehydrogenase

PEP Phosphoenolpyruvate

PT Phosphotransferase

PTS Phosphotransferase system

PRDs PTS regulatory domains

PCR Polymerase Chain Reaction

PSI pounds per square inch

P P-value

prod. Product

P promoter

P. Pseudomonas

RI refractive index

RAM retrotransposition activated marker

rpm revolutions per minute

RNP ribonuclear protein

RNA ribonucleic acid

RHA Right Homology Arm

S. Sacchromyces

s sense

$NaHCO_3$ sodium bicarbonate

NaCl	sodium chloride
Na_2HPO_4	sodium phosphate dibasic
Srl	sorbitol
S-6-P	sorbitol-6-phosphate
SPDH	sorbitol-6-phosphate dehydrogenase
sle	spore lytic enzyme
S.	*Staphylococcus*
S.	*Streptococcus*
H_2SO_4	sulfuric acid
SOC	Super Optimal broth with Catabolite repression
SLP	surface layer protein
Tcd	toxin
T	thymine
Tm	Thiamphenicol
thl	thiolase
TLR	Toll-like receptor
tcdA	toxin A
tcdB	toxin B

™	trade mark
TM	transmembrane
TRAP	Tripartite ATP-independent periplasmic
TY	Tryptose-Yeast
UK	United Kingdom
U	uracil
vs.	versus
V.	*Vibrio*
v/v	volume per volume
V	Volts
WT	wild-type
w/v	weight per volume
YT	yeast-tryptone

1.0 Introduction

1.1 *Clostridia*

Clostridia are an ancient class of bacteria. They are anaerobic spore formers and while mostly known for their pathogenic capacities, the vast majority are benign. Solventogenic Clostridia, such as *Clostridium acetobutylicum*, *Clostridium beijerinckii* and *Clostridium cellulovorans* have long been used to produce biofuels[1,2]. More recently, gas-fermenting Clostridia such as *Clostridium ljunghdahlii* and *Clostridium autoethanogenum* are being manipulated and used for the production of ethanol, butanol and even valuable chemical (such as acetone)[3,4]. Other Clostridia are being applied in cancer therapy (*Clostridium sporogenes, Clostridium novii*), making use of their proteolytic activities[5,6]. *Clostridium botulinum* is especially well known for the toxin it produces, which can kill or cure[7]. There is a range of pathogenic Clostridia, which mostly cause disease through toxins. *Clostridium perfringens* can cause food poisoning or even gas gangrene in humans, and is well known for causing necrotic enteritis in chickens[8]. *Clostridium difficile* is also a toxin producer causing potentially fatal diarrheal disease in humans and also in certain animal (sheep, pigs)[9]. Further pathogenic species include *Clostridium tetanii, Clostridium sordellii*, and *Clostridium septicum*[10-12]. Lastly, there is also a variety of clostridial species present in the healthy gut microbiota, for example, *Clostridium scindens*, just to mention one of them. *C. scindens* has recently gained interest as a bile acid converter, converting primary bile acids (e.g. taurocholate) into secondary bile acids (deoxycholate). These secondary bile acids have been shown to prevent *C. difficile* growth in the intestine, and so, appear to play a major role in combating *C. difficile* disease[13].

1.2 *Clostridium difficile*

Clostridium difficile, an anaerobic, spore-forming, Gram-positive bacterium which colonises the human gut, is implicated in intestinal disorders and has been cited as the main source of healthcare associated diarrhoea in Europe and North America[14,15,16]. Infection usually occurs via the faecal-oral route. The organism is capable of sporulation under stress conditions[17], thereby resisting the acidic conditions of the human stomach, and upon reaching the gut, germinates into vegetative cells. The toxins induce a breakdown of the tight junctions between the mucosal cells, causing diarrhoea through means of toxins[14,18]. Amongst the most vulnerable groups to *C. difficile* infection (CDI) are the elderly, the immuno-compromised, and those undergoing antibiotic treatment. It has been shown that the healthy gut flora plays an important role in preventing CDI through colonisation resistance[19]. Colonisation resistance is used to describe a combination of phenomena, such as competition for nutrients, physically taking up space, and the production of bacteriocins, all of which can be carried out by the normal gut microflora and prevent the germination, growth, and proliferation of *C. difficile*[20,21]. In such weakened host conditions, where disruption of the gut microbiota has occurred, the organism is able to proliferate, where normally, host immune cells, by the detection of the bacterial presence via host cell toll-like receptors (TLRs), would prevent this from occurring[14,18]. Disruption of human epithelial cell tight junctions is induced by *C. difficile* toxin-induced degradation of the human cell actin cytoskeleton[14,22]. Toxin A and toxin B, two large glycosylating toxins, are the primary virulence factors in CDI[14,23].

1.2.1 *Clostridium difficile* virulence factors

Following ingestion of *C. difficile* spores, these travel to the gut, where they can germinate and cause disease. Normally, disease only occurs in people with associated risk factors, mostly a disrupted healthy gut microflora. Symptoms range from a moderate, self-limiting diarrhoea to severe diarrhoea, toxic megacolon and pseudomembranous colitis, which can be fatal. Most *C. difficile* strains produce toxins A and B. These are the main virulence factors of the bacterium. *C. difficile* displays an interrelationship between environmental signals and regulation of virulence factors. For example, toxin production rises as cells enter the stationary phase (excepting certain, so-called, 'hypervirulent' or epidemic strains from *C. difficile* ribotype 027, which initiate toxin production during the logarithmic (log) phase of growth[24]) and is regulated in reaction to different environmental stimuli like the presence of antibiotics and particular amino acids such as cysteine or proline, and also temperature[25-27]. Similarly, as will be discussed in more detail below, toxin genes are modulated by the organism in response to the presence of certain metabolisable sugars such as glucose[23].

1.2.1.1 The large toxins A and B

Following establishment of *C. difficile* vegetative cell growth, the major virulence factors of the organism, the exotoxins toxin A (TcdA) and toxin B (TcdB) are produced[17]. The genes encoding these toxins, *tcdA* and *tcdB*, are situated on a 19.6 kilobase (kb) region named the pathogenicity locus (PaLoc). This region encodes another three ancillary genes, *tcdR*, *tcdE* and *tcdC*[28], which are involved in the regulation and secretion of the toxins (Fig. 1.1). Recently, it has been

shown that the entire PaLoc is potentially mobile and it has been hypothesised to have resulted from an ancient insertion[29-31]. There is a 66% similarity between the toxins at the protein level, indicating that the toxins may have arisen from a replication event[32]. TcdA and TcdB share multiple conserved domains which include a catalytic glucosyltransferase domain situated at the N-terminal, and a cysteine protease domain that is needed for auto-processing and dispatch of the catalytic domain to the cytosol of the intoxicated cell. Also, a hydrophobic translocation domain, which is centrally situated within the toxins, is believed to be involved in pore formation and insertion of the toxins into the endosomal membrane prior to their release into the cytosol. Furthermore, a C-terminal receptor-binding domain, made up of a series of repetitive oligopeptides, is believed to bind to cellular receptors[17,32]. Lately, two receptors for TcdB have been identified and published[33,34].

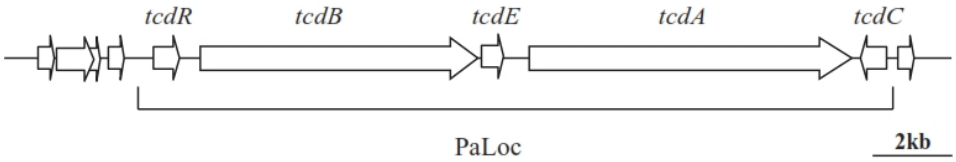

Figure 1.1: Map of the PaLoc containing the toxin genes, *tcdA* and *tcdB*, and the accessory genes *tcdR*, *tcdE*, and *tcdC*[35].
Genetic organisation of the PaLoc illustrating the *tcdR* region encoding an alternative RNA sigma factor; *tcdB*, historically considered as a cytotoxin; *tcdE*, encoding a holin-like protein involved in toxin secretion; the *tcdA* region which codes for an apparent enterotoxin; while *tcdC* encodes a possible repressor[35,36].

TcdR is an extra-cytoplasmic function (ECF) alternative sigma factor directing the transcription from the toxin promoters[37] and its own promoter[38], and playing a major role in upregulating the expression of *tcdA* and *tcdB*[17]. The role of TcdC is still disputed. TcdC is suggested to be an anti-sigma factor negatively regulating *tcdA* and *tcdB* expression by preventing the association between TcdR and the

core RNA polymerase[35,39]. Two studies recently questioned the role of TcdC in regulation of TcdA and TcdB, suggesting that it is not a major predictor or determinant of virulence[40,41]. TcdE is hypothesised to be a holin-like protein involved in the export of the toxins from the cell[42].

CodY is the first regulator situated outside of the PaLoc that has been demonstrated to have a modulatory role in *C. difficile* toxin synthesis[18,43]. In *C. difficile*, *Bacillus subtilis, and Bacillus anthracis*, CodY controls several genes involved in virulence expression as well as those that become induced when cells make the change from log-phase growth to the stationary-phase or sporulation[18,44,45]. Inactivation of the *C. difficile codY* has resulted in de-repression of all genes of the PaLoc during the log and stationary phases[18,43]. CodY binds to the promoter region of *tcdR*, repressing the gene, indicating that growth phase-dependent regulation of toxin production in *C. difficile* is mediated by the effect of CodY on *tcdR* transcription[18,43]. *codY* is a gene encoding a global regulatory protein monitoring the mineral sufficiency of the bacterial environment by responding to the intracellular levels of guanosine triphosphate (GTP) and branched-chain amino acids[18,43].

Recently, it has been demonstrated that Spo0A, the *C. difficile* sporulation master regulator,[46] does not only control sporulation, but also regulates toxin production in a strain dependent manner[47,48]. No Spo0A boxes have been found upstream of *tcdA* and *tcdB*, indicating an indirect effect of Spo0A through a currently uncharacterised regulator[23,49].

Transcription of *tcdA* and *tcdB* is blocked by the presence of rapidly metabolisable sugars such as glucose, fructose, and mannitol, which are taken up

by the phosphotransferase system (PTS)[28,50]. Toxin synthesis is linked to nutrient depletion, which, when this occurs (e.g. at the stationary phase), in general results in the initiation of toxin production, but which is suppressed in the presence of fermentable sugars like glucose and mannitol[28].

The genes encoding toxin A and toxin B are prone to varying degrees of variability giving rise to the many different toxinotypes observed (37, at present), and, thus permitting the organism to be differentiated into various groups described (0-XXXVII). Comparison with the reference strain *C. difficile* VPI10463 (toxinotype 0) is then made to determine to which type a strain belongs[51].

As the toxins are the chief virulence factor they form a target for the development of treatments like vaccines, categorisation of the varying toxin-specific strains into toxinotypes is of importance[51]. Toxin production can be effected or altered as a consequence of variations in the PaLoc, leading to the secretion of toxins with changed properties[51].

This has led to some debate as to which of the two main toxins is more greatly attributed the virulence of the organism. A study by Lyras *et al*. (2009) investigating a toxin A- toxin B+ strain has indicated that expression of *tcdB* alone is enough to produce bacterial virulence[52]. However, it has been separately demonstrated that a *C. difficle tcdB* mutant possessing only a functional *tcdA* produced mortality in a hamster model, showing that researchers and physicians must definitely give due attention to toxin A (as well as toxin B) when developing vaccines and treatments for CDI[14].

1.2.1.2 Binary toxin *Clostridium difficile* transferase (CDT)

Binary toxin, referred to as *C. difficile* transferase (CDT), is an actin-specific adenosine diphosphate (ADP)-ribosyltransferase[53] unrelated to toxins A and B[54], which has been identified in up to 8.6% of *C. difficile* strains[53,55,56]. It has been connected to increased severity of CDI, with the toxin being isolated from patients[57-59], and a 2007 study from a UK hospital found that up to 41.3% isolates in that study were the binary toxin-producing PCR-ribotype, 027[60].

Binary toxin is encoded by two genes, *cdtA* and *cdtB* (respectively encoding an enzymatic component and a binding component)[54]. A regulatory gene, *cdtR*, has been identified as the binary toxin response regulator[61]. A functional copy of *cdtR* is encoded within the *C. difficile* 630 genome, despite this strain lacking binary toxin. Additionally, *C. difficile* 630 CdtR is 96% similar to CdtR in *C. difficile* R20291 and *C. difficile* 196[54] which produce CDT, indicating a further role for CdtR[62].

Host cell surface receptors are recognised by the binding component which results in the internalisation of the enzymatic component into the cytosol, resulting in ADP-ribosylation of monomeric actin, and, as also seen with toxins A and B[14,22], the consequent breakdown of the cell's actin cytoskeleton[53,63]. Due to its covalent modification of target cell proteins and induction of host cell destruction, CDT is, like toxins A and B, implicated in the inflammation of host colonic tissue lining, which may potentiate CDI[64].

1.2.1.3 Spores

Spores are the infectious particles and are vital in *C. difficile* transmission. Since they are able to resist heat, radiation, and the alcohol-based disinfectants used to clean hospital environments, this makes them hard to eradicate, thus, making CDI easily transmissible[17]. Following disruption of the normal gut microbiota, colonisation and subsequent disease occur. Sporulation of the organism can then ensue again, enabling a *C. difficile* sub-population to persist, facilitating the transmission of the organism[17]. The ability of spores to survive in hostile environments is attributable to their structure, with each individual spore having a copy of the bacterial genome enclosed in a protective spore core. The core is surrounded by a thick wall of peptidoglycan, and a loose outer layer, referred to as the exosporium (Fig. 1.2). Spores of other clostridial species, including *C. botulinum* and *C. sordelii*, also possess an exosporium, and it is the first point of contact between the spore and its environment. Germination proficiency has been connected to the exosporium, with spores possessing an intact exosporium germinating less efficiently than spores without one. Disruption of the exosporium exposes the spore coat, the layer of the spore particle giving resistance to unfavourable environments[65,66]. In *Clostridium* species, this spore coat is a thick, proteinaceous, and electron dense covering which surrounds the cortex and the core of the spore. Proteomic and bioinformatics studies of the *C. difficile* spore have shown that the spore is comprised of numerous proteins, but the assignment of the function of these proteins is still ongoing. However, investigations into spore surface proteins in *C. difficile* 630 have found 54 proteins, with several exhibiting a likeness to proteins with suspected enzymatic roles including cell wall hydrolases, oxidoreductases, and catalases[67].

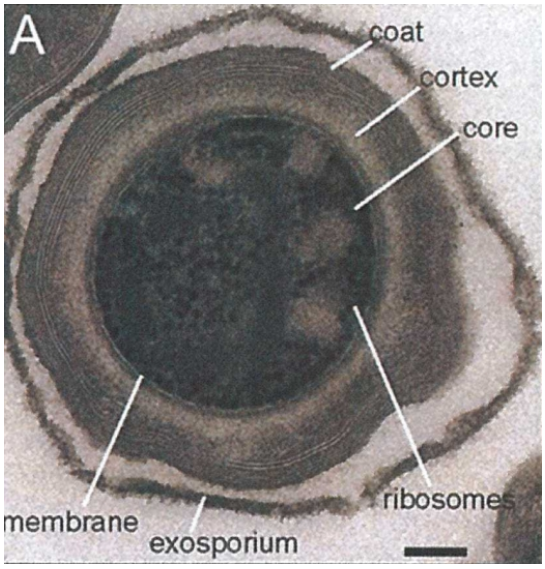

Figure 1.2: Spore structure of *C. difficile* 630 visualised by transmission electron microscopy (TEM)[17,68].
TEM visualisation illustrating the components of a *C. difficile* 630 spore - ribosomes, core, inner membrane, cortex, coat, and exosporium.

C. difficile spore formation is induced by the organism as an attempt to allow survival as a result of exit from the host[69]. Briefly, the generation of a polar septum creates a large mother cell and a smaller forespore[69-72]. The larger cell surrounds the smaller one to make a protoplast engulfed by lipid bilayer membranes inside the mother cell cytosol. The cell wall between the two membranes is then used as the template for the synthesis of a protective peptidoglycan layer referred to as the cortex. At the same time, proteinaceous shells called the spore coat are deposited on the outer membrane of the forespore[69,73,74]. Upon completion of forespore maturation, the mother cell lyses to release the spore[69].

Recently, understanding of the germination of *C. difficile* spores has improved, and several papers have shown that the processes involved are quite different to those in *B. subtilis*[69]. Bile salts, with taurocholate, in particular, being identified as probably the most important amongst germinants in *C. difficile*. SleC, an enzyme

involved in cortex hydrolysis in *C. perfringens*, has been found to be essential for colony formation when germination of *C. difficile* spores was induced in medium which contained the bile salt, taurocholate[46,75]. CspC, a pseudoprotease, has been shown to be the germinant receptor for responding to taurocholate. CspC activates the protease CspB which in turn cleaves inactive SleC. Another pseudoprotease, CspA, has recently also been identified as an important germination regulator[76-80].

1.2.1.4 Motility

Flagella and flagella-mediated motility are important virulence factors, permitting the organism to move towards the site of colonisation. The mucosal site covering the intestinal epithelium of the host constitutes the primary location of host-pathogen interaction in which *C. difficile* must evade the immune response of the host, interact with enterocytes, and bind to surface molecules. *C. difficile* has many potential surface adhesins possibly working as factors of colonisation including cell surface-associated proteins (S-layer, including the surface layer proteins -SLPs), fibronectin-binding protein A (FbpA), proteases like Cwp84, heat shock proteins such as GroEL, hydrolytic enzymes, and the flagellar cap, FliD, and flagellin, FliC, structural segments[81]. FliD and FliC make up parts of the bacterial flagellum, a multi-purpose structure involved in adherence which enables bacterial survival and colonisation[17,82].

The role flagella play in the pathogenesis of CDI appears to be strain-dependent with some studies showing flagella to be important for adherence to cells and host intestinal tissue, while an absence of flagella in the non-epidemic strain *C. difficile* 630Δ*erm* did not reduce adherence *in vivo* to cells of the gut epithelium, but, instead mediated increased adherence to cells[17,82]. A link between toxin

production and flagella regulation has been identified[83], and the involvement of FliC, the flagellar subunit, in global regulation of virulence has been shown[84,85].

1.2.1.5 Adhesins

After germination of *C. difficile* spores, adhesion to specific sites of host tissues is considered to be a first-step in the colonisation of infection of host tissues, and allows the bacteria to avoid host cleansing mechanisms such as excretion[86,87]. The surface components mediating this attachment are referred to as adhesins.

C. difficile adherence to host mucosal surfaces in the gut is believed to enable the organism to attach to the mucosa and commence interaction with host epithelial cells. Adherence by the organism to the mucus layer is considered an initial step for the settlement of *C. difficile* in the gut, and once this niche is occupied, it can initiate an interaction with the host gut epithelial cells and components of the extra-cellular matrix (ECM), making use of the array of virulence factors available to the organism[88].

In the past, high-molecular weight SLP was shown to mediate tissue-binding, while Fbp68 has been demonstrated to bind fibronectin[89], an ECM protein. More recently, lipoprotein 0872, identified as a putative adhesin[90], and Collagen binding protein A (CbpA), a *C. difficile* surface protein[88], have been found to have clear adhesive properties due to their binding to host cells and proteins (and thereby, potentially contributing to the colonisation of the gut), and are, therefore, recognised as likely contributors to *C. difficile* virulence[88,90]. CbpA binds to human collagen (having high affinity to collagens I and V), the structural proteins of the ECM[88].

1.2.2 Growth and Adaptation of *C. difficile*

Bacterial survival under altering environmental conditions requires, on the part of the organism, a capability to sense and to swiftly respond to different stimuli. For *C. difficile*, this capability is essential for its growth proliferation in the gastrointestinal tract[43].

Survival and growth of the organism is dependent upon its ability to counter changes in nutrient availability, relying on mechanisms such as the phosphoenolpyruvate (PEP)-dependent carbohydrate phosphotransferase systems (PTS), ATP-Binding Cassette **(**ABC) transporters, the Major Facilitator Superfamily (MFS) transporters, as well as two-component regulatory systems which sense diverse stimuli and enact an appropriate physiological response involving the altered transcription of a large number of genes[91,92].

1.2.2.1 Carbohydrate Transport in Prokaryotes

Transport systems are of immense importance to all living organisms, and specific permeability to nutrients and metabolites was likely the first clear property of primitive cells[93]. Transporters permit the utilisation of vital nutrients and ions, excretion of the end products of metabolism and deleterious substances, as well as communication between cells and the surrounding environment[94].

Bacteria have developed mechanisms which permit the selective utilisation of carbohydrates, allowing rapid growth, which provides the bacterium with a competitive advantage over other organisms[95]. The major transport systems which seem to be widely represented within bacterial genomes are the MFS, ABC transporters, and the PTS.

1.2.2.2 Major Facilitator Superfamily (MFS)

The major facilitator superfamily (MFS) is a class of membrane transport proteins with the ability to transport small molecules as a response to chemiosmotic ion gradients (Fig. 1.3 C)[94]. The MFS has varying roles from sugar and oligopeptide transport[94,96] to drug efflux pumps[94]. They are found in all domains of life, eukaryotic and prokaryotic (bacteria and archaea).

The MFS can be divided into two families (which are both found in *C. acetobutylicum*): the gluconate: H+ (GntP) family, and the glycoside-pentoside-hexuronide (GPH) family[96]. In *C. acetobutylicum*, several members of the GPH family are modulated by PTS through phosphorylation or other direct interaction[97]. According to NCBI genbank, the *C. difficile* 630 genome encodes up to 20 putative MFS (NCBI).

1.2.2.3 ATP-Binding Cassette (ABC) Transporters

The highly conserved ATP-binding cassette (ABC) transport systems are found in prokaryotic and eukaryotic cell systems[98]. Within prokaryotes, ABC transporters are found in both Gram-negative[93,98] as well as in Gram-positive bacteria[93]. In *Escherichia coli,* up to 5% of the entire genome encodes ABC transporters, encoding about 80 distinct transporter systems[98].

The system utilises adenosine triphosphate (ATP) for energy, which is coupled to a large amount of biological processes, not only related to transmembrane transport, but also to others such as deoxyribonucelicacid (DNA) repair[99]. As well as mainly being involved in transmembrane transport, ABC transporters have a role in non-transport-related activities like translation and elongation, and, as

mentioned, DNA repair. ABC transporters (Fig. 1.3 E, F) can be vital for viability, virulence, and pathogenicity[93], an example of this being the ABC iron-uptake systems[93]. It is possible for an ABC transporter to operate as an importer or as an exporter (seemingly, however, not both), moving molecules in or out of the cell. In prokaryotes, ABCs function mainly as importers[98], but also as exporters[100]. Searches via NCBI genbank have revealed that *C. difficile* 630 harbours ~111 potential ABC transport systems (NCBI).

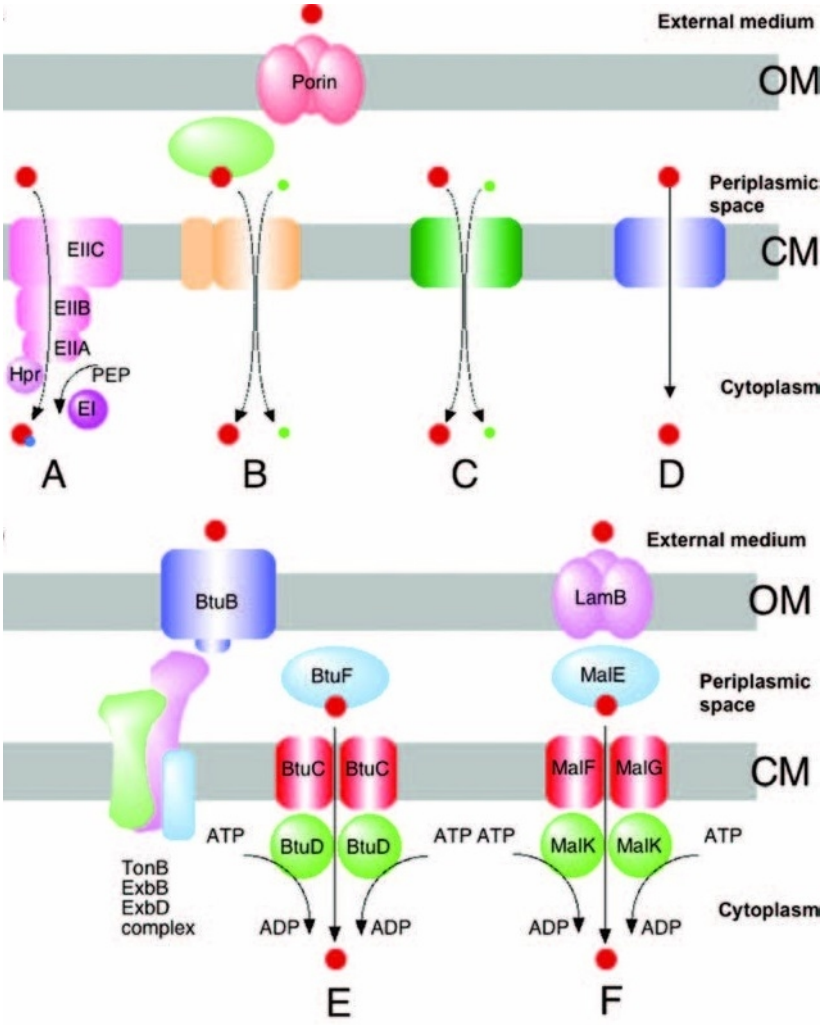

Figure 1.3: Schematic view of the organisation of different transport systems[93].
In Gram-negatives, as seen in the example here, the substrate can pass through the outer membrane (OM) by facilitated diffusion via porins.
PTS (A), which are made up of energy-coupling proteins found in the cytoplasm, and sugar-specific membrane permeases; Tripartite ATP-independent periplasmic (TRAP) transporters (B) which consist of two membrane components, a large transmembrane (TM) subunit involved in the translocation process and a smaller component of unknown function; MFS transporters (C) are usually made up of 12 TM pieces which couples transport of small solutes to gradients of ions; uniporters (D); and ABC transporters (E & F)[93].
The *C. difficile* 630 genome appears to encode over 100 putative ABCs (NCBI).

A substrate binding site, accessing the intracellular and extracellular parts of the cell membrane, undergoes conformational changes induced by ATP binding and hydrolysis resulting in an interchanging exposure of the binding site to both sides of the membrane. The relative binding affinities of the two conformations for the

substrate determines the overall direction of molecule transport. With importer systems found in prokaryotes, the outward-facing conformation is likely to have a greater attraction for the substrate than the inward-facing conformation will (while for eukaryotic export systems the exact opposite holds true). Sugar molecules are not phosphorylated concomitantly with transport[93].

The first structural determination of a bacterial ABC transporter, the vitamin B_{12} importer, BtuCD, in *E. coli*, was determined in 2002, and has led to an explosion in the study of ABC structures[98]. With this particular system (Fig. 1.3 E), a high affinity outer membrane receptor (OMR), BtuB, in an energy-dependent step, translocates the substrate across the outer cell membrane. Substrates are captured by the periplasmic binding protein (BP), BtuF, in the periplasm, and then passed to a cytoplasmic complex consisting of two copies each of BtuC and BtuD. The cytoplasmic complex mediates the ATP hydrolysis-dependent translocation of vitamin B_{12}[93]. The MFS and ABC-type permeases do not take part in metabolic and transcriptional regulation to the extent seen with the PTS[101].

1.2.2.4 Phosphotransferase Systems (PTS)

The phosphotransferase system (PTS), a major mechanism in the uptake and transport of fermentable sugars and their derivatives, is an enzyme transporter only found in prokaryotes, which phosphorylates its carbohydrate substrates during transport, resulting in an intracellular build-up of sugar phosphate esters[102].

The ability of bacterial species to adapt to environmental changes involves physiological responses and complicated modulatory circuits. Carbohydrate substrates embody an important signal used for compartment-specific regulation of virulence genes during infection[22]. PTS are particularly prominent in obligate

or facultative anaerobes[101] and, as yet, are undiscovered in eukaryotes[101]. The PTS is a very complex system both from a structural and a functional viewpoint[103]. In a single bacterium such as *Listeria monocytogenes*, as much as 3.2% of the genome may encode genes for PTS proteins[101]. In *C. difficile* 630, there are 49 putative PTS encoded within the genome[104] (Mitchell, unpublished). The system comprises a multicomponent structure made up of several cytoplasmic and membrane proteins or domains which constitute a chain of phosphoryl transfer passing a phosphate group from the donor phosphoenolpyruvate (PEP) to the substrate, which is then phosphorylated as it passes into the cell[101,102,105] (Fig. 1.4). The system catalyses the uptake and phosphorylation of carbohydrates, and consists of proteins forming a phosphor-relay, transferring the phosphoryl group from PEP to the incoming sugar[101,105].

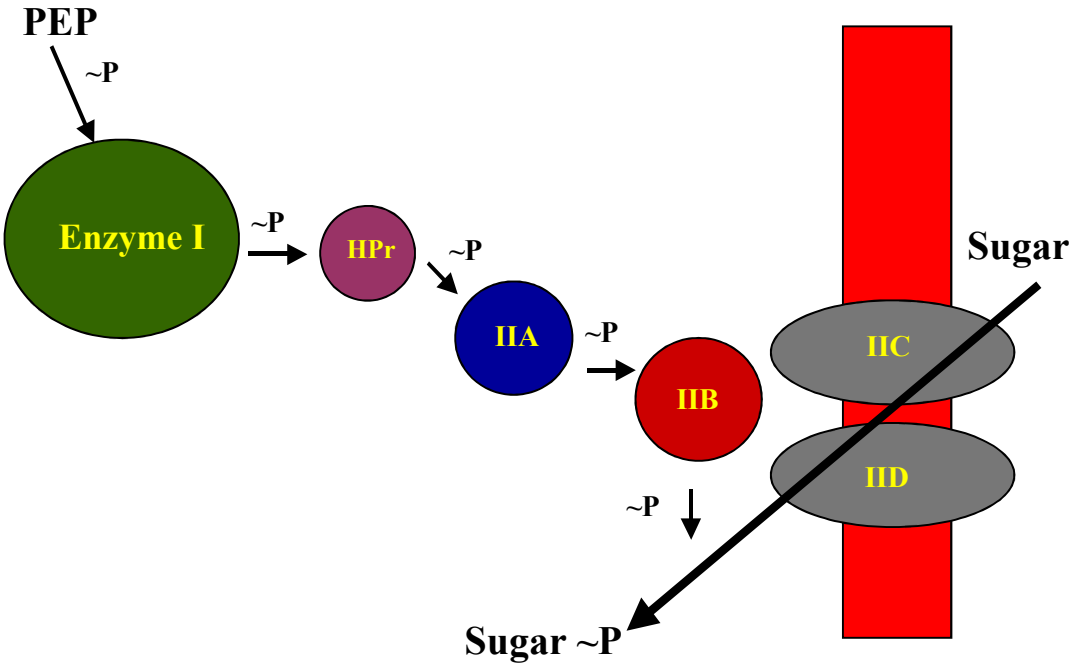

Figure 1.4: The bacterial PEP-dependent phosphotransferase system[106].
The PTS uses phosphoenolpyruvate (PEP) as a phosphoryl donor for sugar phosphorylation and is characterised by the presence of three catalytic entities called Enzyme I, Enzyme II, and HPr (heat-stable, histidine-phosphorylatable protein). The incoming sugar is phosphorylated as it traverses the bacterial cell membrane, and is subsequently converted to fructose-6-phosphate (F-6-P).

The typical PTS structure comprises an enzyme I (EI) and histidine-containing phosphor-carrier protein (HPr), which are in the cytoplasm. These first two components, EI and HPr, are general energy-coupling proteins which are common to all phosphotransferases. These two proteins are generally required for the first step in transport and phosphorylation of PTS carbohydrates, which results in the phosphorylation of HPr at the expense of PEP[107].

The membrane-associated enzyme II (EII) complex is specific to each substrate, usually comprising three identifiable protein domains termed IIA, IIB, and IIC, while some systems possess an additional IID domain (e.g. like the mannose transporter -hypothesised mannose/sorbose PTS IID in *C. difficile* 630) (Fig. 1.4).

The two cytoplasmic IIA and IIB domains are hydrophilic and take part in phosphate transfer, while the transmembrane IIC domain (and IID, if present) is hydrophobic and provides the transmembrane channel for sugar entry[101,105]. The IIC component of the PTS is responsible for the selective transportation of the substrate molecule across the inner bacterial cell membrane, preventing efflux of the sugar molecule back across the cell membrane[108]. The EII domains may reside on different proteins, or depending on sugar specificity, may be fused in different combinations within one or more polypeptide chains (creating IIAB, IIBC, or IIABC domains).[107] The EII mannitol-specific transporting and phosphorylating enzyme from *E. coli*, has all three domains covalently linked. Mannitol, for example, becomes phosphorylated during transport and is released in the cytoplasm as mannitol-1-phosphate (M-1-P)[109]. Similarly, the IIB and IIC components of a *C. acetobutylicum* ATCC824 sucrose PTS are fused into a single protein[110]. Fusions possibly increase the perfomance of a single EII complex, but may also impede phosphoryl transfer to other complexes. Phosphorylation, within an EII complex, reduces the energy barrier for release of the sugar by the IIC domain, so that almost all of the transported sugar emerges inside the cell as a phosphate ester[102].

The primary functions of the PTS include sugar reception, transport, and phosphorylation,[101,105,111] while an array of secondary functions, with consequences for metabolic and transcriptional regulation[23] includes an influence on toxin expression in *C. difficile*[22,23].

1.3 PTS Families

So far, at least four distinct evolutionary super-families of PTS EII complexes are recognised based on the most prominent sugar they take up. These are the Glucose (Glu)-Fructose (Fru)-Lactose (Lac) superfamily; the Ascorbate (Asc)-Galactitol (Gat) superfamily; the Mannose (Man) family; and the Dihydroxyacetone (Dha) family[101]. Analyses suggest that two of these evolving systems (Gat and Dha) are still in transition, as they have yet to acquire the fully-fledged characteristics of PTS EII complexes[101].

Using the phylogeny of IIC domains, seven permease families of PTS are recognised[101,102], of which representatives of all are found in *C. difficile* (Mitchell 2012, unpublished). These are the Glucose (Glu) family; the Fructose (Fru)-Mannitol (Mtl) family; the Lactose (Lac) family, the Ascorbate (Asc) family; the Galactitol (Gal) family; the Mannose (Man) family; and the Glucitol (Gut) family[101].

1.4 Carbon Catabolite Repression (CCR)

Carbon catabolite repression (CCR) in bacteria is regarded as a modulatory mechanism to ensure a steady utilisation of sugars. In Gram-positive bacteria, CCR is a conserved form of regulation[22] and is regarded as a mechanism which responds to carbohydrate availability[23]. Glucose is the preferred, or primary, carbon source for the majority of heterotrophic bacteria[23]. In the presence of glucose, transcription of genes needed for the uptake of secondary carbohydrates is repressed, and pre-existing enzymes are quite often inactivated to maximise (via the suppression of the genes of the less preferred sugar uptake system through the attachment to a catabolite responsive element (*cre*), thus, preventing

their transcription and activation) the utilisation of the primary sugar, in spite of the availability of secondary sugars[22,23].

In low guanine and cytosine (G+C) Gram-positives such as *C. difficile*, CCR is modulated by CcpA, which belongs to the LacI/GalR family of regulators. In *Bacillus subtilis* (but not in *C. difficile*), CcpA activity is stimulated by a serine-phosphorylated form of HPr[23].

Repression of toxin production when in the presence of glucose or other quickly metabolisable carbohydrates such as mannitol or fructose shows that toxin genes are subject to catabolic repression[23]. CcpA has been demonstrated to be involved in glucose-dependent repression of *C. difficile* toxin synthesis. CcpA binds to the regions induced by glucose, such as the putative glucose PTS genes carbon repression resistant (*crr*) and *ptsG* at loci CD630_2666-7, and also to the regulatory parts of the *tcdA* and *tcdB* genes[22]. However, as possibly seen with sorbitol-specific genes, indications are that those genes which are not repressed by glucose are not controlled by CcpA[22].

1.5 PTS in *Clostridium difficile*

At present, it is known that the *C. difficile* 630 genome harbours 49 potential complete PTS[104] (Mitchell, unpublished), which includes representatives of all seven families of PTS (glucose, fructose-mannitol, glucitol/sorbitol, mannose, ascorbate, lactose, and galactitol), indicating that the PTS is playing an important role in *C. difficile* carbohydrate utilisation (Fig. 1.5).

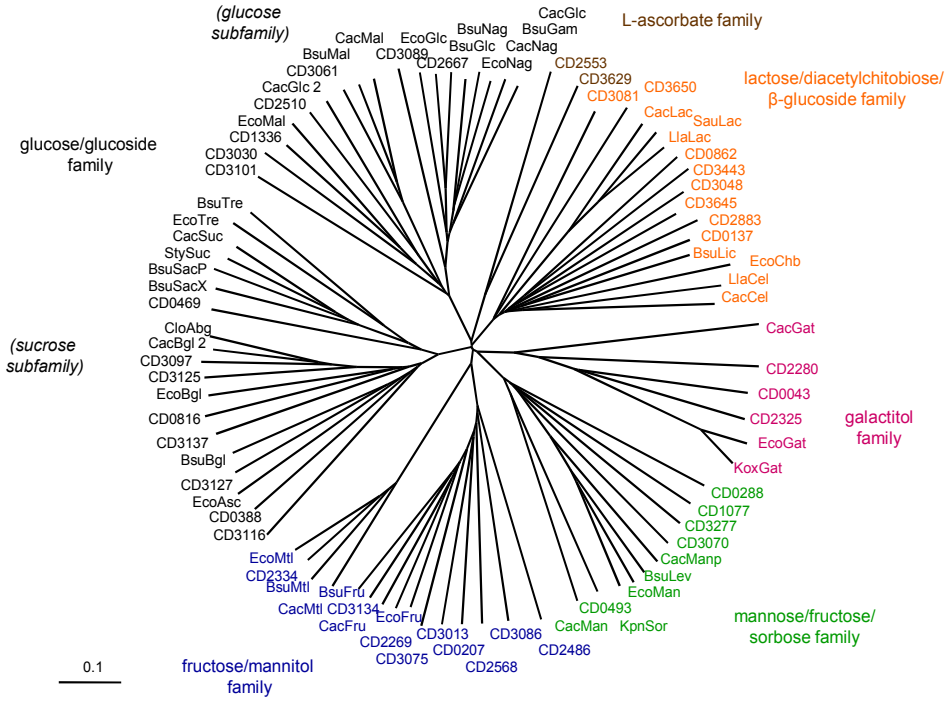

Figure 1.5: Phylogenetic tree of PTS in *C. difficile* 630 (Mitchell, Heriot-Watt University, unpublished).
The phylogenetic tree shows the PTS IIC domain genes in the *C. difficile* 630 genome and the families of PTS to which they belong. Putative representatives of each family [Glu (25), Fru-Mtl (15), Lac (4), Asc-Gat (8), Man (10)] of PTS are encoded within the *C. difficile* 630 genome.

Glucose is, as it is for the majority of heterotrophic organisms, the most preferred sugar in *C. difficile*[23]. The main route for glucose importation in *C. difficile* is via the PTS[23]. Encoded within the *C. difficile* 630 genome, there appear to be six complete PTS IIABC annotated as being glucose-specific. However, at locus CD630_1336, there is also a putative glucose IIBC which may be part of a functional PTS, as it is known that Gram-positive bacteria have 'orphan' PTS genes. It is possible for the $IIBC^{Glu}$ or IIC^{Glu} components to be functional, making use of the IIA/B proteins present in one of the complete glucose PTS. This has been observed repeatedly, as many glucose-specific PTS are without their own IIA, and, so, make use of the IIA of a genuine PTS^{Glu}. This phenomenon has not been observed in other PTS families[101].

The PTS at loci CD630_2666-7 is highly expressed when *C. difficile* is in the presence of glucose[22], indicating that this system may be the main glucose-specific system encoded in the genome primarily responsible for glucose uptake. Supporting this is the phylogenetic grouping of the PTS present in *C. difficile* 630 indicating the glucose system at loci CD630_2666-7 (Fig. 1.6) as being the most genetically divergent within the glucose family of PTS, and hence, more likely to play a distinctive role (due to it probably having an altered functional protein as a consequence of this genetic divergence from the others) when questioning which of the six glucose-specific systems plays the greatest role in uptake of this important sugar (Fig. 1.5) (Mitchell, unpublished).

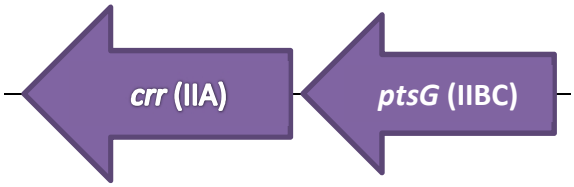

Figure 1.6: PTS^{Glu} at loci CD630_2666-7 in *C. difficile* 630 (Artemis).
Location of the putative glucose PTS in the *C. difficle* 630 genome which illustrates the probable fusion of the IIB and IIC domains. Encoded immediately upstream, at locus CD630_2668, is a putative transcriptional antiterminator (*licT*).

It seems that *C. difficile* is unusual in the number of PTS it harbours in its genome. To date, the highest number found in other bacteria which may grow in the human gut are found in *C. perfringens* strain 13 (14)[112], *L. montocytogenes* (30), and *Vibrio cholorae* 10432-62 (13) (NCBI), less in comparison to the number of putative PTS found in *C. difficile* 630 (49)[104] (Mitchell, unpublished). *C. difficile* and the non-pathogen *C. beijerinckii* (47)[113] appear to be the only Clostridia which harbour such high numbers of PTS.

1.5.1 PTS and Toxin Production

In pathogenic Gram-positive bacteria such as *C. difficile*, transcription of virulence factor genes is often changed in reaction to carbon source availability[23]. As mentioned, in *C. difficile*, transcription of *tcdA* and *tcdB* is repressed by the presence of metabolisable sugars[28]. CcpA, EI, and HPr are required for the regulation of toxin production in response to the availability of glucose[23]. CcpA binds to the regulatory regions of *tcdA* and *tcdB*, but not through a consensus *cre* site motif[23]. Repression of toxin production mediated by glucose is due to a common modulatory mechanism, CcpA, which is related to the presence of fermentable carbohydrates[23]. Since 18% of the genes within the *C. difficile* genome are under the control of glucose[23] (50% of which are under the control of CcpA),[23] the control this mechanism exerts has been shown to include PTS genes responsible for the uptake of those other sugars, such as fructose and mannose[28], that also suppress toxin synthesis and are also under the control of CcpA[22].

1.5.2 PTS, Motility, and Metabolism

Chemotaxis is the movement of bacteria in response to a chemical stimulus, allowing bacteria to follow gradients of metabolisable nutrients, environmental stimuli, and signalling molecules, thus, improving the chances of survival and proliferation[114]. Via a series of chemoreceptors, which are multifunctional membrane-bound protein complexes, bacteria will sense chemotactic stimuli. Following the bacteria encountering a stimulus, transmembrane methyl-accepting chemotaxis proteins (MCPs), which are found in prokaryotic organisms, initiate information gathering, through a signal transduction pathway, about the surrounding environment[105,111]. Binding to or dissociation of the substrate from its

chemoreceptor constitutes the stimulus which eventually triggers a positive or negative behavioural response[103,105,111].

The PTS is capable of interaction with the proteins of the MCP-chemotaxis pathway, influencing the motility of the bacterial cells in the direction of a PTS sugar[115]. In *E. coli*, the EI domain, following the presence of a detectable sugar, and, hence, now unphosphorylated, is capable of interacting with CheA, the sensor kinase of a two-component system that is part of a larger signal transduction pathway, resulting in an increase in motility[114]. The PTS has been demonstrated to play an interactive role in bacterial swimming[114].

1.5.3 PTS and Sporulation/Germination

To date, there is no clear established link between the PTS and *C. difficile* sporulation/germination. However, a couple of genes involved in fructose metabolism have exhibited upregulation during the germination of spores. Phosphofructokinase, an enzyme responsible for phosphorylation of fructose-6-phosphate (F-6-P) (to convert it to fructose 1,6-bisphosphate (FBP) which results in the creation of adenosine diphosphate (ADP) following entry into glycolysis of F-6-P)[116], has been potentially connected to *C. difficile* sporulation[116]. A possible phosphofructokinase in *C. difficile* 630, CD_2270, and a putative fructose PTS IIABC, *fruABC* (CD_3134), were significantly up-regulated in germinating spores (75.2 and 79.8 fold respectively)[116].

Also, toxin expression in *C. difficile* may have a connection to sporulation[47]. The onset of sporulation coincides with the increasing expression of *tcdA* and *tcdB* at the commencement of the stationary phase of growth[28], and Spo0A has been implicated in toxin gene expression[47]. Additionally, sugars taken up by the *C.*

difficile PTS (glucose, mannitol, fructose) affect toxin synthesis[28], so, possibly linking sporulation to PTS sugar uptake, via toxin production, and, thus, conceivably, the genes involved in the uptake of these sugars potentially play a role, directly or indirectly, in *C. difficile* sporulation.

1.6 Aims of the project

This study aims to characterise the main PTS of *C. difficile*, determining their role in carbohydrate uptake and their effect on regulation of virulence.

The following steps were undertaken:

- Identification of the main candidates involved in mannitol and sorbitol uptake.
- Inactivation and restoration of these PTS using insertional mutagenesis (ClosTron), in-frame deletion, and complementation.
- Phenotypic characterisation of the generated mutants and complements to prove their role in uptake of the relevant sugar, and to elucidate their role in regulation of bacterial virulence, analysing growth, sugar consumption, cytotoxicity, and motility.

2.0 Materials and Methods

2.1.1 Bacterial strains

Table 2.1: Bacterial strains used in this study.

Strain Name	Properties	Reference
E. coli Top10	Cloning strain (from Invitrogen™)	Invitrogen
E. coli CA434	Conjugational donor	Williams *et al*. 1990
C. difficile 630	Wild type (WT)	Sebaihia *et al.* 2006
C. difficile 630Δ*erm*Δ*pyrE*	Parental strain	Ng *et al.* 2013
C. difficile 630Δ*erm*	Control strain	Hussain *et al.* 2005
C. difficile 630Δ*erm*_CT*spo0A*	Spore assay control strain	Heap *et al.* 2007
C.difficile 630Δ*erm*_CT*fliC*	Motility assay control strain	Baban *et al*. 2013
C. difficile M120	Motility assay control strain	Valiente *et al*. 2012
C. difficile 630Δ*erm*Δ*mtlD*	Mtl phosphatedehydrogenase deleted	Ng *et al.* 2013
C. difficile 630Δ*erm*_Δ*mtlD*_*mtlD* complemented	Mtl phosphatedehydrogenase mutant complemented	Ng *et al.* 2013
C. difficile 630Δ*erm*_Δ*mtlD*_*mtlD* overexpressed	Mtl phosphatedehydrogenase mutant overexpressed	Ng *et al.* 2013
C. difficile 630Δ*erm* CT*mtlF*	CT mutagenesis of Mtl IIA	This study
C. difficile 630Δ*erm*_CT*mtlF*_*mtlF* complemented	Mtl IIA mutant complemented	This study
C. difficile 630Δ*erm*_CT*mtlF*_*mtlF* overexpressed	Mtl IIA mutant overexpressed	This study
C. difficile 630Δ*erm*Δ*pyrE* _CT*mtlR*	CT mutagenesis of Mtl regulator (*pyrE*-)	This study
C. difficile 630Δ*erm*_CT*mtlR*	CT mutagenesis of Mtl regulator	This study
C. difficile 630Δ*erm*_CT*mtlR*_*mtlR* complemented	Mtl regulator mutant complemented	This study
C. difficile 630Δ*erm*_CT*mtlR*_*mtlR* overexpressed	Mtl regulator mutant overexpressed	This study
C. difficile 630Δ*erm*Δ*pyrE*Δ*mtlA*	Deletion of Mtl IIBC (*pyrE*-)	This study
C. difficile 630Δ*erm*Δ*mtlA*	Deletion of Mtl IIBC	This study

C. difficile 630Δ*ermΔmtlA* _*mtlA* complemented	Mtl IIBC mutant complemented	This study
C. difficile 630Δ*ermΔpyrE*_CT*gutA*	CT mutagenesis of Srl IIC	This study
C. difficile 630Δ*ermΔpyrE*_CT*srlE_N*	CT mutagenesis of Srl IIC/IIB N-terminus	This study
C. difficile 630Δ*ermΔpyrE*_ CT*srlE_C*	CT mutagenesis of Srl IIB C-terminus	This study
C. difficile 630Δ*ermΔpyrE* _CT*srlB*	CT mutagenesis of Srl IIA	This study
C. difficile 630Δ*ermΔpyrE* Δ*gutD*	Srl phosphate dehydrogenase deleted	This study

2.1.2 Plasmids

All plasmid maps were created using Snapgene™.

Table 2.2: Plasmids used in this study.

Plasmid Name	**Description**	**Reference**
pMTL007C-E_*mtlF*	ClosTron plasmid	Heap *et al.* 2010/this study
pMTL007C-E_*mtlR*	ClosTron plasmid	Heap *et al.* 2010/this study
pMTL007C-E_*gutA*	ClosTron plasmid	Heap *et al.* 2010/this study
pMTL007C-E_*srlE_N*	ClosTron plasmid	Heap *et al.* 2010/this study
pMTL007C-E_*srlE_C*	ClosTron plasmid	Heap *et al.* 2010/this study
pMTL007C-E_*srlB*	ClosTron plasmid	Heap *et al.* 2010/this study
pMK-RQ_*mtlA* LHA-RHA	Invitrogen plasmid	This study
pMK-RQ_*gutD* LHA-RHA	Invitrogen plasmid	This study
pMTL-YN3_*mtlA* LH-RHA	Cloning plasmid	Ng *et al.* 2013
pMTL-YN3_*gutD* LH-RHA	Cloning plasmid	Ng *et al*. 2013
pMTL-YN1C	Complem. plasmid	Ng *et al*. 2013
pMTL-YN1X	Overexpr. plasmid	Ng *et al*. 2013

2.1.3 Primers

Table 2.3: Primers used for CT targeting of PTS genes.

Oligo	Sequence (5'-3')	Prod. Size (kb)
*mtlF*_F	GTAAAGATTTAAGTGAGCTTATTGAAGACTCATCAAGAATATTTG	2.7
*mtlF*_R	GCTTTTATGGAAGCTTTTGCCAACTAATCTTAGGAGGG	
*mtlR*_F	GGAGCAGGAAATATTGGAAGGGGTTTTATTGGAGGC	4.3
*mtlR*_R	GGTTTGAAGATGACCTTTGCTTTGCACCTCTTATATGCATGG	
*gutA*_F	GGCAAGAGTAAAGTAAAGTCATTTGAAGGTTTGGTAGGAAGAGC	2.9
*gutA*_R	GGTCCACCCCATCCTCCTCCAGAACC	
*srlE_N*_F	GGAAGATTCTTGCCAGAAAAGTTTAAACCTAGTTACTTTGCAGC	2.6
*srlE_N*_R	CCTAGTGCTATACCTATTTTTGCAACAATTCCTTGACTCTGC	
*srlE_C*_F	GTGACTGGGGGAGCAAAGCC	2.5
*srlE_C*_R	GGTTCAGCTTCTGCAAGACCAAGACCTACTGG	
*srlB*_F	GTGACTGGGGGAGCAAAGCC	4.1
*srlB*_R	CCCTGCACTCCAACAGGGACCACC	
0765-6_F	GCAGTTAGATATTTGTTAGTGGGTATAGTTGCAAACTTTATTAAAGG	

0765-6_R	GGTGAAAAAGATGGAGCAATTGGAGGAACC	1.4
EBS universal	CGAAATTAGAAACTTGCGTTCAGTAAAC	

Table 2.4: Primers used for cloning.

Oligo	**Sequence (5'-3')**	**Prod. Size (kb)**
pMK-RQ_F1	GGCTGCGCAACTGTTGGGAAG	1.4
pMK-RQ_R1	CCCGAACGACCGAGCGC	
mtlA LHA_P1	AAAAAAGGACGTCCGACCTTTTAAGTAGACA CCAAGCCCTG	3.0
mtlA RHA_P4	TTTTTTCCGCGCGGGCCACTTTGTGGGATTTA ACACGTGCTACC	
Δ*mtlA*_A	GCTACTGTAGAATGTCCAGTTTTTTCTTTTAA GTCAAGTATGTCTTTTAATGTGTTATCAGG	1.5
Δ*mtlA*_B	GGCATATGTAAATCTTATATACGATTCATTCA ATGAAAAAGAAATACTAGATATGG	
gutD LHA_P1	TTTTTTCCTGCAGGCCGTTTCTTGGACCAGGA GCTGTTATAGC	2.3
gutD RHA_P4	CCCTGTTGGAGTGCAGGGATGCATGCGCCGC GCCTTTTT	
Δ*gutD*_A	CCATTAATCGGAAATGTTGGAGGTTTAGTTG TCTTATCAATAATATGTTCATTTCCG	1.7
Δ*gutD*_B	GGAGTAGCTAAGAGTCATGCTATAGAAGATA TGTTAAATAGTAAAAGTATATTTGTGTGGGG	

M13_F	CTGATGAGTGTCCTTTATGTAAGG	

Table 2.5: Primers used for complementation.

Oligo	Sequence (5'-3')	Prod. Size (kb)
*Not*I_*Pmtl*_F	TTTTTTGCGGCCGCGTACAAGAAGGTATTCACTGAAAGTATGTGATGG	0.67
*Pmtl*_R_*Nde*I	GAATATAATTCAAGAGGAGGTAAAATTCATATGTTTTTT	
*Nco*I_*mtlF*_F	TTTTTTCCATGGATGAGTAAAGTATTGAATGAGAATAATATATTTTTAGGG	0.43
*mtlF*_R_*Nhe*I	AAAAAAGCTAGCTTAGTTGGCAAAAGCTTCCATAAAAGC	
*Sac*I_*mtlF*_F	TTTTTTGAGCTCATGAGTAAAGTATTGAATGAGAATAATATATTTTTAGGG	0.42
*mtlR*_F_*Nco*I	TTTTTTCCATGGGTGGATAATTTGAAAAAAAAGAAGATTACATCTAGGC	2.16
*mtlR*_R_*Nhe*I	AAAAAAGCTAGCTTATTTATCTATCTATAAATGCTTTTAATCTGTTTG	
*Sac*I_*mtlR*_F	TTTTTTGAGCTCGGTGGATAATTTGAAAAAAAAGAAGATTACATCTAGGC	2.15
*Not*I_*Pmtl*_F	TTTTTTGCGGCCGCGTACAAGAAGGTATTCACTGAAAGTATGTGATGG	1.42
*mtlA*_R_*Nhe*I	CCAAATTTAGATGCATTATTTAAAAGATTAGAATCTAAATAAGCTAGCTTTTTT	

YN1_*Not*I_F	GGAAGTAGAGAGTTCAAGGAATTAGGGATGTAA TAAGC	0.32
YN1_*Nhe*I_R	CTCTAAAAAATTTACATTTTTTAAGTAAGTAACA CTATAAATAATTAAGTTTGC	
YN1_*Sac*I_F	GTAATTTTTAAGGAGGTTGTGTTACATATGACCA TGATTACG	0.29
630-*pyrE*-sF1	TAGACTTAGTAGTAGGACCAGCTATGG	0.68
630_*1880*_Rs	GCTCCTACAGCACCTACTCCA	

2.2 Media and growth conditions

All media were obtained from Sigma^{TM} or Oxoid^{TM}, unless otherwise stated. Autoclaving (Rodwell MP24 Control) was for 15 minutes (min.) at 121° Celsius (^{O}C) with 1500 pounds per square inch (PSI) pressure.

C. difficile 630WT, *C. difficile* 630Δ*erm*, *C. difficile* 630Δ*erm*Δ*pyrE*, *C. difficile* 630Δ*erm*_CT*fliC, C. difficile* M120, *C. difficile* 630Δ*erm*_CT*spo0A*, and all *C. difficile* mutants and complemented mutants were grown at 37°C in an anaerobic cabinet (Don Whitely^{TM} Whitley MG1000). Gas mixture was 5% carbon dioxide (CO_2), 5% hydrogen (H_2), 90% nitrogen (N_2). Pressure was 14.5 bar.

BHIS agar and broth (18.8g brain heart infusion agar/14.8g BHI broth, 2g yeast extract, and 0.2g L-cysteine (all from Oxoid) in 400mL distilled water (dH_2O). BHIS medium was used for the general growing of *C. difficile*. BHIS agar also contained (when required) 1.5% weight per volume (w/v) agar (BHI).Minimal medium (MM) plates[24] consisting of the following (all of which were pre-sterilised): amino acid solution (10g Cas-amino acids (from Becton, Dickson and

Company (BD) diagnostics™), 0.5g L-cysteine, 0.5g tryptophan (from Sigma) in 200mL dH_2O), vitamin solution (20mg biotin, 20mg pantothenate, 20mg pyridoxine (all from Sigma) to a final volume of 200mL in dH_2O), salt solution (1.8g KH_2PO_4, 1.8g sodium chloride (NaCl), 10g sodium phosphate dibasic (Na_2HPO_4), 10g sodium bicarbonate ($NaHCO_3$) (all from Sigma) to a final volume of 20mL in dH_2O), iron sulphate (from Sigma) (20mg/50mL dH_2O), trace salt solution (260mg calcium chloride ($CaCL_2.2H_2O$), 100mg manganese chloride tetrahydrate ($MnCl_2.4H_2O$), 10mg cobalt chloride hexahydrate ($CoCl_2$ $6H_2O$), 200mg magnesium chloride hexahydrate ($MgCl_2$ $6H_2O$), 400mg ammonium sulphate [$(NH_4)_2SO_4$] (all from Sigma) to a final volume of 200mL in dH_2O) with, and without, each relevant sugar (glucose/mannitol/fructose/sorbitol/sucrose) (from Sigma) at a final volume of 1% volume per volume (v/v) were used (stock concentration was 20% w/v) for determining which sugars the organism could utilise for growth on, and for cloning and complementation purposes (MM +glucose) (see section 2.7.1.1).

Defined medium (DM) agar plates[117] consisted of the following: 2.4% w/v proteose peptone (Oxoid), 0.5% w/v sodium phosphate dibasic, 0.2% w/v NaCl, 0.1% potassium phosphate monobasic, 0.01% magnesium sulfate (all from Sigma), and 1% w/v bacto agar (from BD) with, and without, each relevant sugar (mannitol/sorbitol/glucose) at a concentration of 0.6% (w/v) in 400mL dH_2O, and was used to determine which sugars the organism required for growth.

DM broth[117] consisted of the following: 2.4% w/v protease peptone (Sigma), 0.5% w/v sodium phosphate dibasic, 0.2% w/v sodium chloride (NaCl), 0.1% potassium phosphate monobasic, 0.01% magnesium sulfate, and was supplemented with, when needed, 0.15% w/v mannitol/sorbitol/glucose (all from

Sigma) in 400mL dH_2O. DM broth was sterilised using a 500mL volume vacuum filtration system (Thermo^{TM} Nalgene Rapid-Flow 75mm unit).

Tryptose-Yeast (TY) broth consisted of the following: 12g tryptose, 8g yeast extract (both from Oxoid), 0.4g thioglycholate (Sigma), and, when required, 2g mannitol/sorbitol/glucose (0.5% w/v final sugar concentration) in 400mL dH_2O. TY broth was sterilised using a vacuum filtration system (see above).

Lysogeny broth (Luria-Bertani) (LB) with chloramphenicol (cm) (25µg/mL) (broth and agar) and LB with cm/kanamycin (km) (12.5µg/mL) (broth and agar) was used for culturing *E. coli*. *E. coli* was cultured aerobically at 30°C and at 37°C with shaking at 200 rpm as required (Table 2.1).

Media for the two types of motility assays consisted of: (1) Semi-solid 2xYTG (yeast-tryptone-glucose) medium. This was composed of 16g of tryptone (from Oxoid), 10g yeast extract (Sigma), 4g of NaCl, 2.4g of gelzan (Sigma) in 975mL dH_2O. Glucose/mannitol/sorbitol was only added (aseptically as a liquid -25mL of a 20% w/v glucose stock solution) following autoclaving. Each plate was filled equally with 25mL of medium. (2) Top agar consisted of 0.75% (0.5% when in tubes) w/v Agar Biological Number 1 (Oxoid), 14.8g of BHI (Oxoid), 2g of yeast extract, 0.4g of L-cysteine (Sigma) in 400mL dH_2O was autoclaved and then used as a 7mL top layer which was poured onto the top of regular BHIS +CC plates. When preparing in tubes, agar was aliquoted directly into the tube.

Super Optimal broth with Catabolite repression (SOC) (Sigma) medium was used for *E. coli* Top10/CA434 recovery during electroporation.

BHIS +0.1% w/v taurocholate (Sigma) agar plates were utilised for spore assays.

All strains of *C. difficile* and *E. coli* were stored in BHIS broth +15% v/v glycerol (Sigma) at -80°C (New Brunswick Scientific^{TM} U570).

2.3 Media supplements

'*Clostridium difficile* Selective Supplement' commercially available (Oxoid) media supplement consisting of 250µg/mL D-cycloserine and 4µg/mL cefoxitin (CC). The final concentration was 200µg/mL.

Table 2.6: Antibiotics used in this study.

Supplement Name	Organism	Supplier	Stock conc. (mg/mL)
Cycloserin Cefoxitin	*C. difficile*	Oxoid	50
Chloramphenicol	*E. coli*	Sigma	25
Kanamycin	*E. coli*	Sigma	50
Thiamphenicol	*C. difficile*	Sigma	15
Erythromycin	*C. difficile*	Sigma	50

2.4 General molecular techniques

2.4.1 Genomic DNA extraction

Genomic DNA extraction from *C. difficile* was performed with the Qiagen^{TM} 'Blood & Tissue' DNA extraction kit according to the manufacturer's instructions.

2.4.2 Plasmid DNA extraction

Plasmid DNA from *E. coli* Top10_pMK-RQ, *E. coli* Top10_pMTL-YN3, *E. coli* CA434_ pMTL-YN3, *E. coli* Top10_ pMTL-YN1C, *E. coli* CA434_ pMTL-YN1C, *E. coli* Top10_ pMTL-YN1X, and *E. coli* CA434_ pMTL-YN1X was isolated using a Qiagen 'Plasmid Miniprep Kit' according to the manufacturer's instructions.

2.4.3 Restriction digest, dephosphorylation, ligation

mtlA/gutD knock-out cassette was amplified from pMK-RQ using primers specific to the plasmid (see Table 2.4), and purified using a 'GenElute PCR Clean-up Kit' (Sigma) according to the manufacturer's instructions. Following this, the cassette was restricted using *Asc*I and *Sbf*I (from New England Biolabs^{TM} -NEB) for 65 min. at 37°C followed by heat inactivation for 10 min. at 65°C. The vector, pMTL-YN-3, was then dephosphorylated using Antarctic phosphatase (from NEB) and incubated for 65 min. at 37°C followed by heat inactivation for 10 min. at 65°C.

Vector DNA and insert DNA were ligated using 'T4 DNA Ligase' (Promega^{TM}). A vector: insert ratio of 1:3 was used. The ligation mixture was then left on ice overnight. Following this, the ligation mixture was dialysed for 45 min. on dialysis disks (Fisher) in dH_2O and then transformed (see 2.4.5) into *E. coli* Top10.

2.4.4 Making electrocompetent cells

E. coli cells were prepared by adding a 1mL inoculum from an overnight *E. coli* Top 10/CA434 LB culture to 200mL of sterile, pre-warmed LB in a sterile 500mL

conical flask and growing at 37°C at 200 revolutions per minute (rpm) to an OD_{600} of 0.5-0.7. Cells were harvested by centrifugation (BeckmanCoulter Allegra X-30R Centrifuge) at 3684 x gravity (*g*) (in 50mL Falcon™ tubes, filled to 40mL) for 10 min. at 4°C. While always working on ice, two pellets were combined, and then the cells were washed in sterile ice-cold dH_2O and centrifuged at 3684 x *g* for 10 min. at 4°C. This pellet was re-suspended in 20mL sterile ice-cold dH_2O and centrifuged at 3684 x *g* for 10 min. at 4°C. Once more, cells were re-suspended in 10mL sterile ice-cold dH_2O, and centrifuged at 3684 x *g* for 10 minutes at 4°C. Finally, the pellet was re-suspended in 1mL 1mM 4-Morpholinepropanesulfonic acid (MOPS) with 10% (v/v) glycerol (ice-cold). Cells were then aliquoted into 50µL samples and stored at -80°C in micro-centrifuge tubes.

2.4.5 Electroporation

2µL of plasmid DNA (for CT plasmid)/ligation mixture containing plasmid with insert (for deletion or complementation) was added aseptically to 50µL of electro-competent *E. coli* Top10/CA434 cells in a 1mL electroporation cuvette (Bio-Rad™) and subjected to an electronic pulse (2000 Volts [V] on 'Programme 2') using a Gene-Pulsar (Bio-Rad), so as to permit the uptake of the plasmid. Top10/CA434 cells were then incubated in SOC medium for 1 hour (h) at $37^{O}C$ to allow the cells to recover and start growing, before plating on selective medium (LB agar plates +cm), and incubated overnight at $37^{O}C$.

2.4.6 Conjugation

An overnight culture was set-up by taking a single colony of CA434 containing the appropriate CT plasmid or knockout/knock-in cassette from the LB +cm agar plates and inoculating in 5mL of LB +cm and incubating at 37°C. 1mL of cells in broth was taken from the overnight culture and centrifuged (Eppendorf^{TM} Centrifuge 5415D) for 1 min. at 1500 x *g*, and then washed with 0.5mL phosphate buffered saline (PBS), and centrifuged again for 1 min. at 1500 x *g*. The pellet of cells was then brought into the anaerobic cabinet and mixed with 200µL overnight culture of the recipient organism (*C. difficile* 630Δ*erm*Δ*pyrE*, and later, the mutants to be complemented). The conjugant/recipient mixture was then spotted onto non-selective BHIS plates, and incubated anaerobically overnight at 37°C.

2.4.7 DNA sequencing

To confirm the successful transformation of the *mtlA/gutD* knock-out cassettes in the pMTL-YN-3 vector into *E. coli* Top10/CA434, and also deletion of *mtlA*/*gutD*, plasmid/genomic DNA bands were extracted (using a Qiagen 'DNA Gel Purification Kit' according to the manufacturer's instruction) and were sequenced (all sequencing was done by Source Bioscience^{TM}) using primers, pMK-RQ_F1 and pMK-RQ_R1, which were specific for the knock-out cassettes; and *mtlA*/*gutD*_A and_B primers, which were specific for the left homology arm (LHA) and right homology arm (RHA) of *mtlA*/*gutD*.

Complementation cassettes were also sequenced (following ligation of complementation cassettes to pMTL-YN1C/X vectors and transformation into *E. coli* Top10, restriction, running of the plasmid DNA on agarose gel, and then

DNA extraction) using primers immediately up and downstream of the relevant restriction sites of pMTL-YN1C/YN1X (YN1_*Not*I_F/ YN1_*Sac*I_F and YN1_*Nhe*I_R). *pyrE* primers (630-*pyrE*-sF1 and 630_*1880*_Rs)were used to sequence DNA isolated from agarose, which showed restoration of the genes of interest.

2.4.8 Polymerase Chain Reaction (PCR)

2.4.8.1 Primer design

Primers, to enable amplification of the desired region, were designed using several primer design tools. Criteria required for primer design were a melting temperature of 55-60°C (using www.insilico.ehu.es) and no multiple binding within the genome (using BLAST). The ideal number of base pairs is about 20 (although it may be more). For screening of CT mutants, a universal primer, exon binding site (EBS), was also used with the designed forward (F) or reverse (R) primer (depending on whether the intron target was on the sense (s**)** or antisense (a**)** strand).

Table 2.7: PCR conditions used in this study.

No. of Cycles	Temperature (°C)	Time (seconds)	Function
1	95	120	Initialisation
34	95	20	Denaturation
	54-60	10	Annealing
	70	205	Elongation
1	70	300	Final Elongation
1	15	Pause	Hold

PCR machine was a Biometra™ Professional Trio Thermocycler. KOD polymerase (from Novagen™) was used throughout as the DNA polymerase.

2.5 ClosTron (CT) mutagenesis

Selected genes were targeted for inactivation via CT mutagenesis (Fig. 2.1) as described previously[118]. Briefly, the target sequences were inputted into the algorithm design tool (www.clostron.com), giving a recommended target region within the gene (s/a strand).

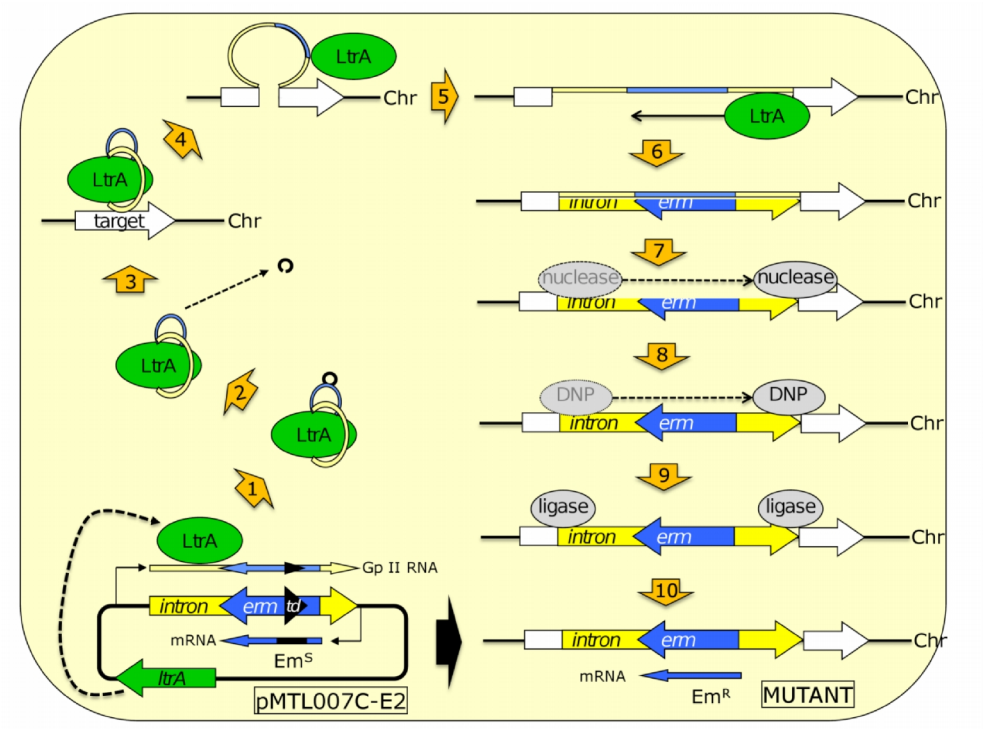

Figure 2.1: ClosTron mutagenesis[119].

The CT plasmid encompasses a group II intron into which an Erm-resistance gene (*ermB*) is inserted, which is inactivated by a small phage *td* group I intron. Upon transcription of the DNA strand encompassing the group II intron region, LtrA binds to the transcript giving rise to (1) the formation of a ribonuclear protein (RNP) complex. (2) The *td* group I intron is now in the correct orientation, so, it is then spliced out. (3) The RNP recognises and attaches to sequences in the target region in the genome. (4) LtrA nicks the DNA target and (5) inserts the RNA. (6) The reverse transcriptase activity of LtrA manufactures the complimentary strand. (7) Host nucleases degrade the insert RNA and (8) DNA polymerase (DNP) synthesises the opposite strand. (9) Host ligases seal the gaps, resulting in (10) the process being concluded in which an activated *ermB* gene is now present in the targeted region of the genome[119].

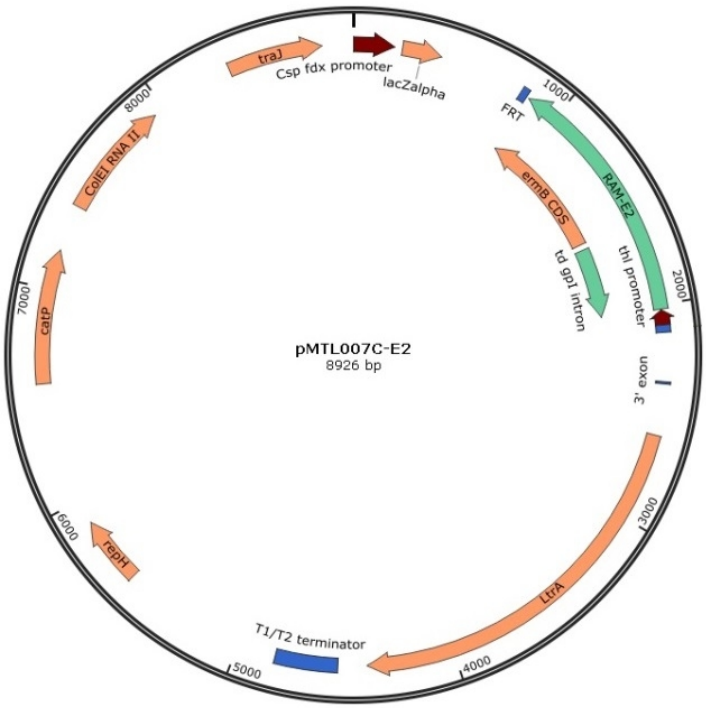

Figure 2.2: Map of the ClosTron plasmid pMTL007C-E2[118].
Amongst the regions encoded within the plasmid are: *catP* gene conferring thiamphenicol-resistance; phage group I intron, *td*; group II intron, *ltrB*; intron encoded protein, *ltrA*; thiolase (*thl*) promoter; ferredoxin (*fdx*) promoter; erythromycin-resistance gene (*ermB*); *colE1* (for replication in *E. coli*); and *repH* (for replication in *C. difficile*).

2.5.1 ClosTron targets

Table 2.8: Genetic loci and intron position of the PTS genes targeted for CT mutagenesis.

Target Gene	Insertion Site (sense/antisense)
CD630_2332 (*mtlF*)	64s
CD630_2333 (*mtlR*)	733s
CD630_0764 (*gutA*)	402a
CD630_0765 (*srlE_N*)	282a
CD630_0766 (*srlE_C*)	240a
CD630_0767 (*srlB*)	184s

CT plasmids (synthesised by DNA 2.0^{TM}) (Fig. 2.2), containing the retargeted sequence specific for each individual selected target, were transformed into electrocompetent *E. coli* Top10 and CA434 cells. Top10 and CA434 cells were then incubated in SOC medium for 1 h at 37°C to allow bacterial recovery and

growth, before plating on selective medium (LB agar plates +cm), and incubated overnight at 30°C. Plates with Top10 transformants were harvested, stocks were made (using Microbank^{TM}) and stored at -80°C. Plates with CA434 were used to set-up an overnight culture by taking a single colony from the LB +cm agar plates, inoculating in 5mL LB +cm, and then incubated overnight at 30°C. These transformed cells were used as the donor cells to pass the plasmid to *C. difficile* during conjugation.

2.5.2 Isolation of putative CT integrants

Following conjugation, the cells were scraped from the plate and transferred to 1mL of PBS and 160µL of the mixture was spread onto plates of BHIS +0.4% v/v CC +0.1% v/v Tm, and incubated for up to 3 days anaerobically at 37°C. Following growth on the plates, the colonies were re-streaked to purity on fresh plates containing the same antibiotics. Following this, the cells were then transferred to plates of BHIS +0.4% v/v CC +0.1% v/v erythromycin (Erm), incubated in the anaerobic cabinet for 3-4 days at 37°C, and again re-streaked onto to fresh Erm plates to purify them.

Erm-resistant colonies were subjected to genomic DNA extraction (see 2.4.1 genomic DNA extraction above) and PCR screening (see 2.4.8 PCR above) to determine if the CT insertion had occurred in the correct position.

2.5.3 Agarose Gel Electrophoresis (AGE)

The PCR products were loaded with 6X running buffer (NEB) and ran on 1% agarose (from Sigma) gel at 100 V. The fragments were visualised using a Bio-

Rad Gel Doc XR+. Following PCR, CT mutants were checked by Southern blotting to confirm the creation of the mutant.

2.5.4 Southern blotting confirmation of CT mutagenesis

Protocol as per Heap *et al.* 2010[120]. CT mutants (CT*srlE_N*, CT*mtlF*, and CT*mtlR*) (Chapters 4 and 5, Fig. 4.34 and Fig. 5.34) were tested by Southern blot to determine if the CT insertion had occurred only in the correct position.

Following confirmation of a single-insertion mutant by Southern blot, the mutant was re-streaked on plates of BHIS + CC, and stored in 0.5mL of BHIS broth +15% v/v glycerol at -80°C.

2.6 In-frame deletion of *mtlA* and *gutD*

Method used according to Ng *et al.* 2013[117]. Knock-out cassettes were constructed consisting of the left and right-homology arms (LHA/RHA) of *mtlA* (CD630_2334) and *gutD* (CD630_0768). The LHA/RHA arms encompass the regions 500 base pairs up and downstream of the target gene(s).

Knock-out/deletion cassettes were ordered (from Invitrogen), and were delivered within a plasmid, pMK-RQ. The plasmid was then transformed into *E. coli* Top10 (see section 2.4.5 electroporation above). *E. coli* Top10 harbouring the plasmid was grown in LB supplemented with 25µg/mL kanamycin (Km) at 30°C overnight. The next morning, plasmid DNA was extracted (see 2.4.2 plasmid DNA extraction above), and the *mtlA/gutD* knock-out cassettes amplified from the pMK-RQ plasmid using primers, pMK-RQ_F1 and pMK-RQ_R1 which were designed specific to the regions in the plasmid immediately upstream and downstream of the cassettes.

2.6.1 Knock-out cassette cloning

Following amplification, purification, and restriction of the *mtlA/gutD* knock-out cassettes, PCR products were ran on 1% w/v agarose gel (see section 2.5.3 AGE above), allowing a single PCR band to be extracted, purified, and sequenced (see section 2.4.7 DNA sequencing above) which showed complete homology to the designed cassette (data not shown). Gel extraction was performed using a 'QIAquick Gel Extraction Kit' from Qiagen in accordance with the manufacturer's instructions. Purified knock-out cassette DNA was then restricted with AscI and SbfI, and inserted into YN3 (see 2.4.3).

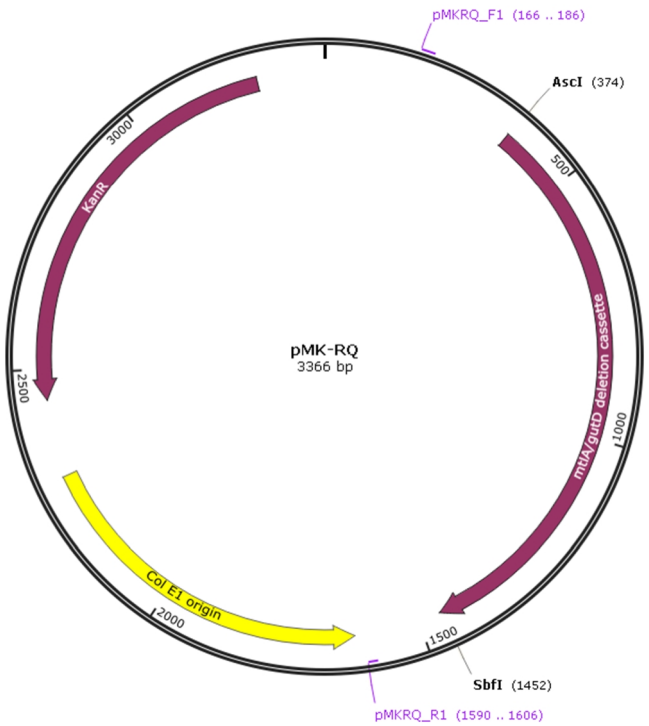

Figure 2.3: Map of the pMK-RQ plasmid containing *mtlA/gutD* knockout cassette (Invitrogen).
mtlA/*gutD* were received in the plasmid and later amplified via PCR using pMKRQ_F1 and pMKRQ_R1 primers. The knockout cassette was restricted using AscI and SbfI, and then inserted into the pMTL-YN3 plasmid (conjugation vector).

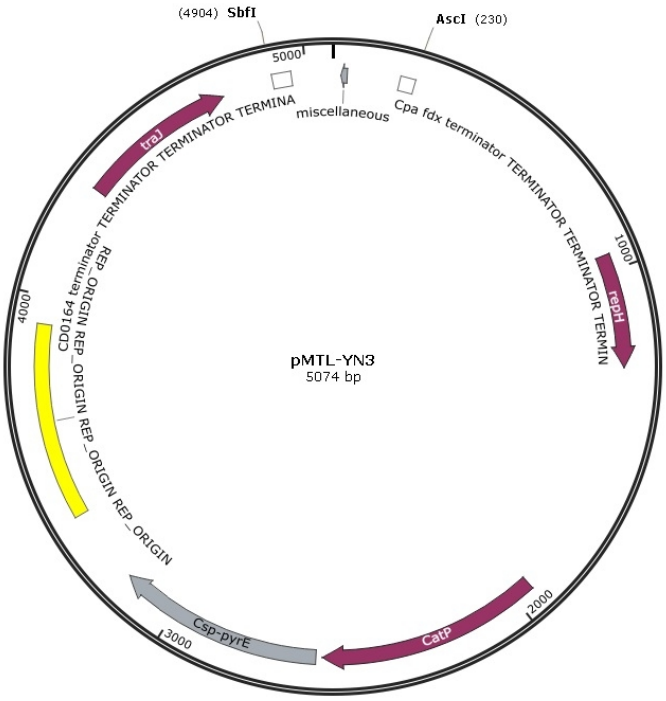

Figure 2.4: Map of the pMTL-YN3 vector used for allelic exchange manipulation of *C. difficile* 630Δ*erm*Δ*pyrE*[117].
Vector was used to deliver the *mtlA*/*gutD* knock-out cassette to the parental strain (630Δ*erm*Δ*pyrE*). Successful delivery of the plasmid into the parental strain is determined by Tm-resistance, conferred by *catP*.

pMTL-YN3 (see restriction digest, dephosphorylation, ligation section 2.4.3) containing the amplified knock-out cassette (*mtlA*/*gutD*) was then transformed into *E. coli* CA434 (see electroporation section 2.4.5 above). Transformants were spread onto LB agar containing cm following recovery in SOC medium for 1 h and incubated for 48 h at 30°C. Following incubation, individual colonies were selected, grown overnight in 5mL LB +cm, subjected to plasmid miniprep DNA extraction (see plasmid DNA extraction section 2.4.2 above), restricted with AscI and SbfI, and the DNA run 1% w/v agarose, and sequenced using pMK-RQ_F1 and pMK-RQ_R1 primers to verify which colonies contained the knock-out cassette (data not shown). Following verification of the presence of the knock-out cassette, each colony containing the cassette was spread onto a fresh LB +cm plate, incubated for 48 h at 30°C, and harvested to make a frozen stock (using

Microbank), which was used to prepare an overnight culture to be used as a donor (see section 2.4.6 conjugation above).

2.6.2 Selecting for single cross-over and double cross-over events

According to Ng *et al.*[117], single cross-over events (Fig. 2.5) are facilitated by a plasmid (pMTL-YN-3 containing the knock-out cassette) carrying a *catP* gene which confers Tm resistance (Fig. 2.5). This results in large *C. difficile* colonies on plates of BHIS +Tm. Following this, single cross-over clones are transferred to minimal media selective plates (containing FOA and no uracil) to identify those cells which had lost the pMTL-YN-3 plasmid and which had undergone the desired double cross-over event, and were consequently *pyrE*-negative (Fig. 2.6).

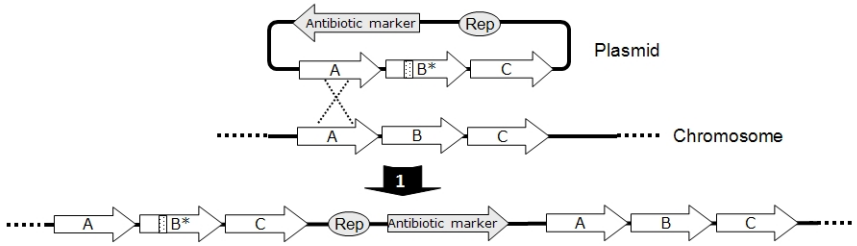

Figure 2.5: Schematic representation of gene knock-out by double cross-over (allelic exchange) selecting for an initial single crossover event (University of Nottingham, 2010).
Tm-resistance was used as a marker to determine the uptake of the pMTL-YN3 plasmid containing the knock-out cassette by the recipient strain (630Δ*erm*Δ*pyrE*) that was to be transformed.

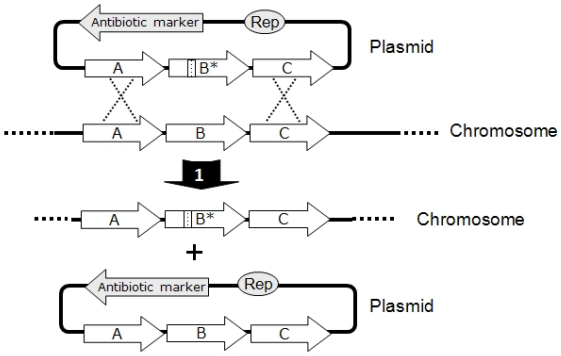

Figure 2.6: Schematic representation of gene knock-out by double cross-over (allelic exchange) (University of Nottingham, 2010).
Left and right homology arms (A and C), directly up and downstream of the target gene (*mtlA*/*gutD*) (B), were used to create the knockout cassette in order that the cassette [(contained in pMTL-YN3 along with the antibiotic selection marker, *catP*, conferring Tm-resistance) (A and C) would replace, by homologous recombination, the chromosomal target regions (A and C, and also B (*mtlA*/*gutD*)].

2.6.3 Complementation of mutants

Mutants made by targeting the PTS^{Mtl} at CD630_2331-4 were complemented with the genes that were orginally targeted in each individual mutant. For example, CT*mtlR* was complemented with *mtlR*. Complementation studies aimed at restoring the gene of interest using its own promoter (*Pmtl*), and also, overexpressing the gene using a stronger promoter (*fdx*).

Each mutant had originally been created in a *pyrE*-negative background in order that they could be easily complemented later on following the observation of a phenotype with the mutant. Restoration of the gene of interest would occur in tandem (and alongside *pyrE* at the *pyrE* locus –Fig. 2.9) with the restoration of *pyrE*. The ability to grow on MM plates without uracil was used as an indicator to determine if the gene had been restored.

Primers specific for the gene of interest and the native promoter were designed with restriction sites on each for *Not*I (promoter), *Nco*I (promoter and gene), *Nhe*I

(gene), and *Sac*I (when overexpressing the gene). Following amplification with these primers, PCR fragments were purified on 1.3% w/v agarose gel and restricted. After restriction, the restricted DNA was then ligated using the previously mentioned method (see section 2.4.3) to pMTL-YN1C/X which had been restricted with *Not*I/*Nco*I/SacI and *Nhe*I. The ligation mixture was dialysed (see section 2.4.3) and then transformed into *E. coli* Top 10 and grown for 3 days at 30°C on LB +cm plates, and then the cm-resistant colonies were grown in LB +cm broth at 30°C overnight and subjected to plasmid miniprep DNA extraction, restricted again, run on 1.3% w/v agarose gel to see if insertion of the genes of interest into the plasmid(s) had occurred, and then sequenced the plasmid DNA to confirm this. After sequencing, plasmid DNA was transformed into *E. coli* CA434, grown on LB +cm plates, and plasmid DNA isolated and once more restricted with *Not*I/*Nco*I/SacI and *Nhe*I.

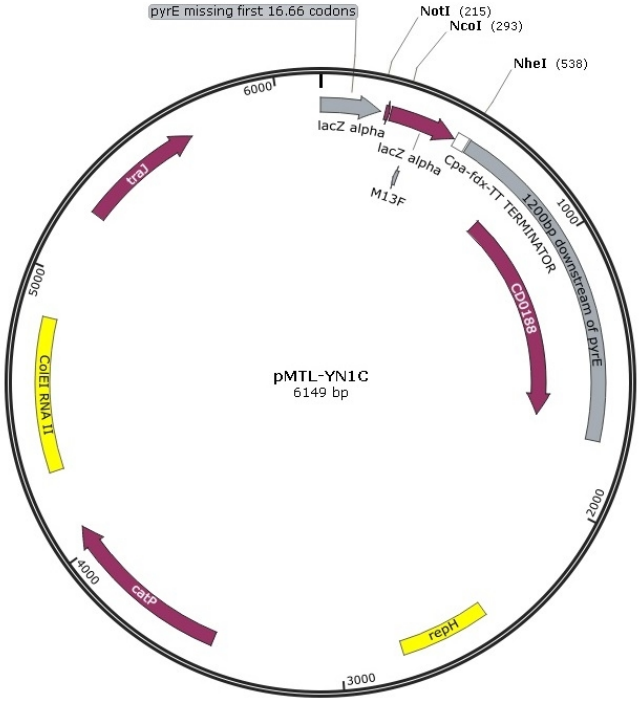

Figure 2.7: Map of the pMTL-YN1C plasmid used for complementation of mutants[117].

Vector used to complement mutants with the desired gene. All mutants were created in a *pyrE*-negative background, hence the use of *C. difficile* 630Δ*erm*Δ*pyrE* as the parental strain. During complementation, at the same time that the gene is inserted into the *C. difficile* 630 genome, *pyrE* is restored, and therefore, *pyrE* restoration is used as a marker of genetic insertion.

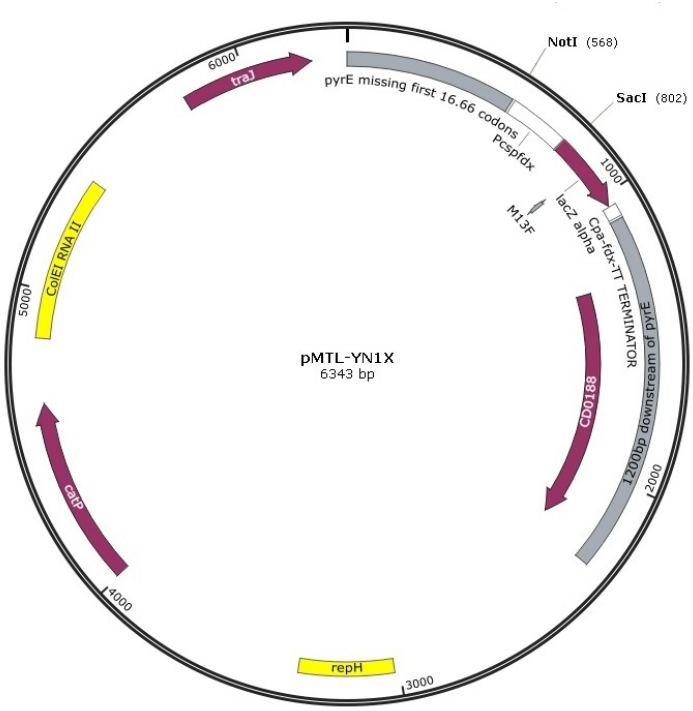

Figure 2.8: Map of the pMTL-YN1X plasmid used to overexpress PTS genes of interest[117].
Vector (containing the constitutive *fdx* promoter) used for complementation of mutants so as to overexpress the gene of interest. All mutants were created in a *pyrE*-negative background, hence the use of *C. difficile* 630Δ*erm*Δ*pyrE* as the parental strain. During complementation, at the same time that the gene is inserted into the *C. difficile* 630 genome, *pyrE* is restored, and, therefore, *pyrE* restoration is used as a marker of the genetic insertion.

E. coli CA434 harbouring pMTL-YN1C/X was grown overnight in LB +cm at 30°C, washed once with sterile PBS, mixed in an aerobic cabininet with 200µL overnight culture of the recipient strain (the original mutant in the *pyrE*-negative background) and spotted onto non-seletive BHIS plates and incubated overnight at 37°C. Transconjugants were then plated onto BHIS +CC +Tm and incubated for 3 days in the anaerobic cabinet. Following growth on plates, eight single colonies were taken from each plate and individually restreaked onto fresh BHIS +CC +Tm plates and incubated for a further 3 days. This step was repeated once more, after which, a streak of Tm-resistant colonies was spread onto MM +glucose plates without uracil. After 2-3 days, single colonies growing on MM

+glucose plates were restreaked onto fresh MM +glucose plates and incubated for a further 2-3 days. Single colonies growing on these plates were then spread on BHIS +CC plates, and DNA isolated from the resulting colonies, which were then amplified using primers to show *pyrE* restoration in tandem with restoration of the gene of interest. PCR products were run on 1% w/v agarose gel to demonstrate the restoration of *pyrE* and the gene of interest. Following this, DNA bands of interest on the gel were cut and purified (see sequencing section 2.4.7) and DNA isolated, which was then sequenced (data not shown), which verified the restoration of *pyrE* and the gene of interest.

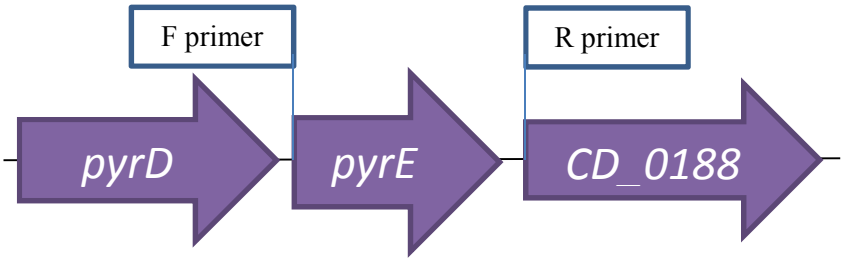

Figure 2.9: *pyrE* locus at CD630_0187 within the *C. difficile* 630 genome. Primers, 630-*pyrE*-sF1 and 630_*1880*_Rs, specific for the regions immediately outside of *pyrE*, were used to screen colonies growing on MM (without uracil) for the restoration of the genes of the PTS^{Mtl} at loci CD630_2331-4 which had been deleted or inactivated.

After the confirmation of the creation of a complemented mutant, each complement was assayed (growth, sugar uptake, cytotoxicity, and motility) alongside the control strain (630Δ*erm*) and the original mutant (*pyrE*).

2.7 Phenotypic assays

Experiments were performed in order to help elucidate the role of the target genes, and the systems of which they are part, in sugar uptake, toxin regulation,

and motility. Each generated mutant was compared with the parent using assays to determine growth, motility, toxicity, and sugar uptake.

2.7.1 Growth

2.7.1.1 Growth on Minimal Medium (MM) agar

MM agar plates were used to determine the growth of the parental strain, (630Δ*erm*Δ*pyrE*) using each of the following sugars: glucose, fructose, mannitol, sorbitol, and sucrose as the sole carbon source (in triplicates).

2.7.1.2 Growth on Defined Medium (DM) agar

The growth of each strain was tested (in triplicates) on plates of DM agar. 1µL of DM (no sugar) overnight culture (which had been inoculated with a fresh single colony from each strain to be tested growing on plates of BHIS without CC) was streaked onto DM agar plates (DM, DM +mannitol, and DM +sorbitol). Following 16 h incubation, plates were removed and photographed (Bio-Rad Gel Doc XR+).

2.7.1.3 Growth in Defined Medium (DM) broth

Time course growth experiments in DM broth (up to 24 h) were performed in triplicate by inoculating 1mL of DM (no sugar) with single colonies of each stain and incubating anaerobically overnight at 37°C, and then, the next morning, using this overnight culture to inoculate (1:100 dilution) 20mL of DM, and DM + 0.15% sugar for the time course experiment. OD_{600} was measured (using a Thermo^{TM} Biomate 3) every two hours until the 12 h time point. OD_{600} was then measured at the 24 h time point. At time 0 h, 6-24 h (mannitol with glucose

samples), and 8-24 h (sorbitol with glucose samples), a further 1mL was extracted for HPLC analysis (see section 2.7.3).

2.7.1.4 Growth in Enriched Media (EM)

Time course growth assays (up to 72 h –PTS^{Mtl} or 120 h –PTS^{Srl}) were performed (in triplicates) by inoculating 1mL of TY broth with single colonies of each strain and incubating anaerobically overnight at $37^{O}C$, and then, the next morning, using this overnight culture to inoculate (1:100 dilution) 20mL of TY broth and TY broth + 0.5% sugar for the time course experiment. OD_{600} was measured every two hours until the 12 h time point. OD_{600} was then measured at the 24 h time point, and every 24 hours until the 72 h time point (PTS^{Mtl} targets) or the 120 h time point (PTS^{Srl} targets). A further 1mL extract from each sample was taken at the 24-72 h time points and stored at $-20^{O}C$ until use in the cytotoxicity assays (see section 2.7.2).

2.7.2 Cytotoxicity assays

Cytotoxicity was determined using Vero cells, passages (p) 25-36, in a cytotoxicity assay as described in Kuehne *et al.* (2010)[14]. Briefly, supernatants collected during the growth assays (in triplicates) were serially diluted (from 10^{0} to 10^{-9}), applied to Vero cell monolayers in 96-well plates, and incubated overnight at $37^{O}C$ and 5% carbon dioxide (CO_2) (Thermo BB15 Heraeus). Cells were observed under the microscope (Motic AE 2000) for rounding after 24 h.

All work was performed sterilely and aseptically. Only pipette tips which had been autoclaved and unopened (unless opened under a Bunsen flame) were used. Vero cell stocks maintained in 20mL volume cell flasks (with filter cap to allow

oxygen) containing Dulbecco's Minimal Essential Medium (MEM) (from Sigma) + 1% v/v penicillin/streptomycin (from Sigma) +5% v/v fetal bovine serum (FBS) (from Sigma) –hereon referred to as 'Vero medium', were grown to confluence at $37^{O}C$ and 5% CO_2 in an incubator (Thermo BB15 Heraeus).

Working inside a laminar air flow (LAF) (Biomat^2), Vero cells were washed once with 10mL sterile PBS (room temperature). 5mL of 1% v/v trypsin (from Sigma) (pre-warmed in the incubator) was added and cells were incubated at $37^{O}C$ for several minutes. Detaching cells were observed under the microscope (Motic AE2000). When the cells had detached (5 mins. maximum), the flask was transferred to the LAF. 5mL of 'Vero medium' (pre-warmed in the incubator) was added and the gently moved around the inside of the flask to collect all the cells. The liquid containing the resuspended cells was removed to a sterile universal tube and spun for 10 mins. at 200 x *g* (Eppendorf^{TM} Centrifuge 5702R). The liquid was extracted and the pellet was resuspended pellet in 10mL of fresh 'Vero medium' (this was the stock of cells). 7mL of stock + 63mL of 'Vero medium' (1 in 10 dilution) was mixed in a sterile square dish (with lid) (Fisher). 100µL of cells were pipetted into each well of a sterile 96-well plate (Costar^{TM}) that had a lid. Plates containing cells were then transferred to the incubator and left for 24 h after seeding for the cells to recover before applying the bacterial supernatants obtained from the growth assays using TY.

When taking 24, 48, and 72 h measurements (in triplicates) during the growth assay in TY, 1mL was extracted for OD_{600} reading and 1mL for the cytotoxicity assay.

1mL *C. difficile* TY extracts that were frozen (-20°C) following the growth assays in enriched media broth (see section 2.7.1.4) were gently defrosted on ice. Defrosted extracts (each condition was performed in triplicates –parent vs. mutant in TY, TYM, and TYS; except the positive control, in TYG, which was performed in duplicates due to 96-well plate limitations), were centrifuged at 17000rpm for 5 mins., and filter sterilised (while using a Bunsen flame) using a 0.22µM filter (Whatman^{TM}) and a 1mL syringe (from BD).

Serial dilutions of extract supernatant were prepared in a sterile 96-well plate that had a lid (ranging from neat to 10^{-9}) under a Bunsen flame. 200µL of neat supernatant went into the first well, while 180µL sterile PBS went into each following well, and then the supernatant was serially diluted by transferring 20µL of it into the next well (10^{-1}), gently mixed up and down a couple of times, and this process was continued until reaching 10^{-9}). The final two columns on the plate (11 and 12) were used as controls. The wells in column 11 contained sterile TY broth in PBS as a 'vehicle control'. The wells in column 12 had nothing added. The use of these controls confirmed that the cells were healthy throughout assay (12) and that the medium used was not inducing cell death (11).

The lid on the 96-well plate was replaced and all of the plates were taken to the cell lab, and 20µL of supernatants applied (starting at the lowest concentration, 10^{-9}, and working from right to left up to the neat concentration) to the top of the cells, and then removed into the incubator, and incubated overnight. Following incubation, the plates were observed under the microscope to determine which dilution was the highest (lowest concentration of toxin) of supernatant which resulted in cell death.

2.7.3 High Pressure Liquid Chromatography (HPLC) evaluation of mannitol/sorbitol/glucose consumption

1mL overnight cultures (in triplicates) of the control (630Δ*erm* -mannitol targets/630Δ*erm*Δ*pyrE* -sorbitol targets), mutant, and complemented strains were set-up in DM broth, and 200µL was used to inoculate 20mL of DMM/DMS/DMG (containing 0.15% w/v mannitol/sorbitol/glucose). Starting at 0 h, 1mL of each sample was taken, and then (from 6 h incubation with the mannitol samples and from 8 h with the sorbitol samples) at 2 h intervals, centrifuged at 13400 x *g*, filtered using a Spartan 0.45µM HPLC filters (Whatman), and frozen at -20°C until use.

Subsequently, 100µL of each sample was added to glass phials containing a 200µL deactivated glass insert (Fisher) containing 100µL mobile phase (see below). 20µL ELGA^{TM} water was first used to clear and initialise the system. Following this, 20µL of each sample was loaded onto the column. The eluate was detected through changes in the refractive index (RI), and absorbance of ulta-violet (UV) light.

The HPLC consisted of a Thermo Dionex Ultimate 3000 Autosampler/Column Compartment with Diode Array Detector. The HPLC column was a Rezex ROA-Organic Acid H+ (8%) 150mm x 7.8mm x 8µm (Bio-Rad). The RI detector consisted of a Refracto Max 520 which was used with the UV detector at 210nm. The software used was Chromeleon Console (from Thermo). The flow rate was 0.5mL/min. The column temperature was maintained at 35°C, while the pressure was 42 bar. The mobile phase consisted of 5mM sulfuric acid (H_2SO_4) dissolved in ELGA water. The internal standard was 50mM valeric acid in 5mM sulfuric

acid, which came off the column at 22 min. Total run time for each sample for 30 min. The injection volume was 20µL.

Peak area (cm^2) was used to determine the concentration of each given peak [always coming off the column at 6.5 min. (mannitol), 6.7 min. (sorbitol), or 5.7-5.8 min. (glucose)] by the use of a calibration curve for mannitol, sorbitol, and glucose [0.5mM-64mM sugar dissolved in dH_2O, and mobile phase (1:1)].

2.7.4 Motility assays

During the motility assays, *C. difficile* 630Δ*erm*_CT*fliC*[82] and *C. difficile* M120[121] were used as negative controls.

2.7.4.1 Motility assays on YT +glucose/mannitol/sorbitol plates

Motility assays on YTG/M/S plates were initially prepared over two days. Overnight cultures (in triplicates) for each strain were prepared in 1mL TY broth. Motility assay plates were prepared (see section 2.2) and reduced overnight in an anaerobic cabinet. The following day fresh cultures in 1 mL TY were prepared from the overnight culture (1:100) and incubated for 6 h. 2µL of bacterial culture was applied to the middle surface of each motility plate. Motility plates were incubated for 48 h until removal from the anaerobic cabinet and photographing (using Gel Doc XR+).

2.7.4.2 Motility assays on BHIS +top agar plates

Strains to be tested were spread (inside an anaerobic cabinet) onto plates of BHIS one day in advance of the assay. BHIS plates were prepared as normal (see section 2.7.1.4). To the top of those plates was added 7ml of 0.6% w/v top agar. The plates were quickly dried at 37^OC in a warm room. Plates were removed to

the anaerobic cabinet and reduced for 8 h. Strains which were growing on normal BHIS +CC plates were used to inoculate BHIS +top agar plates by a single colony being plucked from each plate with a sterile cocktail stick and the centre of the top agar was then pierced with the stick to a depth of 2 mm. This process was performed in triplicates. The plates were returned to the lid side down position, and allowed to grow for 48 h until removal and photographing.

2.7.4.3 Motility assays in tubes

18mL of 0.5% w/v top agar was aliquoted into each sterile glass test tube (Pyrex^{TM}). Tubes were prepared in triplicates for each strain to be tested. Once the medium had solidified, the tubes were transferred to an anaerobic cabinet and reduced for 8 h. With a sterile cocktail, a fresh single colony from a BHIS +CC plate was plucked, and the surface of the agar was pierced to a depth of 2mm. The test tubes were then incubated in the anaerobic cabinet for 48 h until removal and photographing on a lab bench (using a Canon^{TM} Ixus 801S).

2.7.5 Spore assays

CT*mtlR* and Δ*mtlA* were tested to determine if knocking-out these (*mtlR* and *mtlA*) genes produced an effect on the sporulation of *C. difficile*.

Heat-resistant colony forming units (CFU) produced by CD630Δ*ermΔpyrE*, CD630Δ*ermΔpyrE*, CD630Δ*ermΔpyrE*_CT*mtlR*, CD630Δ*ermΔpyrEΔmtlA*, and CD630Δ*erm*_CT*spo0A* were measured over a 5-day period.

To ensure that no spores were present when the BHIS broth was inoculated, a starter culture was prepared (using the same medium) with a 1 in 100 inoculum of an overnight culture (10µL overnight culture into 1mL starter culture). The

starter culture was incubated for 6 h. Finally, the BHIS broth was inoculated with a 1 in 100 inoculum of the starter culture.

Heat-resistant CFU of *C. difficile* cultures were prepared (in triplicate) at 0 h, 24 h, 48 h, 72 h, 96 h, and 120 h. Non-heat-treated *C. difficile* cultures were also prepared at 0 h and 120 h (in triplicates). Two 500µL extracts of each replicate were removed from the anaerobic cabinet. One sample was incubated at 80°C for 10 min., while the second sample was left unheated. Samples were then returned to the anaerobic cabinet and serially diluted (10^0-10^{-3}) in sterile PBS. 20µL of each dilution of the heat-treated culture and 20µL of each dilution of the non-heat-treated culture onto was spotted onto plates of BHIS agar +0.1% taurocholate (to ensure recovery of the spores). The plates were incubated for 24 h, after which, CFUs were enumerated on each plate using the appropriate dilution factors.

2.8 Statistical analysis

All analyses were performed in 'triplicates', meaning that three independent overnight samples of each strain (e.g. 630WT) in each condition (e.g. TY, TYM, and TYG) were set-up, sourced from three separate respective colonies, which were then used to individually inoculate the growth medium in each tube (three), which was then subsequently used to provide samples for analysis (for growth, cytotoxicity, and HPLC). This use of triplicates was also used in same way for the motility assays.

Statistical analysis of growth, toxin levels, sugar concentration, and spore production between different sample groups was carried out using one-way ANOVA (available at vassarstats.net/1u.html). One-way ANOVA (which tests

the null hypothesis that samples in two groups or more are taken from populations with the same means) was used to compare the mean of each sample group and to determine if the differences between those means were statistically significant, and, thus, helping to evaluate the effect of inactivating/deleting, and later, complementing the target genes of interest. A P-value of < 0.05 was considered significant.

Slope of the curve ($\Delta Y/\Delta X$) was used to determine the growth and decline rate of each strain.

2.9 Bioinformatics

Basic Local Alignment Search Tool (BLAST) was used to compare gene (blastn) and protein (blastp) sequences. Sequenced samples were also compared using this programme. Clustal programme at the European Bioinformatics Institute (EBI) was used to create the phylogenetic tree of PTS in *C. difficile* 630 (Mitchell, unpublished) and was also used to align the amino acid sequences of MtlR in the different Clostridia. DNAStar was used to align the sequenced *C. difficile* 630 *srlE* (CD630_0765-6) fragments from the publicly available *C. difficile* 630 *srlE* sequences on NCBI.

3.0 Results Chapter I

3.0 Results Chapter I – Preliminary investigations of *C. difficile* 630 PTS

Prior to this study, there have been no published investigations into the characterisation of the operons hypothesised to encode the mannitol and sorbitol PTS in *C. difficile*. Mannitol and sorbitol are fermentable carbon sources to the organism[22,28]. Previous studies looking at the relationship between these sugars and the PTS in *C. difficile* have only considered whether the sugar in question is fermentable by the organism (mannitol)[28], if its presence elicits an effect on toxin production (mannitol -yes, sorbitol -no, hypothesised)[22,28], and whether the genes hypothesised as encoding the proteins responsible for uptake of these sugars are under the control of CcpA (mannitol-specific genes at loci CD630_2331-4 –not known; sorbitol-specific genes at loci 0762-8 -no)[22]. Therefore, it was imperative to specifically target the genes speculated as being involved in mannitol/sorbitol uptake to firstly, experimentally prove their roles in sugar uptake, and secondly, elucidate their role in growth, toxicity, and motility.

Phylogenetic grouping of all PTS present in CD630 revealed 49 potential systems, which included representatives of all seven families of PTS (Mitchell 2012, unpublished, Fig. 1.5)[101].

Glucose has been well established as the primary sugar (the sugar of highest preference above all) in *C. difficile*[22,28], so it has been used throughout this study as a positive control for effects of sugars on growth and cytotoxicity.

Growth on fructose was also previously tested, as fructose has also been shown to be a primary sugar in *C. difficile*, just next to glucose in order of preference[22].

Within the entire *C. difficile* 630 genome, a fully sequenced strain which we are using to study the PTS in *C. difficile*, there are only three genes that are annotated as putative sucrose-specific PTS. Annotation on Artemis shows these three genes, at loci CD630_0388, CD630_0469 (both IIABC), and CD630_3103 (IIA) as being 'glucose/sucrose'-specific, and also, as merely being stand-alone genes and not comprising part of an actual full sucrose PTS. This indicated that *C. difficile* 630 may not be able to utilise sucrose. It was therefore of interest to test the growth of the organism on this sugar to determine if *C. difficile* 630 possesses the ability to use sucrose.

The hypothesised mannitol system at loci CD630_2331-4 (PTS^{Mtl}) was selected, firstly, because of its genetic divergence from other PTS encoded within the genome (Mitchell, unpublished); secondly, due to the apparent absence of a substantial number of strong homologues for components of this operon, with the partial exception of the putative IIA, MtlF (homologue of MtlF at locus CD630_0206 -55% identity); and thirdly, because this system strongly resembles the thoroughly-studied PTS^{Mtl} in *C. acetobutylicum* DSM 792[95].

The putative sorbitol PTS (PTS^{Srl}) encoded at CD630_0762-8 was selected, instead of another potential PTS^{Srl} at loci 2414-8, because within the same operon as the IIA, IIB, and IIC components of the PTS, is encoded a sorbitol PDH, a gene likely to be imperative to the successful fermentation of sorbitol; and also due to its structural resemblance to the PTS^{Srl} studied in *C. beijerinkii*[122].

3.1 Culturing of *C. difficile* 630 in the presence of PTS Sugars

A growth test involving minimal medium (MM) and a sugar as a carbohydrate source was used to determine if *C. difficile* 630 could grow on the sugars glucose, fructose, mannitol, sorbitol, and sucrose. Glucose was tested, by reason of its importance in *C. difficile* due to it being the preferred carbon source above all other sugars[22]; fructose was tested, because like glucose it is one of the primary sugars[22] and because searches of the *C. difficile* 630 genome revealed five complete putative fructose PTS. Sucrose was tested because phylogenetic studies (Fig. 1.5) indicated that there may only be two potential sucrose PTS encoded within the genome at loci CD630_0388 and CD630_0469. It appeared unlikely that the organism would be able to readily grow with sucrose as the sole carbon source, and so, it was of interest to observe the level of growth on this sugar.

3.1.1 Culturing of 630Δ*erm*Δ*pyrE* on MM agar plates

Strong growth of the organism was observed on glucose, fructose, mannitol, and sorbitol (Fig. 3.1A-D), but not on sucrose, which was weaker (as the colonies look smaller) than the growth seen on the other sugars (Fig. 3.1E).

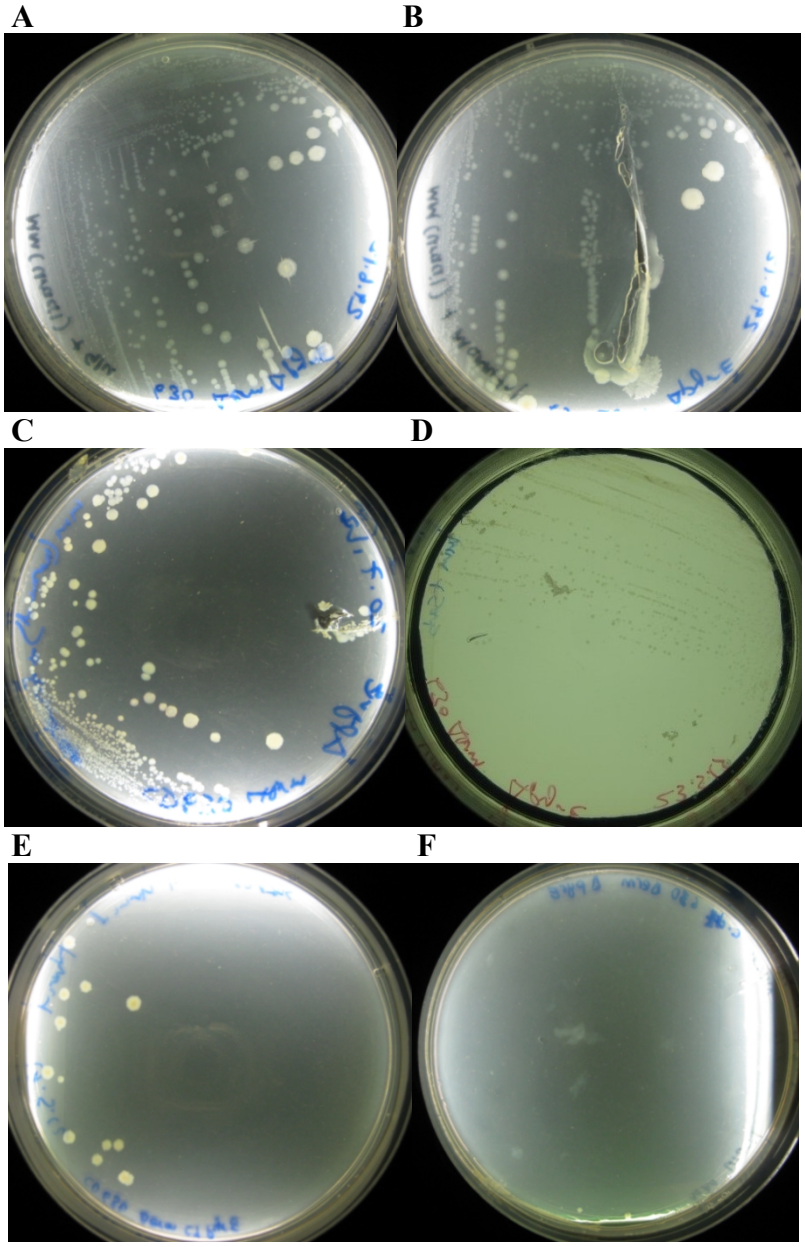

Figure 3.1: Phenotypic appearance of 630Δ*erm*Δ*pyrE* growing on MM +PTS sugar (A-E).
A. Glucose **B.** Mannitol **C.** Fructose **D.** Sorbitol **E.** Sucrose **F.** No sugar. The ability of *C. difficile* 630Δ*erm*Δ*pyrE* to utilise glucose, mannitol, fructose, sorbitol, and sucrose, was assessed. MM with no sugar is shown as a negative control. Plates (in triplicates) contained 1% sugar (w/v) and were incubated anaerobically for 48 h.
Good growth was observed on the plates containing sugar with the partial exception of sucrose, which had far fewer colonies.

It was decided to focus on the PTS involved in mannitol and sorbitol uptake as the organism had been shown to be able to subsist well on both of those sugars alone, the mechanisms of mannitol and sorbitol transport have not been studied in much

detail in *C. difficile*, and finally, because encoded within the *C. difficile* 630 genome are three identifiable operons possibly involved in the uptake of these sugars.

3.2 *In silico* analysis of PTS

In silico analysis of the PTS operons of interest helps in determining those which are the most worthwhile targets initially for ClosTron (CT) mutagenesis and deletion. It is possible to generate CT mutants quickly, enabling the chosen components of the target PT systems to be rapidly characterised. Making an 'educated guess' increases the chances of quickly determining which systems and their genes are the most likely to provide phenotypes, which can then be used to determine the genes of the greatest importance in the fermentation of mannitol and sorbitol, and toxin expression to the organism.

3.2.1 *In silico* analysis of CD630_2331-4

The putative *C. difficile* 630 PTS^{Mtl} at loci CD630_2331-4 (> 5 kb) is homologous (99% identity) to its respective putative PTS^{Mtl} counterparts in *C. difficile* 196, R20291, M120, 2007855, BI1, BI9, ATCC 9689/DSM 1296, BJ08, CF5, and M68 (which represent a variety of ribotypes), indicating a common evolutionary origin for this operon in the different *C. difficile* strains.

The well-studied PTS^{Mtl} in *C. acetobutylicum* DSM 792[95] (Fig. 3.2) organisationally bears a strong resemblance to the operon at loci CD630_2331-4 in *C. difficile* 630. Although not revealing a high level of homology (only > 30%) in terms of the nucleotides and their transcribed protein sequences, the model of the operon is very similar to the *C. acetobutylicum* DSM 792 PTS^{Mtl95}. The

putative *C. difficile* 630 PTS^{Mtl} at loci CD630_2331-4 consists of a fused IICB, a putative transcriptional regulator containing two PRDs, a soluble IIA, and a mannitol-1-phosphate dehydrogenase (MPDH) seemingly under the control of a single promoter[95] (Fig. 3.2).

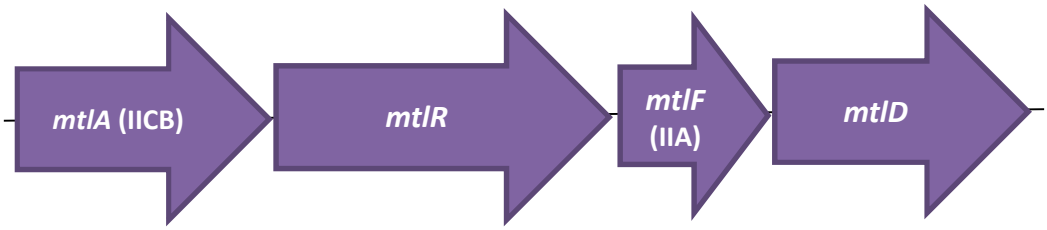

Figure 3.2: Constituent genes of PTS^{Mtl} in *C. acetobutylicum* DSM 792[95].
Like the putative *C. difficile* 630 PTS^{Mtl} at loci CD630_2331-4, the mannitol operon in *C. acetobutylicum* DSM 792 has a single promoter with four identifiable *orfs*, and a fused IICB, unlike the PTS^{Mtl} in other organisms which have a separate promoter for *mtlR* (*B. subtilis*)[123], and a fused IICBA (*E. coli* and *B. subtilis*)[95,123].

MtlD, a putative MPDH, is a 383AA protein encoded by a 1.14 kb gene (Artemis), bearing 92-99% identity in all of the hitherto sequenced strains of *C. difficile* (NCBI). Searches of the *C. difficile* 630 genome have revealed MtlD as apparently the only potential MPDH making this a strong candidate to target in order to inhibit growth in mannitol and to observe the potential effects on cytotoxicity.

MtlF, a 140AA protein hypothesised as a IIA domain and encoded by a 0.42 kb gene at locus CD630_2332 is annotated as being a fructose/mannitol-specific IIA (Artemis). The AA sequence of a putative 'fructose/mannitol'-specific IIA at locus CD630_0206 has a significant amount of similarity (29% identity) to MtlF, indicating that CD_0206 has a potential role in mannitol uptake, possibly phosphorylating the IIB domain that is responsible for phosphorylating incoming mannitol. This homologue could potentially also play a role in mannitol uptake,

possibly phosphorylating a mannitol-specific IIB, as this is the main role of an IIA[102], or perhaps as an auxiliary or back-up mannitol IIA outside of the main PTS^{Mtl}. As a result of this information, *mtlF* was an interesting target for CT mutagenesis in order to determine if turning off what appears to be the primary protein responsible for phosphorylation of IIB PTS^{Mtl} prevented utilisation of mannitol, or if the *mtlF* mutant would continue to exhibit growth in mannitol.

MtlR, the apparent regulator of the system, is annotated as a putative antiterminator. Transcriptional antiterminators have been shown to interact with the HPr domain and the EII domains of the PTS that they are part of, which results in an alternative form of catabolic repression to that seen with CcpA[123,124]. LevR of the LicT system in *B. subtilis* was the first antiterminator studied in-depth[125] and provided the general description by which this class of regulators work[95]. This study reported that in the absence of glucose and the sugar which is specific for the operon on which the relevant antiterminator resides, PTS proteins of the system are present in the phosphorylated state. Under such conditions, the PTS-regulatory domains (PRDs) are phosphorylated, and, therefore, inactive. When an inducer (such as the sugar for which the system is specific) is present, the IIC transfers its phosphate to the inducer, and the PRD becomes dephosphorylated. The regulator is now active in the control of transcription of the operon (Fig. 3.3)[125].

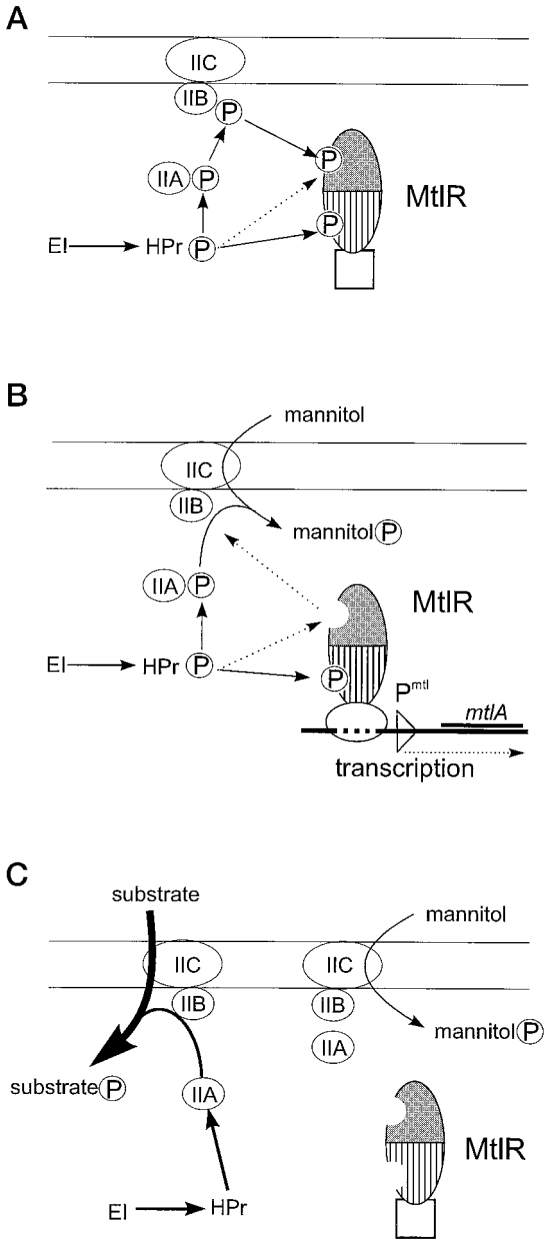

Figure 3.3: Model for the regulation of MtlR[126].
Variations of the model propose that phosphorylation of MtlR generally occur on two domains of the protein, with phosphorylation by HPr (striped region) resulting in MtlR having greater affinity for the promoter; while with phosphorylation by IICB a different domain (grey region) prevents binding to the promoter. **A.** MtlR phosphorylation may occur via IICB or via HPr. **B.** IICB is dephosphorylated by transfer of the phosphoryl group to mannitol. **C.** Mannitol increases, P-HPr decreases. MtlR is dephosphorylated and the operon is no longer activated[126].

Phosphorylation of MtlR usually occurs at the PRDs (Fig. 3.3). It has generally been observed that phosphorylation occurs via the IIBC domain of the PTS[95,125]. However, studies have demonstrated that phosphorylation of MtlR may occur by

HPr[95,123,126]. MtlR becomes activated as PRD-I becomes dephosphorylated when an inducer, such as mannitol, is present[95]. Provided that there is no preferred glucose in the bacterial surroundings, PRD-I is dephosphorylated and MtlR is then activated. HPr phosophorylation of PRD-II is also a requirement for activation[123].

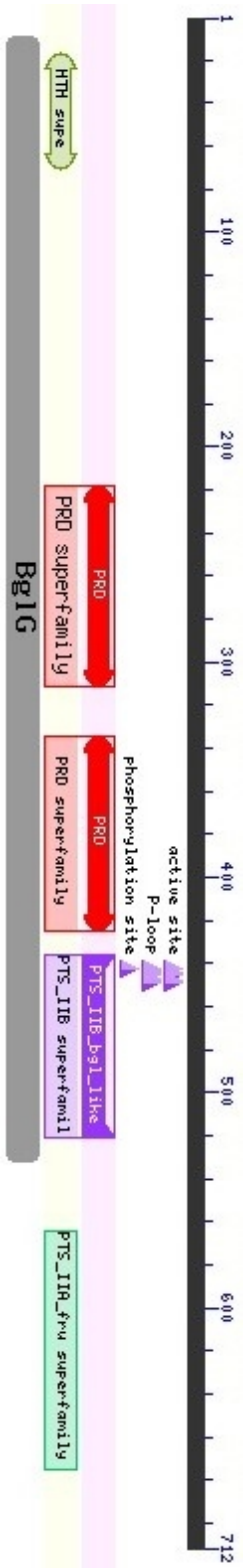

Figure 3.4: MtlR protein organisation. Figure of MtlR showing the two-centrally located PRDs and the IIB_bglG_like and IIA_fru-like domains towards the C-terminus (NCBI).

Putative *C. difficile* 630 MtlR encoded at locus CD630_2333 with two potential PRDs (the sites of phosphorylation), indicative of a transcriptional antiterminator. There appears to be no other gene in the *C. difficile* 630 encoding a PTS^{Mtl} transcriptional antiterminator.

The organisation of *C. difficile* 630 MtlR (Fig. 3.4) contains PRDs located in the centre of the protein (NCBI), which are the sites of phosphorylation[126], and IIB-like and IIA-like domains. In keeping with the typical organisation of transcriptional regulators like antiterminators, the central locus of *C. difficile* 630 MtlR consists, from the 218AA interval to the 425AA interval, of two PRDs belonging to the PRD family that are found in the antiterminators of the *E. coli* BglG superfamily family[95]; and like the MtlR studied in *C. acetobuylicum* DSM 792, towards the C-terminus, there is an IIB-like domain, and also, there is a signature motif resembling members of the fructose-mannitol IIA[95] (Fig. 3.4). PRDs are large conserved domains with low variation across many different bacterial species with a particular indicator being the presence of the conserved histidine residues (which is where phosphorylation of the regulator actually occurs) found in the PRDs[95]. For example, BLAST comparisons of MtlR found homologues in *C. perfringens* WAL-14572, *C. difficile* 630, *C. difficile* R20291, *C. difficile* 196, and *C. acetobuylicum* ATCC 824 illustrating the conserved nature of the MtlR PRDs.Many conserved histidine residues were present (four were common in all of the strains, five in all except *C. acetobuylicum* ATCC 824) found in the vicinity of the MtlR PRDs in each strain of these different Clostridia (Fig 3.5).

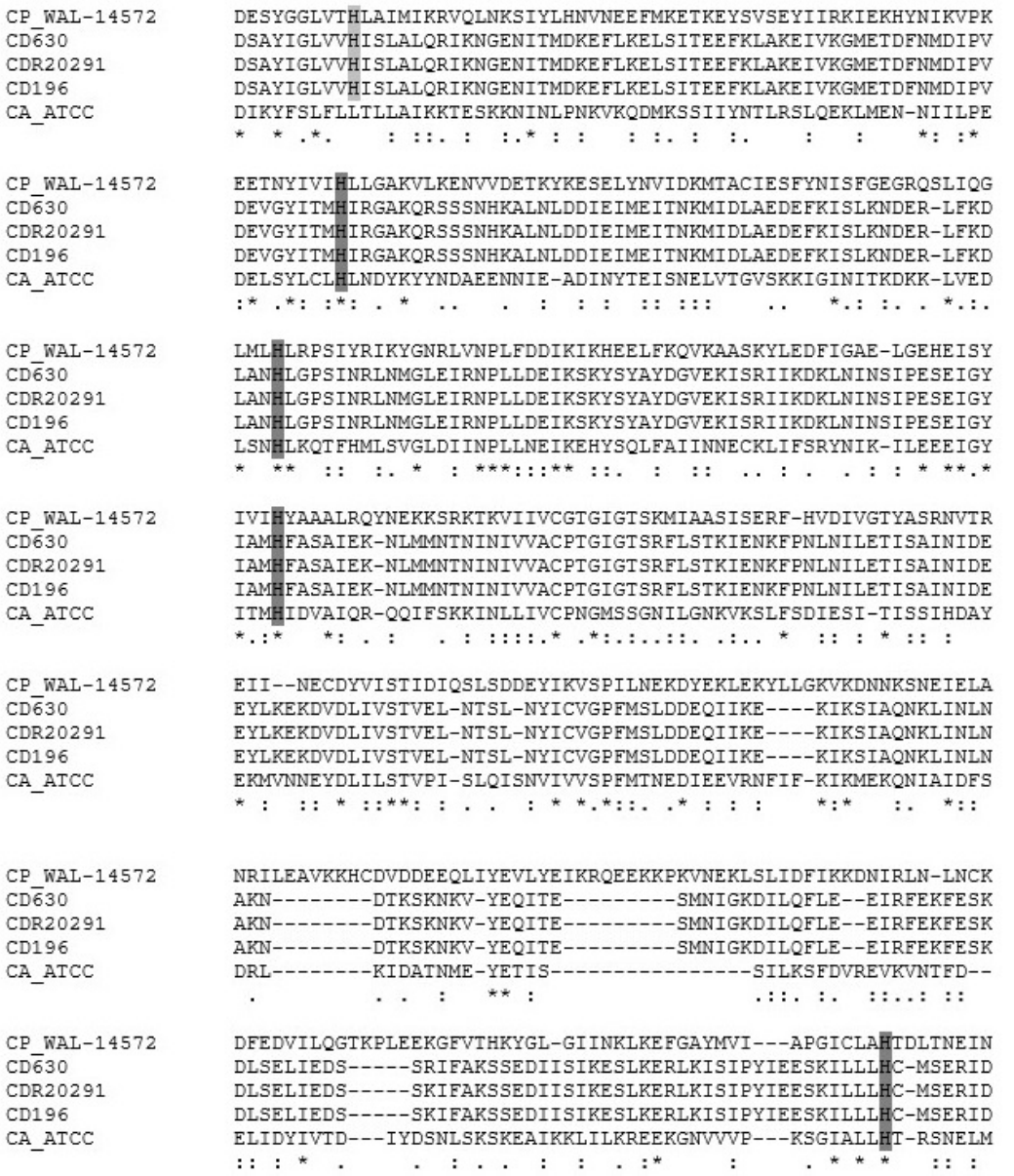

Figure 3.5: Alignment of MtlR in pathogenic and non-pathogenic Clostridia illustrating the conserved nature of the MtlR PRDs.

Alignment of MtlR in *C. perfringens* WAL-14572, *C. difficile* 630, *C. difficile* R20291, *C. difficile* 196, and *C. acetobuylicum* ATCC 824. Figure shows 420AA out of a total 711AA (AA position 198 to AA position 618) found in MtlR. Alignment showed the conserved MtlR histidine residues (highlighted in dark grey from AA position 267 to AA position 610) common to each of the strains, and that, with the exception of AA position 610, are typically found at the centrally located PRDs, thus illustrating the conserved nature of the PRDs across different Clostridia. Highlighted in light grey at AA position 208 is another histidine residue common to each except *C. acetobuylicum* ATCC 824, but which is not within one of the two PRDs of the MtlR protein, like those found from AA position 266 to AA position 381 (Clustal MUSCLE).

All of this would indicate that *mtlR* at locus CD630_2333 in *C. difficile* 630 encodes for a DNA-binding protein, the activity of which may be regulated by the phosphorylation of the PTS^{Mtl} [125,126]. *C. difficile* 630 MtlR shares 99% identity with MtlR in most other *C. difficile* strains (excepting, for example, CD160 -94% identity). Protein BLAST comparison of MtlR with SrlR (661AA) at locus CD630_0762, the putative regulator of the sorbitol PTS at loci CD630_0762-8, revealed a degree of homology (26% identity); while a further BLAST comparison of MtlR with a transcriptional regulator at locus CD630_2416 (657AA), which is part of a second putative sorbitol PTS at loci CD630_2414-8, also revealed a level of homology (25% identity). SrlR and CD_2416 have a higher amount of homology to each other (37% identity). Another MtlR homologue (31%) was found at locus CD630_0040 which is annotated as a 'fructose/mannitol-specific IIA', having homology (25%) to SrlR and CD_2416 (29%).

These proteins are similar in organisation to MtlR, and to each other, in that they possess, similar to MtlR, IIB-like (except CD_0040, which has a IIA there instead) and IIA-like domains towards the C-terminus of the protein. But, unlike MtlR they contain only a single PRD, which is also centrally located (Fig. 3.6).

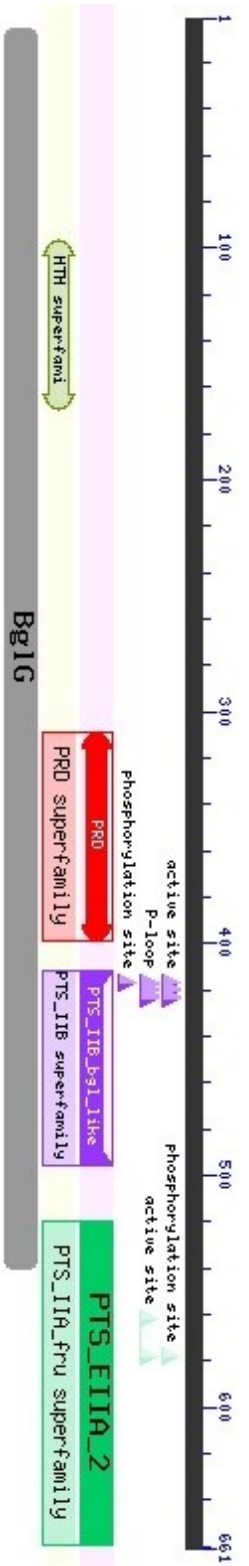

Figure 3.6: Homologue (25%) of *C. difficile* 630 MtlR at locus CD630_2416. In contrast to MtlR, CD_2416 possesses only a single PRD, indicating that it may not be a true mannitol transcriptional regulator[125] and is unlikely to be involved in PTS^{Mtl} regulation.

With MtlR, judging from the large 711AA protein size, the presence of two centrally-located conserved PRDs, and the IIB-like and IIA-like domains toward the C-terminus, as well as the annotation, it appears extremely likely that *mtlR* encodes a transcriptional antiterminator which induces PTS^{Mtl} (such as that at loci CD630_2331-4) when mannitol is present in the bacterial environment. As mentioned above, usually a key feature of the MtlR protein of a PTS involved in mannitol utilisation in Gram-positives is the presence of two PRDs in the central region of the protein, which are the probable sites of phosphorylation[126]. This would make it seem unlikely that the genes encoding SrlR, CD_2416, and CD630_0040 are playing a regulatory role when *C. difficile* 630 detects the presence of mannitol in its vicinity as they each possess only one PRD each. It is possible that SrlR, CD_2416, and CD630_0040 are non-functional regulators. Other than SrlR, CD_2416, and CD630_0040, there appear to be no further homologues of *mtlR* in the rest of the *C. difficile* 630 genome, so it seems that no other gene is playing the role of PTS^{Mtl} transcriptional antiterminator. Targeting *mtlR* for CT mutagenesis would, therefore, potentially experimentally confirm an important role for this gene in mannitol uptake.

MtlA, the 474AA protein encoded by a 1.425 kb gene at locus CD630_2334, consists of a large transmembrane IIC and a smaller IIB fused protein (Fig. 6.2). Near total homology (97-99% identity) was seen with all other sequenced strains of *C. difficile* (NCBI). There appear to be no other genes annotated within the *C. difficile* 630 genome as mannitol-specific IIBs or IICs. BLAST comparison was performed of *mtlA* with the most likely genes to be homologous to *mtlA*, namely the IIBs and IICs of the putative PTS at loci CD630_0041-3 (which contained an IIB annotated as 'fructose/mannitol-specific'), the PTS at loci CD630_0205-8

(which contained a IIA homologue of *mtlF*-see above), and the putative IIABC fructose PTS at loci CD630_3075 and CD630_3134. No homology was found between *mtlA* and any of these genes suggesting that MtlA is the primary route of mannitol uptake. This does not completely exclude a role for compatible IIB and IICs encoded within the rest of the genome (most likely fructose-specific systems), but targeting *mtlA* seemed the best single chance of preventing, or inhibiting, mannitol transport and phosphorylation by the organism. It was decided that targeting *mtlA* would potentially prevent growth in mannitol, as well as result in possible changes in the cytotoxic (and perhaps, motility) behaviour of *C. difficile* 630 when grown in mannitol, as the presence of the sugar is known to suppress toxin production[28].

3.2.2 *In silico* analysis of CD630_0762-8

Bioinformatics analysis was used to help decide which of the two potential sorbitol PTS encoded in the *C. difficile* 630 genome was the best one to target. BLAST queries of the putative *C. difficile* 630 PTS^{Srl} at loci CD630_0762-8 (Fig. 5.2) (> 5 kb) revealed near total (99%) homology with a respective operon in *C. difficile* ATCC 9689/DSM, BI9, BI1, 200785, R20291, CD196, and also M120 (96% homology). Encoded at loci CD630_2414-8, there is another operon which is annotated as a complete sorbitol-specific PTS consisting of a IIA, an operon activator, a regulator, a IIB, and a IIC (Fig. 3.7). No significant similarity was found between the nucleotide sequences when comparing this entire operon (> 5kb) with the entire operon (> 5kb) at loci CD630_0762-8. Nonetheless, as will be discussed in more detail below, individual parts of this operon such as the hypothesised sorbitol IIB (also named *srlE*) at locus CD630_2417 bears substantial genetic similarity to *srlE* at loci CD630_0765-6; and also, *srlR*, at

locus CD630_0762 has a large amount of homology with the supposed sorbitol regulator at locus CD630_2416.



Figure 3.7: Second putative PTS^{Srl} encoded in *C. difficile* 630 at loci CD630_2414-8 (Artemis).
Overall, the operon has no significant homology with the operon at loci CD630_0762-8 (Fig. 5.2). However, individual components have homology – *CD_2416* (with *srlR*, 55% identity), *srlA* (with *gutA*, 44% identity), and *srlE/CD_2417* (with *srlE/CD_0765-6*, 55% identity).

SrlR, a putative sorbitol regulator at locus CD630_0762 consisting of a 661AA protein (Fig. 3.8), is homologous (55% identity) to CD630_2416, a 657AA protein (Fig. 3.7). This protein and CD_2416 somewhat resemble MtlR (Fig. 3.4). Judging from the presence of a centrally-located PRD, a IIB-like domain, and a IIA-like near the C-terminus (Fig. 3.8), it can be speculated that these proteins are potential transcriptional antiterminators, like MtlR. However, unlike MtlR, these proteins contain only a single PRD domain, and this may exclude them from being considered true mannitol transcriptional regulators (antiterminators) as it has been postulated that regulators of this class usually possess two PRDs (the functions of single PRD proteins are, so far, not known)[125]. The single PRDs that are found in both of these proteins are also found in homologues in all the available sequenced strains of *C. difficile*, including those strains in which the respective gene/protein homologue is showing the lowest degree of homology to SrlR and CD_2416. For example, the *C. difficile* CD160 homologue having 93% identity with CD630_2416 also contains only a single PRD (NCBI).

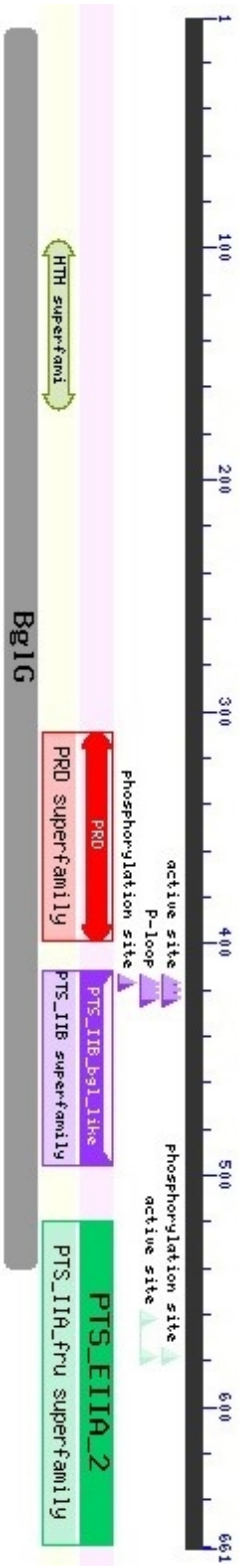

Figure 3.8: SrlR protein showing a single PRD (NCBI).

In contrast to MtlR, and, to what is generally considered the clear characteristics of a mannitol PTS transcriptional regulator (antiterminator), SrlR and CD_2416 possess only a single centrally-located PRD.

The gene name *gutM* is used to annotate potential operon activators at both the operon at loci CD630_0762-8 (CD_0763 –giving a 144AA protein product) (Fig. 5.2) and the one at loci CD630_2414-8 (CD_2415 –giving a 119AA protein) (Fig. 3.7). No homology was found between *gutM* and the gene at locus CD630_2415 (encoding a putative operon activator).

gutA, encoding a 186AA EII-Gut/Srl superfamily protein presumed to be a sorbitol IIC at locus CD630_0764 (Fig. 5.2), has homology (44% identity) with a gene named *srlA*, a putative sorbitol IIC at locus CD630_2414 (NCBI), and therefore, it is possible for one or both of the proteins to have a role in sorbitol uptake, potentially as transmembrane transporters facilitating the motility of sorbitol across the *C. difficile* 630 cell membrane.

Annotated within the *C. difficile* 630 genome, there are genes encoded as two entirely separate proteins (which are separated from each other in the genome by more than 1500 other genes) speculated as being IIBs responsible for the phosphorylation of incoming sorbitol. Both are named SrlE. The first at loci CD630_0765-6 (310AA total protein product) is part of the operon at loci CD630_0762-8 (Chap. 4, Fig. 4.2), while the second at locus CD630_2417 (337AA protein) forms part of the operon at CD630_2414-8 (Fig. 3.7). Both are structurally identical, with EII N and C termini belonging to the Gut-superfamily of EIIs encoded in each protein. Protein BLAST comparison of the sequences revealed a significant degree of homology (55% identity). Targeting *srlE* (*CD_0765-6*) for CT inactivation seemed a better choice since it would appear that there is a greater chance of obtaining a growth phenotype with this IIB than *srlE* at locus CD630_2417 due to *srlE* (*CD_0765-6*) seemingly operating from the

same promoter as the apparent sorbitol-6-phosphate dehydrogenase (SPDH), *gutD*, at locus CD630_0768.

srlB, the gene encoding the putative IIA of the sorbitol PTS at locus CD630_0767 (Fig. 5.2), encodes a 121AA protein (which is described as belonging to IIA-Gut/Srl superfamily), and shares high similarity (97-99% identity) with its homologues in other *C. difficile* strains such as CD22, T23, CD160 (and also a 100% identity with a homologue in CD132). No homology was found with the hypothesised sorbitol IIA, also termed *srlB*, at locus CD630_2414 (Fig. 3.7), which is described as belonging to the same superfamily of IIA as *srlB* at locus CD630_0767 (NCBI).

GutD, the putative SPDH, presumably responsible for catalysing the conversion of phosphorylated sorbitol to F-6-P, consists of a 257AA protein (Fig. 5.2). Seemingly, *gutD* is the only gene encoded within the *C. difficile* 630 genome involved in converting Srl-6-P to F-6-P. Hence, targeting *gutD* for deletion appeared worthwhile; firstly, because it seemed possible that removing this gene would prevent Srl-6-P conversion to F-6-P, preventing *C. difficile* growth in sorbitol; and secondly, complete removal of the gene (instead of CT inactivation) would eliminate any possibility of continued growth of the *gutD* mutant in sorbitol, as a truncated *mtlD* (a MPDH) in *Klebsiella pneumoniae* KAY2026 still exhibited dehydrogenase activity in mannitol despite the inactivation of two-thirds of the gene (the non-truncated N-terminal was shown to primarily be the catalytic domain)[127].

Following the above use of the bioinformatics analysis of the putative mannitol and sorbitol operons as a guide to determine the most suitable genes to focus on,

it was decided to target all of the genes of the potential PTS^{Mtl} at loci CD630_2331-4; and the IIA, IIB, IIC, and SPDH of the putative PTS^{Srl} at loci CD630_0765-8 (Table 3.1), and subject the resulting mutants to growth, cytotoxicity, and motility tests in order to help confirm or determine the roles of the genes, and consequently, the operons of which they form part, in mannitol and sorbitol fermentation, toxin regulation, and motility (Table 3.1).

Deletion of the genes identified as potentially involved in the conversion of phosphorylated mannitol (*mtlD* at locus CD630_2331) and sorbitol (*gutD* at locus CD630_0768), and also the putative $IICB^{Mtl}$ (*mtlA* at locus CD630_2334), was undertaken via allelic-coupled exchange (ACE). CT mutants were created targeting the putative IIA (*mtlF*) and regulator (*mtlR*) of the mannitol PTS at loci CD630_2332-3; and the IIC, IIB, and IIA of the sorbitol system at loci CD630_0765-7. The growth, sugar uptake ability, cytotoxicity, and motility of each mutant was then tested (see Chapter 4, Results Chapter II and Chapter 5, Results Chapter III).

4.0 Results Chapter II –Mannitol PTS (CD630_2331-4)

4.1 Mannitol Operon

Mannitol constitutes one of the primary carbon sources for *C. difficile*[22] and has been demonstrated as exerting an influence on the cytotoxicity of the organism[28]. An understanding of the exact mechanisms by which the bacterium utilises mannitol will increase understanding of the growth and cytotoxicity of *C. difficile* in relation to the sugar. This involves targeting the bacterial systems and their constituent genes, in this case the putative PTS^{Mtl} at loci CD630_2331-4, most likely involved in *C. difficile* growth and cytotoxicity when the organism is in the presence of mannitol.

Mannitol ($C_6H_{14}O_6$) is a six-carbon, non-cyclic polyol (Fig. 4.1) which is produced by plants, protozoa, fungi, and bacteria as a storage compound for carbon. It is the most abundant sugar alcohol found in the natural environment[128], and is used as an additive in various foodstuffs, being extracted in large amounts from seaweed[129].

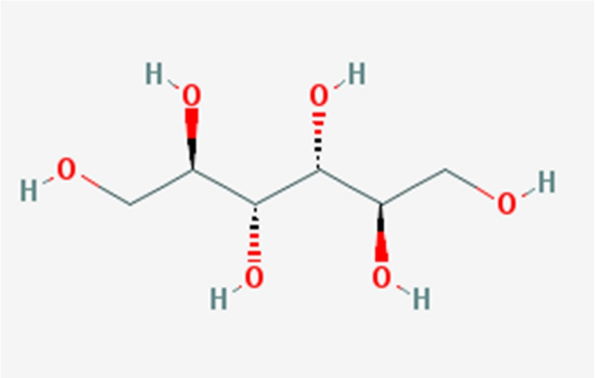

Figure 4.1: Structural diagram illustrating the six-carbon chain mannitol (PubChem).
Mannitol is utilised as a primary source of carbon by *C. difficile* and its presence will suppress toxin production when the sugar is available to the bacterium[28].

The mannitol-specific PTS forms part of the 'fructose-mannitol' family of PTS[95,101]. Within the *C. difficile* 630 genome, there are up to six different IIA

domain proteins annotated as being 'fructose/mannitol specific' (Artemis). Located at CD630_2331-4, there is a putative mannitol PTS. Within this putative PTS^{Mtl}, four open reading frames (*orfs*) are identified, coding for a fused IICB domain (*mtlA* -for transmembrane transport and phosphorylation), a regulator (*mtlR* –transcriptional antiterminator), an IIA domain (*mtlF* – phosphorylation of IIB), and a mannitol-1-phosphate dehydrogenase (MPDH) (*mtlD* –responsible for the conversion of phosphorylated mannitol (M-1-P) to F-6-P) (Fig. 4.2).

The putative *C. difficile* 630 PTS^{Mtl} resembles the PTS^{Mtl} in *C. acetobutylicum* DSM 792[95]. Research into *C. acetobutylicum* DSM 792 has revealed that the *mtlARFD* genes constitute a polycistronic operon which is induced by mannitol and repressed by glucose[95].

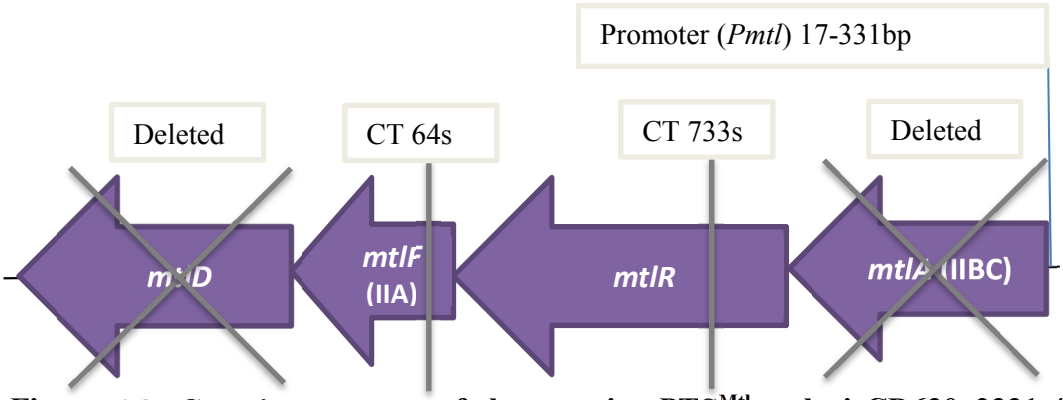

Figure 4.2: Constituent genes of the putative PTS^{Mtl} at loci CD630_2331-4 showing genes targeted for CT mutagenesis, indicated by the chosen insertion site, and deletion, marked by a cross (Artemis).
The putative PTS^{Mtl} encodes a complete PTS with a fused IICB, a regulator, an IIA, and an MPDH, apparently under the control of a single promoter.

4.1.1 MtlA –IIBC domain

As a putative PTS^{Mtl} IICB domain protein, MtlA is speculated as being responsible for facilitating the passage of mannitol across the cell membrane and also phosphorylating the incoming sugar as it enters the cell so that it may be

taken up and then converted to F-6-P. MtlA, which is encoded by a 1.425kb gene, strongly resembles in appearance the $IICB^{Mtl}$ that is part of PTS^{Mtl} in *C. acetobutylicum* DSM 792[95]. Within *C. acetobutylicum* DSM 792, transcription of *mtlARFD* is initiated directly upstream of *mtlA*[95]. The presence of a TATAATT sequence 17bp upstream and a TAATATTA sequence (which indicated the presence of a promoter) 331bp upstream of *mtlA* in *C. difficile* 630 would indicate that this is the transcriptional start site for this operon.

4.1.2 MtlR –transcriptional regulator

The sequence of CD630_*mtlR*, consisting of a 2.13kb size gene, resembles transcriptional regulators such as antiterminators and repressors. This gene is one of the conserved components of the mannitol operon across many bacterial species including *C. acetobutylicum* and *E.coli*[95].

Phosphorylation of MtlR by HPr has been shown to increase the affinity of MtlR for its binding site, but phosphorylation by $IICB^{Mtl}$ results in reduction of this affinity. Regulation of MtlR by two components of the PTS is considered an example of a complex control system detecting both the presence of mannitol and the need to utilise this substrate[126]. The central part of MtlR consists of two PTS regulatory domains (PRDs). PRDs are considered to be targets of PTS-mediated phosphorylation, which serve to moderate transcriptional regulation[95]. The most probable targets for phosphorylation are these phosphorylation domains, PRD-1 and PRD-2, which are conserved in antiterminators[126].

4.1.3 MtlF – IIA domain

mtlF encodes a putative IIA domain protein that would assumedly receive a phosphate from the HPr present in the organism, and MtlF would then pass the phosphate molecule to the IIB^{Mtl} (MtlA) (Fig. 1.4)[95].

4.1.4 MtlD – Phosphate Dehydrogenase

Searches of the *C. difficile* 630 genome have revealed only one phosphate dehydrogenase responsible for converting the phosphorylated mannitol, M-1-P, to F-6-P, indicating that this protein is possibly processing all of the M-1-P coming through all the six annotated PT systems potentially compatible with mannitol phosphorylation.

4.2 Growth, sugar uptake, cytotoxicity, and motility of wild-type (WT) and control strains

The control strain, 630Δ*erm*, to which each mutant was to be compared, was compared to 630 wild-type (WT) to confirm that there were no phenotypic differences in growth, toxicity, sugar uptake, or motility resulting from the deletion of *C. difficile* 630 *erm*[117], which could be mistakenly attributed to those PTS genes which were being targeted for inactivation or deletion. 630Δ*erm*Δ*pyrE* was used as the parental strain so that in the event of achieving a growth or toxin phenotype the mutant would be easily complemented by restoring the inactivated/deleted gene alongside a restored *pyrE*.

4.2.1 Growth of 630WT vs. 630Δ*erm* on defined medium (DM) agar

630WT and 630Δ*erm* were grown on DM and DM +mannitol (DMM) agar to see if any differences in growth could be observed.Both strains showed strong growth with and without (not shown here) mannitol (Fig. 4.3).

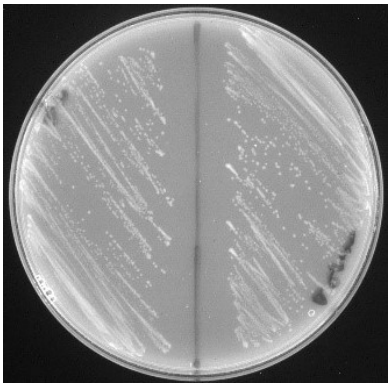

Figure 4.3: Representative image showing growth of WT (left) and control strain (right) on DMM agar.
Strains (in triplicates) were streaked on plates of DM agar containing 0.6% w/v mannitol, and incubated at 37°C for 16 h to see if it was possible to observe a growth phenotype. Strong growth was observed with 630WT and 630Δ*erm* (control strain).
Differences in the ability to metabolise mannitol could not be determined with this assay.

4.2.2 Growth of 630WT vs. 630Δ*erm* in DM, DMM, and DMG broth

No phenotypic differences in growth (Fig. 4.4) were observed between 630WT and 630Δ*erm*, the control strain to which all the mutants made from targeting the PTS^{Mtl} at CD630_2331-4 have been compared. Growth patterns and trends of 630WT and 630Δ*erm* remain the same with significantly increased growth exhibited by both strains between 6-12 h in the presence of mannitol and glucose when compared to growth with no sugar (e.g. 630WT/630Δ*erm* in DM vs. 630WT/630Δ*erm* in DMM/DMG at 8 h **** $P < 0.0001$). For example, at 8 h (which was peak OD_{600} for both strains in DMM and DMG), 630WT in DMM reached an OD_{600} of 0.824, while 630Δ*erm* in the same conditions was 0.803. Slope 0-8 h in DMM: 630WT = 2.06, 630Δ*erm* = 2.0. Slope 0-8 h in DMG: 630WT = 2.21, 630Δ*erm* = 2.16 (Fig. 4.4).

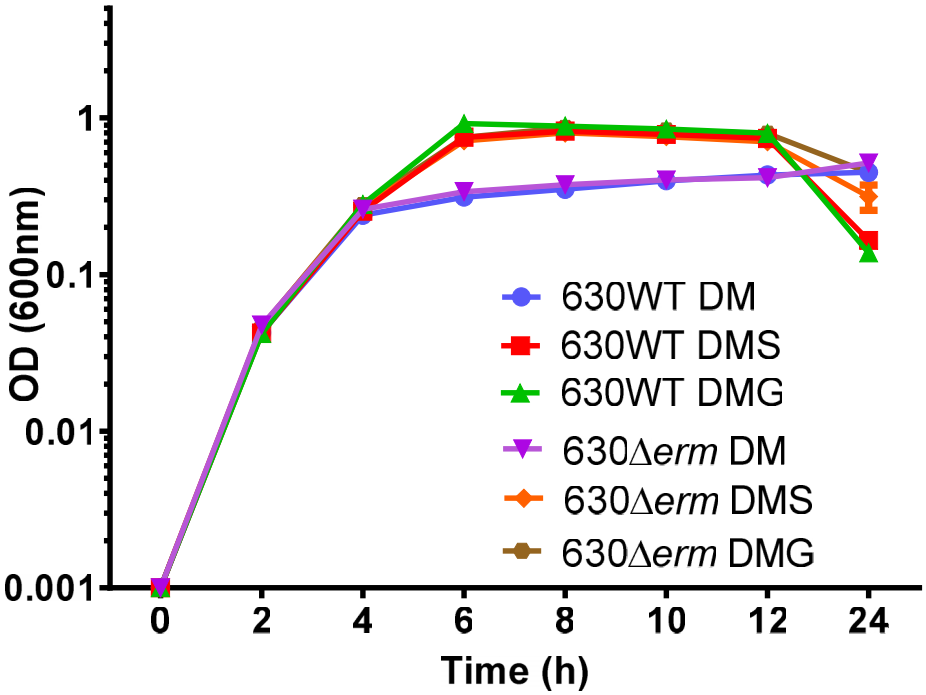

Figure 4.4: Growth of 630WT vs. 630Δ*erm* in DM with or without mannitol or glucose.
630WT and 630Δ*erm* (control strain) were incubated in DM for 24 h at 37°C.1mL extracts (triplicates) were taken at regular time points and the OD_{600} measured.
No differences in growth patterns were seen between the WT and the control strain, with both strains exhibiting a significant increase in growth in mannitol or the presence of glucose, and hence, no phenotypic differences were observed.
Slope 0-8 h (peak growth) in DMM 630WT = 2.06, 630Δ*erm* = 2.0. Slope 0-8 h (peak growth) in DMG 630WT = 2.21, 630Δ*erm* = 2.16.
One-way ANOVA was used to determine statistical significance.
630WT/630Δ*erm* in DM vs. 630WT/630Δ*erm* in DMM/DMG at 8 h **** $P < 0.0001$.

4.2.3 HPLC evaluation of mannitol/glucose consumption in DM

630WT and 630Δ*erm* levels of mannitol uptake up to 24 h were measured via HPLC. Mannitol levels in the 630WT samples fell from 11.84mM at 0 h to 1.65mM at 6 h (**** $P < 0.0001$), to 0.18mM at 8 h (**** $P < 0.0001$), until by 10 h, there was no remaining mannitol. Slope of curve 0-8 h = 3.94 (Fig. 4.5).

At the same time, 630Δ*erm* mannitol levels fell from 10.6mM to 2.5mM by 6 h of incubation (**** P < 0.0001), to 0.19mM at 8 h (**** P < 0.0001), with no mannitol left by 10 h. Slope of curve 0-8 h = 3.55 (Fig. 4.5).

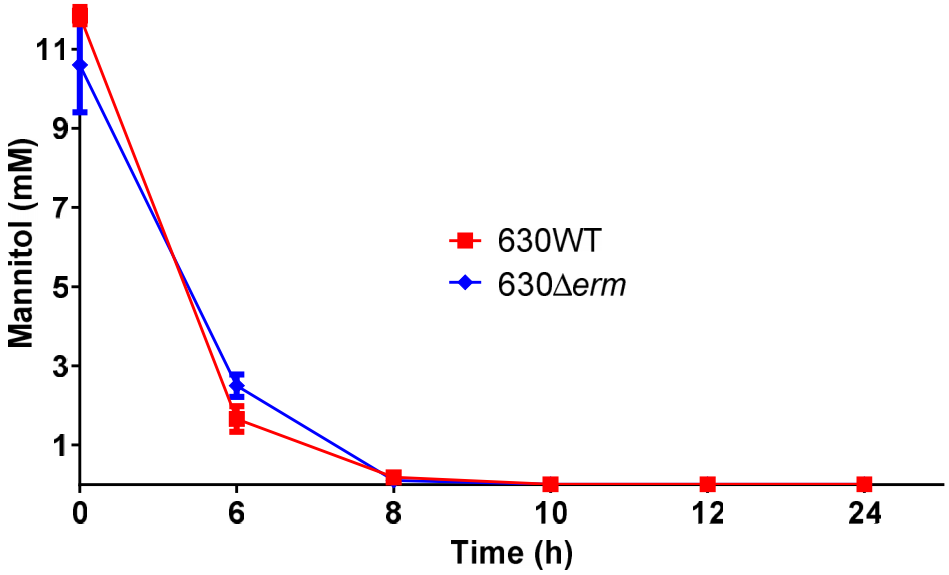

Figure 4.5: HPLC evaluation of mannitol uptake in DM by 630WT and 630Δ*erm* (control strain).
Extracts (triplicates) from the growth assay were used to determine by HPLC the exact amount of sugar remaining in the medium at each time point.
The trends of mannitol uptake by 630WT and 630Δ*erm* were similar from 0-24 h incubation with only residual amounts of mannitol left in both sets of samples by 8 h, and with no mannitol remaining in both sets by 10 h.
630WT slope of curve 0-8 h = 3.94.
630Δ*erm* slope of curve 0-8 h = 3.55.
One-way ANOVA was used to determine statistical significance.
630WT/630Δ*erm* 0 h vs. 6 h **** P < 0.0001.

Glucose levels in all strains were steadily depleted, as was expected, from 0 h until 24 h (**** P < 0.0001). No differences emerged between the strains, indicating that deleting *ermB* produced no overall effect on glucose metabolism (Fig. 4.6).

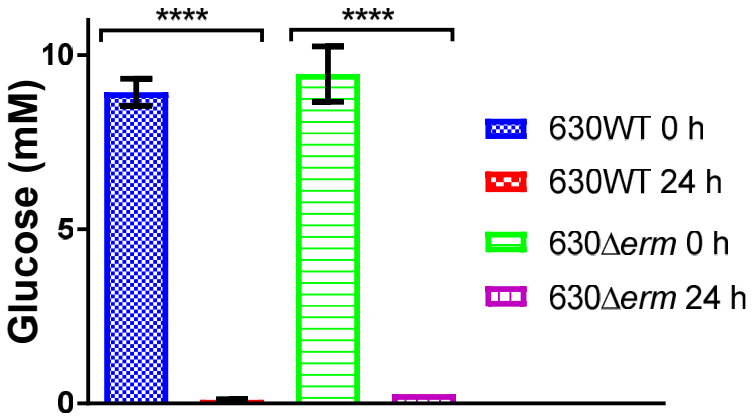

Figure 4.6: HPLC evaluation of glucose uptake in DM by 630WT and 630Δ*erm* (control strain).
Extracts (triplicates) from the growth assay in DM were used to determine by HPLC the exact amount of sugar remaining in the medium at the start and end of the assay.
Glucose utilisation by both strains was similar with a depletion of glucose (**** $P < 0.0001$).
One-way ANOVA was used to determine statistical significance.

4.2.4 Growth of 630WT vs. 630Δ*erm* in TY, TYM, and TYG

No phenotypic differences in growth (Fig. 4.7) were observed between 630WT and 630Δ*erm*, the control strain to which all mutants in this study have been measured alongside. Overall growth of 630Δ*erm* in mannitol and glucose was very similar in comparison to 630WT. Growth patterns and trends remain the same with significantly increased growth exhibited by both strains in the presence of mannitol and glucose, compared to when grown without sugar. For example, at 12 h, which was peak growth, 630WT TY vs. 630WT TYM *** $P < 0.0002$; 630WT TY vs. 630WT TYG **** $P < 0.0001$; 630Δ*erm* TY vs. 630Δ*erm* TYM *** $P < 0.00013$; 630Δ*erm* TY vs. 630Δ*erm* TYG **** $P < 0.0001$ (Fig. 4.7).

630WT slope 0-12 h in TYM = 2.7, in TYG = 2.89. 630Δ*erm* slope 0-12 h in TYM = 2.78, in TYG = 3.02 (Fig. 4.7).

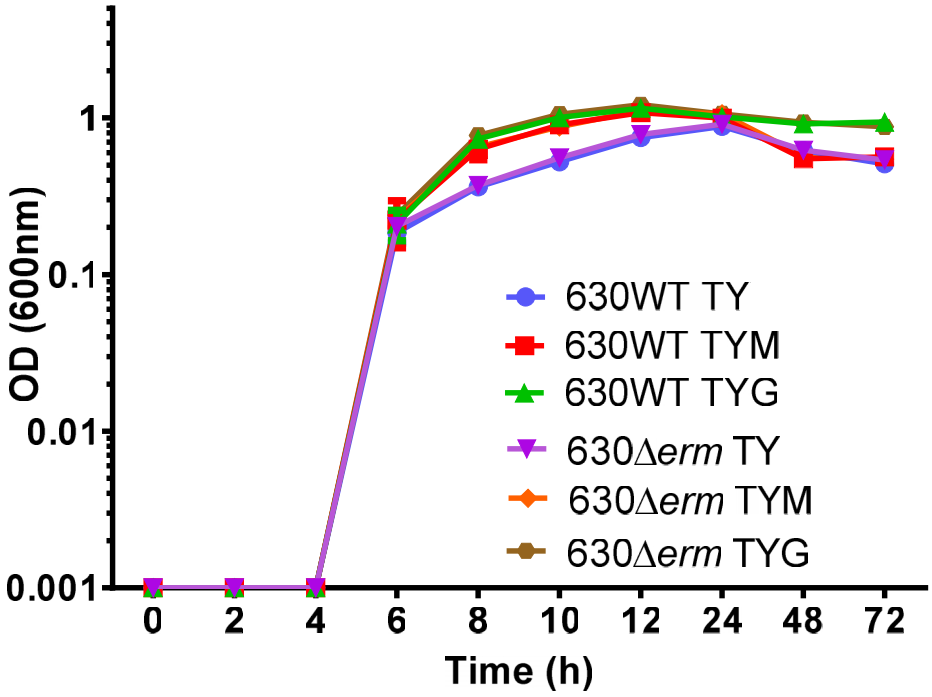

Figure 4.7: Growth of 630WT vs. 630Δ*erm* in TY with or without mannitol or glucose.
630WT and 630Δ*erm* (control strain) were incubated in TY with and without mannitol/glucose for 72 h at 37°C. 1mL extracts (triplicates) were taken at regular time points and the OD_{600} measured.
No differences in growth patterns were seen between the WT and the control strain, with both strains exhibiting a significant increase in growth in mannitol and glucose, and hence, no phenotypic differences were observed.
630WT slope 0-12 h in TYM = 2.7, in TYG = 2.89. 630Δ*erm* slope 0-12 h in TYM = 2.78, in TYG = 3.02.
One-way ANOVA was used to determine statistical significance.
630WT TY vs. 630WT TYM *** $P < 0.0002$.
630WT TY vs. 630WT TYG **** $P < 0.0001$.
630Δ*erm* TY vs. 630Δ*erm* TYM *** $P < 0.00013$.
630Δ*erm* TY vs. 630Δ*erm* TYG **** $P < 0.0001$.

4.2.5 Cytotoxicity of 630WT and 630Δ*erm*

No differences in cytotoxicity patterns and trends emerged between the 630WT and 630Δ*erm* at each time point tested (24, 48, and 72 h) (Fig. 4.8-4.10). The cytotoxin titre was reduced in both the WT and the control strains in TYM and TYG.

Toxin levels for 630WT and 630Δ*erm* were very similar with toxin production by 630WT at 24 h going from a titre of 1.1 x 10^1 in TY to 0 in TYM (**** P < 0.0001) and 0 in TYG (**** P < 0.0001), and 630Δ*erm* going from a titre of 1.0 x 10^1 in TY to 0 in TYM (**** P < 0.0001) and 0 in TYG (**** P < 0.0001). 630WT produced marginally more toxin than 630Δ*erm* (* P < 0.02) (Fig. 4.8).

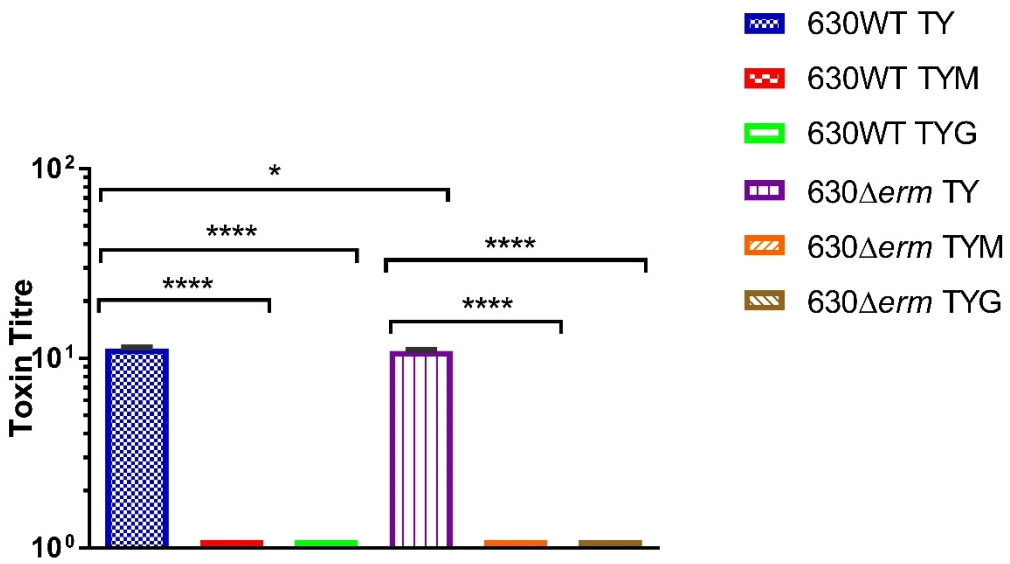

Figure 4.8: Cytotoxicity of 630WT and 630Δ*erm* at 24 h in TY.
Serial dilutions (10^0-10^{-9}) of bacterial supernatants (triplicates) were applied to Vero cell monolayers (p36) to determine toxin titre of both WT and the control strain (630Δ*erm*).
No differences in cytotoxicity patterns were seen between the WT and the control strain, mannitol and glucose suppressing toxin production in both strains.
One-way ANOVA was used to determine statistical significance.
630WT/630Δ*erm* in TY vs. TYM/TYG **** P < 0.0001.
630WT in TY vs. 630Δ*erm* in TY * P < 0.02.

Toxin levels for 630WT and 630Δ*erm* at 48 h were very similar with toxin production by 630WT going from a titre of 1.6 x 10^2 in TY to 1.7 x 10^1 in TYM (**** P < 0.0001), and to 1.0 x 10^1 in TYG (**** P < 0.0001), while 630Δ*erm* toxin production by 630Δ*erm* went from a titre of 1.6 x 10^2 in TY to 1.7 x 10^1 in TYM (**** P < 0.0001), and to 1.0 x 10^1 in TYG (**** P < 0.0001) (Fig. 4.9).

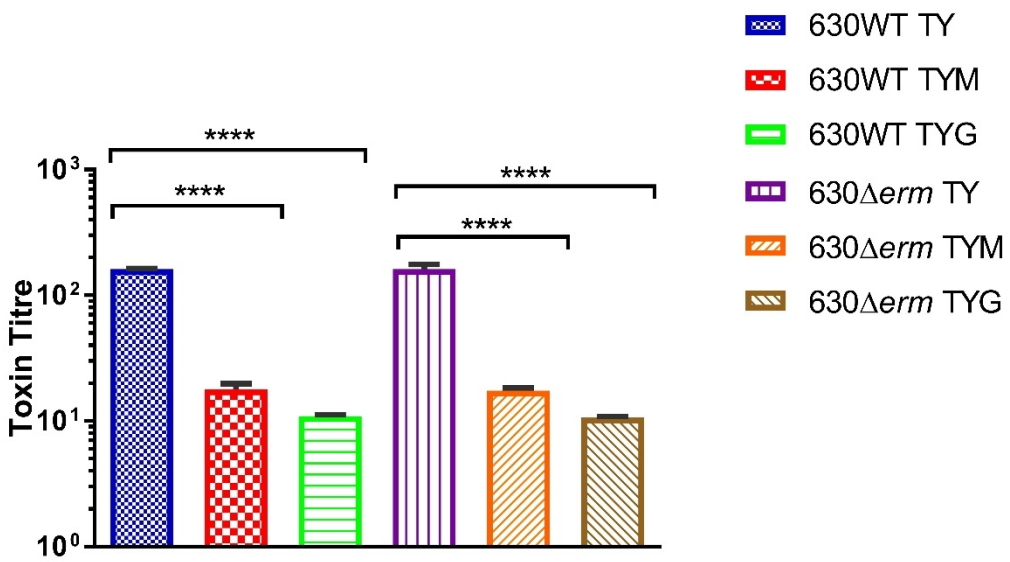

Figure 4.9: Cytotoxicity of 630WT and 630Δ*erm* at 48 h in TY.
Serial dilutions (10^{0}-10^{-9}) of bacterial supernatants (triplicates) were applied to Vero cell monolayers (p36) to determine toxin titre of both the WT and the control strain (630Δ*erm*). 630WT and 630Δ*erm* significantly (**** $P < 0.0001$) suppressed toxin levels in TYM.
No differences in cytotoxicity patterns were seen between the WT and the control strain, with both strains suppressing toxin levels in mannitol and glucose, and, hence, no phenotypic differences were observed.
One-way ANOVA was used to determine statistical significance.
630WT/630Δ*erm* in TY vs. TYM/TYG **** $P < 0.0001$.

Toxin levels for 630WT and 630Δ*erm* at 72 h were very similar with toxin production by 630WT going from a titre of 1.9 x 10^{3} in TY to 1.7 x 10^{1} in TYM (**** $P < 0.0001$), and to 1.0 x 10^{1} in TYG (**** $P < 0.0001$), while 630Δ*erm* went from a titre of 1.8 x 10^{3} in TY to 1.8 x 10^{1} in TYM (**** $P < 0.0001$), and to 1.1 x 10^{1} in TYG (**** $P < 0.0001$) (Fig. 4.10).

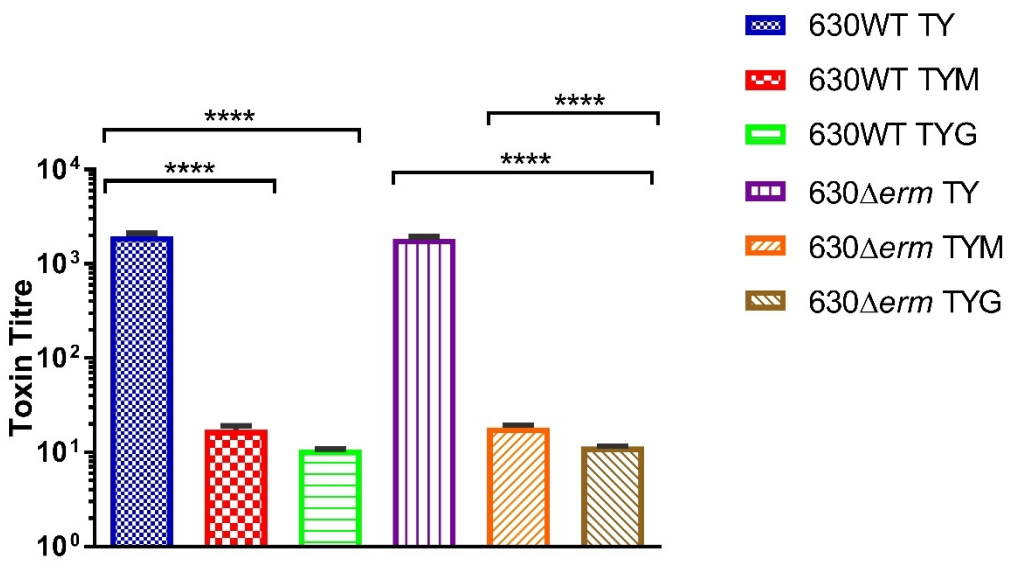

Figure 4.10: Cytotoxicity of 630WT and 630Δ*erm* at 72 h in TY.
Serial dilutions (10^{0}-10^{-9}) of bacterial supernatants (triplicates) were applied to Vero cell monolayers (p36) to determine toxin titre of both WT and parent.
No differences in cytotoxicity patterns were seen between the WT and the control strain (630Δ*erm*), with both strains suppressing toxin levels in mannitol and glucose, and hence, no phenotypic differences were observed.
One-way ANOVA was used to determine statistical significance.
630WT/630Δ*erm* in TY vs. TYM/TYG **** $P < 0.0001$.

4.2.6 Motility assays

Four variant assays were used to determine effects of deleting *C. difficile* 630 *ermB* on the motility of the organism (Fig. 4.11-4.14). The control strain, 630Δ*erm* was tested alongside 630WT, *C. difficile* 630Δ*erm*_CT*fliC*, and *C. difficile* M120. It appears that deleting *C. difficile* 630 *ermB* did not produce an effect on motility.

4.2.6.1 Motility assays on YT +glucose

No differences in motility could be observed between 630WT and 630Δ*erm* when tested on YTG, agar as the motility on the plates seen with each strain was similar. 630WT had a zone diameter of 2cm, while 630Δ*erm* had 2cm (Fig. 4.11).

M120 was used as the negative control, and exhibited reduced motility in comparison to the wild-type and the parent (not shown).

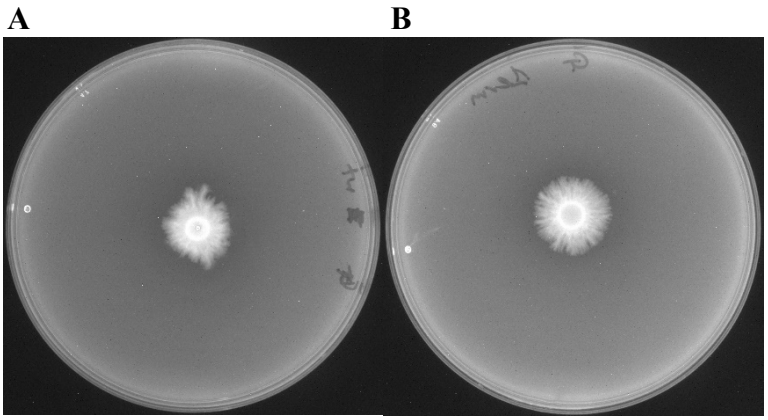

Figure 4.11: Representative images of motility assays of 630WT (A) and 630Δ*erm* (control strain) (B) on YTG.
2µL of each strain (in triplicates) was spotted onto plates of YTG agar containing 1% w/v glucose and incubated at 37°C for 48 h to see if it was possible to observe a motility phenotype.
630WT and the control strain (630Δ*erm*) exhibited a similar level of motility on the plates.

4.2.6.2 Motility assays on YT +mannitol

Motility assays on YT +mannitol were undertaken in order to determine if potential differences in motility could be observed between 630WT and 630Δ*erm* when tested on this medium.

A slightly larger zone of motility was observable with 630WT (1.7cm zone diameter) than with 630Δ*erm* (1.3cm zone diameter) (Fig. 4.12). CT*fliC* was used as the negative control, and exhibited reduced motility in comparison to the wild-type and the parent (not shown).

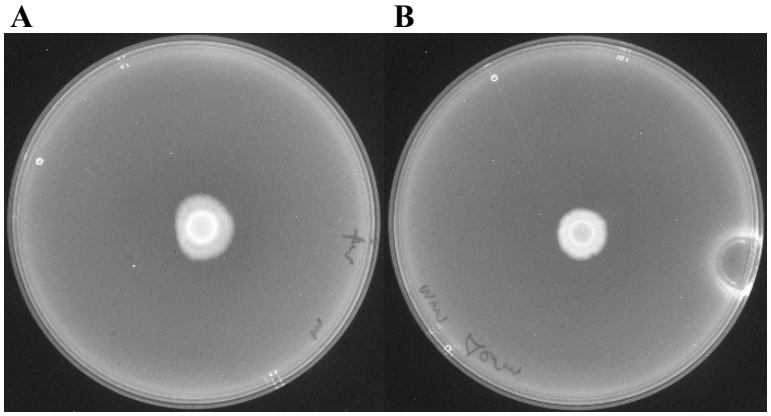

Figure 4.12: Representative images of motility assays of 630WT (A) and 630Δ*erm* (control strain) (B) on YTM.
2µL of each strain (in triplicates) was spotted onto plates of YTM agar containing 1% w/v mannitol and incubated at 37°C for 48 h to see if it was possible to observe a motility phenotype.
630WT and the control strain (630Δ*erm*) exhibited similar motility, but 630WT exhibited slightly larger motility.

4.2.6.3 Motility assays on BHIS +top agar

BHIS +top agar was used as another method to determine potential differences in motility between 630WT and 630Δ*erm*.

No differences were observed, with similar motility seen with both strains (both had a zone diameter of 1cm). CT*fliC* was used as the negative control, and exhibited reduced motility (a zone diameter of 0.7cm) on the plates in comparison (Fig. 4.13).

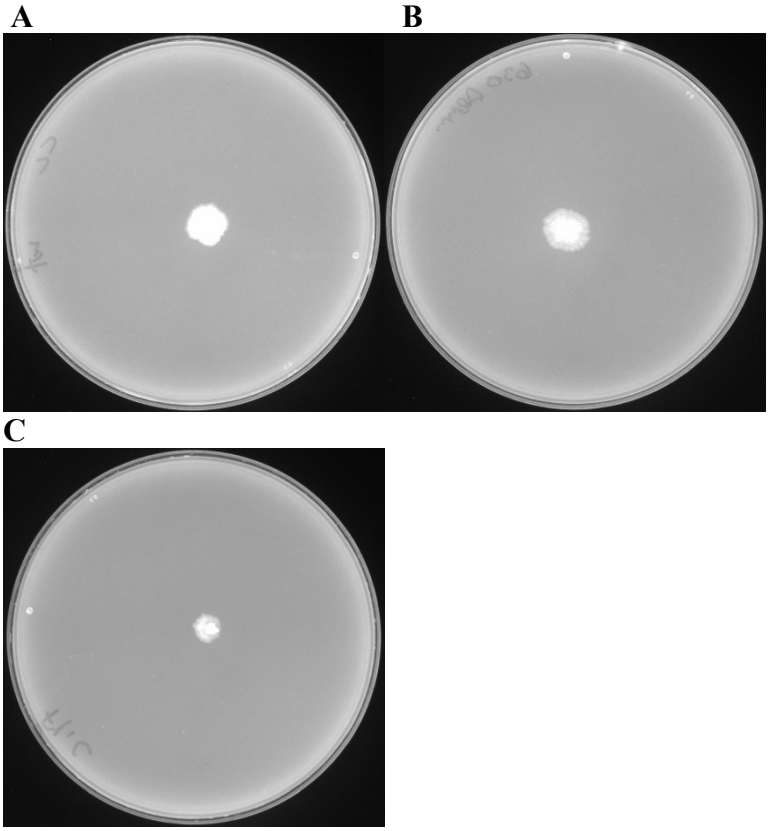

Figure 4.13: Representative images of motility assays on BHIS +top agar showing 630WT (A), control strain (B), and negative control (C).
The surface of the top agar was pierced with a single colony of each strain (in triplicates) and incubated at 37°C for 48 h to see if it was possible to observe a difference in motility.
No differences were observed between 630WT and the control strain with similar motility on the plates seen with both strains.

4.2.6.4 Motility assays in tubes

Motility assays in glass tubes was set-up using the same medium that was used as the top layer medium for the BHIS +top layer agar plates (see section 4.3.6.3). 630WT and 630Δ*erm* both exhibited good turbidity and migrated a distance of 11cm from the point of inoculation to the base of the tubes. *C. difficle* M120 was used as the negative control, showed growth at the very top of the tubes, but did not exhibit any turbidity nor migrate any distance through the tubes (Fig. 4.14).

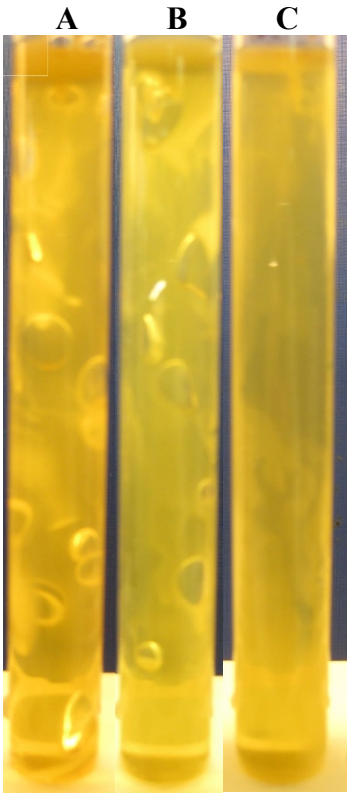

Figure 4.14: Representative images of motility assays showing migration of 630WT (A) and control strain (B) through the agar in the tubes. The negative control, M120 (C), did not migrate.

The surface of the agar was pierced using a sterile cocktail stick to a depth of 2mm to inoculate a single colony of each strain (in triplicates) into the medium and incubated at 37°C for 24 h to see if it was possible to observe a difference in motility.

630WT and the control strain (630Δ*erm*) both exhibited good turbidity and migrated to the base of the tubes (11cm), while the negative control (M120) did not migrate any distance.

4.3 Investigation and Characterisation of PTS^{Mtl} Phosphate Dehydrogenase –MtlD

mtlD was targeted for deletion using allele-couple exchange (ACE)[117] in order to observe the effects on mannitol uptake, general growth, cytotoxicity, and motility. This mutant was generated and then complemented separately using the native promoter (*Pmtl*) and the stronger *fdx* promoter as described in Ng *et al*., 2013[117] by Rachel Ng prior to this study. The characterisation, as described below, was carried out during this study.

4.3.1 Characterisation of 630Δ*erm*Δ*mtlD* (CD630_2331)

The previously generated mutant, Δ*mtlD*, and the complemented mutants, *mtlD* comp and *mtlD* overex[117], were subjected to growth, cytotoxicity, and motility assays spanning a time period of 0-72 h.

4.3.1.1 Growth on DM and DMM agar

630Δ*erm*, Δ*mtlD*, *mtlD* comp, and *mtlD* overex were streaked on DMM agar to see if there were any differences in growth.

630Δ*erm* (control strain) exhibited strong growth. Δ*mtlD* (mutant) failed to grow on DM (not shown) and DMM. Growth on DMM was restored with the complemented mutants, *mtlD* comp and *mtlD* overex (Fig. 4.15).

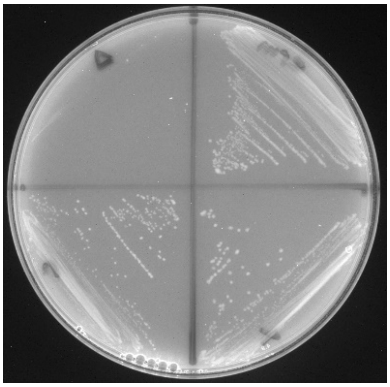

Figure 4.15: Representative image showing growth of Δ*mtlD* (top left), control strain (top right), complemented mutant (bottom left), and overexpressed mutant (bottom right) on DMM agar.
Strains (in triplicates) were streaked on plates of DMM agar containing 0.6% w/v mannitol and incubated at 37°C for 16 h to see if it was possible to observe a growth phenotype.
Unlike the control strain (630Δ*erm*), the mutant (Δ*mtlD*) failed to grow. Growth was restored with the complemented (*mtlD* comp) and overexpressed (*mtlD* overex) mutants.

4.3.1.2 Growth in DM, DMM, and DMG broth

The addition of mannitol to the 630Δ*erm* (control strain) samples provided a major increase in growth from 6-12 h incubation (e.g. 630Δ*erm* in DM (OD_{600} 0.36) vs. 630Δ*erm* in DMM (OD_{600} 0.75) at 8 h (peak growth) *** $P < 0.001$). Slope of the curve 0-8 h in DMM = 1.89; in DMG = 2.13 (Fig. 4.16).

This was not seen with Δ*mtlD* (the mutant). Peak growth in DMM at 24 h was at an OD_{600} of 0.25. Indeed, growth of Δ*mtlD* in DMM was consistently much below growth in DM alone from 4-24 h (e.g. 24h OD_{600} in DM = 0.491). Δ*mtlD* growth in DMM was significantly below that of the control strain in DMM (**** < 0.0001) (Fig. 4.16).

The Δ*mtlD* control samples in DMG also continuously exhibited much significantly reduced growth levels in comparison with 630Δ*erm* in DMG. For example, at 8 h growth of the control strain in DMG reached an OD_{600} of 0.85, while the mutant in DMG merely reached an OD_{600} of 0.42 (*** $P < 0.001$). Slope of the graph 0-12 h in DMM = 0.385; in DMG = 0.76 (Fig. 4.16).

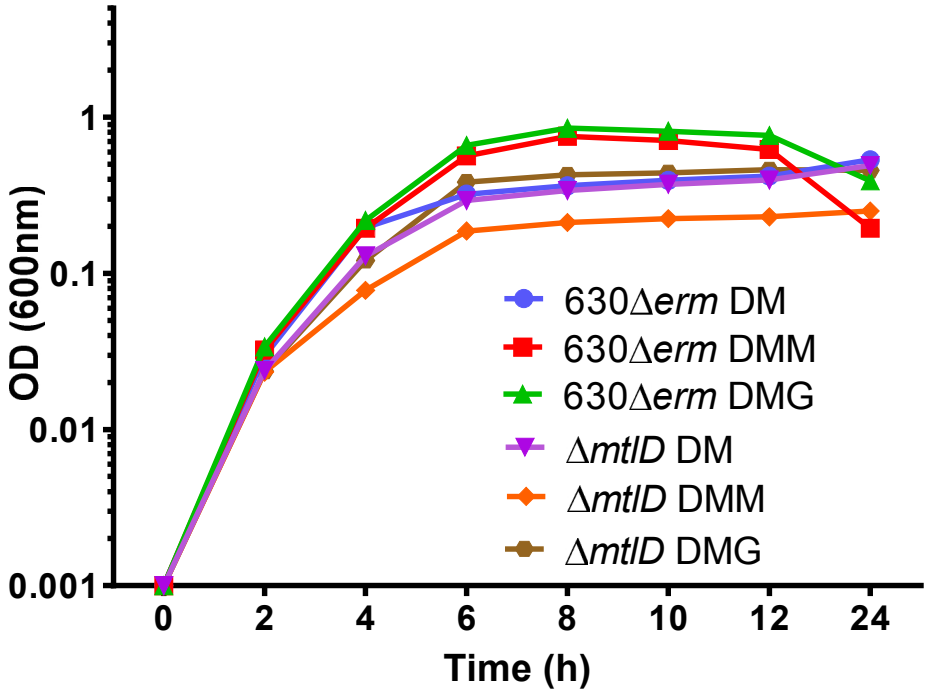

Figure 4.16: Role of *mtlD* in *C. difficile* 630Δ*erm* growth in DM.
630Δ*erm* (control strain) and Δ*mtlD* (mutant) were incubated for 24 h at 37°C. 1mL extracts (triplicates) were taken at regular time points and the OD_{600} measured.
Growth of the mutant, in all conditions (DM, DMM, DMG), lagged noticeably behind growth of the control strain in DM, DMM, and DMG.
630Δ*erm* slope of the curve 0-8 h in DMM = 1.89; in DMG = 2.13.
Δ*mtlD* slope of the curve 0-8 h in DMM = 0.52; in DMG = 1.06
One-way ANOVA was used to determine statistical significance.
630Δ*erm* in DM vs. 630Δ*erm* in DMM at 8 h *** $P < 0.001$.
630Δ*erm* in DMM (peak growth) vs. Δ*mtlD* in DMM (peak growth)
**** $P < 0.0001$.
630Δ*erm* in DMG (peak growth) vs. Δ*mtlD* in DMG (peak growth) *** $P < 0.001$.

Unlike Δ*mtlD* (mutant), the addition of mannitol to the *mtlD* comp cultures significantly increased growth from 4 h until the final time point at 24 h. At 10 h, growth of *mtlD* comp in DM reached an OD_{600} of 0.39, while in DMM it reached a peak of 0.75 (**** $P < 0.0001$). This indicated, when compared to 630Δ*erm*, a delayed, but complete restoration of growth levels in mannitol, as 630Δ*erm* growth in DMM peaked at 0.75 at 8 h (Fig. 4.17). Growth in DMG mirrored

630Δ*erm* growth in DMG, peaking at 8 h (OD_{600} 0.85). Slope of the curve 0-10 h in DMM = 1.51; 0-8 h in DMG = 2.15 (Fig. 4.17).

Overexpression of *mtlD* (*mtlD* overex) restored OD_{600} levels in mannitol to the same levels as seen with 630Δ*erm* in mannitol. Growth in DMM, like that of 630Δ*erm*, peaked at 8 h of incubation, with an OD_{600} of 0.74 (*mtlD* overex DM (OD_{600} 0.36) vs. *mtlD* overex DMM **** $P < 0.0001$) (Fig. 4.17).

Like 630Δ*erm* and *mtlD* comp, *mtlD* overex had no difficulty utilising glucose and exhibited similar levels of growth at the same time points. For example, at 8 h, the peak OD_{600} in DMG of 0.85 was almost exactly the same as the control strain (0.85) and the complemented mutant (0.86) in DMG at this time point (Fig. 4.16 & 4.17).

The slopes of the curves from 0-8 h (peak growth) in DMM for 630Δ*erm* (1.89) and for *mtlD* overex (1.86) were similar. Slope of the graph 0-8 h in DMM = 1.86; 0-8 h in DMG = 2.13 (Fig. 4.16 & 4.17).

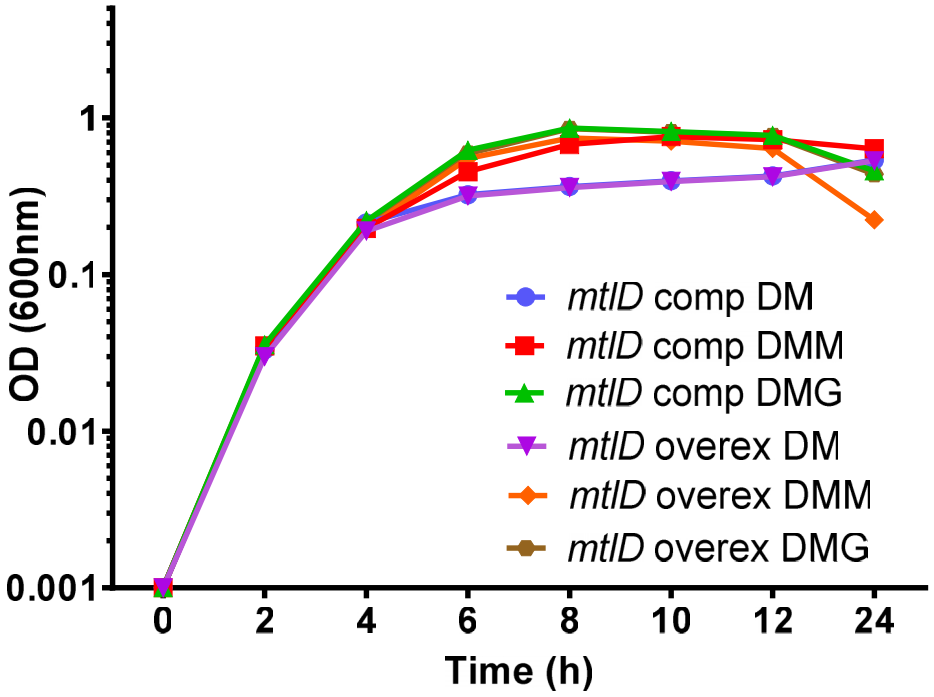

Figure 4.17: Role of *mtlD* in *C. difficile* 630Δ*erm* growth in DM.
mtlD comp (complemented mutant) and *mtlD* overex (overexpressed mutant) were incubated for 24 h at 37°C. 1mL extracts (triplicates) were taken at regular time points and the OD_{600} measured.
Growth of the mutant, in all conditions (DM, DMM, DMG), lagged significantly behind growth of the control strain in DM, DMM, and DMG.
Restoration of *mtlD* in both strains resulted in mannitol uptake being restored.
mtlD comp slope of the curve 0-10 h (peak growth) in DMM = 1.51; 0-8 h in DMG = 2.15.
mtlD overex slope of the curve 0-8 h (peak growth) in DMM = 1.86; 0-8 h in DMG = 2.13.
One-way ANOVA was used to determine statistical significance.
mtlD comp at 10 h in DM vs. DMM **** $P < 0.0001$.
mtlD overex at 8 h DM vs. DMM *** $P < 0.0001$.

4.3.1.3 HPLC evaluation of mannitol/glucose consumption in DM

Uptake of mannitol by 630Δ*erm* and *mtlD* overex (and to a lesser extent *mtlD* comp. [630Δ*erm* vs. *mtlD* comp at 6 h *** $P < 0.0014$]) occurred with the mannitol levels for the 630Δ*erm* samples falling from 7.5mM at 0 h to 2.22mM at 6 h, to 0mM by 8 h; for *mtlD* overex they fell from 7.6mM at 0 h to 2.46mM at 6 h, to 0mM by 8 h; while uptake by the complemented mutant, *mtlD* comp, was

slower, with mannitol levels dropping from 7.63mM at 0 h to 3.85 at 6 h, then to 1mM at 8 h, before reaching 0mM at 10 h. 630Δ*erm* slope 0-8h = 1.875; *mtlD* comp slope 0-8h = 1.65; *mtlD* overex slope 0-8h = 1.9 (Fig. 4.18).

All of this was in complete contrast to the behaviour of *mtlD*, which although by the completion of the assay had utilised a significant amount of added mannitol (22.4%), had 5.82mM of mannitol remained at 24h. At 6 h and 8 h, when every other strain had used the available mannitol, Δ*mtlD* still had 6.22mM and 6.27mM mannitol remaining at these respective time points (Δ*mtlD* vs. 630Δ*erm* and *mtlD* overex at 6 h **** $P < 0.0001$; Δ*mtlD* vs. *mtlD* comp at 8 h *** $P < 0.0003$). Δ*mtlD* slope 0-8 h = 0.30 (Fig. 4.18).

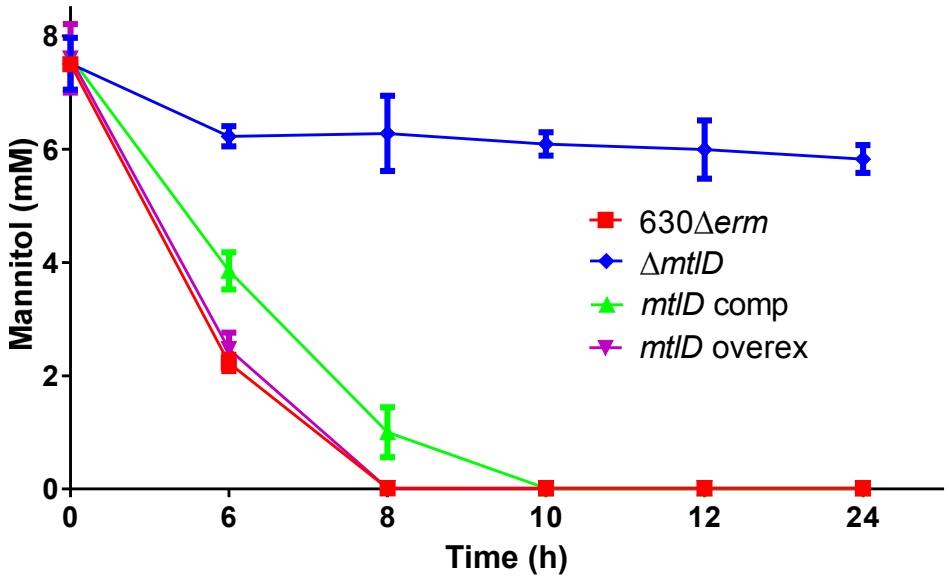

Figure 4.18: HPLC evaluation of mannitol uptake in DM by 630Δ*erm* (control strain), Δ*mtlD* (mutant), and the complemented mutants (*mtlD* comp and *mtlD* overex).
Extracts (triplicates) from the growth assay in DM were used to determine by HPLC the exact amount of sugar remaining in the medium at each time point.
The amount of mannitol left in the mutant strain medium at 6-24 h was significantly above that left by the control strain and the complemented mutants at these time points (**** $P < 0.0001$).
630Δ*erm* slope 0-8h = 1.875.
mtlD comp slope 0-8h = 1.65.
mtlD overex slope 0-8h = 1.9.
Δ*mtlD* slope 0-8 h = 0.30.
One-way ANOVA was used to determine statistical significance.
630Δ*erm* vs. *mtlD* comp at 6 h *** $P < 0.0014$.
Δ*mtlD* vs. 630Δ*erm* and *mtlD* overex at 6 h **** $P < 0.0001$.
Δ*mtlD* vs. *mtlD* comp at 8 h *** $P < 0.0003$.

In each strain tested, with the exception of Δ*mtlD*, glucose was almost totally depleted, as was expected, between 0-24 h (**** $P < 0.0001$). No differences in overall glucose uptake emerged between these strains, indicating that once *mtlD* was restored, there was no overall effect on glucose uptake. However, the amount of glucose remaining in the Δ*mtlD* samples (0.4mM), although it was a small fraction of the total glucose at the start of the assay, was slightly above that of all of the other strains (the next highest being 630Δ*erm* with 0.13mM) (Fig. 4.19).

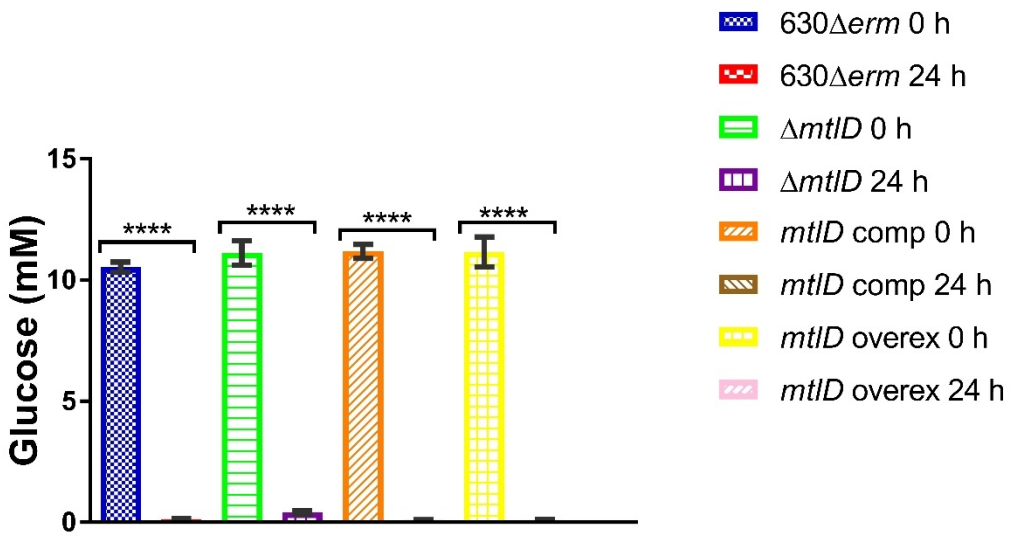

Figure 4.19: HPLC evaluation of glucose uptake in DM by 630Δ*erm* (control strain), Δ*mtlD* (mutant), and the complemented mutants (*mtlD* comp and *mtlD* overex).
Extracts (triplicates) from the growth assay were used to determine by HPLC the exact amount of sugar remaining in the medium at the start and end of the assay. The amount of glucose utilisation by each strain was similar with a depletion of the sugar (**** $P < 0.0001$). A residual amount of glucose was noticeably left remaining at 24 h with the mutant, Δ*mtlD*.
One-way ANOVA was used to determine statistical significance.

4.3.1.4 Growth in TY, TYM, and TYG

Growth of the mutant, Δ*mtlD*, in TY, TYM, and TYG from 2 h onwards lagged significantly behind growth of the parent throughout the entire assay (Fig. 4.20). With regard to mannitol uptake, as well as lagging far behind parental growth levels in TYM up to 24 h (e.g. at 12 h, which was peak growth for the control strain and the mutant strain in TYM), mutant growth in TYM, instead of being above that of the mutant in TY, was consistently slightly below throughout the entire assay, indicating an inability to utilise the mannitol in the medium (Fig. 4.20).

The presence of mannitol led to a slight increase in 630Δ*erm* OD_{600} levels. At 12 h (peak growth), OD_{600} in TY was 0.98, while in TYM it was 1.07 (**** $P < 0.000106$). Slope of the curve 2-12 h in TYM = 2.14, in TYG = 2.14 (Fig. 4.20).

With the mutant, Δ*mtlD*, the presence of mannitol did not at any time point induce an increase. For example, at 12 h, which was peak growth of the mutant in mannitol, OD_{600} in TY was 0.55, and in TYM it was 0.45 (Fig. 4.20). Mutant growth in all conditions consistenly lagged behind that of the control strain. 630Δ*erm* in TY reached a peak OD_{600} of 0.98 (at 12 h), while Δ*mtlD* only reached a peak of 0.76 in TY (at 48 h) (** $P < 0.0016$). 630Δ*erm* in TYM (peak growth) vs. Δ*mtlD* in TYM (peak growth) differed very significantly (**** $P < 0.0001$). In TYG, 630Δ*erm* peaked at an OD_{600} of 1.07 (at 12 h), while Δ*mtlD* reached 1.01 (at 24 h). Slope of the curve 2-12 h in TYM = 0.91, 2-24 h, in TYG = 1.68 (Fig. 4.20).

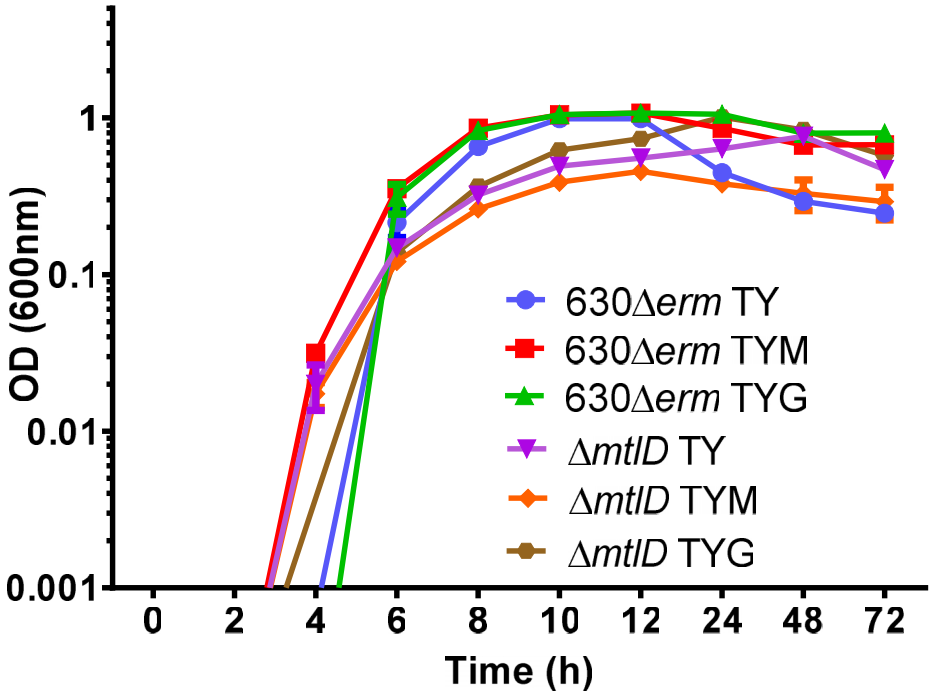

Figure 4.20: Role of *mtlD* in *C. difficile* 630Δ*erm* growth in TY.
630Δ*erm* (control strain) and Δ*mtlD* (mutant) were incubated in TY with and without mannitol/glucose for 72 h at 37°C. 1mL extracts (triplicates) were taken at regular time points and the OD_{600} measured.
Deletion of *mtlD* inhibited growth in each condition tested. Δ*mtlD* was unable to grow in TY, TYM, and TYG to the levels seen with the control strain.
630Δ*erm* slope of the curve 2-12 h in TYM = 2.14, in TYG = 2.14.
Δ*mtlD* slope of the curve 2-12 h in TYM = 0.91, 2-24 h in TYG = 1.68.
One-way ANOVA was used to determine statistical significance.
630Δ*erm* at 12 h (peak growth) in TY vs. in TYM **** $P < 0.000106$.
630Δ*erm* in TY at 12 h (peak growth) vs. Δ*mtlD* in TY at 48 h (peak growth) ** $P < 0.0016$.
630Δ*erm* in TYM at 12 h (peak growth) vs. Δ*mtlD* in TYM at 12 h (peak growth) **** $P < 0.0001$.

Complementation of Δ*mtlD* with *mtlD* using the native (*Pmtl*) promoter (*mtlD* comp) resulted in a slight increase in growth in the presence of mannitol from 6 h to 12 h (not significant). However, by 24 h (peak OD_{600} in TY and TYM) this was no longer observable as OD_{600} in TY was 0.98, in TYM it was 0.86, in TYG it was 1.0. Slope of the curve 2-12 h in TYM = 1.74, in TYG = 2.02 (Fig. 4.21).

Complementing the mutant with *mtlD* using the *fdx* promoter (*mtlD* overex) resulted in an increase in OD_{600} levels in mannitol from 6 h. For example, at 24 h, OD_{600} in TY was 0.96, while in TYM it reached 1.0 (** $P < 0.0075$). Slope of the curve 2-12 h in TYM = 2.08, in TYG = 2.14 (Fig. 4.21).

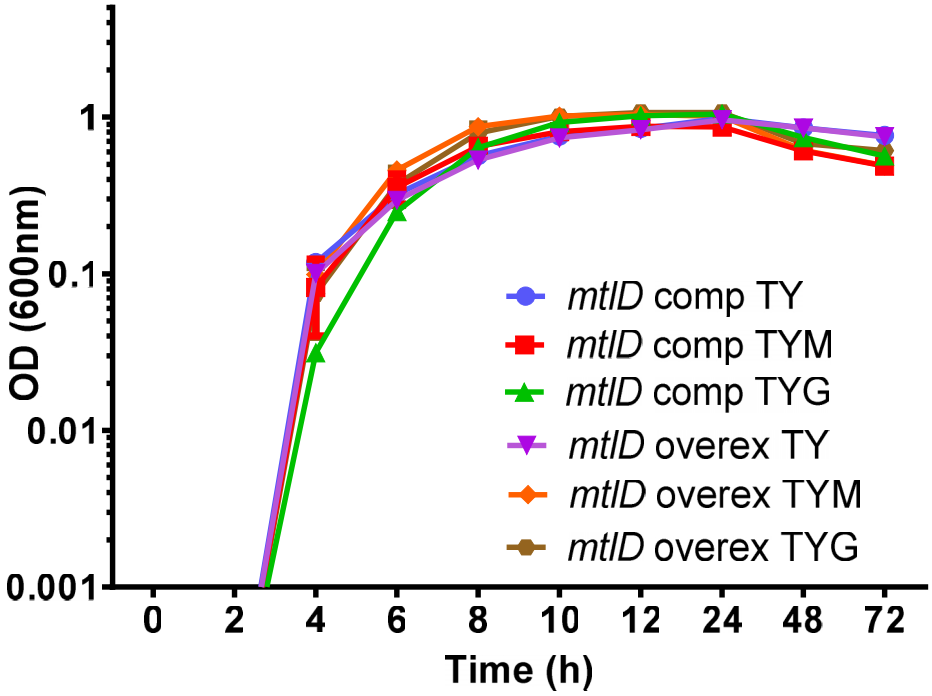

Figure 4.21: Role of *mtlD* in *C. difficile* 630Δ*erm* growth in TY.
mtlD comp and *mtlD* overex were incubated in TY with and without mannitol/glucose for 72 h at 37°C. 1mL extracts (triplicates) were taken at regular time points and the OD_{600} measured.
Restoration of *mtlD* using the native promoter (*mtlD* comp), overall, did not induce an increase in growth in mannitol, but did restore the ability restore the ability to increase growth in glucose. Overexpressing *mtlD* (*mtlD* overex) resulted in an OD_{600} increase in TYM (** $P < 0.0075$) and TYG (in comparison to when *mtlD* overex was in TY) (** $P < 0.01$).
mtlD comp slope of the curve 2-12 h in TYM = 1.74, in TYG = 2.02.
mtlD overex slope of the curve 2-12 h in TYM = 2.08, in TYG = 2.14.
One-way ANOVA was used to determine statistical significance.
mtlD overex at 24 h TY vs. TYM ** $P < 0.0075$.
mtlD overex at 24 h TY vs. TYG ** $P < 0.01$.

4.3.1.5 Cytotoxicity of 630Δ*erm* and 630Δ*erm*Δ*mtlD*

At 24 h, toxin levels were suppressed in the control strain, 630Δ*erm*, as the presence of mannitol caused toxin levels to fall from a toxin titre of 2.2 x 10^1 in TY to 0 in TYM (**** P < 0.0001) (Fig. 4.22).

This reduction in toxin levels was not seen with the mutant, Δ*mtlD*, with toxin levels increasing from a toxin titre of 1.5 x 10^2 in TY to 2.6 x 10^2 in TYM (*** P < 0.0008). Indeed, toxin levels of the mutant in TY and TYM were significantly above those of the control strain in the same conditions (in TY **** P < 0.0001; in TYM **** P < 0.0001) (Fig. 4.22).

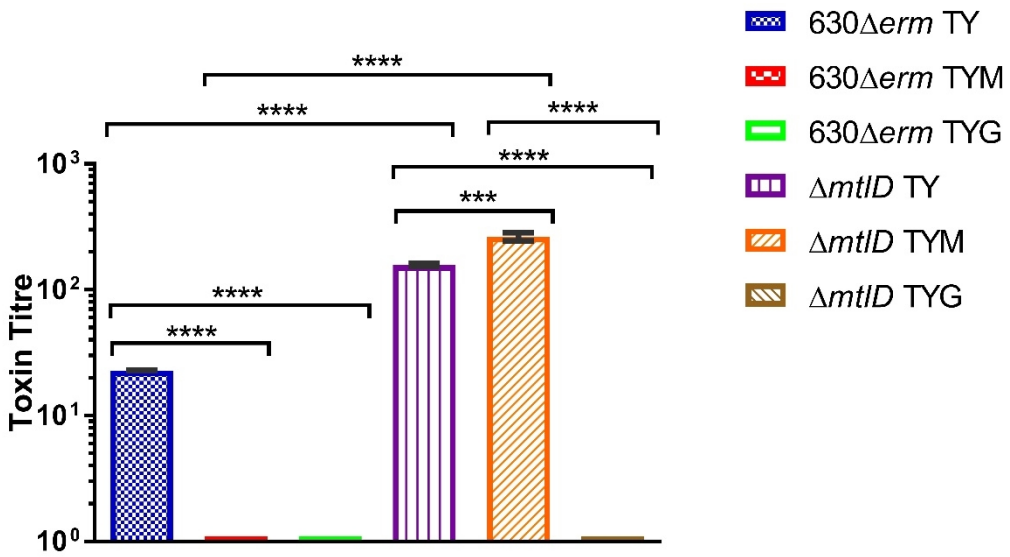

Figure 4.22: Role of *mtlD* in *C. difficile* 630Δ*erm* toxin production at 24 h in TY.
Cytotoxicity of Δ*mtlD* at 24 h incubation. Serial dilutions (10^0-10^{-9}) of bacterial supernatants (in triplicates) were applied to Vero cell monolayers (p30) to determine toxin titre of the control strain (630Δ*erm*) and the mutant (Δ*mtlD*).
No toxin suppression was observed with Δ*mtlD* in TYM. Mutant toxin production significantly increased in TYM compared to when in plain TY (*** P < 0.0008).
One-way ANOVA was used to determine statistical significance.
630Δ*erm* in TY vs. TYM **** P < 0.0001.
630Δ*erm* vs. Δ*mtlD* in TY **** P < 0.0001; in TYM **** P < 0.0001.
Δ*mtlD* TY vs. TYM *** P < 0.0008.

Both complemented strains, *mtlD* comp and *mtlD* overex, restored suppression of toxin production, with toxin levels dropping from a titre of 1.0 x 10^1 for *mtlD* comp and 1.0 x 10^1 for *mtlD* overex in TY to 0 for both strains in TYM (**** P < 0.0001). *mtlD* overex exhibited slightly higher toxicity in TY than *mtlD* comp (* P < 0.02) (Fig. 4.23).

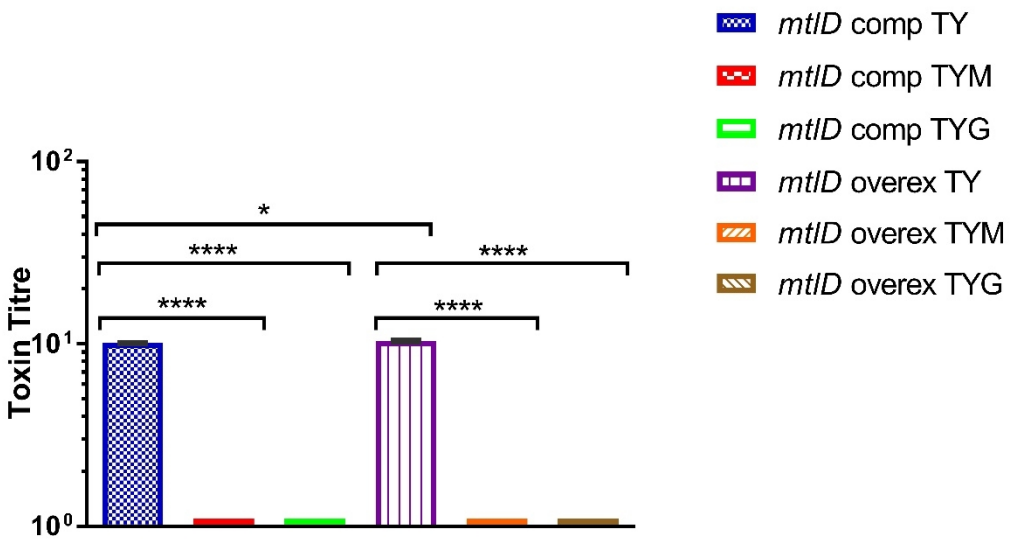

Figure 4.23: Role of *mtlD* in *C. difficile* 630Δ*erm* toxin production at 24 h in TY.
Cytotoxicity of *mtlD* comp and *mtlD* overex at 24 h incubation. Serial dilutions (10^0-10^{-9}) of bacterial supernatants (in triplicates) were applied to Vero cell monolayers (p30) to determine toxin titre of the complemented mutant (Δ*mtlD* comp) and the overexpressed mutant (Δ*mtlD* overex).
A significant level (**** P < 0.0001) of toxin suppression was observed with both strains in TYM.
One-way ANOVA was used to determine statistical significance.
mtlD comp TY vs. TYM **** P < 0.0001.
mtlD overex TY vs. TYM **** P < 0.0001.
mtlD comp TYM vs. *mtlD* overex TYM * P < 0.02.

At 48 h, 630Δ*erm* (control strain) toxin levels were suppressed in mannitol going from a toxin titre of 3.3 x 10^1 in TY to 0 in TYM (**** P < 0.0001) (Fig. 4.24).

Toxin levels in mannitol were upregulated by the mutant, Δ*mtlD*, going from a titre of 1.3 x 10^1 in TY to 2.6 x 10^2 in TYM (**** P < 0.0001) (Fig. 4.24).

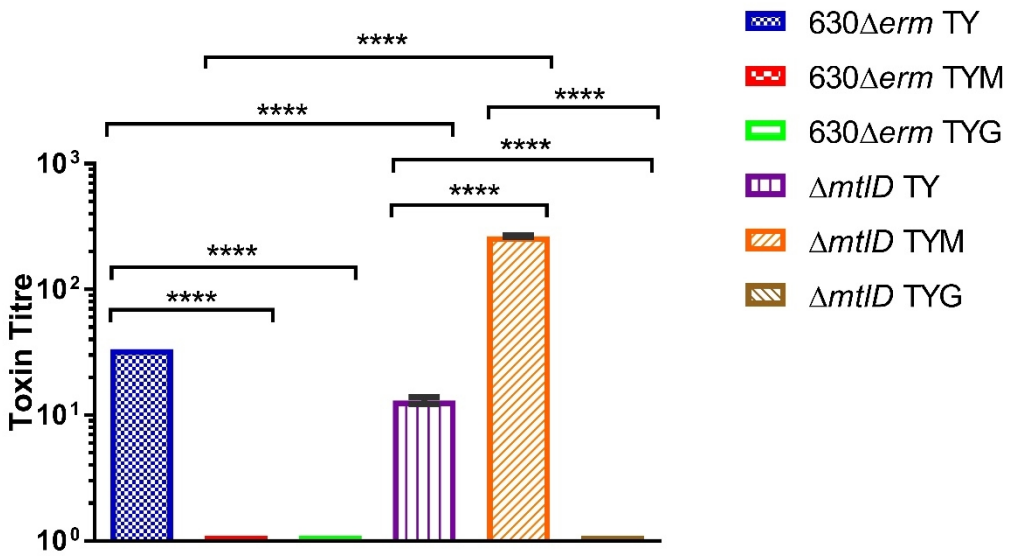

Figure 4.24: Role of *mtlD* in *C. difficile* 630Δ*erm* toxin production at 48 h in TY.

Cytotoxicity of Δ*mtlD* at 48 h incubation. Serial dilutions (10^{0}-10^{-9}) of bacterial supernatants (in triplicates) were applied to Vero cell monolayers (p30) to determine toxin titre of the control strain (630Δ*erm*) and the mutant (Δ*mtlD*).
While mannitol suppressed toxin levels in 630Δ*erm* (**** P < 0.0001), an upregulation of cytotoxicity with Δ*mtlD* in mannitol was observed (**** P < 0.0001).
One-way ANOVA was used to determine statistical significance.
630Δ*erm* vs. Δ*mtlD* in TY **** P < 0.0001; in TYM **** P < 0.0001.
Δ*mtlD* TY vs. TYM **** P < 0.0001.

mtlD comp exhibited an increase in toxin levels in mannitol compared to when in TY alone, with toxin production going from a titre of 1.1 x 10^{1} to 1.6 x 10^{1} (** P < 0.0016) (Fig. 4.25).

mtlD overex completely suppressed toxin production with toxin levels going from a titre of 1.1 x 10^{1} in TY and falling to 0 in TYM (**** P < 0.0001) (Fig. 4.25).

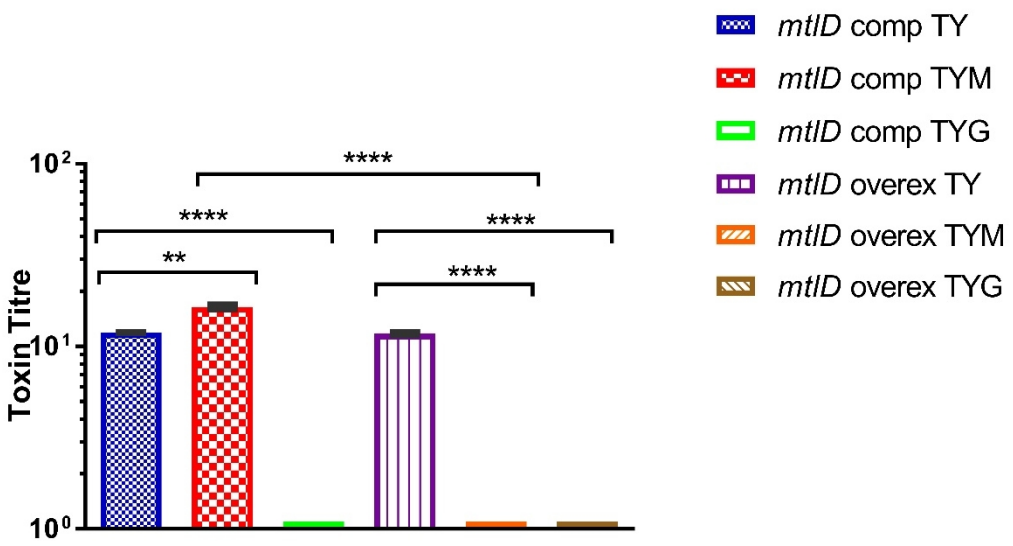

Figure 4.25: Role of *mtlD* in *C. difficile* 630Δ*erm* toxin production at 48 h in TY.

Cytotoxicity of *mtlD* comp and *mtlD* overex at 48 h incubation. Serial dilutions (10^{0}-10^{-9}) of bacterial supernatants (triplicates) were applied to Vero cell monolayers (p30) to determine toxin titre of the mutant complemented with the native promoter (*mtlD* comp) and the mutant complemented with the *fdx* promoter (*mtlD* overex).

mtlD comp toxin levels in mannitol appear to have increased. Toxin suppression in mannitol was totally restored by *mtlD* overex (**** $P < 0.0001$).

One-way ANOVA was used to determine statistical significance.

mtlD comp TY vs. TYM ** $P < 0.0016$.

mtlD overex TY vs. TYM **** $P < 0.0001$.

mtlD comp TYM vs. *mtlD* overex TYM **** $P < 0.0001$.

At 72 h, 630Δ*erm* toxin levels in mannitol were reduced going from a toxin titre of 4.0×10^{2} in TY to 1.4×10^{1} in TYM (**** $P < 0.0001$) (Fig. 4.26).

Δ*mtlD* toxin levels increased from a titre of 2.1×10^{2} in TY to 2.9×10^{3} in TYM (**** $P < 0.0001$) (Fig. 4.26).

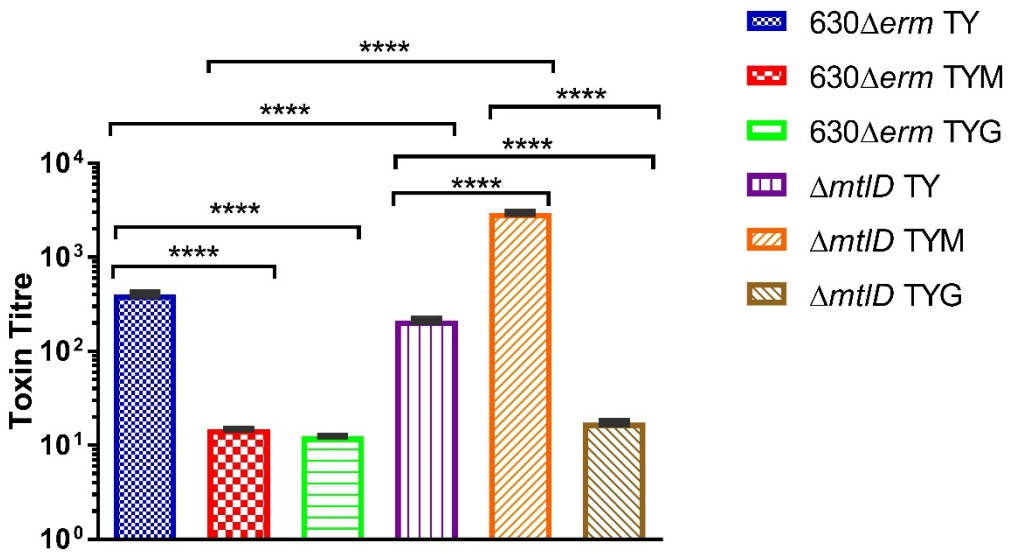

Figure 4.26: Role of *mtlD* in *C. difficile* 630Δ*erm* toxin production at 72 h in TY.

Cytotoxicity of Δ*mtlD* at 72 h incubation. Serial dilutions (10^{0}-10^{-9}) of bacterial supernatants (triplicates) were applied to Vero cell monolayers (p30) to determine toxin titre of the control strain (630Δ*erm*) and the mutant (Δ*mtlD*).
Toxin levels were suppressed in the control strain in TYM. In contrast to the control strain which suppressed cytotoxicity (**** $P < 0.0001$), Δ*mtlD* increased toxin production in TYM (**** $P < 0.0001$).
One-way ANOVA was used to determine statistical significance.
630Δ*erm* vs. Δ*mtlD* in TY **** $P < 0.0001$; in TYM **** $P < 0.0001$.
Δ*mtlD* TY vs. TYM **** $P < 0.0001$.

At 72 h, *mtlD* comp exhibited an increase in toxin production in mannitol, with toxin levels going from a titre of 1.3 x 10^2 in TY to 2.1 x 10^2 in TYM (** $P < 0.0016$) (Fig. 4.27).

mtlD overex, meanwhile, showed decreased toxin production in mannitol, with toxin levels dropping from 1.3 x 10^2 in TY to 2.0 x 10^1 in TYM (**** $P < 0.0001$) (Fig. 4.27).

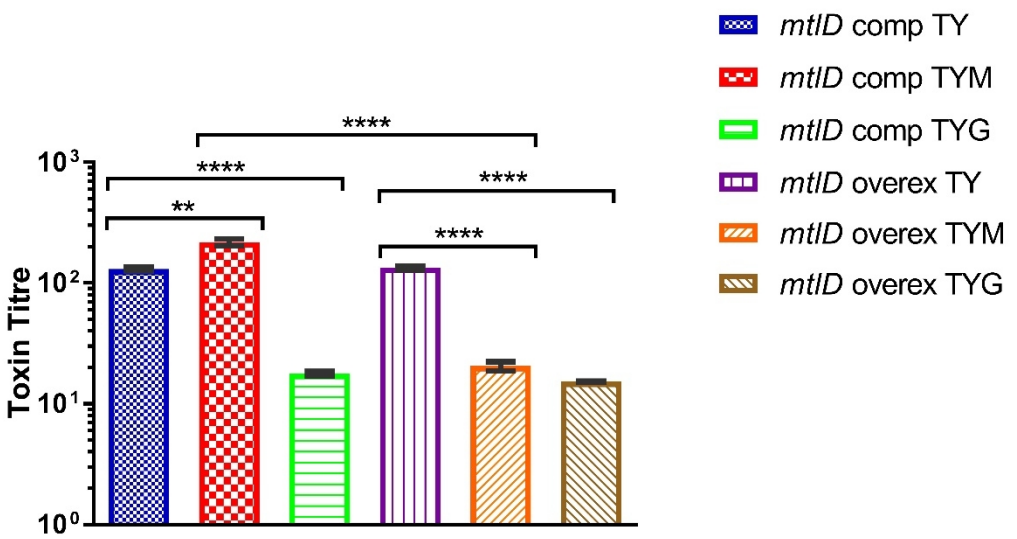

Figure 4.27: Role of *mtlD* in *C. difficile* 630Δ*erm* toxin production at 72 h in TY.
Cytotoxicity of *mtlD* comp and *mtlD* overex at 72 h incubation. Serial dilutions (10^{0}-10^{-9}) of bacterial supernatants (triplicates) were applied to Vero cell monolayers (p30) to determine toxin titre of the mutant complemented using the native promoter (*mtlD* comp) and the mutant complemented using the *fdx* promoter (*mtlD* overex).
mtlD comp toxin levels in mannitol increased. Toxin suppression in mannitol was restored in *mtlD* overex.
One-way ANOVA was used to determine statistical significance.
mtlD comp TY vs. TYM ** $P < 0.0016$.
mtlD overex TY vs. TYM **** $P < 0.0001$.
mtlD comp TYM vs. *mtlD* overex TYM **** $P < 0.0001$.

4.3.1.6 Motility assays

Motility was tested using four variant motility assays. The mutant and the complemented mutants were tested alongside 630Δ*erm*, 630Δ*erm* _CT*fliC*, and *C. difficile* M120.

4.3.1.6.1 Motility assays on YT +glucose

Spotting each strain on agar plates of YT +glucose revealed that the ability of Δ*mtlD* to move across the plates to be less than the control strain and the complemented mutants. 630Δ*erm* exhibited a zone of motility with a zone diameter of 2cm, while Δ*mtlD* had a zone diameter of only 0.7cm. The

complemented mutants, *mtlD* comp and *mtlD* overex, appeared to have increased in motility (when compared with Δ*mtlD*) with *mtlD* comp having a zone diameter of 0.8cm, and *mtlD* overex having a zone diameter of 0.9cm (Fig. 4.28). *C. difficile* M120 was used as the negative control, and exhibited reduced motility in comparison to the parent, the mutant, and the complemented mutants (not shown).

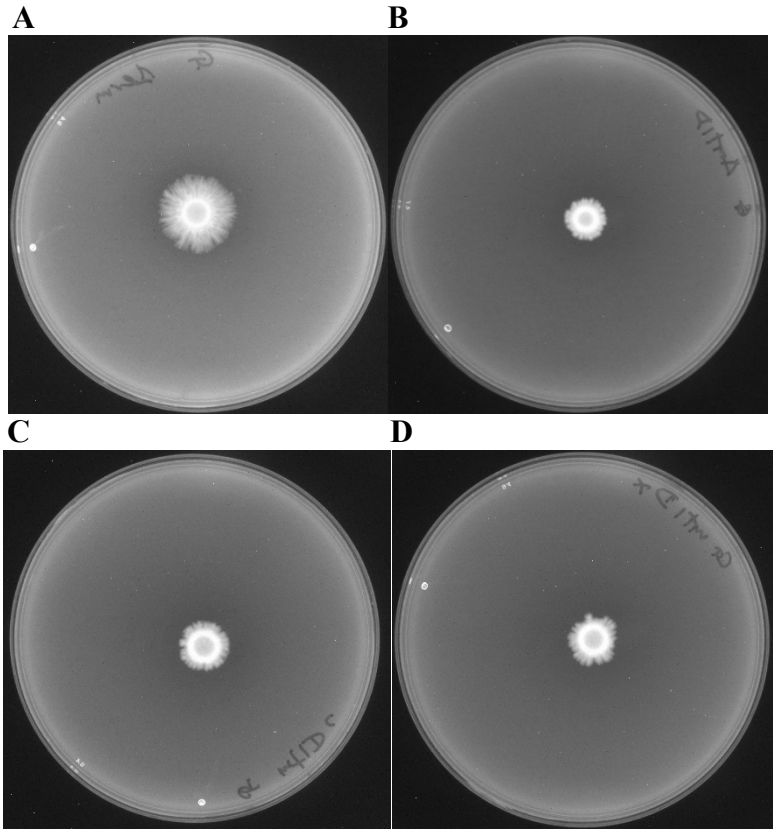

Figure 4.28: Representative images of motility assays showing control strain (A), mutant (B), complemented mutant (C), and overexpressed mutant (D) on YTG.

2µL of an overnight culture of each strain (in triplicates) was spotted onto plates of YTG agar containing 1% w/v glucose and incubated at 37°C for 48 h to see if it was possible to o a difference in motility.

A large zone of motility was observed with the control strain (630Δ*erm*) (A), a reduced zone was seen with the mutant (Δ*mtlD*) (B), while slightly smaller zones (in comparison to the mutant) were observed with the complemented mutants [*mtlD* comp (C) and *mtlD* overex (D)].

4.3.1.6.2 Motility assays on YT medium +mannitol

On YT + mannitol, each strain, with the exception of Δ*mtlD*, showed motility on the plates. However, it was possible to observe a difference in motility on the plate when each strain was spotted on YTM plates. 630Δ*erm* exhibited the highest degree of motility (1.3cm zone diameter). Δ*mtlD* exhibited little or no motility. *mtlD* comp showed greater motility (1cm zone diameter) than Δ*mtlD*, but still less than 630Δ*erm*. *mtlD* overex exhibited increased motility (1.3cm zone diameter) which was comparable to 630Δ*erm* (Fig. 4.29). *C. difficile* CT*fliC* was used as the negative control, and exhibited reduced motility in comparison to the parent, the mutant, and the complemented mutants (not shown).

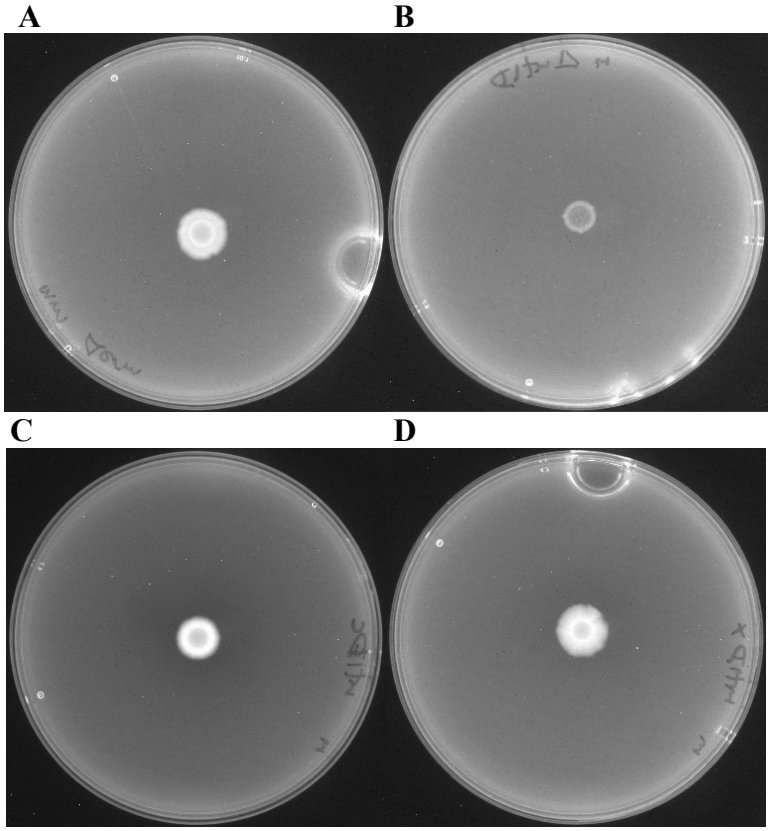

Figure 4.29: Representative images of motility assays showing control strain (A), mutant (B), complemented mutant (C), and overexpressed mutant (D) on YTM.

2µL of an overnight culture of each strain (in triplicates) was spotted onto plates of YTM agar containing 1% w/v mannitol and incubated at 37°C for 48 h to see if it was possible to observe a motility phenotype.

Large zones of motility were observed with the control strain (630Δ*erm*) (A), the complemented mutant (*mtlD* comp) (C), and the overexpressed mutant (*mtlD* overex) (D). The mutant (Δ*mtlD*) (B) exhibited no, or severely reduced, motility.

4.3.1.6.3 Motility assays on BHIS +top agar

BHIS +top agar was used to determine differences in motility between 630Δ*erm* Δ*mtlD*, *mtlD* comp, and *mtlD* overex (Fig. 4.30). The diameters of the zones of motility for strains tested were: 630Δ*erm* was 1cm, Δ*mtlD* was 0.6cm, *mtlD* comp was 0.8cm, and *mtlD* overex was 1cm. CT*fliC* (negative control) produced a zone of motility of 0.7cm zone diameter (Fig. 4.30).

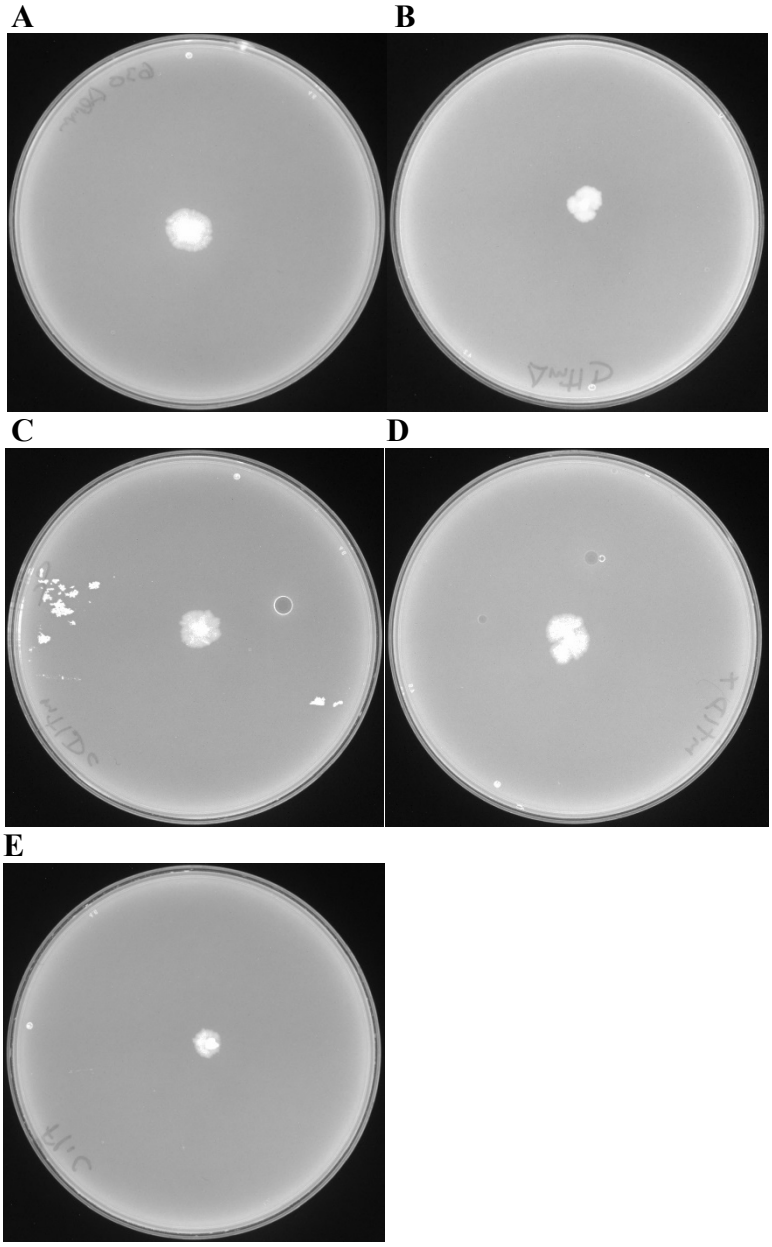

Figure 4.30: Representative images of motility assays on BHIS +top agar showing control strain (A), mutant (B), complemented mutant (C), overexpressed mutant (D), and negative control, CT*fliC* (E).

The surface of the top agar was pierced to a depth of 2mm with a single colony of each strain (in triplicates) and incubated at 37°C for 48 h to see if it was possible to observe a difference in motility.

Motility was observed with the mutant (Δ*mtlD*) showing slightly less motility (0.6cm) (B) than the control strain (630Δ*erm*) (0.85cm) (A), the complemented mutant (*mtlD* comp) (0.6cm) (C), and the overexpressed mutant (*mtlD* overex) (0.8cm) (D). CT*fliC* (negative control) (E) produced a zone of motility with a 1.4cm zone diameter.

4.3.1.6.4 Motility assays in tubes

Motility assays in glass tubes were prepared using the same medium as was used for the top layer medium on the BHIS +top layer agar plates (see section 4.4.1.6.3). The control strain (630Δ*erm*), *mtlD* comp, and *mtlD* overex produced turbidity in the medium and migrated 11cm from the inoculation point to the bottom of the tubes. The mutant (Δ*mtlD*) showed less turbidity, but still migrated 11cm from the point of inoculation to the bottom of the tubes. The 630Δ*erm* tubes showed the most turbidity. *C. difficile* M120 was used as the negative control, showed growth at the very top of the tubes, but did not exhibit any turbidity nor migrate any distance through the agar (Fig. 4.31).

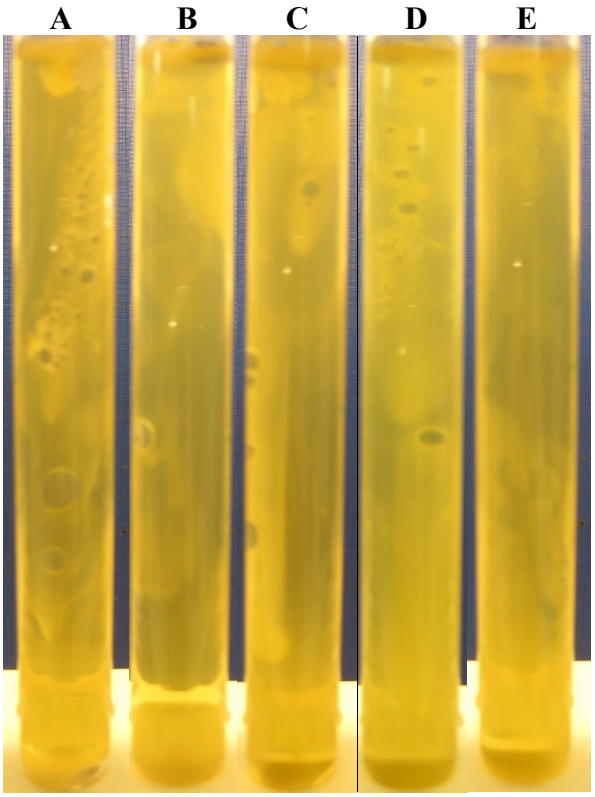

Figure 4.31: Representative images of motility assays showing migration of control strain (A), mutant (B), complemented mutant (C), and overexpressed mutant (D) through the agar in the tubes. The negative control, M120 (E), did not migrate.

The surface of the agar was pierced to depth of 2mm with a single colony of each strain (in triplicates) and incubated at 37°C for 24 h to see if it was possible to observe a difference in motility.

Each strain tested exhibited good turbidity and migrated to the base of the tube (11cm), although a higher level of turbidity was seen with the control strain, 630Δ*erm* (A), and seemingly also with the complemented mutant (*mtlD* comp) (C) and the overexpressed mutant *mtlD* overex (D) than what was seen with the mutant (Δ*mtlD*) (B), while the negative control (M120) did not migrate any distance.

4.4 Investigation and Characterisation of PTS^{Mtl} IIA domain -MtlF

The PTS^{Mtl} IIA domain, *mtlF*, was targeted for CT inactivation so as to investigate the role this gene plays in mannitol uptake. Since there are several other (five) genes scattered about the *C. difficile* 630 genome which are annotated as encoding mannitol-specific IIA domains (at least four of which are solely described as 'fructose/mannitol' at loci 0040-1, 0206, 3015, 3132), it was of

interest to determine if the organism was capable of making use of mannitol without the functioning Mtl IIA at locus CD630_2332. The resultant mutant, CT*mtlF*, was tested for differences in growth, sugar uptake, cytotoxicity, and motility.

4.4.1 Characterisation of 630Δ*erm*_CT*mtlF* (CD_2332) and complements

CT insertion into *mtlF* (Fig. 4.32) was determined by amplifying genomic DNA isolated from the colonies of the parental strain, and erythromycin-resistant *C. difficile* 630Δ*erm*Δ*pyrE* colonies, with primers specific for both the target gene and the CT insertion, and then running the PCR products on a 1% w/v agarose gel, and comparing the fragment sizes for the parent (0.89 kb) and the mutant (2.79 kb) (Fig. 4.33). Southern blotting confirmed that the CT insertion had occurred in a single location (Fig. 4.34).

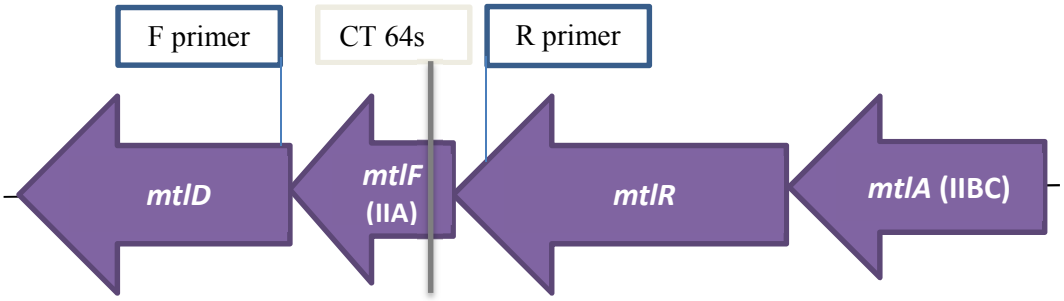

Figure 4.32: Position within the putative PTS^{Mtl} at loci CD630_2331-4 of the gene of interest, *mtlF*, the CT insertion into the gene, and the primers used to screen for the insertion.
Primers, specific for the regions immediately outside of the predicted CT insertion site in *mtlF* (in the target region), were used to amplify DNA from Erm-resistant colonies to screen for the insertion.

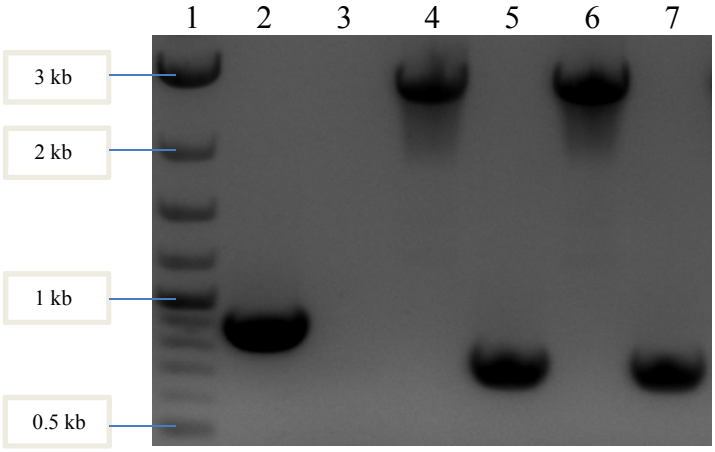

Figure 4.33: PCR screening for CT insertion in CT*mtlF*.
Primers, specific for the regions immediately outside of the predicted CT insertion site in *mtlF*, were used to screen for the insertion on 1% w/v agarose. Table 4.1 below shows the lane order.

Table 4.1: Content of each well when showing by PCR the CT insertion in CT*mtlF*.

Well	Content	Size (kb)
1	Marker	
2	630Δ*ermΔpyrE*, F + R primer	0.89
3	630Δ*ermΔpyrE*, F + EBS primer	-
4	CT*mtlF* mut. A, F + R primer	2.79
5	CT*mtlF* mut. A, F + EBS primer	0.69
6	CT*mtlF* mut. B, F + R primer	2.79
7	CT*mtlF* mut. B, F + EBS primer	0.69

Following initial screening, by PCR, of *C. difficile* 630Δ*ermΔpyrE* erythromycin-resistant colonies for the presence of the CT insertion (as described in Materials and Methods, section 2.4.8), Southern blotting was undertaken in order to verify a single CT insertion in *C. difficile* 630Δ*ermΔpyrE* (Fig. 4.34, Table 4.2).

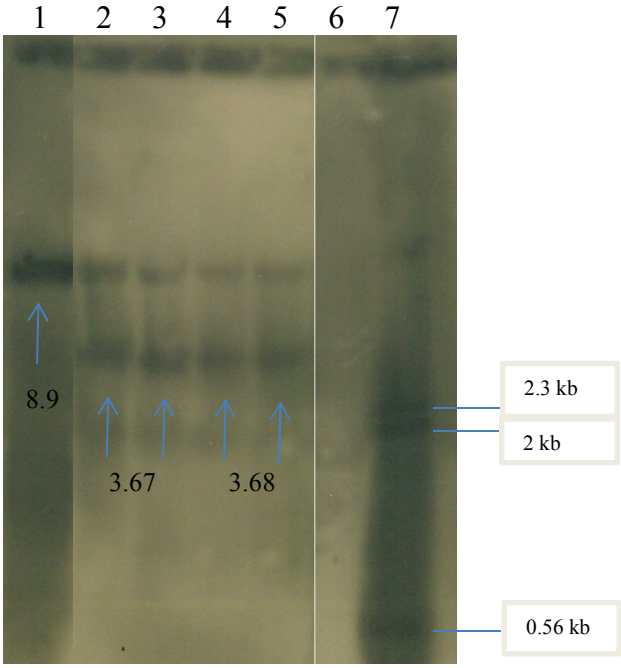

Figure 4.34: Southern blot showing CT insertion in CT*mtlR* and CT*mtlF*. Chromosomal genomic DNA was cut with *Hind*III. Arrows show the group II intron insertion fragment of the expected size. Mutant samples indicating a successful insertion were loaded twice (mutants A and B). Table 4.2 below shows the lane order.

Table 4.2: Southern blot confirmation of CT insertion.

Well	**Content**	**Size (kb)**
1	CT plasmid -positive control	8.9
2	CT*mtlR* mut. A	3.67
3	CT*mtlR* mut. B	3.67
4	CT*mtlF* mut. A	3.68
5	CT*mtlF* mut. B	3.68
6	630Δ*ermΔpyrE* -negative control	-
7	λ *Hind*III marker	

CT*mtlF* (mutant A) was later complemented using the native promoter (*Pmtl*) (*mtlF* comp) and an overexpression promoter (*fdx*) (*mtlF* overex). CT*mtlF* was also restored to *pyrE*-positive, so that each strain could be assayed in a *pyrE*-positive background. Complementation of CT*mtlF* was determined by amplifying genomic DNA isolated from CT*mtlF* colonies growing on MM (without uracil), with primers specific for the restored *pyrE* and which would also encompass the restored gene, and then running the PCR products on 1% w/v agarose gel, and verifying the fragment sizes for *mtlF* complemented (*mtlF* comp) (1.75 kb) and *mtlF* overexpressed (*mtlF* overex) (2.81 kb) (Fig. 4.35). Sequencing confirmed the complementation of the mutant (data not shown).

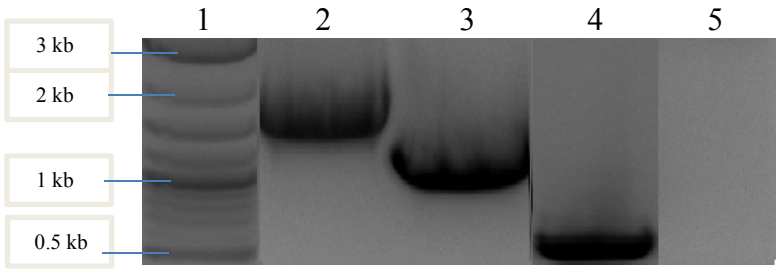

Figure 4.35: PCR screening for restoration of *mtlF* in CT*mtlF*.
Primers, specific for the regions immediately outside of the *C. difficile* 630 *pyrE* locus (CD630_0187), were used to screen for the restoration of *mtlF* and *pyrE* (firstly, with the native promoter, and secondly, with the *fdx* promoter) on 1% w/v agarose. Table 4.3 below shows the lane order.

Table 4.3: Content of each well when showing by PCR the restoration of *mtlF*.

Well	Content	Size (kb)
1	Marker	
2	*mtlF* comp	1.75 (0.42 + 0.65 + 0.68)
3	*mtlF* overex	1.3 (0.42 + 0.2 + 0.68)
4	CT*mtlF pyrE*+	0.68
5	630Δ*ermΔpyrE*, F + R	-

4.4.1.1 Growth on DM agar

630Δ*erm*, CT*mtlF*, *mtlF* comp, and *mtlF* overex were streaked on DM (not shown) and DMM agar to see if there were any differences in growth. Each strain showed strong growth on DM (not shown) and DMM. Differences in the ability to metabolise mannitol could not be discerned (Fig. 4.36).

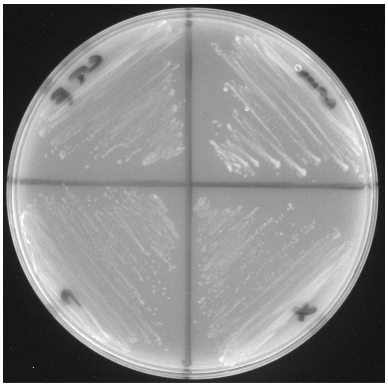

Figure 4.36: Representative image showing growth of mutant (top left), control strain (top right), complemented mutant (bottom left), and overexpressed mutant (bottom right) on DMM agar.
Strains (in triplicates) were streaked on plates of DM agar containing 0.6% w/v mannitol and incubated at 37°C for 16 h to see if it was possible to observe a growth phenotype.
Strong growth was observed with the control strain (630Δ*erm*), the mutant (CT*mtlF*), the complemented mutant (*mtlF* comp), and the overexpressed mutant (*mtlF* overex). Differences in the abilities of the control strain, mutant, and complemented mutants to use mannitol could not be determined by this assay.

4.4.1.2 Growth in DM, DMM, and DMG broth

The addition of mannitol to the medium allowed 630Δ*erm* (control strain) to exhibit a significant increase in growth from 6 h until 12 h compared to when it was in DM alone. At 8 h (peak growth in DMM), OD_{600} levels of 630Δ*erm* in DM were 0.36, while in DMM they were 0.78 (630Δ*erm* in DM vs. 630Δ*erm* in DMM at 8 h **** $P < 0.0001$). Slope of the curve 2-8 h in DMM = 2.55 (Fig. 4.37).

The mutant, CT*mtlF*, unlike the control strain, showed, at 6-8 h, an inability to utilise mannitol to the same extent as the control strain, with OD_{600} levels at 8 h, for example, at 0.35 in DM, and 0.38 in DMM (** $P < 0.002$). At 10-12 h, there was an increase in OD_{600} levels in DMM in comparison to when CT*mtlF* was in plain DM (e.g. at 12 h OD_{600} in DM was 0.39, in DMM it was 0.49) (**** $P < 0.0001$). Slope of the curve 2-8 h in DMM = 1.19, 2-24 h in DMM = 1.44 (Fig. 4.37).

At 24 h of incubation, there was an upsurge in CT*mtlF* growth in DMM to an OD_{600} of 0.84 (in DM alone it remained at 0.46). This represented a highly significant increase in OD_{600} from the previous time point (**** $P < 0.0001$) (Fig. 4.37).

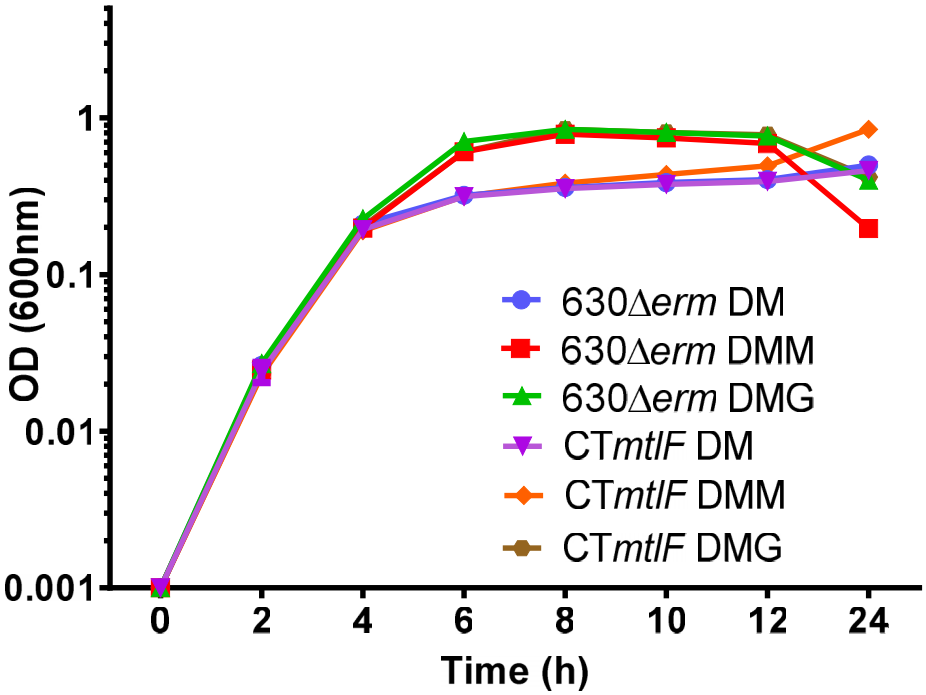

Figure 4.37: Role of *mtlF* in the growth of *C. difficile* 630Δ*erm* in DM.
630Δ*erm* (control strain) and CT*mtlF* (mutant) were incubated for 24 h at 37°C. 1mL extracts (triplicates) were taken at regular time points and the OD_{600} measured. CT inactivation of *mtlF* partially inhibited growth in DMM (in comparison to the control strain) up to 24 h, but the decline of CT*mtlF* in DMM was much less pronounced than when it was in DM, and much less than the control strain in DM and DMM.
630Δ*erm* slope of the curve 2-8 h in DMM = 2.55.
CT*mtlF* slope of the curve 2-8 h in DMM = 1.19, 2-24 h in DMM = 1.44.
One-way ANOVA was used to determine statistical significance.
630Δ*erm* in DM vs. 630Δ*erm* in DMM at 8 h **** $P < 0.0001$.
CT*mtlF* at 12 h in DM vs. DMM **** $P < 0.0001$.

Complementing CT*mtlF* using the native promoter (*Pmtl*) of *mtlF*, permitted an increase in growth levels when in the presence of mannitol (DMM) compared to when not in mannitol (DM). This represented a partial restoration of the level and timing of mannitol uptake as had been seen with the control strain, 630Δ*erm*. For example, from 8 h, *mtlF* comp showed an ability to utilise mannitol with the significantly higher OD_{600} observed in DMM (0.45) compared to those observed in DM (0.35) (**** $P < 0.0001$). At 12 h, OD_{600} in DM was 0.39, while in DMM

it was 0.64 (**** P < 0.0001). Slope of the curve 2-24 h in DMM = 1.28 (Fig. 4.38).

mtlF overex, the mutant with *mtlF* overexpressed using the *fdx* promoter, also displayed a partially restored ability to use mannitol. At 8 h, OD_{600} in DM was 0.38, in DMM it was 0.48 (*** P < 0.0004). By 12 h, the disparity in OD_{600} had widened with the optical density reaching 0.39 in DM and 0.53 in DMM (**** P < 0.0001) Slope of the curve 2-24 h in DMM = 1.36 (Fig. 4.38).

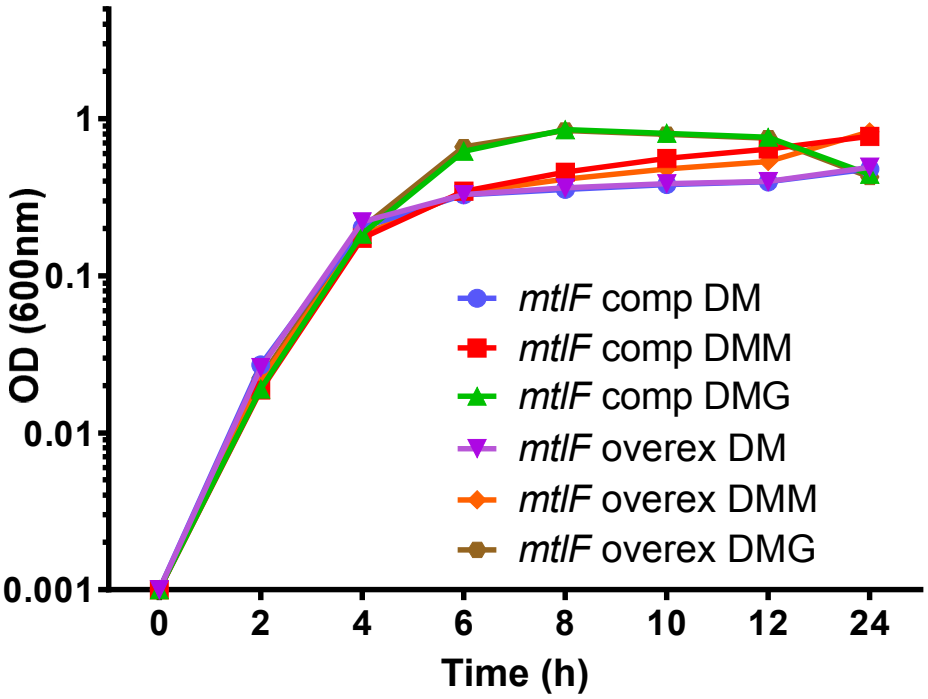

Figure 4.38: Role of *mtlF* in the growth of *C. difficile* 630Δ*erm* in DM.
mtlF comp (complemented mutant) and *mtlF* overex (overexpressed mutant) were incubated for 24 h at 37°C. 1mL extracts (triplicates) were taken at regular time points and OD_{600} measured.
Mannitol-induced increases in growth were partially restored up to 8 h with *mtlF* comp (**** P < 0.0001) and *mtlF* overex (*** P < 0.0004) exhibiting highly significant increases in DMM at 8 h (in comparison to when in DM), unlike CT*mtlF* at that time point (Fig. 4.37).
mtlF comp slope of the curve 2-8 h in DMM = 1.46, 2-24 h in DMM = 1.28.
mtlF overex slope of the curve 2-8 h in DMM = 1.3, 2-24 h in DMM = 1.36.
One-way ANOVA was used to determine statistical significance.
mtlF comp at 8 h DM vs. DMM **** P < 0.0001.
mtlF overex at 8 h DM vs. DMM *** P < 0.0004.

4.4.1.3 HPLC evaluation of mannitol/glucose consumption in DM

HPLC analysis was undertaken to determine the exact level of mannitol uptake by the control strain, 630Δ*erm*, mutant (CT*mtlF*), and complemented mutants (*mtlF* comp and *mtlF* overex).

Mannitol was consumed rapidly by 630Δ*erm*, within 8 h of incubation (630Δ*erm* 0 h vs. 8 h **** $P < 0.0001$), but while the mutant exhibits nowhere near the same level of uptake up to 12 h; by 24 h, there was almost no mannitol remaining in the CT*mtlF* culture. Complementing the mutant using the native promoter (*Pmtl*) of *mtlF* (*mtlF* comp) and overexpressing the gene using the *fdx* promoter (*mtlF* overex) increased mannitol uptake (Fig. 4.39).

At 12 h, 630Δ*erm* differed significantly from the other strains in that all of the available mannitol had been spent, but this was especially noticeable when comparing 630Δ*erm* with CT*mtlF* (630Δ*erm* vs. CT*mtlF* at 12 h **** $P < 0.0001$). Slope of the curve 0-8 h for 630Δ*erm* = 5.71 (Fig. 4.39).

At 12 h, the mutant, with 7.31mM residual mannitol, differs significantly from the complements with *mtlF* comp 3.45mM (** $P < 0.008$) and *mtlF* overex 6.14mM mannitol (* $P < 0.05$) (Fig. 4.39).

CT*mtlF* slope of the curve 0-8 h = 1.46, 0-24 h = 2.33. *mtlF* comp slope of the curve 0-8 h = 1.89, 0-24 h = 2.33. *mtlF* overex slope of the curve 0-8 h = 1.13, 0-24 h = 2.16 (Fig. 4.39).

At 24 h, each strain had used almost all of the available mannitol, but with the CT*mtlF*, *mtlF* comp, and *mtlF* overex samples some residual mannitol was detected (0.007, 0.006, and 0.002mM respectively) (Fig. 4.39).

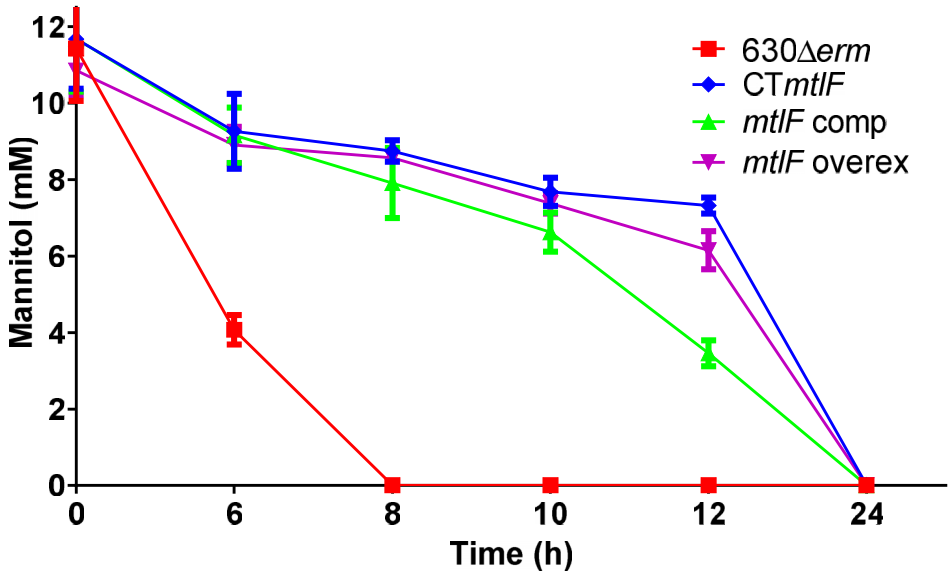

Figure 4.39: HPLC evaluation of mannitol uptake in DM by 630Δ*erm* (control), CT*mtlF* (mutant), and the complemented mutants (*mtlF* comp and *mtlF* overex).
Extracts (triplicates) from the growth assay were used to determine by HPLC the exact amount of sugar remaining in the medium at each time point.
The control strain had used all of the mannitol by 8 h. This was not seen with the mutant and the complements until 24 h.
630Δ*erm* slope of the curve 0-8 h = 5.71.
CT*mtlF* slope of the curve 0-8 h = 1.46, 0-24 h = 2.33.
mtlF comp slope of the curve 0-8 h = 1.89, 0-24 h = 2.33.
mtlF overex slope of the curve 0-8 h = 1.13, 0-24 h = 2.16.
One-way ANOVA was used to determine statistical significance.
mtlF comp vs. CT*mtlF* at 12 h ** $P < 0.008$.
mtlF overex vs. CT*mtlF* at 12 h * $P < 0.05$.

Glucose levels were depleted by each strain, as was expected, between 0 h and 24 h (**** $P < 0.0001$). No differences in glucose uptake emerged between the strains, indicating that interrupting *mtlF* produced no effect on glucose metabolism (Fig. 4.40).

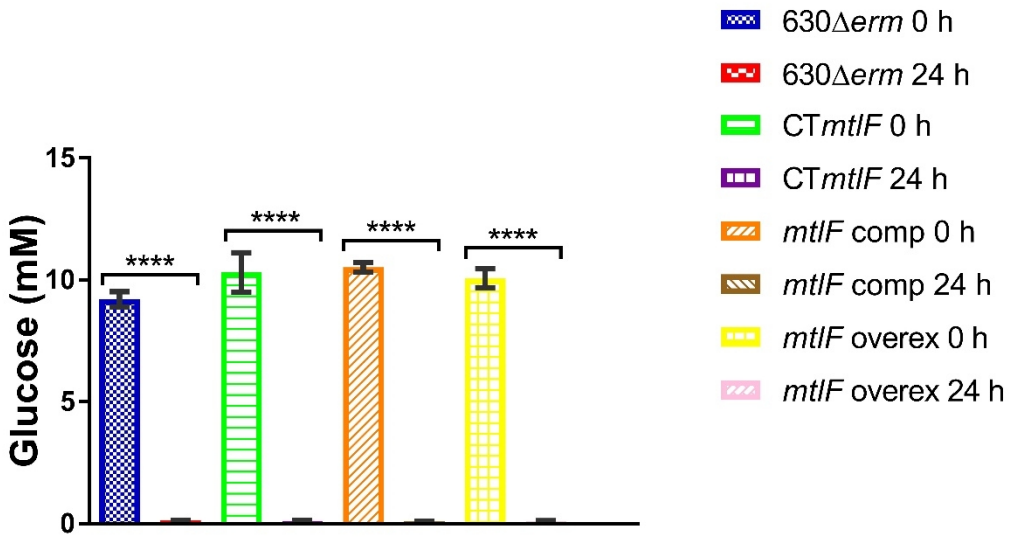

Figure 4.40: HPLC evaluation of glucose uptake in DM by 630Δ*erm* (control strain), CT*mtlF* (mutant), and the complemented mutants (*mtlF* comp and *mtlF* overex).
Extracts (triplicates) from the growth assay were used to determine by HPLC the exact amount of sugar remaining in the medium at the start and end of the assay. Glucose was utilised by each strain between 0 h and 24 h (**** $P < 0.0001$). One-way ANOVA was used to determine statistical significance.

4.4.1.4 Growth in TY, TYM, and TYG

From 10 h, the presence of mannitol in the medium allowed the control strain to maintain a higher OD_{600}. At 24 h, OD_{600} in TY was 0.28 (from a peak of 0.9 at 12 h), while in TYM it was 1.02 (peak growth). 630Δ*erm* in TY at 12 h (peak growth) vs. 630Δ*erm* at 24 h (peak growth) in TYM at 12 h * $P < 0.04$ (Fig. 4.41).

Mutant OD_{600} levels revealed no increase in growth up to 24 h when comparing the mutant in TY and TYM. For example, at peak growth, which was 24 h, CT*mtlF* OD_{600} in TY was 0.9, while in TYM it was 0.85 (Fig. 4.41).

At 48 h and 72 h, mutant OD_{600} levels declined more gradually in TYM than TY. An example being at 48 h when OD_{600} in TY was 0.54, while in TYM it was 0.69 (* $P < 0.05$) (slope of the graph (downward) 24-72 h: in TY = 4, in TYM = 2.6) (Fig. 4.41).

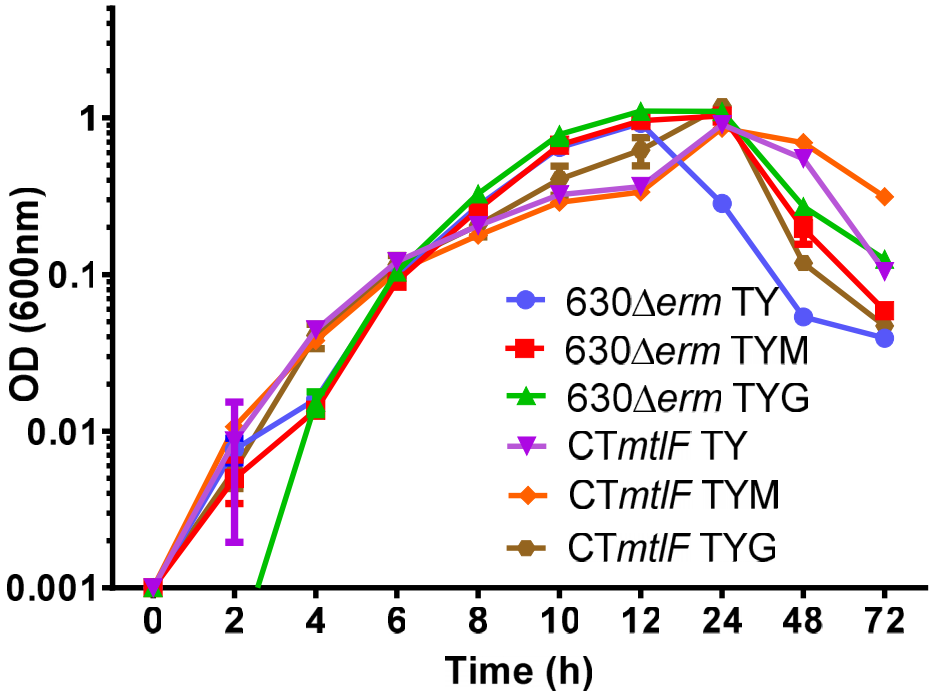

Figure 4.41: Role of *mtlF* in the growth of *C. difficile* 630Δ*erm* in TY.
630Δ*erm* (control strain) and CT*mtlF* (mutant) were incubated in TY with and without mannitol/glucose for 72 h at 37°C. 1mL extracts (triplicates) were taken at regular time points and the OD_{600} measured.
CT inactivation of *mtlF* completely inhibited growth in TYM up to 24 h, but the decline of CT*mtlF* in TYM was much less pronounced than the mutant in TY, and the parent in TY and TYM at 48 h and 72 h.
CT*mtlF* slope (downward) 24-72 h: TY = 4, TYM = 2.6.
One-way ANOVA was used to determine statistical significance.
630Δ*erm* TY vs. TYM at 12 h * $P < 0.04$.

Similarly to CT*mtlF*, growth of *mtlF* comp in TY reached, at 12 h, an OD_{600} of 0.32, and exhibited no increase in TYM until 24 h (peak growth in TY and TYM) with OD_{600} levels in TY at 0.79 and TYM 0.85 (** $P < 0.0017$). From 24-72 h, there was a more gradual OD_{600} decline in TYM than in TY. An example being at 48 h when OD_{600} in TY was 0.4, while in TYM it was 0.5 (* $P < 0.034$) (slope of the graph (downward) 24-72 h: in TY = 3.3, in TYM = 2.2) (Fig. 4.42).

mtlF overex exhibited a comparable trend (to CT*mtlF* and *mtlF* comp) with an OD_{600} of 0.37 in TY at 12 h, exhibiting no increase in TYM until 24 h (peak

growth in TY and TYM) which became significant at 48 h with OD_{600} levels at 0.39 in TY and at 0.72 in TYM (* P < 0.03), and declining more gradually in TYM than in TY (slope of the graph (downward) 24-72 h, in TY = 3.15, in TYM = 2.2) (Fig. 4.42).

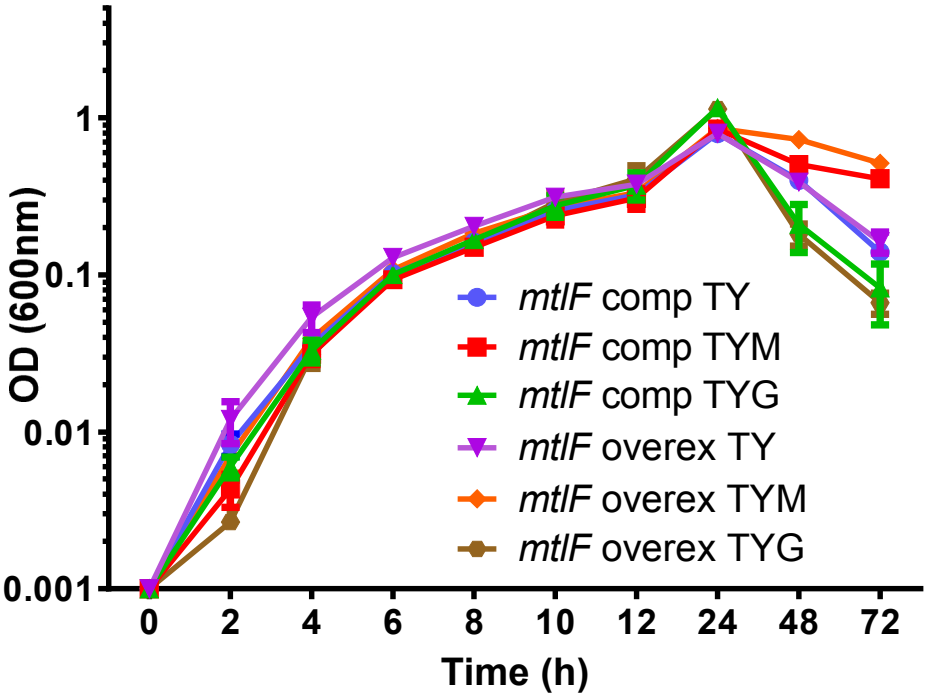

Figure 4.42: Role of *mtlF* in the growth of *C. difficile* 630Δ*erm* in TY.
mtlF comp (control strain) and *mtlF* overex (overexpressed mutant) were incubated for 72 h at 37°C. 1mL extracts (triplicates) were taken at regular time points and the OD_{600} measured.
Restoration of *mtlF* allowed both of the complemented strains to decline after 24 h at a slightly more gradual rate than was seen with the mutant (Fig. 4.41).
mtlF comp slope 24-72 h: TY = 3.3, TYM = 2.2.
mtlF overex slope 24-72 h, TY = 3.15, TYM = 2.2.
One-way ANOVA was used to determine statistical significance.
mtlF comp at 24 h TY vs. TYM ** P < 0.0017.
mtlF comp at 48 h TY vs. TYM * P < 0.034.
mtlF overex at 48 h TY vs. TYM * P < 0.03.

4.4.1.5 Cytotoxicity of 630Δ*erm*, 630Δ*erm*_CT*mtlF*, and complements

The control strain, 630Δ*erm*, in mannitol exhibited a significantly reduced level of toxin secretion compared to when it was in TY alone, going from a toxin titre of 3.5 x 10^4 in TY to 0 in TYM (630Δ*erm* TY vs. 630Δ*erm* TYM **** $P < 0.0001$) (Fig. 4.43).

Mannitol-induced reduction of toxin levels was observed with the mutant, CT*mtlF*, but to nowhere near the same amount as the control strain. The toxin levels of CT*mtlF* went from a toxin titre of 1.1 x 10^3 in TY to 1.1 x 10^2 in TYM, which was considered highly significant (**** $P < 0.0001$) (Fig. 4.43).

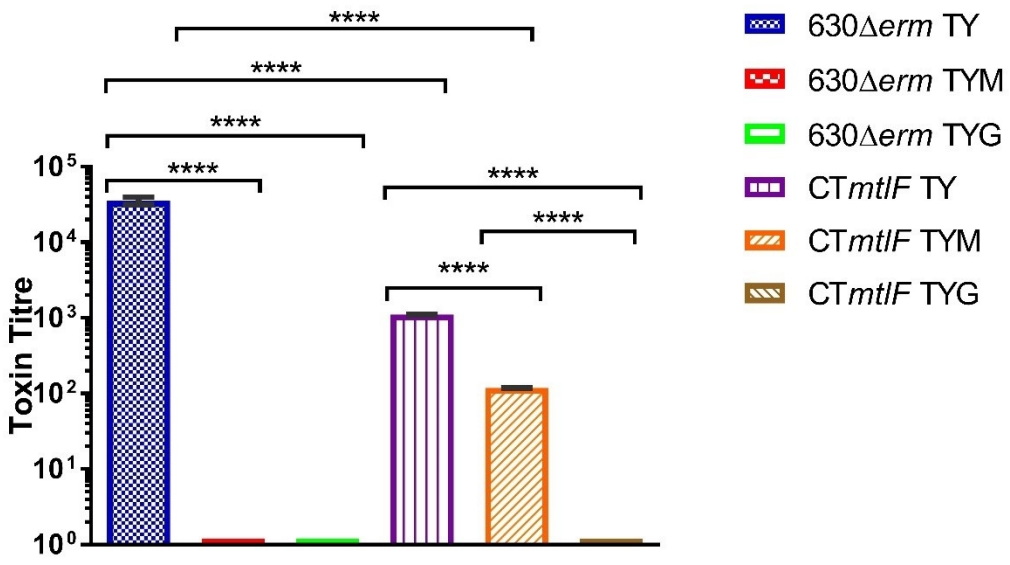

Figure 4.43: Role of *mtlF* in *C. difficile* 630Δ*erm* toxin expression at 24 h in TY.
Cytotoxicity of CT*mtlF* at 24 h incubation. Serial dilutions (10^0-10^{-9}) of bacterial supernatants (triplicates) were applied to Vero cell monolayers (p33) to determine the toxin titre of the control strain (630Δ*erm*) and the mutant (CT*mtlF*).
Unlike the control strain in mannitol, toxin levels showed a restorative trend with CT*mtlF* in mannitol.
One-way ANOVA was used to determine statistical significance.
630Δ*erm* TY vs. 630Δ*erm* TYM **** $P < 0.0001$.
CT*mtlF* TY vs. CT*mtlF* TYM **** $P < 0.0001$.

mtlF comp and *mtlF* overex toxin levels remained at a toxin titre of 1.2 x 10^3 in TY and 1.1 x 10^3 in TYM for both strains (no significant change). Glucose suppressed toxin production in both strains (Fig. 4.44).

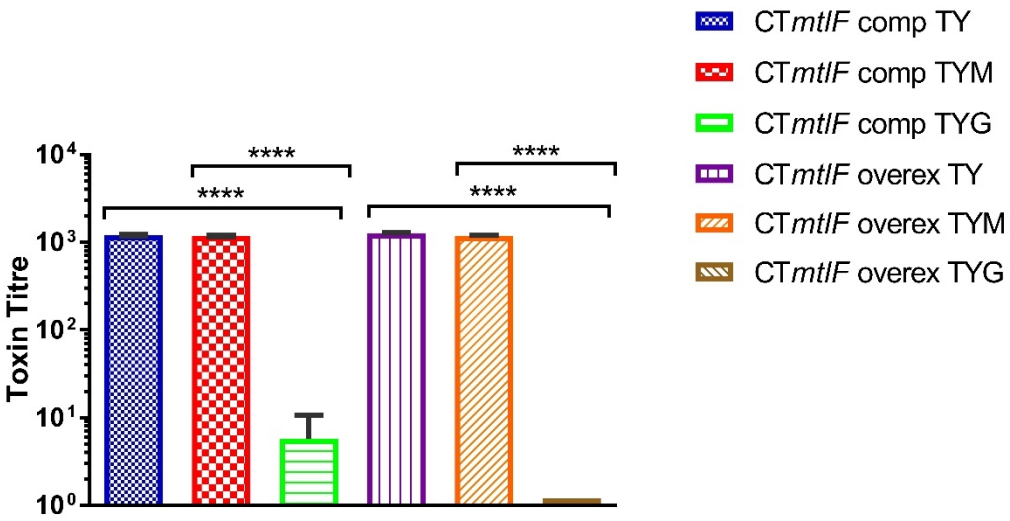

Figure 4.44: Role of *mtlF* in *C. difficile* 630Δ*erm* toxin expression at 24 h in TY.
Cytotoxicity of the *mtlF* complements at 24 h incubation. Serial dilutions (10^0-10^{-9}) of bacterial supernatants (triplicates) were applied to Vero cell monolayers (p33) to determine the toxin titre of the complemented mutant (*mtlF* comp) and the mutant (*mtlF* overex).
Complete restoration of toxin levels was seen with *mtlF* comp and *mtlF* overex in mannitol.
One-way ANOVA was used to determine statistical significance.

At 48 h, there was a trend towards a reduction in toxin levels with the control strain in TYM, when compared to when it was in TY, going from an average of 7.3 x 10^5 (with variance) to 6.0 x 10^1 (**** $P < 0.0001$). With the mutant, CT*mtlF*, toxin levels in TY were 1.8 x 10^4, which was above those in TYM at 1.4 x 10^3 (**** $P < 0.0001$). Mutant toxin levels in TYM were significantly above those of the control strain in TYM (**** $P < 0.0001$) (Fig. 4.45).

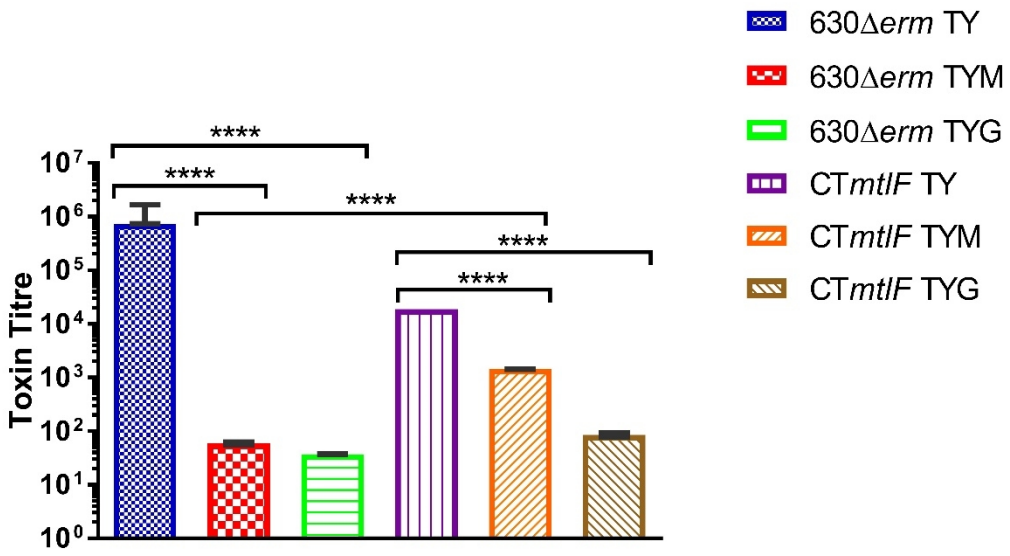

Figure 4.45: Role of *mtlF* in *C. difficile* 630Δ*erm* toxin expression at 48 h in TY.
Cytotoxicity of CT*mtlF* at 48 h incubation. Serial dilutions (10^{0}-10^{-9}) of bacterial supernatants (triplicates) were applied to Vero cell monolayers (p33) to determine the toxin titre of the control strain (630Δ*erm*) and the mutant (CT*mtlF*).
A trend towards restoration of toxin production in mannitol was seen with CT*mtlF* in mannitol.
One-way ANOVA was used to determine statistical significance.
630Δ*erm* TY vs. TYM **** $P < 0.0001$.
CT*mtlF* TY vs. TYM **** $P < 0.0001$.
630Δ*erm* TYM vs. CT*mtlF* TYM **** $P < 0.0001$.

At 48 h, *mtlF* comp toxin levels in TY were at titre of 1.7 x 10^4 (with variance), while in TYM they were 1.9 x 10^3. *mtlF* overex toxin levels fell from a titre of 2.5 x 10^4 in TY to 1.3 x 10^3 in TYM (*** $P < 0.00013$) (Fig. 4.46).

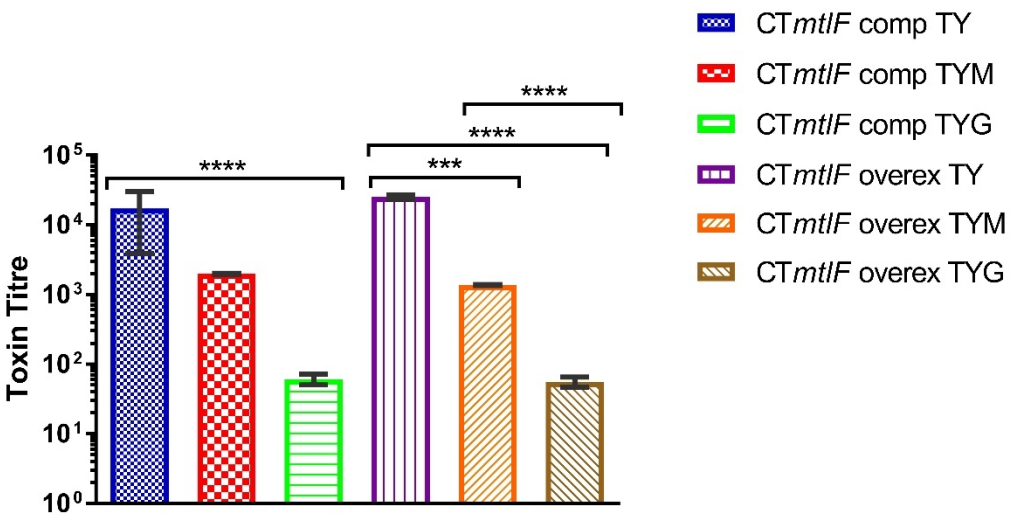

Figure 4.46: Role of *mtlF* in *C. difficile* 630Δ*erm* toxin expression at 48 h in TY.
Cytotoxicity of the *mtlF* complements at 48 h incubation. Serial dilutions (10^0-10^{-9}) of bacterial supernatants were applied to Vero cell monolayers (p33) to determine the toxin titre of the complemented mutant (*mtlF* comp) and the overexpressed mutant (*mtlF* overex).
mtlF overex exhibited a significant decrese in toxicity in TYM (*** $P < 0.0013$). Neither complemented mutant exhibited the level of toxin suppression seen with 630Δ*erm* (Fig. 4.45).
One-way ANOVA was used to determine statistical significance.
mtlF overex TY vs. TYM *** $P < 0.0013$.

At 72 h, 630Δ*erm* cytotoxicity in TYM was, at a titre of 1.6×10^2, below that seen in TY at 2.5×10^6 (**** $P < 0.0001$). With the mutant, this was not so clearly observed, with CT*mtlF* toxin levels dropping from 9.6×10^5 in TY to 3.4×10^5 in TYM (** $P < 0.003$). Mutant toxin levels in TYM were significantly above those of the control strain in TYM (**** $P < 0.0001$) (Fig. 4.47).

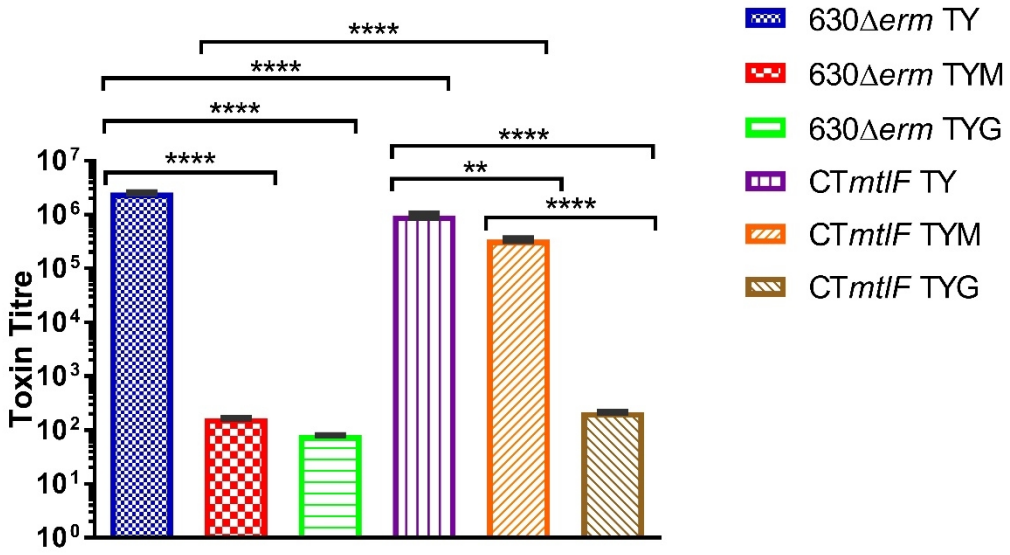

Figure 4.47: Role of *mtlF* in *C. difficile* 630Δ*erm* toxin expression at 72 h in TY.

Cytotoxicity of CT*mtlF* at 72 h incubation. Serial dilutions (10^0-10^{-9}) of bacterial supernatants (triplicates) were applied to Vero cell monolayers (p33) to determine the toxin titre of the parent (630Δ*erm*) and the mutant (CT*mtlF*).

A significant restoration of toxin levels in TYM was seen with CT*mtlF*. Unlike 630Δ*erm*, CT*mtlF* showed a much reduced ability to suppress *C. difficile* toxin production in mannitol.

One-way ANOVA was used to determine statistical significance.

630Δ*erm* TY vs. TYM **** $P < 0.0001$.

CT*mtlF* TY vs. TYM **** $P < 0.003$.

630Δ*erm* TYM vs. CT*mtlF* TYM **** $P < 0.0001$.

Toxin levels of *mtlF* comp and *mtlF* overex were very similar in TY. In TY both strains had a toxin titre of 5.1 x 10^5 (*mtlF* comp) (with some variance) and 5.6 x 10^5 (*mtlF* overex), and in TYM the toxin titre fell to 2.4 x 10^4 (*mtlF* comp) and 1.9 x 104^4 (*mtlF* overex) (*mtlF* overex TY vs. TYM **** $P < 0.0001$) (Fig. 4.48).

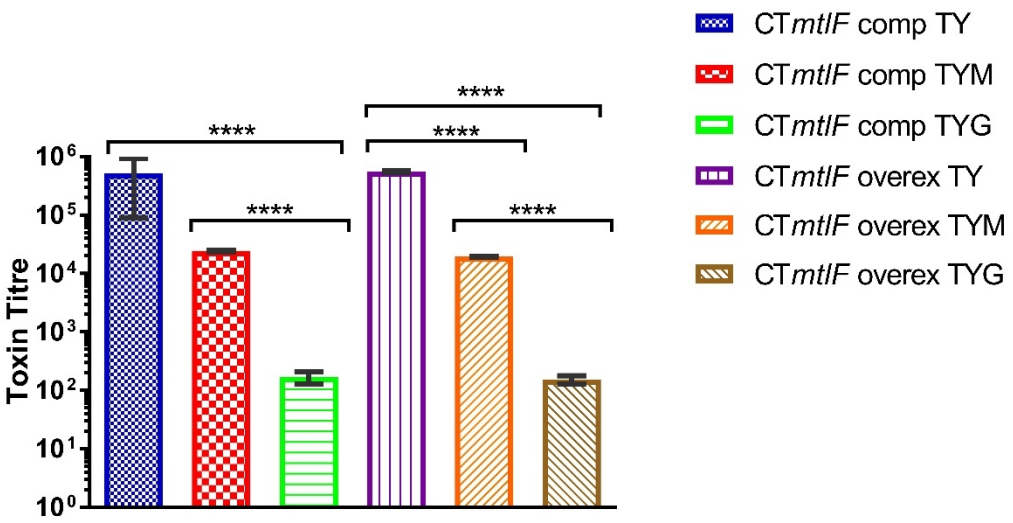

Figure 4.48: Role of *mtlF* in *C. difficile* 630 toxin expression at 72 h in TY.
Cytotoxicity of *mtlF* comp and *mtlF* overex at 72 h incubation. Serial dilutions (10^{0}-10^{-9}) of bacterial supernatants (triplicates) were applied to Vero cell monolayers (p33) to determine the toxin titre of the complemented mutant (*mtlF* comp) and the overexpressed mutant (*mtlF* overex).
A trend towards a partial restoration of toxin suppression in TYM was seen with *mtlF* overex when comparing it to the mutant.
One-way ANOVA was used to determine statistical significance.
mtlF overex TY vs. TYM **** $P < 0.0001$.

4.4.1.6 Motility assays

Four variant motility assays were performed in order to elucidate the possible role of *mtlF* in *C. difficile* 630 motility. *C. difficile* 630Δ*erm*_CT*fliC* and *C. difficile* M120 were used as the negative controls.

4.4.1.6.1 Motility assays on YT +glucose

The control strain (630Δ*erm*) produced a larger zone of motility (5.9cm zone diameter) than what was observed with the mutant (CT*mtlF*) (4cm zone diameter) (Fig. 4.49) and the complemented mutants (*mtlF* comp -1.3cm zone diameter and *mtlF* overex -1.3cm) (not shown). M120 was used as the negative control strain, and exhibited reduced motility in comparison to the parent, the mutant, and the complemented mutants (not shown).

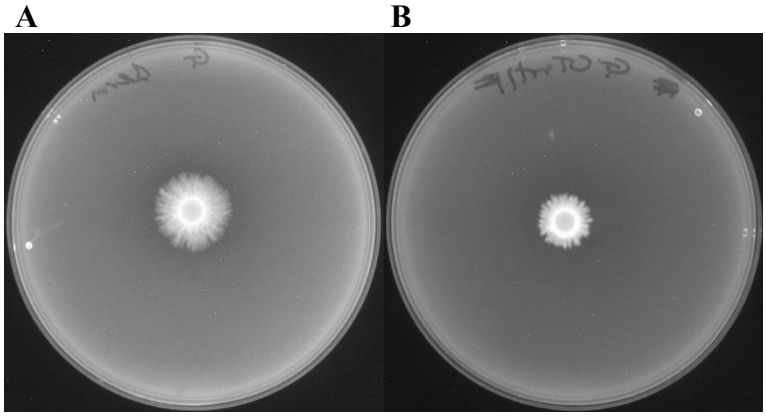

Figure 4.49: Representative images of motility assays showing control strain (A) and mutant (B) on YTG.
2µL of each strain (in triplicates) was spotted onto plates of YTG agar containing 1% w/v glucose and incubated at 37°C for 48 h to see if it was possible to observe a difference in motility.
The control strain (630Δ*erm*) showed greater motility than was seen with the mutant (CT*mtlF*).

4.4.1.6.2 Motility assays on YT +mannitol

630Δ*erm* exhibited the largest zone of motility on the plates with a diameter of 1.3cm. CT*mtlF* exhibited good, but less motility (1cm zone diameter) in comparison to 630Δ*erm*. *mtlF* comp (1.1cm zone diameter) and *mtlF* overex (1.2cm zone diameter) showed similar zones of motility to CT*mtlF*, which were still smaller than 630Δ*erm* (Fig. 4.50). CT*fliC* was used as the negative control, and exhibited reduced motility in comparison to the parent, the mutant, and the complemented mutants (not shown).

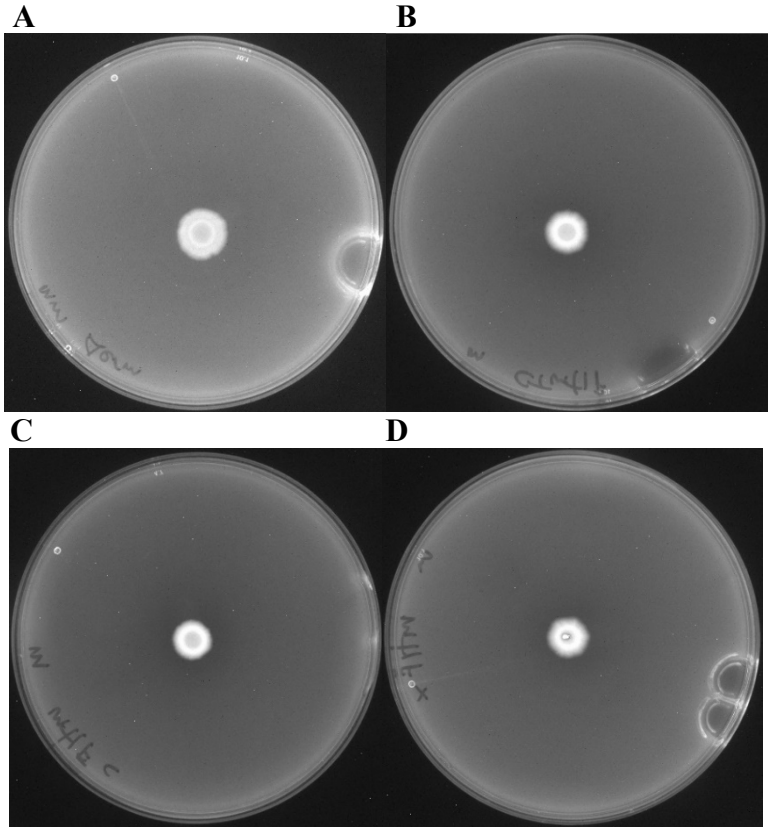

Figure 4.50: Representative images of motility assays showing zones of motility of control strain (A), mutant (B), complemented mutant (C), and overexpressed mutant (D) on YTM.
2µL of each strain (in triplicates) was spotted onto plates of YTM agar containing 1% w/v mannitol and incubated at 37°C for 48 h to see if it was possible to observe a difference.
The control strain (630Δ*erm*) showed the biggest zone of motility. Slight inhibition (in comparison) was observed with the mutant (CT*mtlF*), the complemented mutant (*mtlF* comp), and the overexpressed mutant (*mtlF* overex).

4.4.1.6.3 Motility assays on BHIS +top agar

BHIS +top agar was used to determine potential differences in motility between 630Δ*erm* and CT*mtlF* (and the complemented mutants –not shown). No differences were observed with each strain showing a similar zone of motility (630Δ*erm*, 1cm; CT*mtlF*, 0.9cm; *mtlF* comp, 1cm; *mtlF* overex, 1cm). CT*fliC* was used as the negative control, and exhibited reduced motility (0.7cm zone diameter) in comparison to the control strain, the mutant (Fig 4.51), and the complemented mutants (not shown).

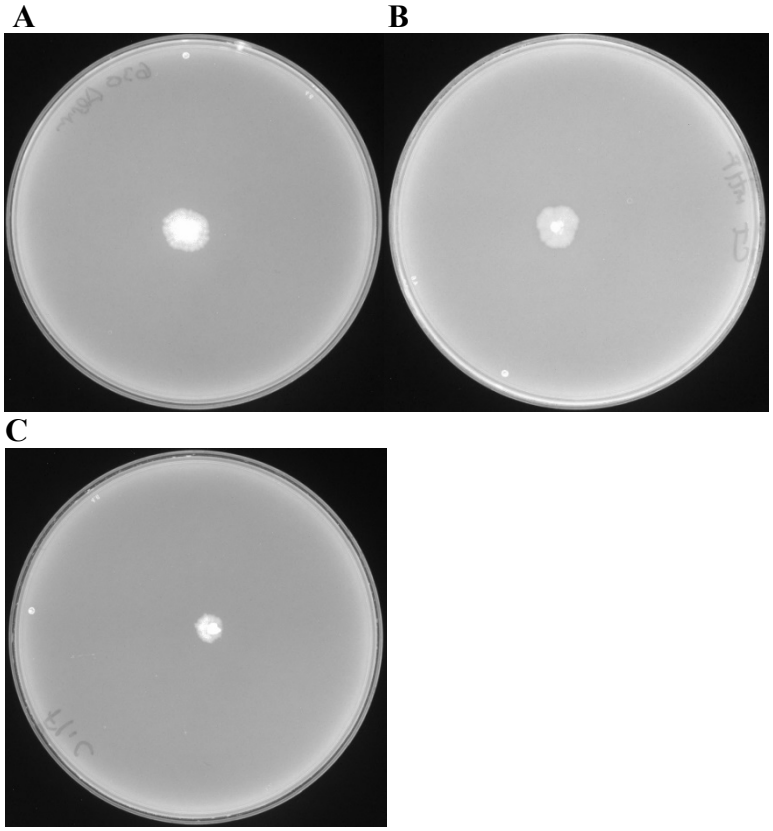

Figure 4.51: Representative images showing motility assays on top agar showing control strain (A), mutant (B), and negative control, CT*fliC* (C).
The surface of the top agar was pierced with a single colony of each strain (in triplicates) and incubated at 37°C for 48 h to see if it was possible to observe a difference in motility.
No differences were observed between the control strain (630Δ*erm*) and the mutant (CT*mtlF*) with similar zones of motility seen with both strains.

4.4.1.6.4 Motility assays in tubes

Motility assays in glass tubes were prepared using the same medium as was used for the top layer medium on the BHIS +top layer agar plates. No differences could be observed between 630Δ*erm* and CT*mtlF* (and the complemented mutants –not shown) with each strain exhibiting good turbidity and migrating (11cm) from the point of inoculation to the base of the tubes. *C. difficile* M120 was used as the negative control, showed growth at the very top of the tubes, but exhibited no turbidity, and did not migrate any distance through the agar (Fig. 4.52).

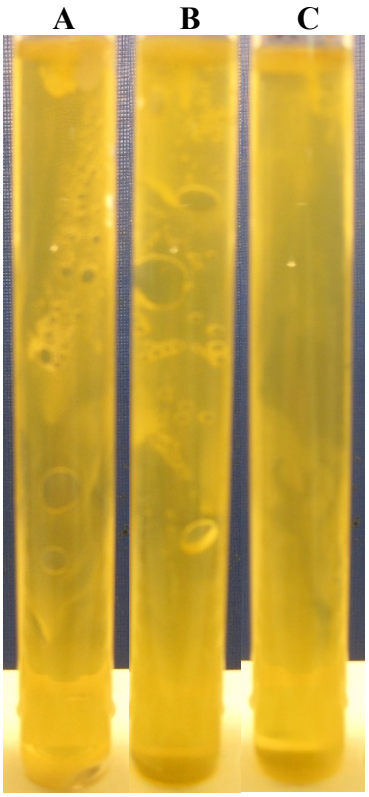

Figure 4.52: Representative images of motility assays showing migration of control strain (A) and mutant (B) through the agar in the tubes. The negative control, M120 (C), did not migrate.
The surface of the agar was pierced with a single colony of each strain (in triplicates) and incubated at 37°C for 24 h to see if it was possible to observe a difference in motility.
The control strain (630Δ*erm*) and the mutant (CT*mtlF*) both exhibited strong growth and migrated to the base of the tubes (11cm), while the negative control (M120) did not migrate any distance.

4.5 Investigation and Characterisation of PTS^{Mtl} Regulator -MtlR

mtlR was targeted for CT mutagenesis (Fig. 4.53) and the resultant mutant complemented in order to observe the effects of inactivating and restoring this putative regulatory gene on mannitol uptake, general growth,cytotoxicity, and motility.

4.5.1 Characterisation of 630Δ*erm*_CT*mtlR* (CD630_2333) and complements

CT insertion into *mtlR* was determined by screening erythromycin-resistant *C. difficile* 630Δ*erm*Δ*pyrE* colonies (potential CT mutants) via PCR with primers specific for the target gene as well as the CT insertion, running the PCR products

on 1% w/v agarose gel, and then comparing the fragment sizes for the parent (2.51 kb) and the mutant (4.31 kb) (Fig. 4.53). Southern blotting confirmed that the CT insertion had occurred in a single location (Fig. 4.32, Table 4.2).

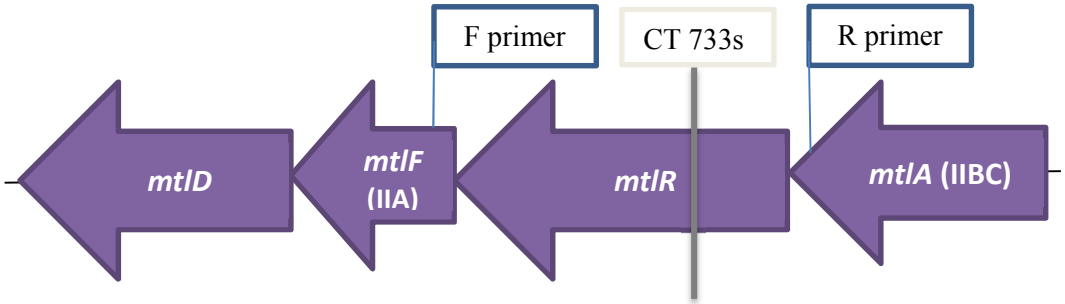

Figure 4.53: Position within the putative PTS^{Mtl} at loci CD630_2331-4 of the gene of interest, *mtlR*, the CT insertion into the gene, and the primers used to test for the insertion.
Primers, specific for the regions immediately outside of the predicted CT insertion site in *mtlR*, were used to amplify colonies from Erm-resistant colonies to screen for the insertion on 1% w/v agarose.

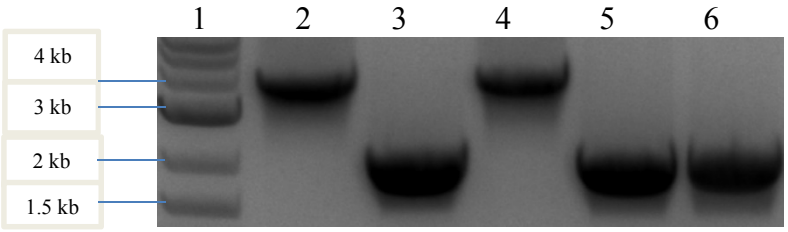

Figure 4.54: PCR screening for CT insertion into CT*mtlR*.
Primers specific for the regions immediately outside of the predicted CT insertion site in *mtlR* were used to screen for the insertion on 1% w/v agarose. Table 4.4 below shows the lane order.

Table 4.4: Content of each well when showing by PCR the CT insertion in CT*mtlR*.

Well	Content	Size (kb)
1	Marker	
2	CT*mtlR* mut. A, F + R primer	4.31
3	CT*mtlR* mut. A, F + EBS primer	2.30
4	CT*mtlR* mut. B, F + R primer	4.31
5	CT*mtlR* mut. B, F + EBS primer	2.30
6	630Δ*erm*Δ*pyrE*, F + R primer	2.51

CT*mtlR* was later complemented at the *pyrE* locus using the native promoter (*Pmtl*) (*mtlR* comp) and an overexpression promoter (*fdx*) (*mtlR* overex). CT*mtlR* was also restored to *pyrE*-positive, so that each strain could be assayed in a *pyrE*-positive background. Complementation of CT*mtlR* was determined by amplifying by PCR genomic DNA isolated from CT*mtlR* colonies growing on MM (without uracil) with primers specific for the restored *pyrE* and which would also encompass the restored gene, running the PCR products on 1% w/v agarose gel, and then verifying the fragment sizes for *mtlR* complemented (*mtlR* comp) (3.46 kb) and *mtlR* overexpressed (*mtlR* overex) (2.81 kb) (Fig. 4.55). Sequencing (see Chapter 2 section 2.7.4) confirmed the restoration of *mtlR* and *pyrE*.

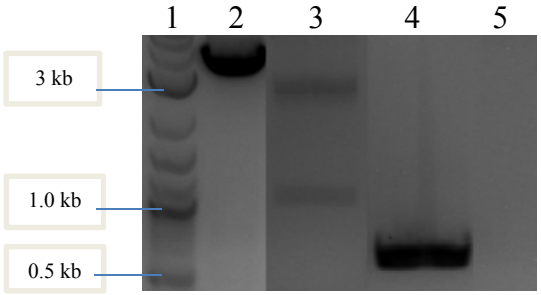

Figure 4.55: PCR screening for restoration of *mtlR* and *pyrE*.
Primers, specific for the regions immediately outside of the restored *pyrE*, were used to amplify DNA from MM plates without uracil to screen for the restoration of *mtlR +Pmtl* with *pyrE* (well 2), *mtlR +fdx* with *pyrE* (well 3), and *pyrE* alone (well 4); and compared to DNA isolated from the parental strain, 630Δ*erm*Δ*pyrE* (well 5). Table 4.5 below shows the lane order.

Table 4.5: Content of each well when showing by PCR the restoration of *mtlR*.

Well	Content	Size (kb)
1	Marker	
2	*mtlR* comp	3.46 (2.13 + 0.65 +0.68)
3	*mtlR* overex	3.01 (2.13 + 0.2 + 0.68)
4	CT*mtlR pyrE*+	0.68
5	630Δ*erm*Δ*pyrE*	-

4.5.1.1 Growth on DM agar

630Δ*erm*, CT*mtlR*, *mtlR* comp, and *mtlR* overex were streaked on DM (negative control -not shown) and DMM agar to see if there were any differences in growth.

Each strain showed strong growth with and without (not shown) mannitol, making it impossible to determine any differences in the ability of each strain to utilise mannitol on DMM agar (Fig. 4.56).

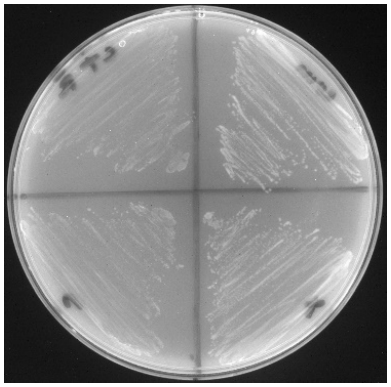

Figure 4.56: Representative image showing growth of mutant (top left), control strain (top right), complemented mutant (bottom left), and overexpressed mutant (bottom right) on DMM agar.
Strains (in triplicates) were streaked on plates of DMM agar containing 0.6% w/v mannitol and incubated at 37°C for 16 h to see if it was possible to observe a growth phenotype.
Strong growth was observed with the control strain (630Δ*erm*), the mutant (CT*mtlR*), the complemented mutant (*mtlR* comp), and the overexpressed mutant (*mtlR* overex) on DM (not shown) and DMM. It was not possible to determine differences in the ability to metabolise mannitol by this assay.

4.5.1.2 Growth in DM, DMM, and DMG broth

The addition of mannitol to the control strain (630Δ*erm*) medium (DMM) significantly increased growth levels, starting at the 6 h (*** $P < 0.0005$) incubation time, with the OD_{600} going from 0.31 in DM to 0.48 in DMM. At 8 h the greatest disparity was observed between growth in DM (OD_{600} of 0.36) and DMM (OD_{600} of 0.81 –peak growth) (**** $P < 0.0001$). Slope of the curve 0-8 h in DMM = 2.03 (see Fig. 4.57).

This was not observed with CT*mtlR*. Growth levels in DMM from 6-12 h slowly rose from an OD_{600} of 0.3 to 0.41 before peaking at 0.51 at 24 h. This was in strong contrast with 630Δ*erm* which showed a significant increase in growth at 8 h (630Δ*erm* vs. CT*mtlR* at 8 h in DMM **** $P < 0.0001$). Slope of the curve 0-8 h in DMM = 0.89, 0-24 h in DMM = 0.75 (Fig. 4.57).

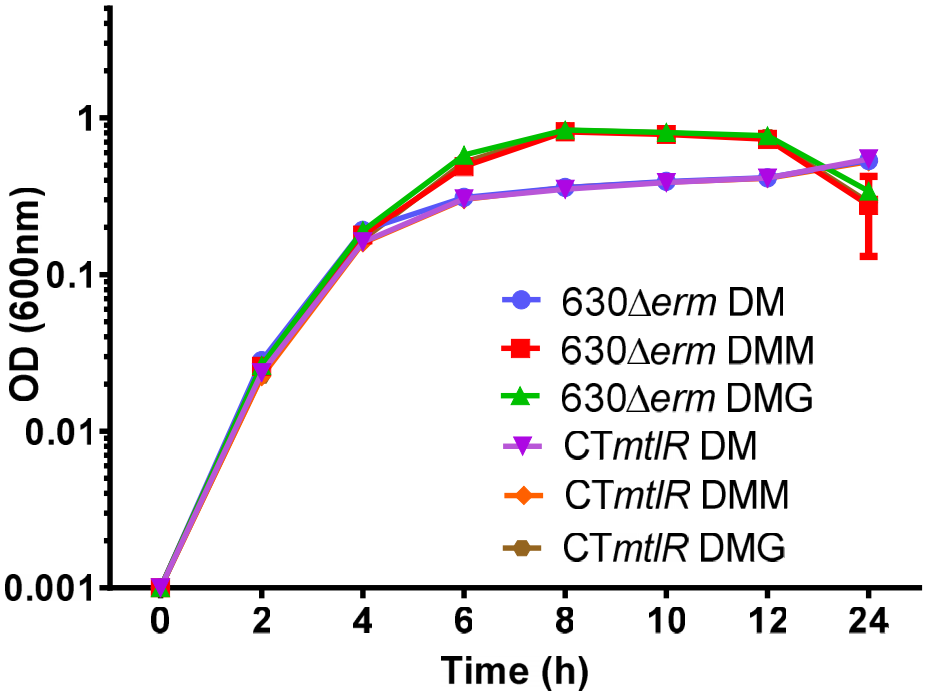

Figure 4.57: Role of *mtlR* in *C. difficile* 630Δ*erm* growth in DM.
630Δ*erm* (control strain) and CT*mtlR* (mutant) were incubated for 24 h at 37°C. 1mL extracts (triplicates) were taken at regular time points and the OD_{600} measured.
CT*mtlR* exhibited significantly attenuated growth levels in DMM in comparison to 630Δ*erm* in DMM (**** $P < 0.0001$) at 8 h, indicating that the mutant is unable to make use of the available mannitol.
630Δ*erm* slope of the curve 0-8 h in DMM = 2.03.
CT*mtlR* slope of the curve 0-8 h in DMM = 0.89, 0-24 h in DMM = 0.75.
One-way ANOVA was used to determine statistical significance.
630Δ*erm* at 6 h DM vs. DMM *** $P < 0.0005$.
630Δ*erm* vs. CT*mtlR* at 8 h in DMM **** $P < 0.0001$.

The complemented mutant (*mtlR* comp) at first (6, 8, and 10 h) exhibited a similar growth pattern to CT*mtlR*, with OD_{600} levels in DMM at 0.31, 0.36, and 0.4 respectively at these times. However, at 24 h there was an increase in OD_{600} levels (in comparison to CT*mtlR* in DMM and *mtlR* comp in DM alone) which increased considerably to 0.84 (*mtlR* comp in DMM vs. *mtlR* comp in DM at 24 h **** $P < 0.0001$; *mtlR* comp in DMM vs. CT*mtlR* in DMM at 24 h **** $P < 0.0001$), indicating a delayed, but, ultimately, complete restoration of mannitol

uptake by *mtlR* using the native promoter (*Pmtl*) in defined media. Slope of the curve 0-8 h in DMM = 0.92, 0-24 h = 1.2 (Fig. 4.58).

mtlR overex, overall, exhibited slightly (but not significantly) higher growth levels in mannitol than the control strain (630Δ*erm*). Like the control strain, *mtlR* overex already showed at 6 h a notable increase in growth in mannitol (OD_{600} 0.44) in comparison to when it was grown in DM alone (OD_{600} 0.3) (**** $P < 0.0001$), and, by 8 h (peak growth), a highly significant difference in growth was observed with *mtlR* overex at an OD_{600} of 0.83 in DMM, while merely at an OD_{600} of 0.35 in DM (**** $P < 0.0001$) Slope of the curve 0-8 h in DMM = 2.09 (see Fig. 4.58). The results indicated a complete and undelayed restoration of mannitol uptake by *mtlR* using the *fdx* promoter.

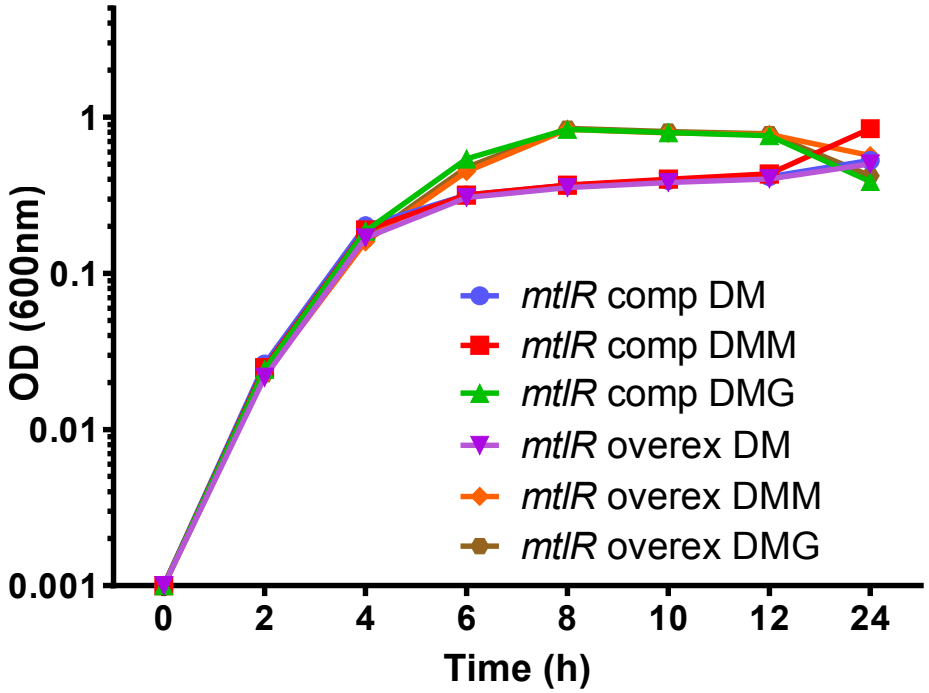

Figure 4.58: Role of *mtlR* in *C. difficile* 630Δ*erm* growth in DM.
mtlR comp (complemented mutant) and *mtlR* overex (overexpressed mutant) were incubated for 24 h at 37°C. 1mL extracts (triplicates) were taken at regular time points and the OD_{600} measured.
mtlR comp completely, but belatedly, restored mannitol-induced increases in growth levels (by 24 h). *mtlR* overex completely restored mannitol-induced increases in growth by 8 h (like the control strain).
mtlR comp slope of the curve 0-8 h in DMM = 0.92, 0-24 h = 1.2.
mtlR overex slope of the curve 0-8 h in DMM = 2.09.
One-way ANOVA was used to determine statistical significance.
mtlR comp in DM vs. DMM at 24 h **** $P < 0.0001$.
mtlR comp in DMM vs. CT*mtlR* in DMM at 24 h **** $P < 0.0001$.
mtlR overex in DM vs. DMM at 24 h **** $P < 0.0001$.
mtlR overex in DMM vs. CT*mtlR* in DMM at 24 h **** $P < 0.0001$.

4.5.1.3 HPLC evaluation of mannitol/glucose consumption in DM

At 6 h, uptake of mannitol in 630Δ*erm* (and *mtlR* overex) rapidly occurred. In the control strain mannitol levels diminished from 7.55mM at 0 h to 4.7mM at 6 h (*** $P < 0.0003$); while *mtlR* overex decreased from 7.14mM to 5.64mM (*** $P < 0.0004$). By 8 h incubation both strains had utilised all of the mannitol. 630Δ*erm* slope of the graph 0-8 h = 3.77. *mtlR* overex slope of the graph 0-8 h = 3.57 (Fig. 4.59).

mtlR comp (complemented mutant) mannitol levels from 0-12 h remained between 7.17 and 7.5mM. This was in stark contrast to 630Δ*erm* and *mtlR* overex at these time points (**** $P < 0.0001$). By 24 h, the level of mannitol in the *mtlR* comp samples had plummeted to 1.92mM, indicating uptake (73.7%) of the sugar had occurred between 12 h and 24 h (*mtlR* comp 12 h vs. 24 h **** $P < 0.0001$) *mtlR* comp slope of the graph 0-8 h = 0, 0-24 h = 0.87 (Fig. 4.59).

CT*mtlR* mannitol levels remained steady throughout the entire assay, ranging from 7.13mM at 0 h to 7.62mM at 24 h, indicating no uptake of the sugar (vs. 630Δ*erm* 8-24 h **** $P < 0.0001$; vs. *mtlR* overex 8-24 h **** $P < 0.0001$; vs. *mtlR* comp 24 h **** $P < 0.0001$). CT*mtlR* slope of the graph 0-8 h = 0, 0-24 h = 0 (Fig. 4.59).

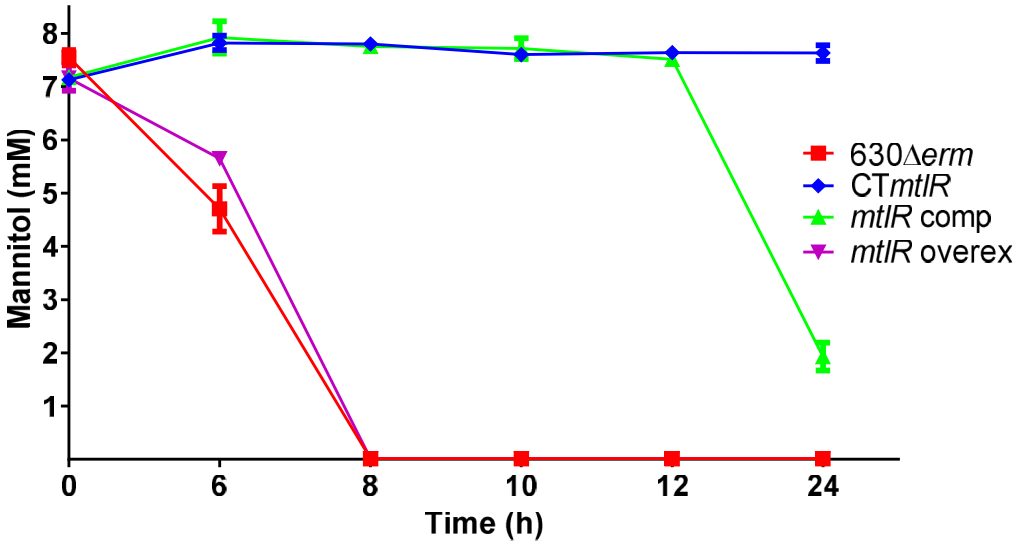

Figure 4.59: HPLC evaluation of mannitol uptake in DM by 630Δ*erm* (control strain), CT*mtlR* (mutant), and the complemented mutants (*mtlR* comp and *mtlR* overex).
Extracts (triplicates) from the growth assay in DM were used to determine by HPLC the exact amount of sugar remaining in the medium at each time point. The mutant, CT*mtlR*, was unable to use the available mannitol. 630Δ*erm* and *mtlR* overex had used all of the sugar by 8 h of incubation. *mtlR* comp, although unable to consume all of the sugar, by 24 h it had utilised most of the mannitol (73.7%).
630Δ*erm* slope of the graph 0-8 h = 3.77.
mtlR overex slope of the graph 0-8 h = 3.57.
mtlR comp slope of the graph 0-8 h = 0, 0-24 h = 0.87.
CT*mtlR* slope of the graph 0-8 h = 0, 0-24 h = 0.
One-way ANOVA was used to determine statistical significance.
630Δ*erm* 0 h vs. 6 h *** $P < 0.0003$.
mtlR overex 0 h vs. 6 h *** $P < 0.0004$.
mtlR comp 12 h vs. 24 h **** $P < 0.0001$.
CT*mtlR* vs. 630Δ*erm* 8-24 h **** $P < 0.0001$.
CT*mtlR* vs. *mtlR* overex 8-24 h **** $P < 0.0001$.
CT*mtlR* vs. *mtlR* comp 24 h **** $P < 0.0001$.

Glucose levels were depleted by each strain, as was expected, between 0 h and 24 h (**** $P < 0.0001$). No differences emerged between the strains, indicating that interrupting *mtlR* produced no effect on glucose metabolism (Fig. 4.60).

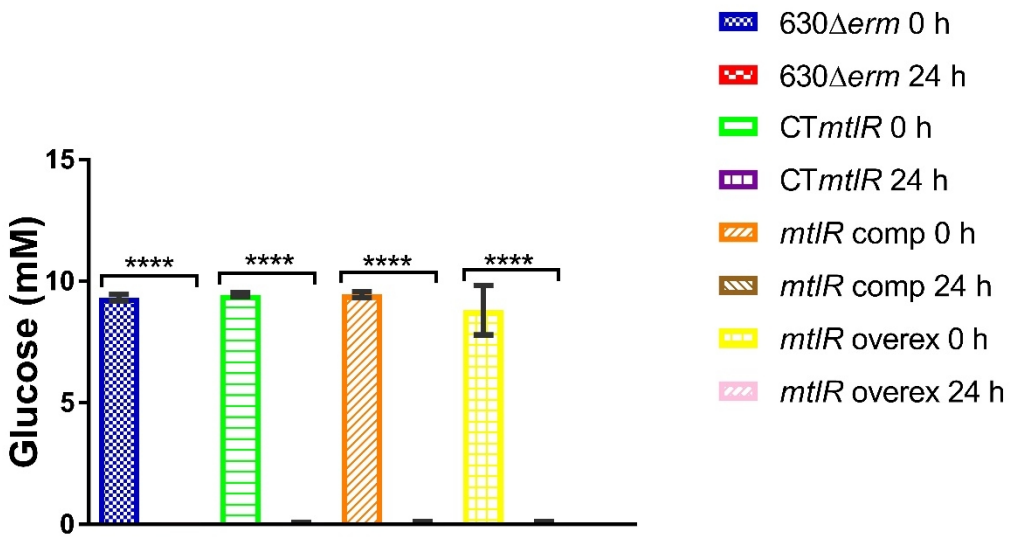

Figure 4.60: HPLC evaluation of glucose uptake in DM by 630Δ*erm* (control strain), CT*mtlR* (mutant), and the complemented mutants (*mtlR* comp and *mtlR* overex).
Extracts (triplicates) from the growth assay in DM were used to determine by HPLC the exact amount of sugar remaining in the medium at the start and end of the assay.
The level and trend of glucose utilisation by each strain was the same with a depletion of glucose (**** $P < 0.0001$).
One-way ANOVA was used to determine statistical significance.

4.5.1.4 Growth in TY, TYM, and TYG

With 630Δ*erm*, supplementing TY broth with mannitol resulted in an increase in OD_{600} levels. This was observed at 6-24 h of incubation, being especially noticeable at 10-24 h. For example, at peak growth, which was 12 h, OD_{600} in TY was 1.01, while in TYM it was 1.11 (* $P < 0.03$). 630Δ*erm* slope of the curve 8-12 h in TYM = 3.67 (Fig. 4.61).

Such a mannitol-induced increase was generally not seen with the mutant, CT*mtlR*. Mutant samples in TY and TYM had very similar OD_{600} at 4-24 h (e.g. at 10 h OD_{600} in TY it was 0.43, in TYM it was 0.40). At 24 h, CT*mtlR* peaked at 0.88 in TY and 0.87 in TYM. The exception to this was the decline of the mutant cultures in TYM seen at 48 h, which occurred at a slower rate, with the samples

in TY having an OD_{600} of 0.29, while those in TYM had an OD_{600} of 0.5 (* P < 0.02). Though, by 72 h, OD_{600} in TY and TYM cultures had both declined steeply (to an OD_{600} of 0.04 and 0.09 respectively). CT*mtlR* slope of the curve 10-24 h in TYM = 2.315. CT*mtlR* slope of the curve (downward) 24-72 h in TY = 4.2, in TYM = 3.8 (Fig. 4.61).

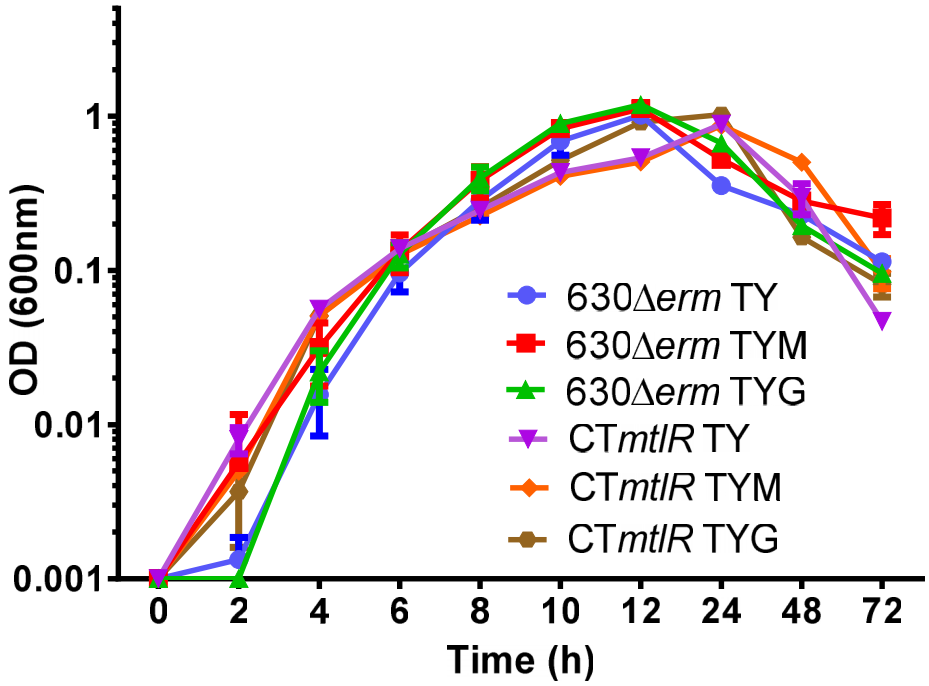

Figure 4.61: Role of *mtlR* in *C. difficile* 630Δ*erm* growth in TY.
630Δ*erm* (control strain) and CT*mtlR* (mutant) were incubated for 72 h at 37°C. 1mL extracts (triplicates) were taken at regular time points and the OD_{600} measured.
CT*mtlR* exhibited significantly attenuated growth levels in TYM in comparison to 630Δ*erm* in TYM.
630Δ*erm* slope of the curve 8-12 h in TYM = 3.67.
CT*mtlR* slope of the curve in TYM 8-12 h = 1.4, 10-24 h = 2.315.
CT*mtlR* slope of the curve (downward) 24-72 h in TY = 4.2, in TYM = 3.8
One-way ANOVA was used to determine statistical significance.
630Δ*erm* TY vs. TYM at 12 h * P < 0.03.
CT*mtlR* TY vs. TYM at 48 h * P < 0.02.
630Δ*erm* in TYM at 12 h vs. CT*mtlR* in TYM at 24 h (** P < 0.01).

Complementing CT*mtlR* with *mtlR* using its native promoter (*Pmtl*), and also complementing using the *fdx* promoter, resulted in the (delayed) ability of the complemented mutant strain (*mtlR* comp) to utilise the available mannitol; and with the overexpressed strain (*mtlR* overex), an ability to grow in TYM to significantly higher (**** $P < 0.0001$) levels than when in plain TY and to reach roughly the same level of growth as observed with 630Δ*erm* in mannitol (Fig. 4.61 & 4.62).

Commencing at 24 h, *mtlR* comp cultures in TYM showed an increase in growth over those samples in TY, as both cultures reached their peak OD_{600} (0.90 in TY, 0.93 in TYM) at this time point. By 48 h, although both OD_{600} of the cultures were declining, a significant disparity in OD_{600} (*** $P < 0.0005$) had opened between the sets, indicating that *mtlR* comp was able to make use of the available mannitol at the later time points (slope 24-72 h (downward): *mtlR* comp in TY = 4.25, *mtlR* comp in TYM = 2.15). Slope of the curve in TYM 8-12 h = 1.4, 10-24 h = 2.15 (Fig. 4.62).

mtlR overex at 6 h in TYM had started exhibiting an increase in OD_{600} levels (0.17) in comparison to *mtlR* overex in TY (0.12), which by 12 h had widened greatly (0.51 in TY, 1.04 in TYM) (**** $P < 0.0001$), which was also the time point of peak growth for the samples in TYM (the samples in plain TY peaked at 24 h with an OD_{600} of 0.79). Slope of the curve in TYM 8-12 h = 3.4 (Fig. 4.62).

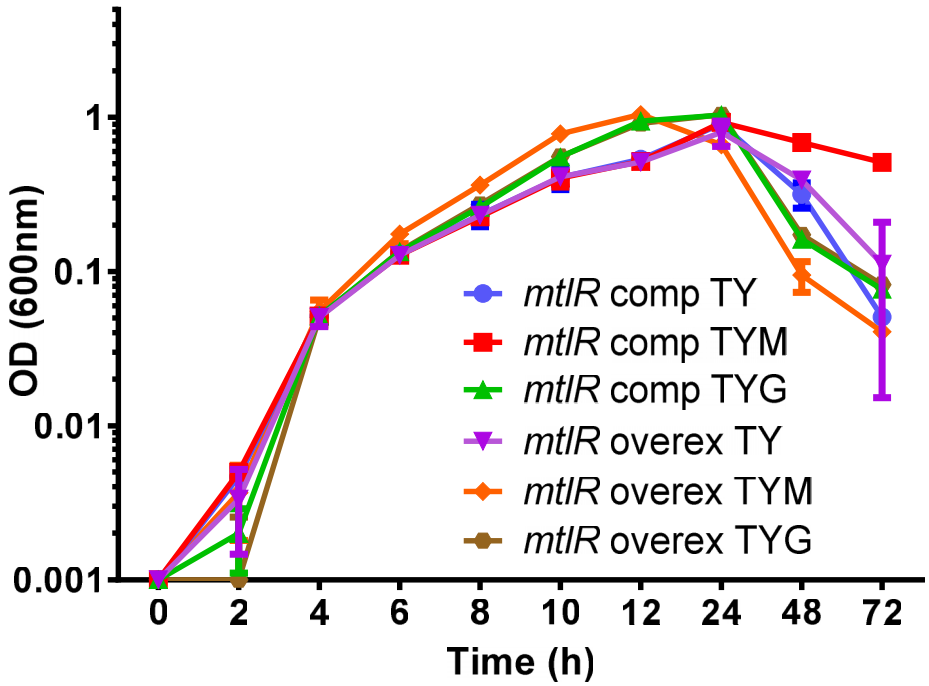

Figure 4.62: Role of *mtlR* in *C. difficile* 630Δ*erm* growth in TY.
mtlR comp (complemented mutant) and *mtlR* overex (overexpressed mutant) were incubated for 72 h at 37°C. 1mL extracts (triplicates) were taken at regular time points and the OD_{600} measured.
mtlR comp exhibited a delayed ability to restore uptake of mannitol in enriched medium. *mtlR* overex showed a completely restored ability to utilise mannitol.
mtlR comp slope of the curve in TYM 10-24 h (upward) = 2.65 ; 24-72 h in TY = 4.25, in TYM = 2.15.
mtlR overex slope of the curve in TYM 8-12 h (upward) = 3.4, 24-72 h (downward) = 3.1.
One-way ANOVA was used to determine statistical significance.
mtlR comp TY vs. TYM at 48 h *** $P < 0.0005$.
mtlR overex TY vs. TYM at 12 h **** $P < 0.0001$.

4.5.1.5 Cytotoxicity of 630Δ*erm*, 630Δ*erm*_CT*mtlR*, and complements

Toxin levels of 630Δ*erm* (control strain) exhibited a reduction in TYM when compared to when it was in TY alone. At 24 h incubation, the toxin titre was 2.8 x 10^3, but in TYM it was 0 (as it was in TYG also) (**** $P < 0.0001$) (Fig. 4.63).

This was not seen with the mutant, CT*mtlR*, as it had a toxin titre of 112.3 x 10^2 being produced in TY, and a titre of 1.1 x 10^2 in TYM, indicating no mannitol-

induced down-regulation of cytotoxicity. However, glucose reduced toxin production (Fig. 4.63).

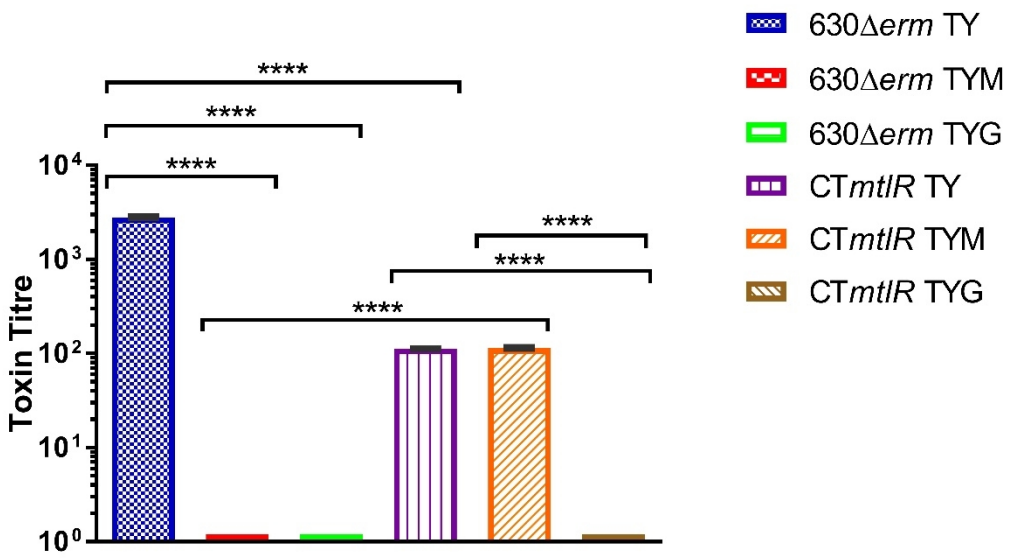

Figure 4.63: Role of *mtlR* in *C. difficile* 630Δ*erm* toxin production at 24 h in TY.
Cytotoxicity of CT*mtlR* at 24 h incubation. Serial dilutions (10^{0}-10^{-9}) of bacterial supernatants (triplicates) were applied to Vero cell monolayers (p35) to determine the toxin titre of the control strain (630Δ*erm*) and the mutant (CT*mtlR*).
Unlike the control strain, toxin production was completely unsuppressed in mannitol by CT*mtlR*.
One-way ANOVA was used to determine statistical significance.
630Δ*erm* TY vs. TYM **** $P < 0.0001$.
630Δ*erm* TY vs. CT*mtlR* TY **** $P < 0.0001$.
630Δ*erm* TYM vs. CT*mtlR* TYM **** $P < 0.0001$.

Toxin production by the complemented mutant, *mtlR* comp, reached a toxin titre of 1.1 x 10^2 in both TY, and 1.0 x 10^2 in TYM, indicating no restoration of mannitol-induced toxin suppression (Fig. 4.64).

Contrastingly, overexpression of *mtlR* (*mtlR* overex) resulted in a restoration of toxin down-regulation in TYM, as the toxin titre levels fell from 1.1 x 10^2 in TY to 0 in TYM (**** $P < 0.0001$) (Fig. 4.64).

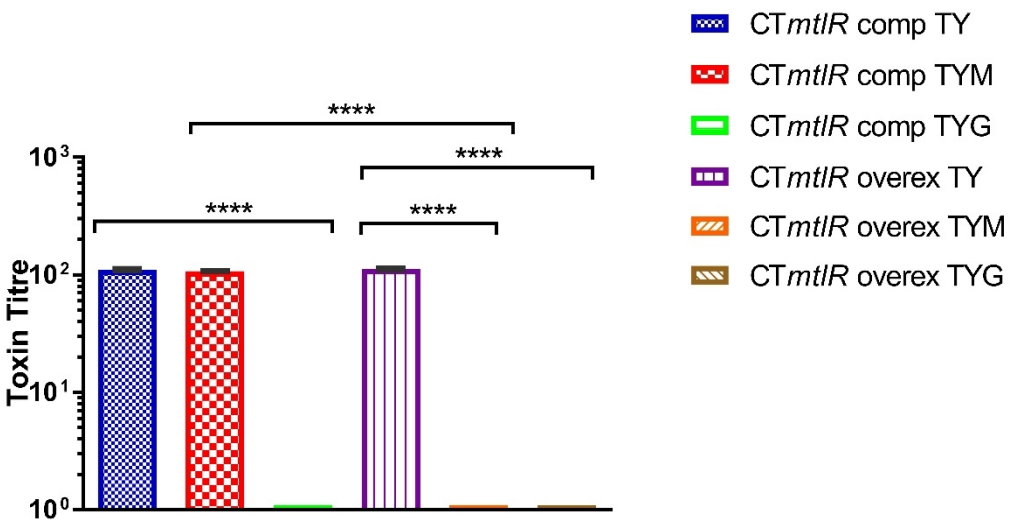

Figure 4.64: Role of *mtlR* in *C. difficile* 630Δ*erm* toxin production at 24 h in TY.

Cytotoxicity of *mtlR* comp and *mtlR* overex at 24 h incubation. Serial dilutions (10^{0}-10^{-9}) of bacterial supernatants (triplicates) were applied to Vero cell monolayers (p35) to determine the toxin titre of both strains.
Toxin suppression was not restored in mannitol by *mtlR* comp, but was fully restored by *mtlR* overex.
One-way ANOVA was used to determine statistical significance.
mtlR comp TYM vs. *mtlR* overex TYM **** $P < 0.0001$.
mtlR overex TY vs. TYM **** $P < 0.0001$.

At 48 h, the presence of mannitol reduced the amount of toxin produced by 630Δ*erm*, with levels going from a toxin titre of 4.5 x 10^3 in TY to 0 in TYM (**** $P < 0.0001$) (Fig. 4.65).

CT*mtlR* showed a minor reduction in toxin levels (in comparison to the control strain) with toxin production in TY at a toxin titre of 3.9 x 10^3, and, at a titre of 1.9 x 10^3 in TYM, albeit, minutely reduced in comparison to when in plain TY (** $P < 0.004$) (Fig. 4.65).

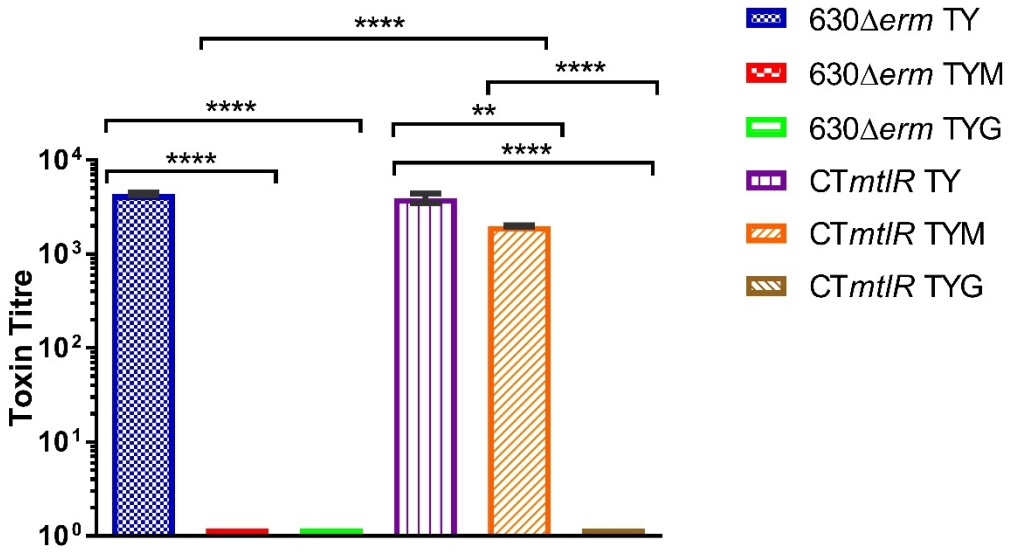

Figure 4.65: Role of *mtlR* in *C. difficile* 630Δ*erm* toxin production at 48 h in TY.
Cytotoxicity of CT*mtlR* at 48 h incubation. Serial dilutions (10^{0}-10^{-9}) of bacterial supernatants (triplicates) were applied to Vero cell monolayers (p35) to determine the toxin titre of the control strain (630Δ*erm*) and the mutant (CT*mtlR*).
630Δ*erm* completely suppressed toxin production in mannitol. Toxin production in mannitol was mostly restored by CT*mtlR*.
One-way ANOVA was used to determine statistical significance.
630Δ*erm* TY vs. TYM **** $P < 0.0001$.
630Δ*erm* TY vs. CT*mtlR* TY **** $P < 0.0001$.
630Δ*erm* TYM vs. CT*mtlR* TYM **** $P < 0.0001$.
CT*mtlR* TY vs. TYM ** $P < 0.004$.

At 48 h, toxin production by the complemented mutant, *mtlR* comp, displayed a reduction in mannitol with toxin levels going from 2.8 x 10^3 in TY to 1.4 x 10^2 in TYM (*** $P < 0.0004$) (Fig. 4.66).

However, toxin levels in the same conditions with the overexpressed mutant, *mtlR* overex, showed a total restoration of toxin suppression in mannitol. While toxin production hit 2.5 x 10^3 in TY, in TYM it was 0 (**** $P < 0.0001$) (Fig. 4.66).

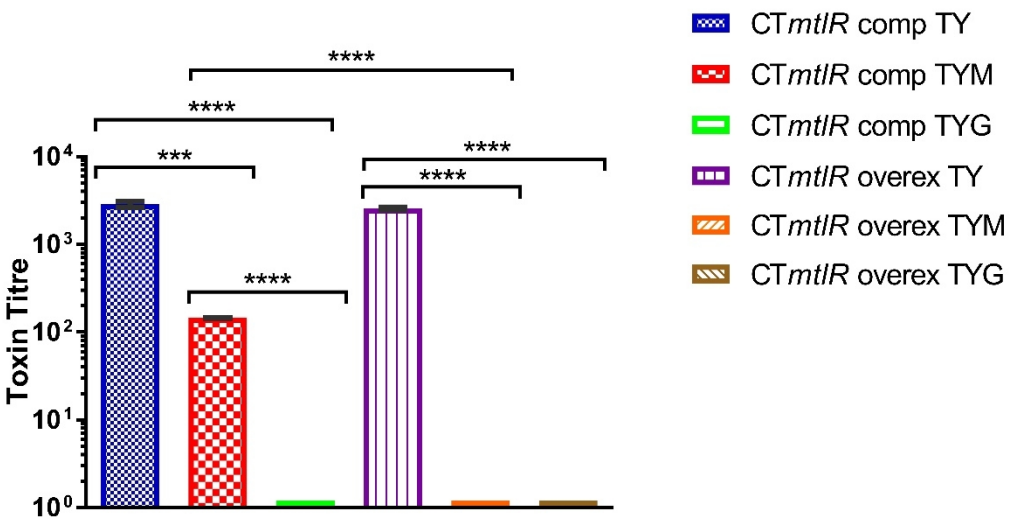

Figure 4.66: Role of *mtlR* in *C. difficile* 630Δ*erm* toxin production at 48 h in TY.

Cytotoxicity of *mtlR* comp and *mtlR* overex at 48 h incubation. Serial dilutions (10^{0}-10^{-9}) of bacterial supernatants (triplicates) were applied to Vero cell monolayers (p35) to determine the toxin titre of the mutant complemented with *mtlR* using its own promoter (*mtlR* comp) and the mutant complemented using the *fdx* promoter (*mtlR* overex).

Toxin suppression in mannitol was partially restored by *mtlR* comp and completely by *mtlR* overex.

One-way ANOVA was used to determine statistical significance.

mtlR comp TY vs. TYM *** $P < 0.0004$.

mtlR comp TYM vs. *mtlR* overex TYM **** $P < 0.0001$.

mtlR overex TY vs. TYM **** $P < 0.0001$.

At 72 h of incubation, toxin production by 630Δ*erm* dropped from 8.8 x 10^{5} in TY to above 3.8 x 10^{1} in TYM (**** $P < 0.0001$) (Fig. 4.67).

CT*mtlR*, although it exhibited trend towards a minor decrease in toxin levels in mannitol, did not significantly suppress toxin production in mannitol with levels at a toxin titre 1.7 x 10^{5} in TY (with variance), and at a titre of 9.0 x 10^{4} in TYM (Fig. 4.67).

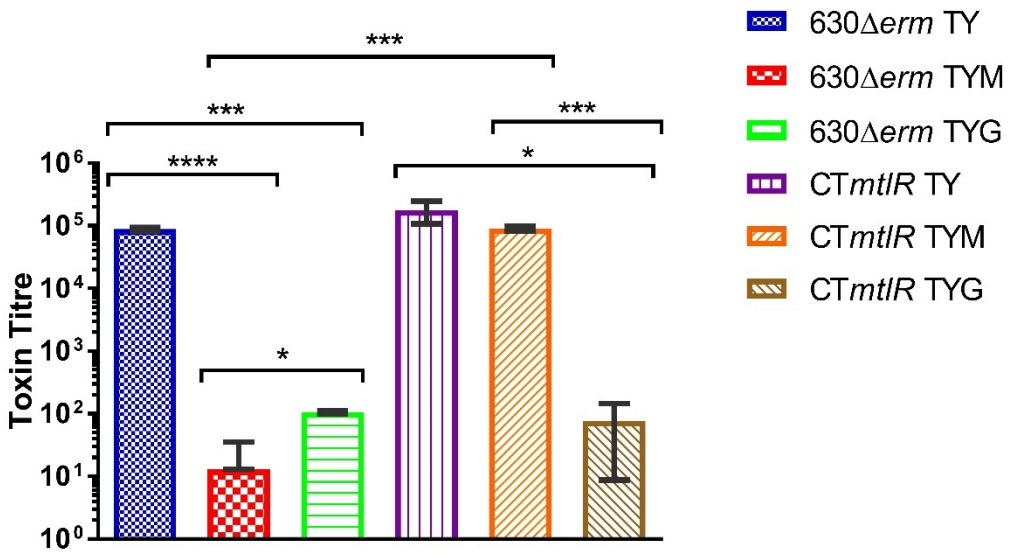

Figure 4.67: Role of *mtlR* in *C. difficile* 630Δ*erm* toxin production at 72 h in TY.
Cytotoxicity of CT*mtlR* at 72 h incubation. Serial dilutions (10^{0}-10^{-9}) of bacterial supernatants (triplicates) were applied to Vero cell monolayers (p35) to determine the toxin titre of the parent (630Δ*erm*) and the mutant (CT*mtlR*).
While 630Δ*erm* suppressed toxin levels in mannitol (**** $P < 0.0001$), toxin production was restored in mannitol by CT*mtlR*.
One-way ANOVA was used to determine statistical significance.
630Δ*erm* TY vs. TYM **** $P < 0.0001$.
630Δ*erm* TYM vs. CT*mtlR* TYM *** $P < 0.001$.

Suppression of toxin production at 72 h in mannitol was restored by *mtlR* comp with a toxin titre of 1.9 x 10^5 in TY to 1.8 x 10^3 in TYM (**** $P < 0.0001$); and more greatly by *mtlR* overex with toxin levels falling from 2.0 x 10^5 in TY to 2.4 x 10^2 in TYM (**** $P < 0.0001$) (Fig. 4.68).

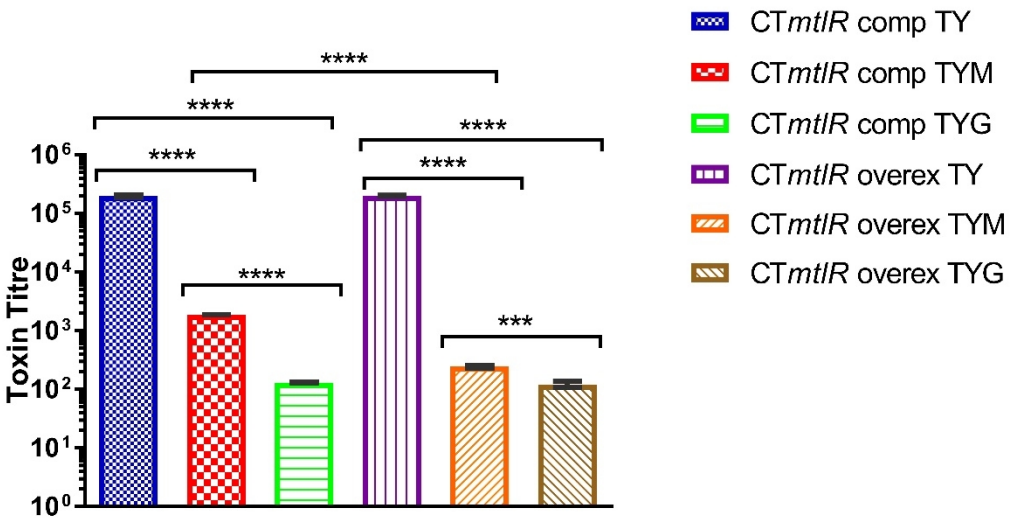

Figure 4.68: Role of *mtlR* in *C. difficile* 630Δ*erm* toxin production at 72 h in TY.
Cytotoxicity of the *mtlR* complemented mutants at 72 h incubation. Serial dilutions (10^{0}-10^{-9}) of bacterial supernatants (triplicates) were applied to Vero cell monolayers (p35) to determine the toxin titre of the complemented mutant (*mtlR* comp) and the overexpressed mutant (*mtlR*).
Toxin suppression in mannitol was restored by both strains (more noticeably by *mtlR* overex).
One-way ANOVA was used to determine statistical significance.
mtlR comp TY vs. TYM **** $P < 0.0001$.
mtlR comp TYM vs. *mtlR* overex TYM **** $P < 0.0001$.
mtlR overex TY vs. TYM **** $P < 0.0001$.

4.5.1.6 Motility assays

Four variant motility assays were performed in order to elucidate the possible role of *mtlR* in *C. difficile* 630 motility. *C. difficile* 630Δ*erm*_CT*fliC* and *C. difficile* M120 were used as the negative controls.

4.5.1.6.1 Motility assays on YT +glucose

Testing each strain on YT +glucose did not reveal noticeable differences in motility. The control strain (630Δ*erm*) displayed a larger zone of motility (2cm zone diameter). Smaller zones that were similar in size were observed with the mutant (CT*mtlR*) (1.4cm diameter) (Fig. 4.69) and the complemented mutants

(*mtlR* comp -1.5cm zone diameter; and *mtlR* overex -1.2cm) (not shown). M120 was used as the negative control, and exhibited reduced motility in comparison to the parent, the mutant, and the complemented mutants (not shown).

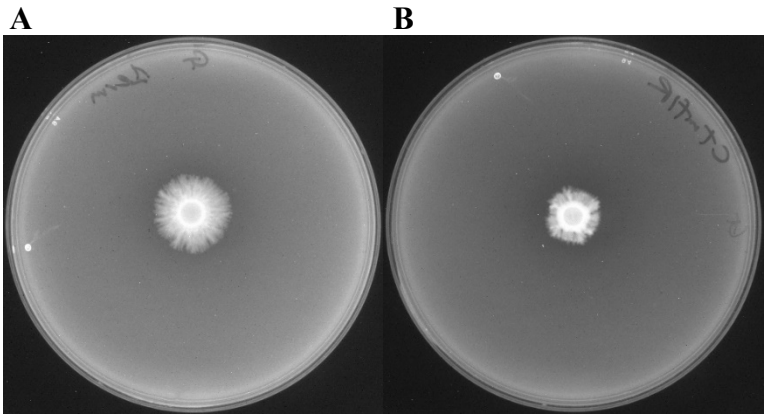

Figure 4.69: Representative images of motility assays showing control strain (A) and mutant (B) on YTG.
2µL of each strain (in triplicates) was spotted onto plates of YTG agar containing 1% w/v glucose and incubated at 37°C for 48 h to see if it was possible to observe a difference in motility.
The control strain (630Δ*erm*) exhibited a larger zone of motility on the plates than was seen with the mutant (CT*mtlR*) and both complements (not shown).

4.5.1.6.2 Motility assays on YT +mannitol

It was possible to observe a difference in motility when each strain was spotted onto YT +mannitol plates. 630Δ*erm* exhibited the largest zone of motility (1.3cm zone diameter) on the plates. CT*mtlR* was motile (1cm zone diameter), but less motile than 630Δ*erm*. *mtlR* comp showed a greater degree of motility (1cm zone diameter) than CT*mtlR*, but still less than 630Δ*erm*. *mtlR* overex showed a zone of motility (1.3cm zone diameter) which was similar to 630Δ*erm* (Fig. 4.70). CT*fliC* was used as the negative control, and exhibited reduced motility in comparison to the parent, the mutant, and the complemented mutants (not shown).

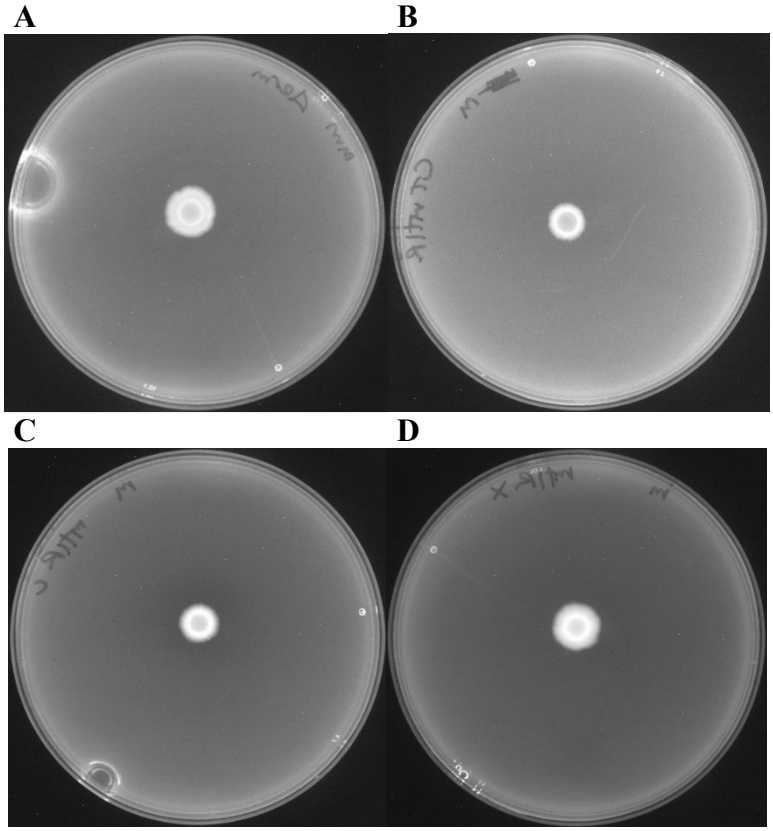

Figure 4.70: Representative images of motility assays showing the control strain (A), mutant (B), complemented mutant (C), and overexpressed mutant (D) on YTM.
2µL of each strain (in triplicates) was spotted onto plates of YTM agar containing 1% w/v mannitol and incubated at 37°C for 48 h to see if it was possible to observe a difference in motility.
The greatest motility was observed with the control strain (630Δ*erm*). Inhibition was observed with the mutant (CT*mtlR*) and the complemented mutant (*mtlR* comp), while motility comparable to the control strain was observed with the overexpressed mutant (*mtlR* overex).

4.5.1.6.3 Motility assays on BHIS +top agar

BHIS +top agar was used to determine possible differences in motility between 630Δ*erm*, CT*mtlR*, *mtlR* comp (not shown), and *mtlR* overex (not shown).

No differences were observed between the strains with similar motility on the plates observed with each strain (630Δ*erm*, 1cm zone diameter; CT*mtlR*, 1cm; *mtlR* comp, 1cm; *mtlR* overex, 1cm). CT*fliC* was used as the negative control,

and exhibited reduced motility (0.7cm zone diameter) in comparison to the control strain, the mutant (Fig 4.71), and the complemented mutants (not shown).

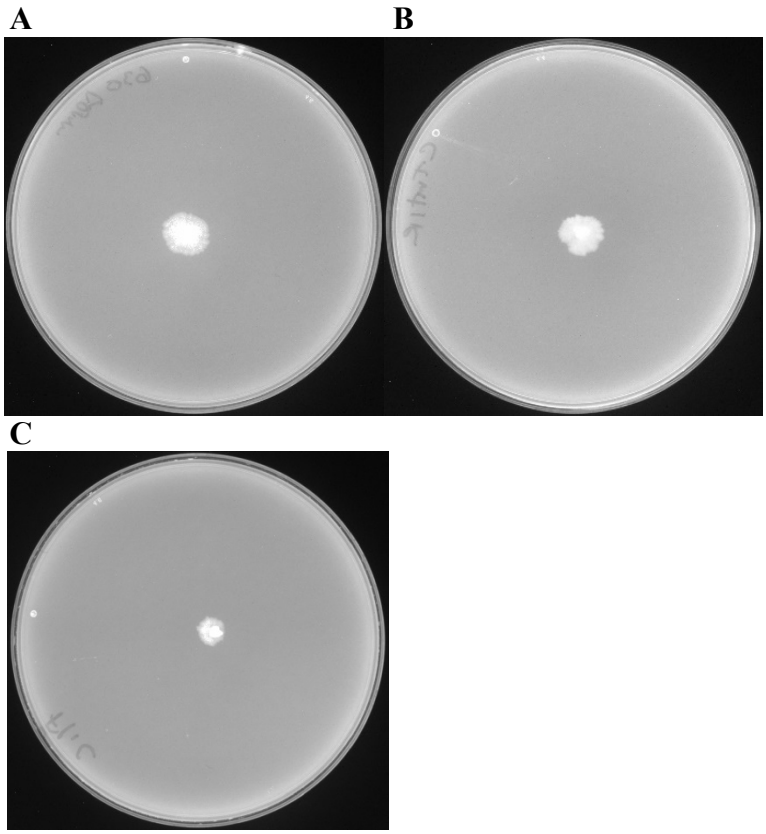

Figure 4.71: Representative images of motility assays showing control strain (A), mutant (B), and negative control, CT*fliC* (C).
The surface of the top agar was pierced with a single colony of each strain (in triplicates) and incubated at 37°C for 48 h to see if it was possible to observe a difference in motility.
No differences were observed between the strains with similar motility observed with the control strain (630Δ*erm*), the mutant (CT*mtlR*), and the complements (not shown).

4.5.1.6.4 Motility assays in tubes

Motility assays in glass tubes were prepared using the same medium as was used for the top layer medium on the BHIS +top layer motility assay agar plates in order to determine potential differences in motility between 630Δ*erm*, CT*mtlR*, *mtlR* comp (not shown), and *mtlR* overex (not shown).

Each strain exhibited good turbidity and migrated from the point of inoculation to the base of the tubes (11cm distance). *C. difficile* M120 was used as the negative control, showed growth at the very top of the tubes, but did not exhibit any turbidity nor did it migrate any distance through the agar (Fig. 4.72).

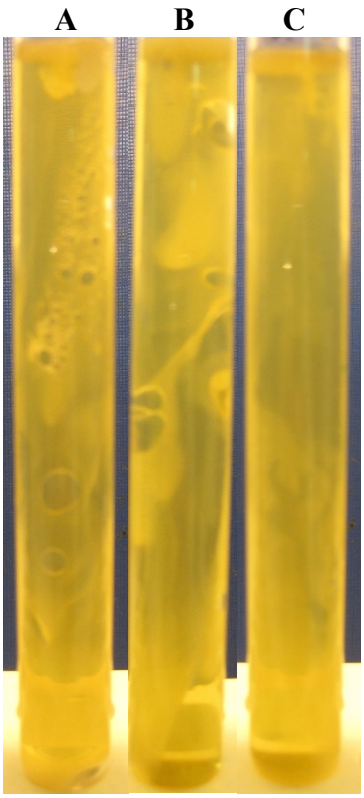

Figure 4.72: Representative images of motility assays showing migration of control strain (A) and mutant (B) through the agar in the tubes. The negative control, M120 (C), did not migrate.
The surface of the agar was pierced with a single colony of each strain (in triplicates) and incubated at 37°C for 24 h to see if it was possible to observe a difference in motility.
The control strain (630Δ*erm*), the mutant (CT*mtlR*), and the complements (not shown) exhibited good turbidity and migrated to the base of the tubes (11cm), while the negative control (M120) did not migrate any distance.

4.5.1.7 Spore assay

A spore assay was performed in order to determine the effect of inactivating *mtlR* on *C. difficile* 630 spore formation.

630Δ*ermΔpyrE*_CT*mtlR* showed no significant difference in its ability to form heat-resistant colonies in comparison to the parental strain, 630Δ*ermΔpyrE*. An example was seen at 120 h showing the number of heat-resistant colonies to be around 10^6/mL for both strains (1.6 x 10^6/mL for 630Δ*ermΔpyrE* and 1.0 x 10^6/mL for CT*mtlR*) (with minor variance) (Fig. 4.73). CT*spo0A* was used as the negative control and formed no heat-resistant colonies (not shown).

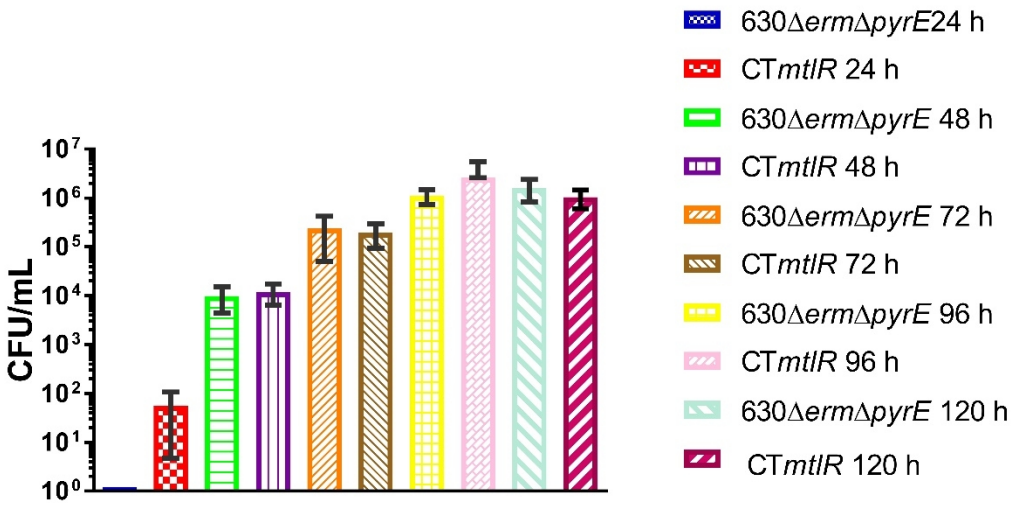

Figure 4.73: Role of *mtlR* in 630Δ*ermΔpyrE* spore formation.
Sporulation of CT*mtlR* at 120 h incubation. Spore assay was performed for up to 5 days with samples (triplicates) taken every 24 h and subjected to heat-treatment (80^OC). Serial dilutions (10^0-10^{-3}) of parental strain (630Δ*ermΔpyrE*) and mutant (CT*mtlR*) samples were spotted on plates of BHIS +taurocholate. Heat resistant-colonies formed by both strains were counted at each time point. The 630Δ*erm spo0*A mutant (data not shown) was used throughout as a negative-control, and failed to form heat-resistant colonies.
Spore formation does not appear to be affected by CT mutagenesis of *mtlR*.
One-way ANOVA was used to determine statistical significance.

4.6 Investigation and Characterisation of PTS^{Mtl} IIBC domain -MtlA

mtlA (Fig. 4.74) was selected for deletion using ACE to obtain an in-frame deletion[117]. Deleting this gene, it was hypothesised, would inhibit the detection, passage, phosphorylation, and consequent uptake of the incoming sugar molecule, and so, would prevent the bacteria from utilising mannitol. The mutant, Δ*mtlA*, was afterwards complemented with *mtlA* using the native promoter (*Pmtl*) in order to observe the effects of restoring the gene. Efforts to overexpress *mtlA* using the *fdx* promoter (with the overexpression vector pMTL-YN1X) failed, perhaps because of MtlA's status as a transmembrane protein making it harder to overexpress.

4.6.1 Characterisation of 630Δ*erm*Δ*mtlA* (CD630_2334)

Deletion of *mtlA* by ACE (Fig. 4.74) was determined by amplifying genomic DNA from colonies of the parental strain (630Δ*erm*Δ*pyrE*), and *C. difficile* 630Δ*erm*Δ*pyrE* colonies growing on minimal media (MM) plates +fluorotic acid (FOA) with primers specific for *mtlA* and its encompassing left and right homology arms (LHA and RHA), running the PCR products on 1% w/v agarose gel, and then, comparing the fragment sizes for the parent (3 kb) and the mutant (1.58 kb) (Fig. 4.75). Sequencing of DNA from the extracted 1.58 kb band (Δ*mtlA*) using *mtlA* _A and _B primers confirmed the deletion of the gene (data not shown).

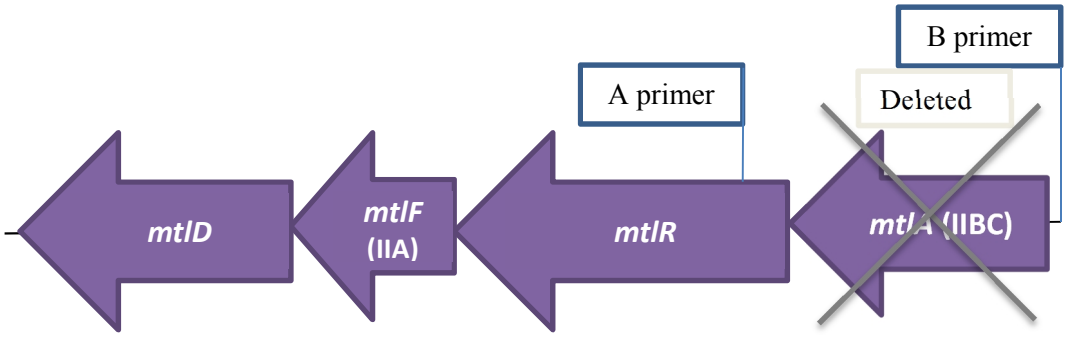

Figure 4.74: Position within the putative PTS^{Mtl} at loci CD630_2331-4 of the gene of interest, *mtlA*, and the primers used to screen for the deletion of *mtlA*. Primers, specific for the regions immediately outside of *mtlA*, were used to screen FOA-tolerant colonies growing on MM for the absence of the gene.

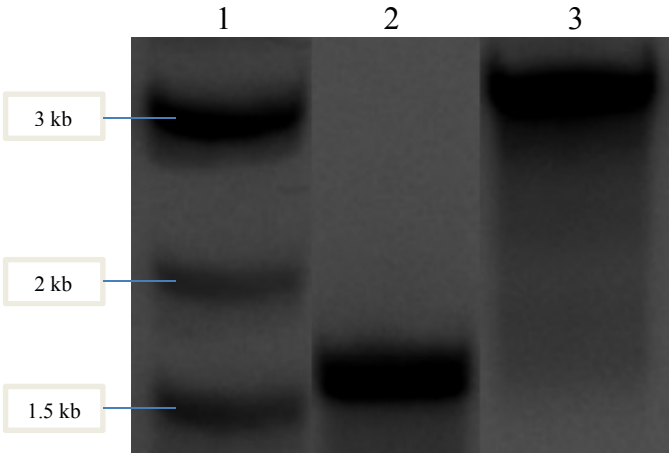

Figure 4.75: PCR screening for deletion of *mtlA*.
Primers (A and B) (Fig. 4.74), specific for the regions immediately outside of the LHA and the RHA, were used to amplify DNA from colonies growing on MM plates +FOA (well 2); and also, to amplify DNA from the parental strain, 630Δ*ermΔpyrE* (well 3). Table 4.6 below shows the lane order.

Table 4.6: Contents of each well when performing PCR analysis to show deletion of *mtlA*.

Well	Content	Size (kb)
1	Marker	
2	630Δ*ermΔpyrEΔmtlA*	1.56 (3.0-1.4)
3	630Δ*ermΔpyrE*	3.0

Complementation of Δ*mtlA*, afterwards, was accomplished using the native promoter (*Pmtl*) and was later determined by amplifying genomic DNA isolated from Δ*mtlA* colonies growing on MM (without uracil), with primers specific for the restored *pyrE* and which also encompassed the restored gene, then running the PCR products on 1% w/v agarose gel, and then verifying the fragment size for *mtlA* complemented (*mtlA* comp) (2.75 kb) (Fig. 4.76). Sequencing confirmed the restoration of *mtlA* and *pyrE* (data not shown).

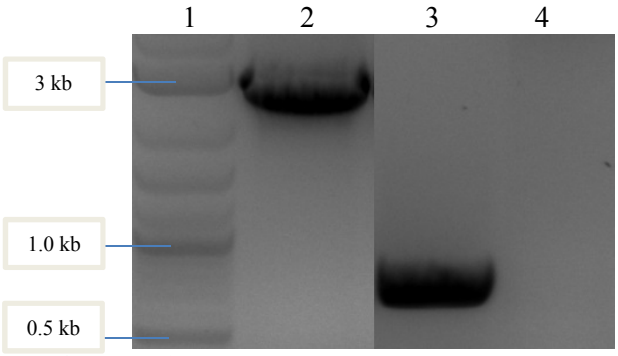

Figure 4.76: PCR screening for restoration of *mtlA* and *pyrE*.
Primers, specific for the regions immediately outside of the *pyrE* locus, were used to amplify DNA isolated from colonies growing on MM plates without uracil to screen for the restoration of *mtlA* with *pyrE* (well 2), and *pyrE* alone (well 3); and compared to DNA from the parental strain, 630Δ*ermΔpyrE* (well 4). Table 4.7 below shows the lane order.

Table 4.7: Contents of each well when performing PCR analysis to show complementation of Δ*mtlA*.

Well	Content	Size (kb)
1	Marker	
2	630Δ*ermΔmtlA_mtlA* comp	2.8 (1.47 + 0.65 + 0.68)
3	630Δ*ermΔmtlA* (*pyrE*+)	0.68
4	630Δ*ermΔpyrE*	-

4.6.1.1 Growth on DM agar

630Δ*erm*, Δ*mtlA*, and *mtlA* comp were streaked on DM and DMM agar to see if it was possible to discern any differences in growth.

Each strain showed strong growth on DM (not shown) and DMM, so it was not possible to determine differences in the ability to use mannitol on this agar (Fig. 4.77).

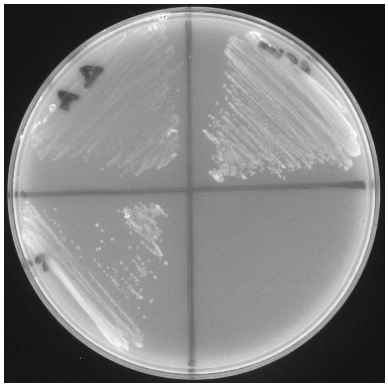

Figure 4.77: Representative image showing growth of mutant (top left), control strain (top right), and the complemented mutant (bottom left) on DMM agar.
Strains (in triplicates) were streaked on plates of DMM agar containing 0.6% w/v mannitol and incubated at 37°C for 16 h to see if it was possible to observe a growth phenotype.
Strong growth was observed with the control strain (630Δ*erm*), the mutant (Δ*mtlA*), and the complemented mutant (*mtlA* comp). It was not possible to determine differences in the ability of each strain to metabolise mannitol with this assay.

4.6.1.2 Growth in DM, DMM, and DMG broth

The presence of mannitol boosted the growth of the control strain, 630Δ*erm*. Starting at 6 h incubation and until the 12 h time point, the OD_{600} levels of 630Δ*erm* in DMM were significantly higher (**** $P < 0.0001$ at 6 h) than those in DM alone. For example, at 8 h (peak growth), OD_{600} in DM was 0.36, while in DMM it was 0.77 (**** $P < 0.0001$). Slope of the curve 0-8 h in DMM = 1.94 (Fig. 4.78).

Growth of the mutant, Δ*mtlA*, did not exhibit the mannitol-mediated upsurge in growth seen with the control strain, 630Δ*erm*. OD_{600} levels of the mutant in DM and DMM were similar throughout (with the exception of a minor increase observed at 24 h). A typical example was at 12 h incubation, OD_{600} in DM was 0.39, and at the same time in DMM was 0.42 (Fig. 4.78), indicating an inability of the mutant to make use of the great majority of the available mannitol. Peak growth of the mutant happened at 24 h (in DM OD_{600} = 0.48 and in DMM OD_{600} = 0.52). The small increase (not significant) of Δ*mtlA* growth at 24 h in DMM (in comparison to when Δ*mtlA* was in DM) indicates that a minor amount of mannitol was being utilised by the mutant. Slope of the curve 0-8 h in DMM = 0.94 (Fig. 4.78).

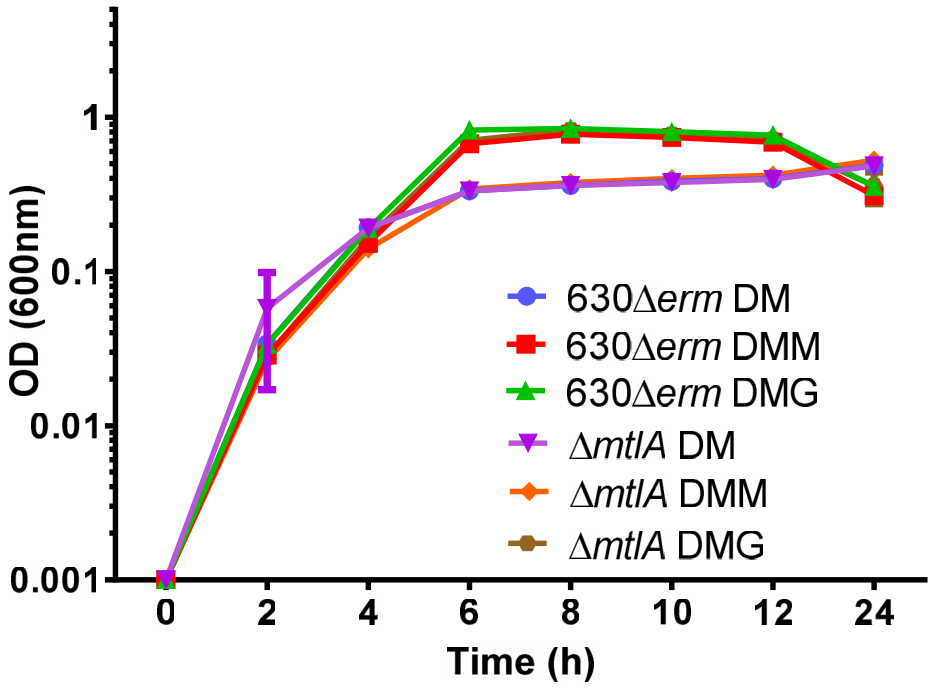

Figure 4.78: Role of *mtlA* in *C. difficile* 630Δ*erm* growth in DM.
630Δ*erm* (control strain) and Δ*mtlA* (mutant) were incubated for 24 h at 37°C. 1mL extracts (triplicates) were taken at regular time points and the OD_{600} measured.
Δ*mtlA* exhibited significantly attenuated growth levels in DMM in comparison to 630Δ*erm* in DMM. Growth of the mutant in DMM resembled growth in DM alone.
630Δ*erm* slope of the curve 0-8 h in DMM = 1.94.
Δ*mtlA* slope of the curve 0-8 h in DMM = 0.94.
One-way ANOVA was used to determine statistical significance.
630Δ*erm* in DM vs. DMM at 6 h **** $P < 0.0001$.
630Δ*erm* in DMM vs. Δ*mtlA* DMM at 6 h **** $P < 0.0001$.

Complementation of the mutant with *mtlA* using the native promoter (*Pmtl*) (*mtlA* comp) restored the ability to use the available mannitol. From 6 h to the end of the assay, *mtlA* comp in DMM displayed higher growth levels in comparison with *mtlA* comp in DM. At 10 h, for example, when growth in mannitol was at its highest, the OD_{600} in DM was only 0.36, while in DMM it reached 0.81 (**** $P < 0.0001$), thus, showing a complete restoration of mannitol uptake by *mtlA* comp in defined medium. Slope of the curve 0-8 h in DMM = 1.62 (Fig. 4.79).

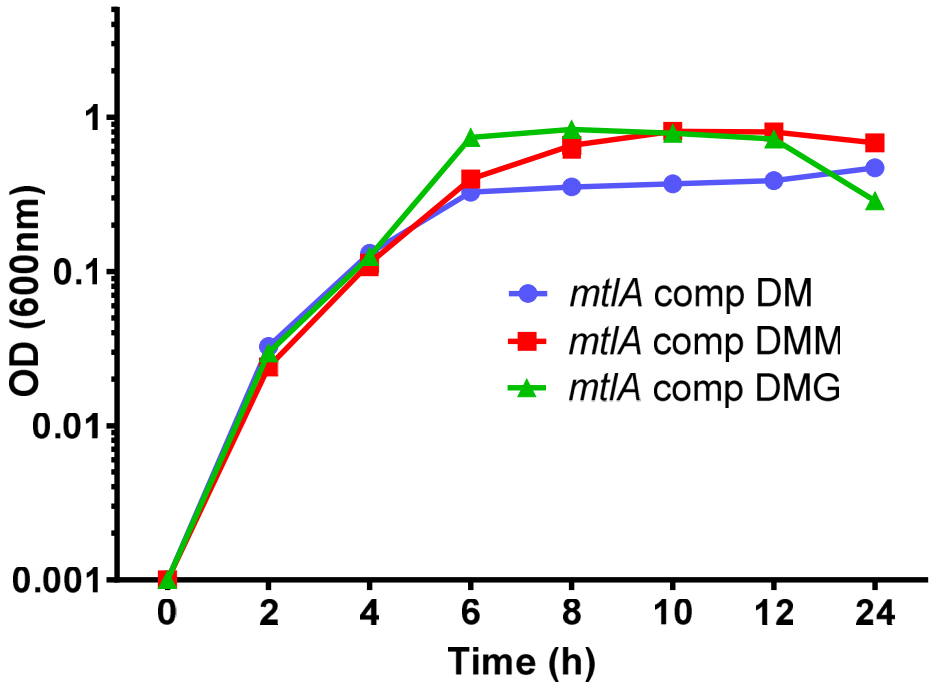

Figure 4.79: Role of *mtlA* in *C. difficile* 630Δ*erm* growth in DM.
mtlA comp (complemented mutant) was incubated for 24 h at 37°C. 1mL extracts (triplicates) were taken at regular time points and the OD_{600} measured.
The ability to utilise mannitol was restored as *mtlA* comp exhibited significantly higher growth levels in DMM in comparison to when it was grown in DM alone (**** $P < 0.0001$ at 10 h). Mannitol-induced increases in growth were belatedly (at 10 h), but fully, restored to 630Δ*erm* levels (Fig. 4.78).
mtlA comp slope of the curve 0-8 h in DMM = 1.62.
One-way ANOVA was used to determine statistical significance.
mtlA comp in DM vs. DMM at 10 h **** $P < 0.0001$.

4.6.1.3 HPLC evaluation of mannitol/glucose consumption in DM

The control strain, 630Δ*erm*, utilised all of the available mannitol, with the amount of mannitol going from 10.61mM at 0 h to 3.65mM at 6 h (**** $P < 0.0001$), to 0mM by 8 h (Fig. 4.80).

Deletion of *mtlA* (Δ*mtlA*) resulted in an inability of the mutant to use the vast majority of the mannitol (75.8%) by the end of the assay, with there being 10.54mM mannitol at the start (0 h) and still 7.99mM at 24 h. However, a

substantial amount (2.55mM -24.2%) of the sugar was still consumed by the mutant between these time points (Fig. 4.80).

Complementing the mutant using the native promoter of *mtlA* (630Δ*erm*Δ*mtlA*_*mtlA* comp) permitted a (tardy) return to control strain levels of mannitol utilisation. At 6 h, mannitol levels (8.34mM) in the *mtlA* comp samples differed widely in comparison to the 630Δ*erm* samples (3.65mM) (*** $P < 0.001$), and were not significantly lower than the Δ*mtlA* samples (9.08mM) (Fig. 4.80). Similarly, at 8 h, 630Δ*erm* had only a tiny fraction of mannitol remaining (0.1mM), while in the *mtlA* comp samples there still remained a large amount of the sugar (3.45mM) (no siginificant difference between *mtlA* comp at 6 h and 8 h). Nonetheless, at 10 h, this large difference was no longer observed (630Δ*erm* 0.09mM, *mtlA* comp 0.11mM), and by 12 h both strains had consumed the remaining mannitol (Fig. 4.80).. 630Δ*erm* slope of the curve 0-8 h = 5.25. Δ*mtlA* slope of the curve 0-8 h = 0.74. *mtlA* comp slope of the curve 0-8 h = 3.4 (Fig. 4.80).

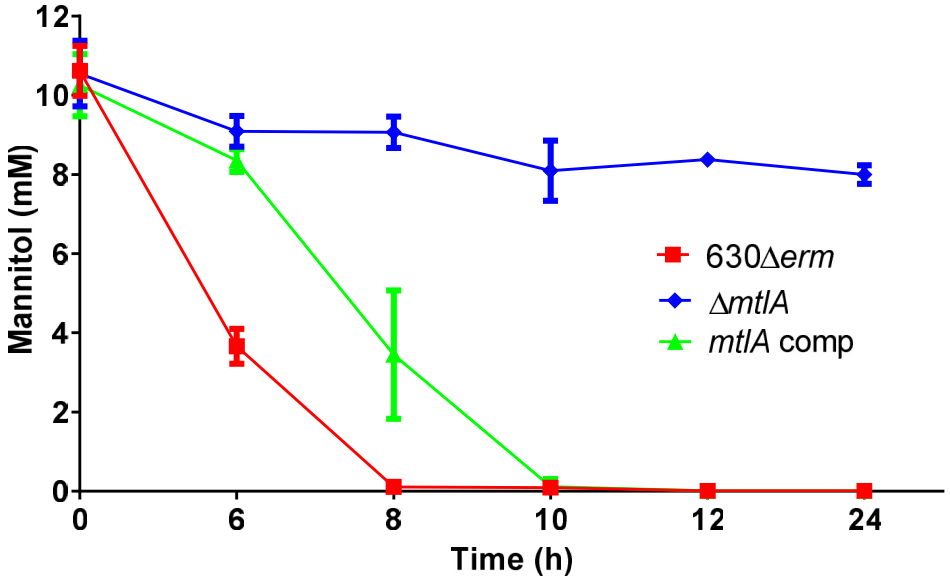

Figure 4.80: HPLC evaluation of mannitol uptake in DM by 630Δ*erm* (control strain), Δ*mtlA* (mutant), and the complemented mutant (*mtlA* comp). Extracts (triplicates) from the growth assay in DM were used to determine by HPLC the exact amount of sugar remaining in the medium at each time point.
The amount of mannitol left in both the control strain (630Δ*erm*) medium and the complemented mutant (*mtlA* comp) medium from 8 h was significantly less than what was left in the mutant (Δ*mtlA*) medium at the 24 h time point (**** $P < 0.0001$). By 10 h, the control and the complemented mutant had spent the available mannitol.
630Δ*erm* slope of the curve 0-8 h = 5.25.
Δ*mtlA* slope of the curve 0-8 h = 0.74.
mtlA comp slope of the curve 0-8 h = 3.4.
One-way ANOVA was used to determine statistical significance.
630Δ*erm* vs. *mtlA* comp at 6 h *** $P < 0.001$.
Δ*mtlA* vs. *mtlA* comp at 8 h ** $P < 0.003$.

Glucose levels of each strain were depleted, as was expected, between 0 h and 24 h (**** $P < 0.0001$). No differences emerged between the strains, indicating that interrupting *mtlA* function did not produce an effect on each strain's ability to metabolise glucose (Fig. 4.81).

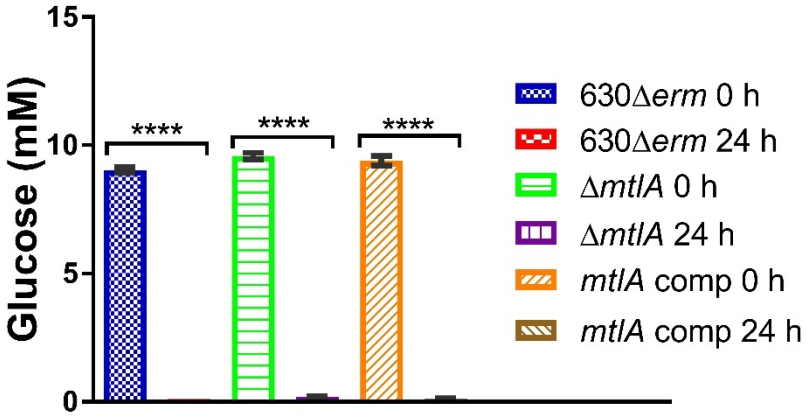

Figure 4.81: HPLC evaluation of glucose uptake in DM by 630Δ*erm* (control strain), Δ*mtlA* (mutant), and the complemented mutant (*mtlA* comp).
Extracts (triplicates) from the growth assay in DM were used to determine by HPLC the exact amount of sugar remaining in the medium at the start and end of the assay.
Glucose utilisation by each strain was the same with a depletion of glucose between 0 h and 24 h (**** $P < 0.0001$).
One-way ANOVA was used to determine statistical significance.

4.6.1.4 Growth in TY, TYM, and TYG

With the addition of mannitol, 630Δ*erm* OD_{600} levels exhibited an increase (from 8 h) in comparison with those samples of 630Δ*erm* in TY alone. This difference in OD_{600} levels became significant at later time points (and also, when the OD_{600} was starting to fall). For example, at 12 h (peak growth), 630Δ*erm* in TY alone resulted in an OD_{600} of 1.03, while in TYM it was 1.12 (*** $P < 0.001$).Slope of the curve 2-12 h in TYM = 2.25 (upward); 12-72 h in TYM = 1.35 (downward) (see Fig. 4.82).

Such a difference in OD_{600} levels between the two conditions was not observed with the mutant, Δ*mtlA*. To select a single example, at 24 h (peak growth) OD_{600} in TY was 1.0, in TYM it was 0.99.Slope of the curve 2-24 h in TYM = 1.65 (upward); 24-72 h in TYM = 2.99 (downward) (Fig. 4.82).

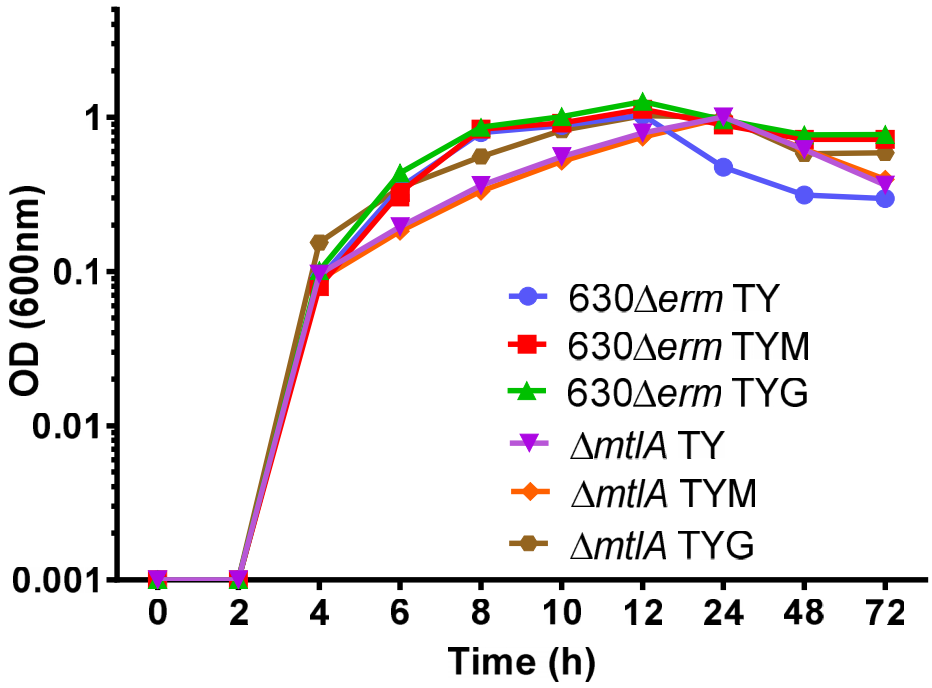

Figure 4.82: Role of *mtlA* in the growth of *C. difficile* 630Δ*erm* in TY.
630Δ*erm* (control strain) and Δ*mtlA* (mutant) were incubated for 72 h at 37°C. 1mL extracts (triplicates) were taken at regular time points and the OD_{600} measured.
Deletion of *mtlA* significantly inhibited growth in mannitol. Mutant peak growth growth in mannitol was attenuated in comparison to the control strain in the same medium (*** $P < 0.001$).
630Δ*erm* slope of the curve 2-12 h in TYM = 2.25 (upward); 12-72 h in TYM = 1.35 (downward).
Δ*mtlA* slope of the curve 2-24 h in TYM = 1.65 (upward); 24-72 h in TYM = 2.99 (downward).
One-way ANOVA was used to determine statistical significance.
630Δ*erm* at 12 h in TY vs. in TYM *** $P < 0.001$.
630Δ*erm* at 12 h in TYM vs. Δ*mtlA* at 24 h in TYM *** $P < 0.001$.

Complementing Δ*mtlA* using the native promoter (*Pmtl*) did not permit *mtlA* comp (complemented mutant) to return to control strain levels of growth in TYM (Fig. 4.83).

Supplementing the medium with mannitol produced, as was seen with the mutant, no increase in growth. At the time point of highest growth in TY and TYM, 24 h, *mtlA* comp samples in TY were at an OD_{600} 0.97, and were 0.95 in TYM. However, at 72 h, OD_{600} levels were significantly higher (* $P < 0.0205$) in TYM

at 0.57, while in TY they were 0.44. Slope of the curve 2-24 h in TYM = 1.59 (upward); 24-72 h in TYM = 1.88 (downward) (Fig. 4.83).

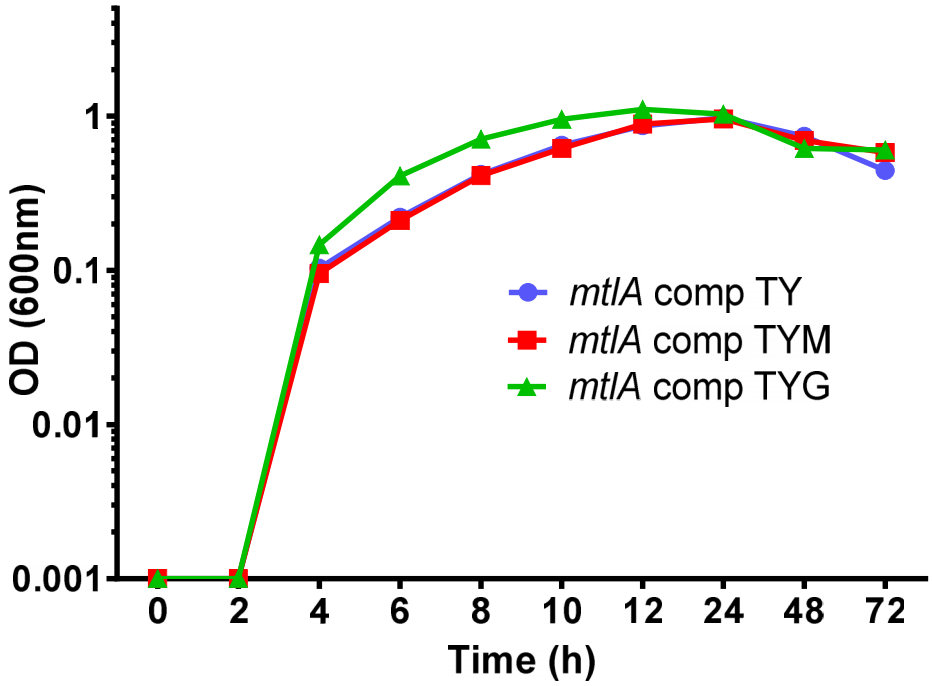

Figure 4.83: Role of *mtlA* in the growth of *C. difficile* 630Δ*erm* in TY.
mtlA comp (complemented mutant) was incubated for 72 h at 37°C. 1mL extracts (triplicates) were taken at regular time points and the OD_{600} measured.
Deletion of *mtlA* significantly inhibited growth in mannitol (Fig. 4.82). Restoration of *mtlA* (*mtlA* comp) using the native promoter (*Pmtl*) did not restore mannitol-induced increase in OD_{600} levels in TYM, and growth remained attenuated in comparison to the control strain (630Δ*erm*) (Fig. 4.82) in the same medium. However, at 72 h, *mtlA* comp OD_{600} in TYM was significantly above (* $P < 0.02$) that of *mtlA* comp in plain TY.
Slope of the curve 2-24 h in TYM = 1.59 (upward); 24-72 h in TYM = 1.88 (downward).
One-way ANOVA was used to determine statistical significance.
mtlA comp at 72 h TY vs. TYM * $P < 0.02$.

4.6.1.5 Cytotoxicity of 630Δ*erm* and 630Δ*erm*Δ*mtlA*

With the cytotoxicity assays, deleting *mtlA* resulted in toxin levels in mannitol similar to those seen in TY alone. 630Δ*erm* (control strain) cytotoxicity was suppressed in mannitol with toxin levels going from a toxin titre of 2.0×10^3 in TY to 0 in TYM (**** $P < 0.0001$). Δ*mtlA* (mutant) exhibited no change in toxin

production with toxin levels in TY and TYM remaining at a titre of 10^2 (9.8 x 10^2 and 1.0 x 10^2 respectively) (Fig. 4.84).

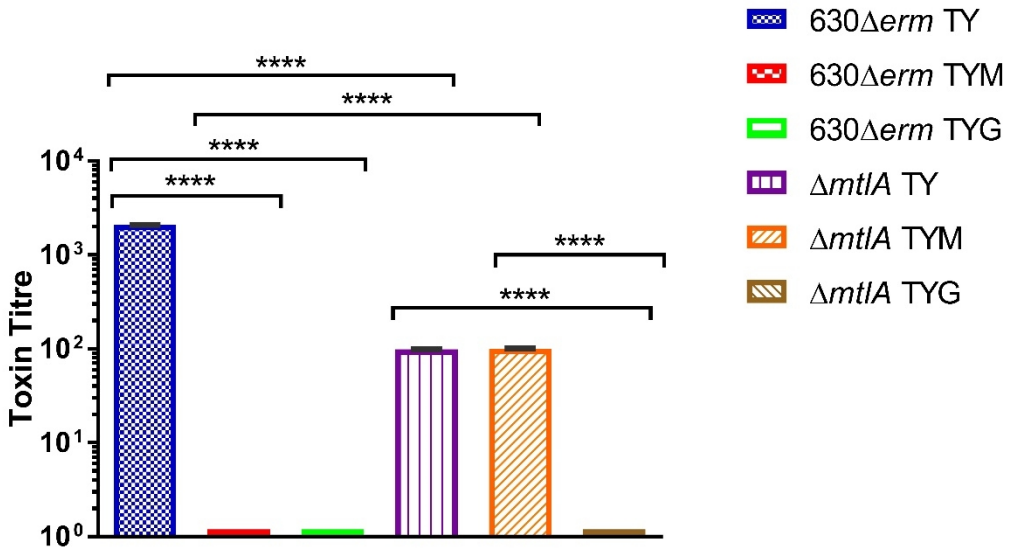

Figure 4.84: Role of *mtlA* in *C. difficile* 630Δ*erm* toxin production at 24 h in TY.
Cytotoxicity of Δ*mtlA* at 24 h incubation. Serial dilutions (10^0-10^{-9}) of bacterial supernatants (triplicates) were applied to Vero cell monolayers (p34) to determine the toxin titre of the control strain (630Δ*erm*) and the mutant (Δ*mtlA*).
The control strain suppressed toxin levels in mannitol (****P < 0.0001), while restoration of cytotoxicity was observed with Δ*mtlA* in mannitol.
One-way ANOVA was used to determine statistical significance.
630Δ*erm* in TY vs. in TYM **** P < 0.0001.
630Δ*erm* in TY vs. Δ*mtlA* in TY **** P < 0.0001.
630Δ*erm* in TYM vs. Δ*mtlA* in TYM **** P < 0.0001.

Complementing Δ*mtlA* with *mtlA* using the native promoter (*Pmtl*) did not re-establish toxin suppression in mannitol at 24 h. Toxin levels in TY and TYM remained at a titre of 10^2 (1.0 x 10^2 and 1.0 x 10^2 respectively) (Fig. 4.85).

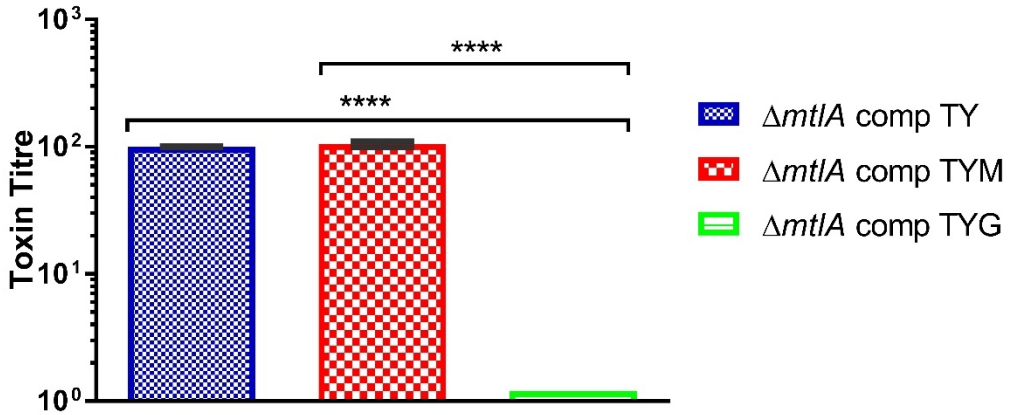

Figure 4.85: Role of *mtlA* in *C. difficile* 630Δ*erm* toxin production at 24 h in TY.
Cytotoxicity of *mtlA* comp at 24 h incubation. Serial dilutions (10^0-10^{-9}) of bacterial supernatants (triplicates) were applied to Vero cell monolayers (p34) to determine the toxin titre of the complemented mutant (Δ*mtlA* comp).
There was no restoration of toxin suppression in mannitol by Δ*mtlA* comp.
One-way ANOVA was used to determine statistical significance.

At 48 h, deletion of *mtlA* restored toxin production in mannitol. 630Δ*erm* toxin levels went from a toxin titre of 3.1 x 10^5 in TY to 1.3 x 10^1 in TYM (**** $P < 0.0001$); while Δ*mtlA* exhibited no difference in toxin levels when grown in TY or TYM with a toxin titre marginally above 10^4 (1.5 x 10^4 and 1.6 x 10^4 respectively) in both conditions (Fig. 4.86).

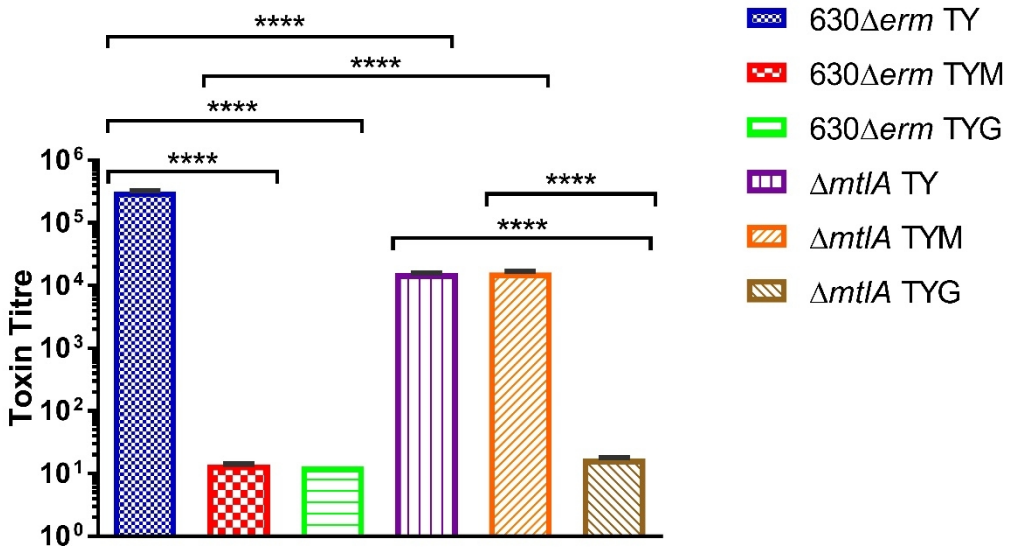

Figure 4.86: Role of *mtlA* in *C. difficile* 630Δ*erm* toxin production at 48 h in TY.

Cytotoxicity of Δ*mtlA* at 48 h incubation. Serial dilutions (10^{0}-10^{-9}) of bacterial supernatants (triplicates) were applied to Vero cell monolayers (p34) to determine the toxin titre of the control strain (630Δ*erm*) and the mutant (Δ*mtlA*).
The control strain suppressed toxin production in mannitol (**** $P < 0.0001$), while restoration of cytotoxicity was observed with Δ*mtlA* in mannitol.
One-way ANOVA was used to determine statistical significance.
630Δ*erm* in TY vs. in TYM **** $P < 0.0001$.
630Δ*erm* in TY vs. Δ*mtlA* in TY **** $P < 0.0001$.
630Δ*erm* in TYM vs. Δ*mtlA* in TYM **** $P < 0.0001$.

Complementing Δ*mtlA* using the native promoter (*mtlA* comp) did not re-establish toxin suppression in mannitol at 48 h. Toxin levels remained at a toxin titre of 1.3 x 10^4 in TY and 1.0 x 10^4 in TYM (with minor variance) (Fig. 4.87).

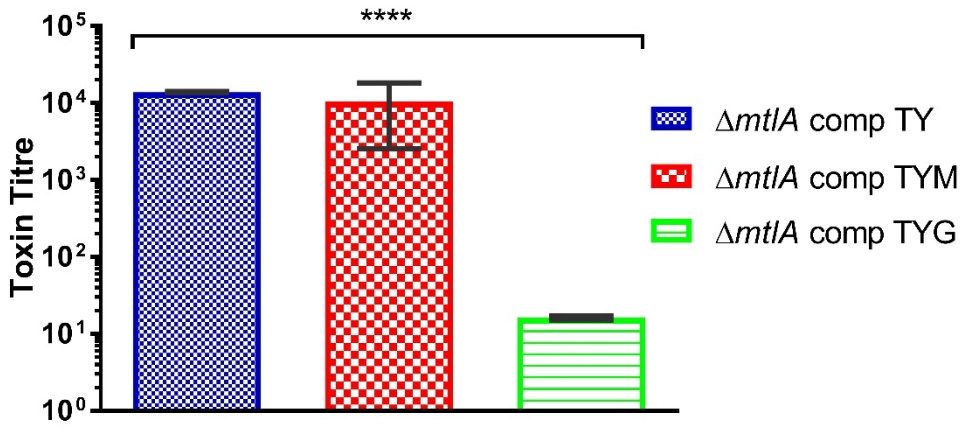

Figure 4.87: Role of *mtlA* in *C. difficile* 630Δ*erm* toxin expression at 48 h in TY.
Cytotoxicity of *mtlA* comp at 48 h incubation. Serial dilutions (10^{0}-10^{-9}) of bacterial supernatants (triplicates) were applied to Vero cell monolayers (p34) to determine the toxin titre of the complemented mutant (*mtlA* comp).
There was no restoration of toxin suppression in mannitol by *mtlA* comp.
One-way ANOVA was used to determine statistical significance.

At 72 h, deletion of *mtlA* restored toxin production in mannitol. 630Δ*erm* toxin levels went from a toxin titre of 3.3 x 10^5 in TY to 1.3 x 10^2 in TYM (**** $P < 0.0001$), while Δ*mtlA* only exhibited small (but, significant) differences in toxin levels when grown in TY and TYM with a toxin titre much above 10^5 in both conditions (2.7 x 10^5 and 2.5 x 10^5 respectively) (* $P < 0.012$) (Fig. 4.88).

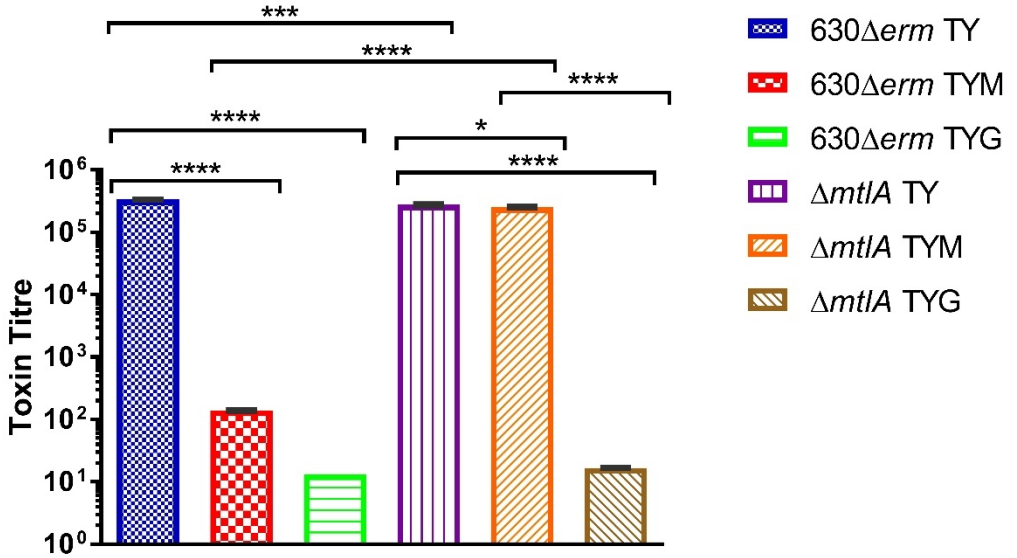

Figure 4.88: Role of *mtlA* in *C. difficile* 630Δ*erm* toxin production at 72 h in TY.

Cytotoxicity of Δ*mtlA* at 72 h incubation. Serial dilutions (10^{0}-10^{-9}) of bacterial supernatants (triplicates) were applied to Vero cell monolayers (p34) to determine the toxin titre of the control strain (630Δ*erm*) and the mutant (Δ*mtlA*).
The control strain suppressed toxin production in mannitol (**** $P < 0.0001$), while near complete restoration of cytotoxicity was observed with Δ*mtlA* in mannitol.
One-way ANOVA was used to determine statistical significance.
630Δ*erm* in TY vs. TYM **** $P < 0.0001$.
630Δ*erm* in TY vs. Δ*mtlA* in TY *** $P < 0.0004$.
630Δ*erm* in TYM vs. Δ*mtlA* in TYM **** $P < 0.0001$.
Δ*mtlA* in TY vs. TYM * $P < 0.012$.

Complementing Δ*mtlA* with *mtlA* using the native promoter partly and significantly re-established toxin suppression in mannitol at 72 h. Toxin levels went from a toxin titre of 2.2 x 10^{5} in TY to 1.2 x 10^{4} in TYM (with variance) (**** $P < 0.0001$) (Fig. 4.89).

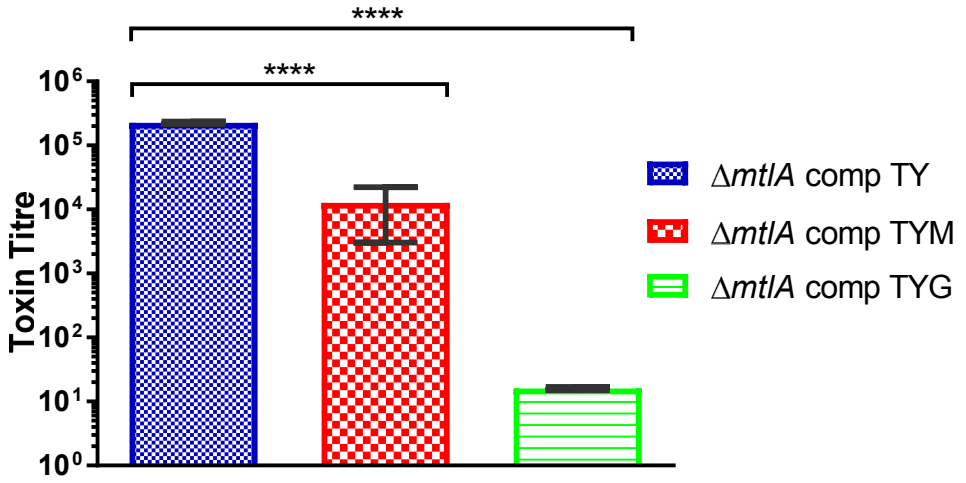

Figure 4.89: Role of *mtlA* in *C. difficile* 630Δ*erm* toxin production at 72 h in TY.
Cytotoxicity of Δ*mtlA* comp at 72 h incubation. Serial dilutions (10^{0}-10^{-9}) of bacterial supernatants (triplicates) were applied to Vero cell monolayers (p34) to determine the toxin titre of the complemented mutant, *mtlA* comp.
A partial, incomplete, yet, significant (**** P < 0.0001) restoration of suppression of cytotoxicity in mannitol by *mtlA* comp was observed.
One-way ANOVA was used to determine statistical significance.
Δ*mtlA* comp in TY vs. TYM **** P < 0.0001.

4.6.1.6 Motility assays

Four variant motility assays were performed in order to elucidate the possible role of *mtlA* in *C. difficile* 630 motility. *C. difficile* 630Δ*erm*_CT*fliC* and *C. difficile* M120 were used as the negative controls.

4.6.1.6.1 Motility assays on YT +glucose

The control strain (630Δ*erm*) displayed the largest zone of motility at a diameter of 2cm. Smaller and similar zones of motility were observed with both the mutant (Δ*mtlA*) (1.3cm zone diameter) (Fig. 4.90) and the complemented mutant (*mtlA* comp) (1.3cm zone diameter) (not shown). M120 was used as the negative control, and exhibited reduced motility in comparison to the parent, the mutant, and the complemented mutant (not shown).

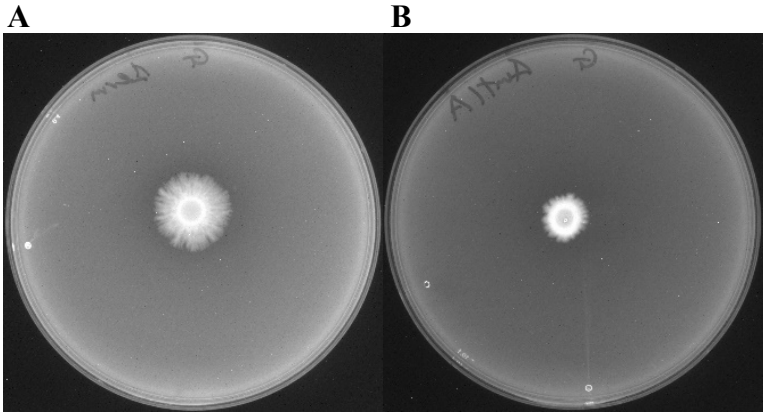

Figure 4.90: Representative images of motility assays showing control strain (A) and mutant (B) on YTG.
2µL of each strain (in triplicates) was spotted onto plates of YTG agar containing 1% w/v glucose and incubated at 37°C for 48 h to see if it was possible to observe a difference in motility.
Wider zones of motility were observed with the control strain (630Δ*erm*) than was seen with the mutant (Δ*mtlA*) and the complemented mutant (*mtlA* comp –not shown).

4.6.1.6.2 Motility assays on YT +mannitol

Spotting each strain on YT +mannitol revealed differences in the zones of motility on the plates. Reduced motility was observed with the mutant (Δ*mtlA*) (1cm zone diameter) in comparison to the motility of the control strain (630Δ*erm*) (1.3cm zone diameter), and increased motility (in comparison to the mutant) was seen with the complemented mutant (*mtlA* comp) (1.2cm zone diameter) (Fig. 4.91). CT*fliC* was used as the negative control, and exhibited reduced motility in comparison to the parent, the mutant, and the complemented mutant (not shown).

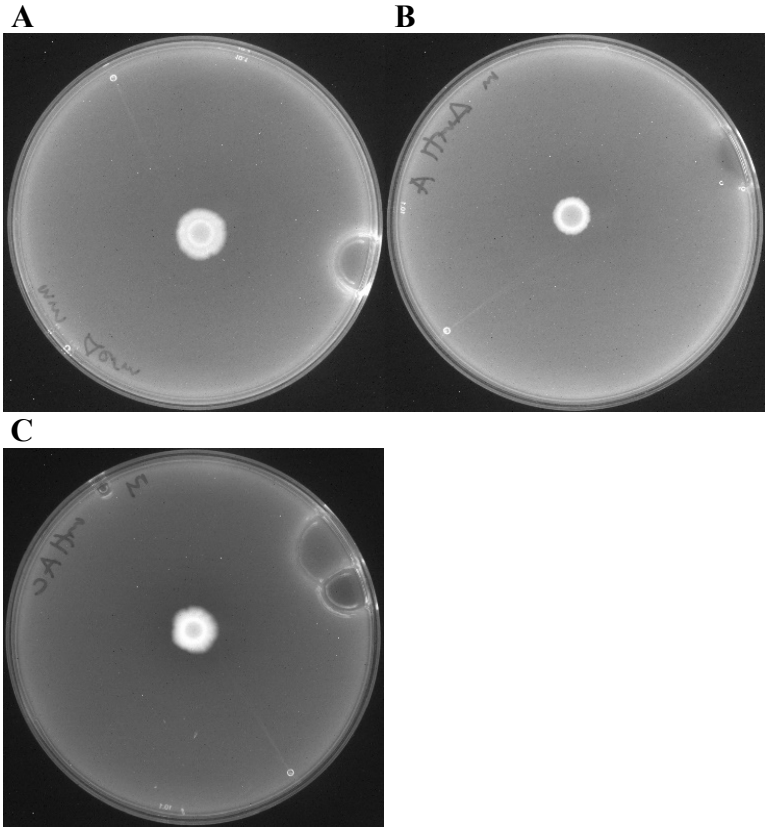

Figure 4.91: Representative images of motility assays showing growth of control strain (A), mutant (B), and complemented mutant (C) on YTM.
2µL of each strain (in triplicates) was spotted onto plates of YTM agar containing 1% w/v mannitol and incubated at 37°C for 48 h to see if it was possible to observe a difference.
The greatest motility was observed with the control strain (630Δ*erm*). Reduced motility was observed with the mutant (Δ*mtlA*), and increased motility (in comparison to the mutant) was seen with the complemented mutant (*mtlA* comp).

4.6.1.6.3 Motility assays on BHIS +top agar

BHIS +top agar was used to determine possible differences in motility between 630Δ*erm*, Δ*mtlA*, and *mtlA* comp (not shown).

No differences were observed, with similar motility by each strain (630Δ*erm*, 1cm zone diameter; Δ*mtlA*, 1cm; *mtlA* comp, 1.1cm). CT*fliC* was used as the negative control, and exhibited reduced motility (0.7cm zone diameter) in comparison to the control strain, the mutant (Fig. 4.92), and the complemented mutant (not shown).

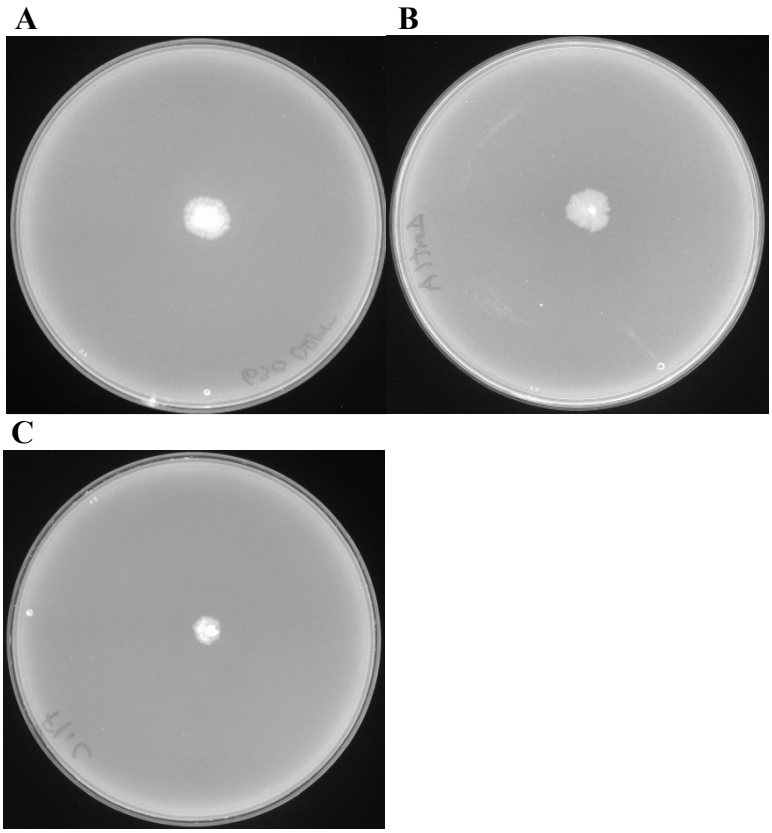

Figure 4.92: Representative images of motility assays on BHIS +top agar showing control strain (A), mutant (B), and negative control, CT*fliC* (C).
The surface of the top agar was pierced with a single colony of each strain (in triplicates) and incubated at 37°C for 48 h to see if it was possible to observe a difference in motility.
No differences were observed between the control strain (630Δ*erm*) and the mutant (Δ*mtlA*) with similar motility seen with both strains.

4.6.1.6.4 Motility assays in tubes

Motility assays in glass tubes were prepared using the same medium as was used for the top layer medium on the BHIS +top layer agar plates.

Each strain tested (630Δ*erm*, Δ*mtlA*, and *mtlA* comp –not shown) showed the presence of the bacteria throughout the length of the tubes and migrated 11cm through the agar from the point of inoculation to the base of the tubes. *C. difficile* M120 was used as the negative control, showed growth at the very top of the tubes, but did not exhibit any turbidity nor migrate any distance through the agar (Fig. 4.93).

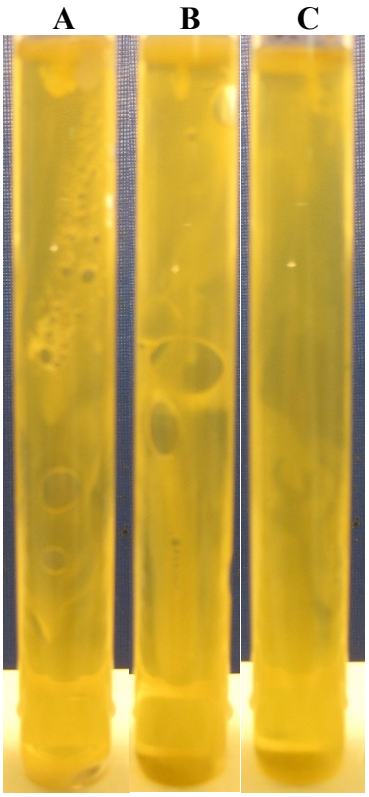

Figure 4.93: Representative images of motility assays showing migration of control strain (A), mutant (B) through the agar in the tubes. The negative control M120 (C), did not migrate.
The surface of the agar was pierced with a single colony of each strain (in triplicates) and incubated at 37°C for 24 h to see if it was possible to observe a difference in motility.
The control strain (630Δ*erm*), the mutant (Δ*mtlA*), and the complemented mutant (*mtlA* comp –not shown) exhibited robust turbidity and migrated to the base of the tube (11cm), while the negative control (M120) did not migrate any distance through the agar.

4.6.1.7 Spore assay

A spore assay was performed in order to investigate the effects of deleting *mtlA* on spore formation.

630Δ*erm*Δ*pyrE*Δ*mtlA* showed no significant difference in its ability to form heat-resistant colonies in comparison to the parental strain, 630Δ*erm*Δ*pyrE*. An example, at 120 h, is shown with the number of heat-resistant colonies seen to be around 10^6/mL for both strains (1.6 x 10^6/mL for 630Δ*erm*Δ*pyrE* and 2.4 x

10^6/mL for Δ*mtlA*) (with variance) (Fig. 4.94). *C. difficile* 630Δ*erm*_CT*spo0A* was used as the negative control and did not form any CFUs (not shown).

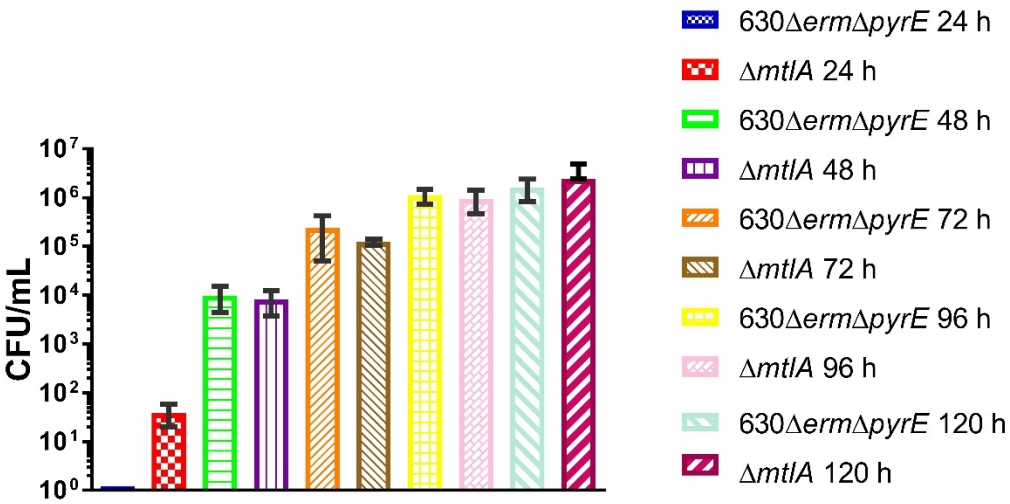

Figure 4.94: Role of *mtlA* in *C. difficile* 630Δ*erm*Δ*pyrE* spore formation.
Formation of heat-resistant colonies by Δ*mtlA* up to 120 h. Spore assay was performed for up to 5 days with samples (triplicates) taken every 24 h and subjected to heat-treatment (80°C). Serial dilutions (10^0-10^{-3}) of parental strain (630Δ*erm*Δ*pyrE*) and mutant (Δ*mtlA*) samples were spotted on plates of BHIS +taurocholate (in triplicates). Heat resistant-colonies formed by both strains were counted at each time point. The *spo0A* mutant (data not shown) was used throughout as a negative-control and failed to form heat-resistant colonies.
Spore formation does not appear to be affected by deletion of *mtlA*.
One-way ANOVA was used to determine statistical significance.

4.7 Discussion

Mannitol represents a fermentable source of carbon for *C. difficile* and has been observed to exert an influence on the production of toxin by the organism[22,28]. An understanding of the exact mechanisms of its uptake and its role in cytotoxicity is imperative in determining the specific role of this sugar in *C. difficile* growth and pathogenesis. Studies of what is hypothesised to be the main *C. difficile* 630 PTS^{Mtl} at loci CD630_2331-4 will help elucidate the mechanisms of mannitol transport and fermentation, as well as toxin regulation and motility in the presence of mannitol.

Testing the growth, sugar uptake, cytotoxicity, and motility of 630WT and 630Δ*erm* (used as the control strain throughout the assays which tested each mutant) revealed no differences (ability to use sugars, ability of mannitol to suppress toxin production, and motility) between these two strains (Fig. 4.4-4.10).

However, it was later consistently observed that the growth rate of the mutants and the complements (which were originally constructed in a *pyrE*-negative background and were later converted back to *pyrE*-positive) in enriched conditions and on YTG/YTM motility assay plates lagged slightly behind that of 630Δ*erm*. As will be seen in chapter 5 (Results Chap. III –Sorbitol PTS) when testing 630WT vs. 630Δ*erm*Δ*pyrE* (parental strain), it was again observed that the *pyrE*-negative strain consistently lagged behind 630WT in a way that all mutants and complements created from targeting PTS^{Mtl} at loci CD630_2331-4 did. This is perhaps due to the inevitable accumulation of single nucleotide polymorphisms (SNPs) acquired over time during the successive passaging when creating 630Δ*erm*Δ*pyrE* (parental strain) from 630WT and 630Δ*erm*. These SNPs are possibly accounting for the altered growth rate of mutants and complements created from $630\Delta erm\Delta pyrE^{130}$.

The altered growth rate resulted in the mutants and the complemented mutants always reaching peak growth slightly later in enriched medium (TY) (e.g. at 24 h instead of 12 h as 630WT and 630Δ*erm* always did) and, assumedly, on the YTG/YTM motility assay plates than 630WT and 630Δ*erm* did. This appears to have had an effect on cytotoxicity with 630Δ*erm* exhibiting higher toxicity (in the controls TY and TYG) at the 24 h time points, and the mutants/complements cytotoxicity levels not catching up until 48 h. Such a delay in growth was generally not observed (or at least to a far less recognisable degree) in defined

media with peak growth in the controls occurring at generally the same time for all strains. As mentioned, this delay observed did not affect the level of growth and cytotoxicity (just the timing).

A more refined control strain to use instead of 630Δ*erm* perhaps may have been to restore the parental strain, 630Δ*erm*Δ*pyrE*, to *pyrE*-positive using pMTL-YN1 (empty vector) at the same time that complementation of the PTS^{Mtl} mutants was being undertaken and to use that as the control strain instead of relying on 630Δ*erm* from the lab culture collection.

The structure of this putative mannitol-specific operon in *C. difficile* 630 closely resembles the apparent PTS^{Mtl} in a diversity of Clostridia such as *C. difficile* R20291, *C. difficile* CD196, *C. perfringens* WAL-14572 (NCBI), *C. acetobutylicum* DSM 792 (Fig. 3.2)[95], and *B. stearothermophilus* (Fig. 4.95)[126], with a gene encoding a fused IICB being transcribed, followed by a regulator, an IIA, and finally, a phosphate dehydrogenase, all of which are seemingly under the control of a single promoter 331bp upstream of *mtlA*, in contrast to the PTS^{Mtl} in many other organisms such as *B. subtilis* and *V. cholerae*, which have a seperate promoter for *mtlR*[126].

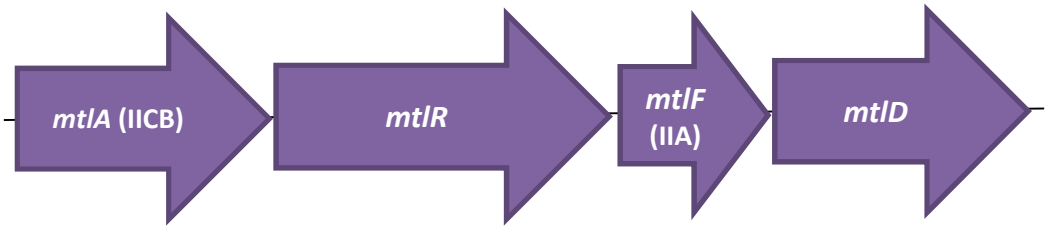

Figure 4.95: Constituent genes of PTS^{Mtl} in *B. stearothermophilus*[95,126].
Like the *C. difficile* 630 PTS^{Mtl} at loci CD630_2331-4, the mannitol operon in *B. stearothermophilus* has a single promoter with four identifiable *orfs*, and a fused IICB, unlike the PTS^{Mtl} in other organisms which have a separate promoter for *mtlR*[123], and a fused IICBA[101].

mtlD, encoding a putative MPDH at locus CD630_2331, was targeted for deletion, as this appeared to be the only gene present in *C. difficile* 630 responsible for the conversion of M-1-P to F-6-P. It was hypothesised that deletion of this gene would prevent mannitol utilisation as, regardless of any other potential mannitol-specific IIA, IIB, and IIC genes, uptake of the sugar without the ability to oxidise phosphorylated mannitol (M-1-P) to F-6-P would still stop growth in mannitol.

Deletion of *mtlD* resulted, firstly, in a significant reduction in the general growth levels of the organism in DM, DMM, and DMG broth (and on DM/DMM agar) as shown by the attenuation in OD_{600} levels (and through inspection of DMM agar plates) under the defined conditions (Fig. 4.15-16). This reduction was also observed in TY, TYM, and TYG, which was consistently observed throughout the assay (from 4 h to 72 h) performed in enriched conditions (Fig. 4.20). Secondly, mutant growth in mannitol did not reach higher levels than when grown in DM/TY alone. Indeed, growth of the mutant in DMM/TYM was consistently lower than growth of the mutant in DM/TY with no sugar (Fig. 4.16 & 4.20).

In DM and TY, mannitol utilisation was partially restored by complementing the mutant with *mtlD* using its native promoter (*Pmtl*), and was completely restored by using a stronger promoter (*fdx*). Also, growth on DMM agar and YTM agar also showed the effect of deleting and restoring *mtlD*, with much weaker growth exhibited by Δ*mtlD*, and with, as was seen clearly on YTM agar, and a partial and a complete restoration of motility on the plates by *mtlD* comp and *mtlD* overex respectively (Fig. 4.29).

Supporting these observations were the HPLC results, obtained from testing the bacterial supernatants obtained from the assay in DMM. This showed that while the control strain and the complements were using significant amounts of mannitol by 6 h and depleting all of the sugar by 10 h; *mtlD*, by 24 h, still had not used the great majority of the available mannitol (77.6%), which still means that a sizable portion (22.4%) of available mannitol was used by the mutant over the course of the assay (Fig. 4.18).

It seems that complementing using the native promoter, which was used in order for the gene to be restored at what would be considered the regular 'gene dosage'[117], was not sufficient to bring back normal levels of mannitol usage. Overexpressing *mtlD* using a stronger promoter, such as *fdx*, was necessary to observe control strain levels of mannitol uptake (Fig. 4.17-21). Perhaps this is due to the location of the restored gene being far removed from its original locus. *mtlD*'s original locus is CD630_2331, but in *mtlD* comp and *mtlD* overex it was restored between CD630_0187 (*pyrE*) and CD630_0188.

The growth assays indicated that *mtlD* is important in the utilisation of mannitol, most probably as a PDH, converting the phosphorylated form of mannitol, M-1-P (following phosphorylation by the IIB, *mtlA*), to F-6-P, thus enabling entry to glycolysis[131].

The growth of Δ*mtlD* at times appeared erratic. To cite several examples, with the assays performed in DM, Δ*mtlD* growth in the positive control, DMG, did not exhibit the major increase in growth observed in the same condition by 630Δ*erm* (and is known to occur in the presence of glucose)[28] (Fig. 4.17). Likewise, the assays in the enriched conditions revealed that Δ*mtlD* growth in TY alone from 6

h lagged far behind the levels reached by 630Δ*erm* in the same conditions. Additionally, growth in TYG did not reach near what would be normal OD_{600} levels in TYG (> 1.0) until 24 h, unlike the control strain and the complements (Fig. 4.21 & 4.22). As seen with the results from the assays performed under defined conditions, the results obtained from the assays performed in TY revealed that deleting *mtlD*, as well as affecting growth in TYM, will also affect growth in TY and TYG, and that such effects are no longer seen when *mtlD* is reinstalled. As will be discussed, Δ*mtlD* must have been using some amount of glucose (however reduced) as the HPLC results showed uptake of glucose in DMG (glucose levels at the final time point of 24 h) appeared to be only slightly above the other strains it was tested alongside (Fig. 4.19), and as will be mentioned below, toxin suppression was still occurring in TYG (Fig. 4.23-4.28).

In addition, in performing motility assays it is not possible to say if there is definitely a link or not between *mtlD* and the motility of the bacterium, as Δ*mtlD* exhibited much weaker growth on the YTG (Fig. 4.29) and YTM (Fig. 4.30) motility plates, on the top agar motility plates (Fig. 4.31), and weaker turbidity in the motility assay in tubes (Fig. 4.32) in comparison to the control strain. Noting that in the motility assay performed in tubes, Δ*mtlD*, like the control strain (and unlike the negative control *C. difficile* M120), was able to migrate the same distance (11cm) to the bottom of the tubes, indicating that the mutant strain was still motile, and that the differences seen in each motility assay were possibly not related to motility, but actually to the general growth deficiencies of the mutant strain in general, which have been seen in the other tests (growth in DM/TY and sugar uptake shown by HPLC) (Fig. 4.16, 4.18, & 4.20).

Complementing Δ*mtlD* with *mtlD* using its native promoter (*Pmtl*) (*mtlD* comp) restored mannitol uptake in DMM, as well as restoring normal growth in glucose. By 6 h, the presence of mannitol pushed *mtlD* comp growth levels significantly ahead of *mtlD* comp growth in DM alone (Fig. 4.17). However, this re-establishment of mannitol uptake by the complemented mutant was not to the same level as would normally be seen, as demonstrated by the control strain, 630Δ*erm*. Overexpression of *mtlD* was required to restore mannitol uptake to this level (Fig. 4.17). Also, it can be seen that merely complementing using the native promoter is sufficient to restore normal growth behaviour in the presence of glucose (fast efficient uptake of the sugar was completely comparable with the control strain and the overexpressed mutant), but not in the presence of mannitol (Fig. 4.17). In enriched medium, *mtlD* comp exhibited, from 6-12 h, a slight increase in OD_{600} in TYM compared to when in TY alone. By 24 h, this increase could no longer be seen, indicating that complementing using the native promoter was not sufficient to restore regular levels of mannitol uptake and allow *mtlD* comp to use the majority of the available mannitol in enriched conditions. From 8-24 h, OD_{600} levels in glucose were significantly (e.g. at 24 h, which was peak growth * $P < 0.013$) above those in TY alone (Fig. 4.23), indicating that glucose uptake in enriched conditions was mostly (but not entirely) restored by *mtlD* comp (Fig. 4.21).

Overexpression of *mtlD* by *mtlD* overex saw OD_{600} levels in TYM (** $P < 0.007$) and TYG (** $P < 0.0018$) significantly above those in TY alone from 6-24 h (Fig. 4.21), signalling that overexpressing *mtlD* will completely restore mannitol and glucose uptake to normal levels in enriched medium.

These findings (the effects observed not just in relation to mannitol, but also in regard to general growth, in glucose, and, perhaps, motility) suggest a wider role for *mtlD* in the survival and growth of the organism, instead of simply being a converter of phosphorylated mannitol. It has been seen in *S. aureus* that an *mtlD* mutant exhibited lower levels of survival in the presence of linoleic acid, an antimicrobial fatty acid, and H_2O_2, thus connecting successful mannitol uptake with the survival and growth of the bacterium, and at the same time demonstrating a wider role for *mtlD* in the proliferation of the organism[132].

With the cytotoxicity assays, Δ*mtlD* did not exhibit the cytotoxic trends displayed by the control strain. At 24 h, there was no suppression of toxin levels in TYM as was seen with the control strain (Fig. 4.22). At 48 h, in direct contrast to the control strain, mutant toxin levels weregreatly up-regulated in TYM. It is possible that the significant increase in toxin levels seen with Δ*mtlD* at 48 h in TYM (Fig. 4.24) is a sign that the bacterium was stressed and exhibited it by the production of more toxin[133]. Mutant toxin production in glucose was suppressed at 24, 48, and 72 h (Fig. 4.22, 4.24, 4.26). Complementing with *mtlD* using *Pmtl* restored toxin suppression in mannitol at 24 h, but not at 48 h and 72 h. This appeared to tally with the OD_{600} values which showed a minor increase in *mtlD* comp values in TYM (in comparison to *mtlD* comp in TY) between 6-12 h, but not at 24 h (as was seen with 630Δ*erm* and *mtlD* overex) (see Fig. 4.20-1). By 48 h and 72 h, *mtlD* comp toxin production in *mtlD* comp was no longer suppressed by mannitol. In contrast, *mtlD* comp toxin production in glucose was suppressed at 24, 48, and 72 h. (Fig. 4.23, 4.25, & 4.27). Overexpressing *mtlD* completely restored toxin suppression in TYM at each time point tested, which agrees with the increase in

growth seen in TYM (in comparison with *mtlD* overex in TY alone) from 6-24 h (Fig. 4.23, 4.25, & 4.27).

The clear differences in cytotoxicity seen between 630Δ*erm* and the *mtlD* mutant (and between the mutant and the complements) in TYM, resulting from the deletion and the restoration/overexpression of *mtlD*, indicates that *mtlD* has a role in toxin production when the organism is transporting mannitol into the cell, but perhaps also a wider regulatory role in toxin expression as evidenced by the differences observed in toxin levels in TYM between the strains *mtlD*-positive (control strain) leading to toxin suppression and *mtlD*-negative (mutant) resulting in toxin increase (Fig. 4.22, 4.24, &-4.26). In recent years, there have been increasing discoveries of multiple function genes outside of the PaLoc such as *codY*[18] and *spo0A*[49], which along with what is perceived to be their primary functions as a regulator monitoring the nutrition of the bacterial environment (*codY*)[43] and a sporulation master regulator (*spo0A*)[134,135], have also been shown to regulate toxin expression. This seems to be a possibility also with *mtlD* in *C. difficile* 630 since removal of this gene from the organism has resulted in distinct phenotypic (in relation to to toxicity) changes in TYM at 48-72 h (Fig. 4.24 & 4.26), which were then not seen when *mtlD* was adequately restored.

Clearly, deletion of *mtlD* has resulted in a weakened strain (as particularly evidenced by the failure of Δ*mtlD* to grow on DM agar –Fig. 4.15, and the weaker growth seen on the YTG and YTM agar motility plates –Fig. 4.28 & 4.29). The reduction in general growth and toxicity as shown by the attenuated and erratic growth and cytotoxicity of Δ*mtlD* in DM and TY would strongly indicate a wider role for *mtlD* in the general growth and virulence of *C. difficile* 630.

mtlF, the putative IIA of the operon at CD630_2331-4, was successfully inactivated via CT mutagenesis (Fig. 4.34). Apparent inactivation of *mtlF* showed an inability of the mutant until 24 h, in both defined and enriched conditions (also on plates of YTM –see Fig. 4.48), to utilise mannitol, resulting in attenuated growth levels (Fig. 4.37), and connectedly, there was also a reduced degree of suppression of toxicity in the mutant (Fig. 4.43, 4.45, & 4.47).

This perceived inability of CT*mtlF* to use mannitol (before 24 h) was confirmed by HPLC which showed far more (**** $P < 0.0001$) mannitol remaining in the mutant samples than the control strain samples from 6 h to 12 h (Fig. 4.39). However, at 24 h, growth of the mutant reached a peak (in DMM) indicating a delayed, yet significant (and complete) uptake of the sugar (Fig. 4.37). Like the control strain, HPLC results showed that CT*mtlF* in defined conditions had used all of the mannitol by 24 h (Fig. 4.39). Interestingly, even though CT*mtlF* was unable to utilise the sugar in defined conditions before 24 h, mutant peak growth (OD_{600} 0.84) in DMM when it belateledly occurred at 24 h, significantly exceeded that of the control strain in DMM which occurred at 10 h (0.78) (**** $P < 0.0001$) (Fig. 4.37).

It seems that *mtlF* may be playing no role in motility as the motility assays did not reveal consistent differences between the control strain and CT*mtlF* in the four variant motility assays utilised (Fig. 4.49-4.52).

Complementing the mutant using the native promoter, *Pmtl* (*mtlF* comp), or using the *fdx* promoter (*mtlF* overex), partially restored normal patterns of mannitol uptake in defined medium. Growth of the complements in DMM peaked at 24 h (the control strain peaked at 8 h, the mutant also peaked at 24 h) (Fig. 4.38). The

HPLC data showed that the complements used significantly more sugar than the mutant between 8-12 h (at 12 h: CT*mtlF* vs. *mtlF* comp * $P < 0.0251$; CT*mtlF* vs. *mtlF* overex * $P < 0.041$). The slope of the curve also indicated a more gradual decline of mutant (slope = 0.48) mannitol levels than those of the *mtlF* complemented (slope = 1.42) or *mtlF* overexpressed mutants (slope = 0.68), indicating increased mannitol uptake by the complements (Fig. 4.39).

In enriched conditions, neither complement clearly restored growth in mannitol. Unlike the results in defined medium, there did not appear to be significant increases in OD_{600} by either complement in TYM compared to when they were in TY alone. Both complements at 24 h exhibited a minor increase in OD_{600} values in TYM compared to when in plain TY. Also, in comparison to CT*mtlF*, *mtlF* comp, and *mtlF* overex declined from 24 h to 72 h at a slightly more gradual rate, as shown by the slope of graph (CT*mtlF* = 2.7, *mtlF* comp = 2.2, *mtlF* overex = 1.7) (Fig 4.42).

Cytotoxicity of CT*mtlF*, was partially restored to levels seen in TY alone at 24 h, 48 h, and 72 h (Fig. 4.43, 4.45, & 4.47), indicating that inactivation of *mtlF*, as well as preventing growth in mannitol, also prevented the suppression of toxicity when in the presence of the sugar. At 24 h, CT*mtlF*, did not exhibit quite the level of suppression seen with the control strain (Fig. 4.43) (**** $P < 0.0001$). At 48 h (Fig. 4.45) and 72 h (Fig. 4.47), there was reduced toxin suppression in TYM by CT*mtlF* in comparison to the control strain (**** $P < 0.0001$). The reduction seen with the mutant at these time points was, however, still significant, albeit reduced in comparison to the control strain (e.g. at 48 h, CT*mtlF* in TY vs. TYM **** P <0.0001, while 630Δ*erm* in TY vs. TYM **** P 0.0001) (Fig. 4.45). The slope of the curve indicates that from 24-72 h, mutant decline in TYM was slightly more

gradual than the decline in TY, suggesting that there was a minor degree of mannitol uptake by the mutant at the later time points, and perhaps that was accounting for the small (but significant) reduction in mutant TYM toxin levels at the last time point of 72 h (CT*mtlF* in TY slope = 4; CT*mtlF* in TYM slope = 2.7).

It seems, however, that the partial restoration of mannitol uptake by the complements will not, until possibly 72 h, induce a degree of toxin suppression. At 24 h and 48 h (with the possible exception *mtlF* overex at the 48 h time point), the cytoxicity of each complement resembled that of the mutant. Both complements actually showed a slightly higher amount of toxin production (as the mutant, CT*mtlF*, showed a reduced level of toxin suppression at 24 h and 48 h – Fig. 4.43 & 4.45)

Nonetheless, unlike the mutant, at 72 h, cytotoxicity of the complemented mutants appeared to be partly restored, as *mtlF* comp (toxin titre at marginally above over 10^4) and *mtlF* overex (toxin titre at slightly over 10^4) showed a stronger trend towards toxin suppression (significantly with *mtlF* overex * $P < 0.0166$) (Fig. 4.49), a consequence perhaps of the more gradual OD_{600} decline the complements exhibited in TYM compared to CT*mtlF* in TYM, which indicated a level of mannitol utilisation (Fig. 4.40 & 4.49).

There appeared to be major differences in the level of restoration of growth and cytotoxicity in mannitol between the two complements, *mtlF* comp and *mtlF* overex. Partial restoration of growth and cytotoxicity was achieved with *mtlF* comp, as was possibly expected (although even this level of restoration was unsatisfactory). But, also, with *mtlF* overex, growth and toxin production was not

returned to that of the control strain, levels as would be expected (and has been seen with *mtlD* overex and *mtlR* overex) when overexpressing the gene which seems to be likely involved in the uptake of the sugar.

Another potential reason for the relative failure of the complementation may be that the phenotypes observed with CT*mtlF* were the consequence of a polar effect (see 5.8 Discussion). Another possibility could be the presence of another IIA compatible with mannitol uptake that is located elsewhere in the genome.

The results indicate that *mtlF* is involved in the uptake of mannitol and is likely the gene that is primarily responsible for the phosphorylation of a mannitol-specific IIB domain (MtlA) involved in phosphorylating the incoming mannitol molecule. Phylogenetic analysis predicts that *mtlF* is a IIA protein, so its assumed role would be that of phosphorylating the IIB upon detection of the sugar by the IIC domain[102]. Without phosphorylation of IIB by IIA, regardless of detection of the incoming mannitol molecule by the IIC, mannitol cannot be taken up (as M-1-P), and subsequently converted to F-6-P and used as a source of energy. In this scenario, the IIB, in this case *mtlA*, remains unphosphorylated, due to the IIA (*mtlF*) being inactivated, while HPr assumedly remain phosphorylated. Without the putative PTS^{Mtl} IIA available to phosphorylate the IIB, which will, in turn, phosphorylate the incoming sugar, it is theoretically impossible for the CT*mtlF* to make use of any mannitol, unless the mannitol may get through via another, perhaps less efficient, system. The most likely route for this would be a PTS compatible with mannitol transport, and that has been postulated as being fructose PTS[106]. As mannitol-specific PTS belong to the 'fructose-mannitol' family of systems, it is plausible that the minor amount of mannitol being taken up by CT*mtlF* is coming through one of the five complete (containing an IIA, IIB, IIC)

potential fructose systems encoded in the *C. difficile* 630 genome. All of the IIA domains (at loci_0040-1, 0206, 3015, 3075, 3132) in these possible fructose PTS have also been labelled as potentially mannitol-specific (Artemis), so it is possible that although the IIA at locus CD630_2332 (*mtlF*) (which itself is annotated as 'fructose/mannitol-specific') appears to be the foremost IIA involved in phosphorylation of a mannitol-specific IIB, there are many potential IIA encoded throughout the genome which may also be involved, perhaps when *mtlF* is not functional, or when it is functional, in an auxiliary role. *In silico* analysis performed in chapter 3 revealed CD630_0206, a putative fructose/mannitol IIA, as a homologue of *mtlF* (29% identity), and therefore, potentially a strong candidate for this role of a putative secondary IIA, which possibly phosphorylates *mtlA*, resulting in the complete consumption of mannitol in defined conditions (Fig. 4.37 & 4.39) and the moderate degree of uptake of the sugar seen in enriched medium at 48 h and 72 h (Fig. 4.41).

It is known that in response to the presence of a PTS sugar such as mannitol, CcpA will induce a suppression of toxin levels via binding portions of the PaLoc, which are the regulatory regions of *tcdA, tcdB, tcdR,* and *tcdC*[23]. Such repression is indicative of the toxin genes undergoing repression of catabolism[23]. It would seem that without a functioning *mtlF* to phosphorylate *mtlA*, CcpA would not bind to those regions of the PaLoc, thus, resulting in no toxin suppression.

With the assays performed, it seems that *mtlF* probably has no role in *C. difficile* 630 motility as different assays did not reveal significant differences. No differences in the motility abilities of CT*mtlF* (in comparison to the control strain) were seen on BHIS +top agar plates (Fig. 4.51) or in tubes (Fig. 4.52). On YTG and YTM plates (Fig. 4.49-50), a difference was observed (which on YTM is

likely related to mannitol uptake), but without adequate complementation it is impossible to fully determine whether this indicated a role for *mtlF* in motility or not.

mtlR, the apparent regulator of the system, is annotated as a putative antiterminator. Transcriptional antiterminators have been shown to interact with the HPr and with the EII domains of the PTS that they are part of, which results in an alternative form of catabolic repression to that seen with CcpA[123,124]. The organisation of *C. difficile* 630 MtlR shows two encoded PRDs located in the centre of the gene (NCBI), the sites of phosphorylation and which interact with the EII domains of the PTS[126].

mtlR was successfully inactivated by the CT (Fig. 4.54). The resultant mutant, CT*mtlR*, exhibited no mannitol-induced increase in growth in defined or enriched conditions (and also on plates of YTM), in clear contrast to the control strain (Fig. 4.57, 4.59, & 4.61).

In DM (Fig. 4.57) and TY (Fig. 4.61), the mutant behaved as if it was incapable of recognising the mannitol in the medium. Also, unlike CT*mtlF* showing some utilisation of mannitol towards the end of the assays (24 h in DM; 48-72 h in TY) (Fig. 4.37 & 4.41), CT*mtlR* OD_{600} in DMM/TYM declined at the same rate as in DM/TY (Fig. 4.57 & 4.61). This was mirrored in the HPLC results revealing no use of any of the sugar by the mutant (Fig. 4.59).

Similarly, with cytotoxicity, CT*mtlR* displayed none of the well-established suppression of toxin levels seen by *C. difficile* in mannitol[28]. At each time point, toxin levels in TYM resembled those in TY alone (Fig. 4.63, 4.65, & 4.67).

Complemented *mtlR* mutants (*mtlR* comp and *mtlR* overex) exhibited the restored ability to use mannitol in DMM (Fig. 4.58), on YTM plates (Fig. 4.71), and in TYM, and connectedly, restored mannitol-induced repression of *C. difficile* 630 cytotoxicity (Fig. 4.64, 4.66 & 4.68). Complementing using the native promoter was not sufficient to fully restore growth and cytoxicity as seen with the growth assays, HPLC data, and toxin assays. *mtlR* comp in mannitol showed an ability to reach levels of growth significantly above that without mannitol, but unlike 630Δ*erm* (6 h) and *mtlR* overex (8 h), this occurred at 24 h of incubation. HPLC confirmed that *mtlR* comp utilisation of mannitol was somewhat delayed (in comparison with 630Δ*erm* and *mtlR* overex) with significant uptake occurring from 12 h and depletion of most of the sugar (73.3%) by 24 h (Fig. 4.61).

mtlR comp showed the ability to suppress toxin levels (unlike CT*mtlR*). Nevertheless, the re-establishment of toxin suppression did not occur, as happened with the control strain and the overexpressed mutant, from 24 h (Fig. 4.63 & 4.64) onwards, but, at the later time points of 48 h and 72 h (Fig. 4.66 & 4.68), tying in with the belated mannitol uptake shown by *mtlR* comp (Fig. 4.62).

Overexpressing *mtlR* completely restored mannitol uptake to control strain levels. Like the control strain in defined medium from 6 h (Fig. 4.57), the presence of mannitol induced a major increase in growth, a result mirrored in the HPLC analysis showing all of the available sugar in the 630Δ*erm* and *mtlR* overex samples gone by 8 h (Fig. 4.59).

Inactivating *mtlR* appears to have produced no effect on motility as testing using four variant motility assays revealed no major differences between the control strain, the mutant, and the complements (Fig. 4.69-72). The mutant and the

complements behaved similarly on YTG plates (Fig. 4.69). Although reduced motility was observed on the YTM plates with the mutant, which was then reversed with the complements, it would appear that this is perhaps connected to the mannitol-fermenting abilities of each strain to show motility on this medium (Fig. 4.70). The motility assays in tubes showed no differences between each strain in their abilities to migrate through the agar in the tube (while the non-motile negative control strain M120 did not migrate at all) (Fig. 4.72).

As mentioned, the central part of MtlR consists of two PRDs. PRDs are considered as being targets of PTS-mediated phosphorylation, which will moderate transcriptional regulation[95]. MtlR belongs to a group of regulators found in a variety of bacteria containing PRDs which control the expression of the PTS, and a general mechanism of regulation of their activity has been put forward based on multiple phosphorylation of PRDs by the components of the PTS[125]. So, in the absence of an inducer (i.e. a sugar like mannitol), the regulator (MtlR), is phosphorylated by its corresponding EII (MtlA) and is inactive. When the inducer is present, it is transported and phosphorylated by the PTS, and the regulator becomes dephosphorylated, and as a result, is activated. Consequently, induction is achieved in response to the presence of the PTS substrate. Also, some PRD-containing regulators are also phosphorylated by the general PTS phosphor-carrier protein, HPr, in order to be active. This activation is prevented if phosphate is diverted from HPr to support transport and phosphorylation of another, more readily, metabolised sugar such as glucose. The consequent inactivation of the regulator underlies a form of catabolite repression[95]. In the case of the MtlR protein of *B. stearothermophilus*, DNA has been demonstrated to be stimulated by HPr-dependent phosphorylation and decreased on phosphorylation

by the EIICB^{Mtl}, showing a direct link between the phosphorylation state of the regulator and transcriptional regulation activity[126].

It would seem that with the CT inactivation of *mtlR*, no regulation of PTS^{Mtl} is occurring, so the system appears to be dependent upon *mtlR*-mediated regulation, resulting in no mannitol-utilisation. Unlike CT*mtlF* [which showed some uptake of mannitol as seen by the HPLC results showing depletion of the sugar by that mutant in defined medium by 24 h (Fig. 4.39), and in enriched medium by the more gradual decline that was observed from 24-72 h in TYM than in TY (Fig. 4.42)], CT*mtlR* appeared to be unable to use any mannitol, as the OD_{600} at these time points dropped at the same rate and to the same level in DM/TY as in DMM/TYM (Fig. 4.57 & 4.61), and the HPLC results indicated no uptake of the sugar by the mutant (Fig. 4.58). As revealed in chapter 3, encoded within *C. difficile* 630 are three MtlR homologues: SrlR, CD_2416, and CD_0040. However, unlike MtlR, these proteins apparently possess only a single PRD (Fig. 3.6). As PRDs are the sites of phosphorylation in antiterminators[95,125,126], it appears that despite the homology of SrlR, CD_2416, and CD_0040 to MtlR, an antiterminator involved in mannitol utilisation requires two PRDs (such as MtlR in *C. acetobutylicum* DSM 792[95] and *B. stearothermophilus*[126]), and, thus, without a functioning MtlR, no mannitol uptake was discerned with CT*mtlR* (in contrast to CT*mtlF* at 24-72 h –Fig. 4.39, 4.41, & 4.43). This was confirmed by the restoration of growth and cytotoxicity by the complemented mutants, *mtlR* comp and *mtlR* overex.

Testing the effect of CT inactivating *mtlR* on sporulation revealed no change to the sporulating ability of the organism. The parental strain, 630Δ*erm*Δ*pyrE* (which was used as the control for the spore assays), produced similar levels of

heat-resistant CFUs/mL as the mutant, CT*mtlR* (Fig. 4.72). This is not very surprising when considering, to date, the lack of a strong link between the PTS and *C. difficile* sporulation.

The *C. difficile* 630 mannitol-specific PTS IIA, IIB, and IIC domains, in contrast to the *E. coli* EIICBA^{Mtl109}, but like that of *C. acetobutylicum* DSM 792 (Fig. 4.95)[95], consists of a fused IICB permease (Artemis), a fusion likely to increase the efficient uptake of the sugar[102].

Deletion of the IICB domain protein, *mtlA*, prevented growth in mannitol (Fig. 4.78) and resulted in no clearly observable mannitol-induced suppression of toxin levels (Fig. 4.84, 4.86, & 4.88).

In DMM, Δ*mtlA* was unable to exhibit the major increase in OD_{600} levels that was seen with 630Δ*erm*, the control strain, from 6 h (Fig. 4.79). As shown by the HPLC analysis, while the control strain had spent almost all of the available mannitol by 8 h; at 24 h, Δ*mtlA* still had 75.6% of the sugar unused (Fig. 4.80).

Growth of the mutant in DMM did show, however, a minor, insignificant increase in OD_{600} compared to when it was in DM from 6 h to 24 h. It was this consistent increase that agreed with the HPLC results which showed that the mutant was capable of using a significant amount (24.4%) of the available mannitol by 24 h (Fig. 4.80). Restoration of *mtlA* permitted the complemented mutant, *mtlA* comp, like the control strain, to utilise mannitol, allowing *mtlA* comp to exhibit from 6 h significantly higher growth in DMM compared to when it was in DM alone (Fig. 4.79). Also, by 10 h, *mtlA* comp had spent the mannitol that was available (Fig. 4.80).

In the enriched medium, while the control strain showed significantly higher growth from 8 h in TYM as compared to when it was in TY alone, growth of the mutant in mannitol resembled that in TY broth without sugar (Fig. 4.82). At 24 h incubation, growth of the mutant peaked in TY (OD_{600} = 1.0) and TYM (OD_{600} = 0.99), but was below the peak OD_{600} reached by the control strain in TYM (1.12 at 12 h). This indicates that the mutant was unable to use the available mannitol in the enriched conditions.

All of the presented evidence strongly suggests that *mtlA* encodes the main route for mannitol detection, phosphorylation, and uptake in *C. difficile* 630. Without a functioning $IICB^{Mtl}$ at loci CD630_2334 it would appear that *C. difficile* 630 cannot use a large amount of mannitol, but would also suggest that perhaps the minor amount of mannitol getting through to the bacteria (as seen with the HPLC results) was coming via a different route. As previously mentioned, the mannitol PTS belongs to the fructose-mannitol family of PT systems[95,101], and it seems possible for mannitol to be taken up by compatible fructose systems. Considering that encoded within the *C. difficile* 630 genome, there are annotated five putative fructose PTS (Artemis), four of which are annotated as 'fructose/mannitol', it may be possible for an amount of mannitol transport to be facilitated by one or more of these potential fructose PTS.

Cytotoxicity of Δ*mtlA* in TYM was at similar levels to that seen with Δ*mtlA* in TY (Fig. 4.84, 4.86, & 4.88). For example, 630Δ*erm* toxin levels at 72 h in TYM were suppressed going from far above a toxin titre of 3.3×10^5 in TY to 1.3×10^2 in TYM (*** $P < 0.001$); while with the mutant, cytotoxicity was completely restored with toxin levels in TY and TYM remaining almost unchanged at a titre of 2.7×10^5 And 2.5×10^5 respectively (Fig. 4.88). With the complemented

mutant, *mtlA* comp, toxin suppression was not restored at 24 h (Fig. 4.85), nor at 48 h (Fig. 4.87), but was later partially re-established in mannitol at 72 h with toxin levels going from a titre of 2.2 x 10^5 in TY to 1.2 x 10^4 in TYM (with variance) (*mtlA* comp TY vs. TYM **** $P < 0.0001$) (Fig. 4.89). This shows that without *mtlA* present, *C. difficile* 630 will not suppress toxin production in the presence of mannitol.

The partial restoration of cytotoxicity seen with *mtlA* comp was related to the partial restoration of mannitol uptake by the complement in TYM (Fig. 4.82). In enriched medium, the presence of mannitol did not result in a significant increase in *mtlA* comp OD_{600} levels. Only at 72 h did the presence of mannitol in the medium result in *mtlA* comp exhibiting a higher OD_{600} compared to when in plain TY. The slope of the curve indicates a more gradual decline of the complement in TYM than in TY alone (slope 24-72 h: in TY = 2.65, in TYM = 1.9). The higher OD_{600} for *mtlA* comp in TYM at 72 h was likely accounting for the reduction in cytotoxicity seen in TYM as the complement was capable of utilising a considerable amount of mannitol which in-turn induced a significant down-regulation of *C. difficile* cytotoxicity (Fig. 4.89).

It seems that *mtlA* is not involved in motility. Although, Δ*mtlA* exhibited reduced motility on plates of YTG in comparison to 630Δ*erm*, the complement (*mtlA* comp) behaved no differently to the mutant (Fig. 4.89). It seems that the differences between 630Δ*erm*, the mutant, and the complement may have more to do to with the differences observed between 630Δ*erm* and 630Δ*erm*Δ*pyrE* (the parental strain from which all mutants and the complements was made from). On YTM, Δ*mtlA* exhibited a reduced zone of motility in comparison to 630Δ*erm*, a reduction which was partly restored by *mtlA* comp (Fig. 4.91). This appears to be

related to the mannitol-metabolising abilities of each strain. Also, the motility assays on top agar (Fig. 4.91) and in the tubes (Fig. 4.93) showed each strain tested to be motile (except M120), with no noticeable differences between 630Δ*erm*, Δ*mtlA*, and *mtlA* comp.

mtlA appears not to play a role in *C. difficile* 630 sporulation as Δ*mtlA*'s ability to form heat-resistant colonies was unimpaired in comparison to the parental strain, 630Δ*erm*Δ*pyrE* (Fig. 4.94).

As mentioned before, the pleiotropic regulator, CcpA[22], suppresses *C. difficile* toxin production through binding to the regulatory portions of *tcdA, tcdB,* and *tcdR* when a fermentable PTS sugar such as mannitol is being transported into the organism[23,28]. It would appear that since the mutant (Δ*mtlA*) seemed incapable of detecting, transporting, and phosphorylating large amounts of mannitol due to the absence of *mtlA*, CcpA was no longer inhibiting toxin synthesis by its binding to the PaLoc genes, and hence, the lack of toxin suppression in mannitol by Δ*mtlA* (Fig. 4.88) and the partial restoration of it by *mtlA* comp (Fig. 4.89).

5.0 Results Chapter III -Sorbitol PTS (CD630_0762-8)

5.1 Sorbitol Operon

Sorbitol (Srl) ($C_6H_{14}O_6$) (Fig. 5.1) (PubChem), also known as glucitol (Gut)[136], is found in many fruits in nature such as berries, cherries, plums, apples, and pears[137,138], and is widely used in the food industry as a sweetener[136].

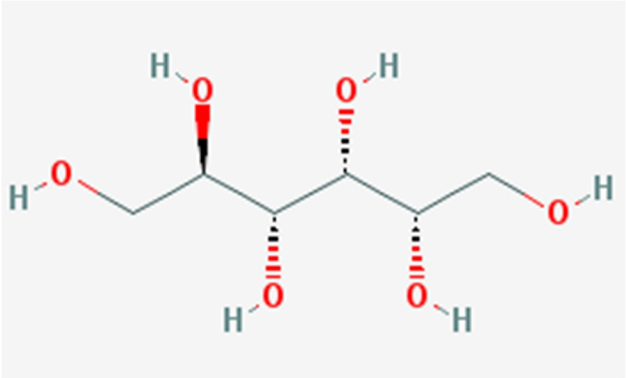

Figure 5.1: Structural diagram illustrating the six-carbon chain sorbitol (PubChem).
Sorbitol is used in the food industry as a sweetener and is utilised by *C. difficile* as a fermentable carbon source (Chapter 3, Fig. 3.1D).

The utilisation of sorbitol as a carbon source for bacteria has been previously described in *C. beijerinkii*[122], *E. coli*[122], and *Lactobacillus casei*[136]. Encoded within the *C. difficile* 630 genome (as well as within the genomes of *C. difficile* R20291 and *C. difficile* 196), amongst others, there are two operons annotated as being sorbitol-specific, the first is at loci CD630_0762-8, and the second one, at loci CD630_2414-8 (Artemis). The following sequences, indicating the presence of a promoter for this operon, GATTATAAT and TTAATT boxes, are respectively located 32bp and 55bp upstream of the operon at loci CD630_0762-8. The operon consists of seven open reading frames (*orf*) encoding a regulator (*srlR*/*gutR*), an operon activator (*gutM*), an enzyme IIC domain (*gutA*), two genes encoding a single protein for the enzyme IIB domain (*srlE_N* and *srlE_C*

termini), an enzyme IIA domain (*srlB*), and finally, a sorbitol phosphate dehydrogenase (SPDH) (*gutD*) responsible for conversion of phosphorylated sorbitol, sorbitol-1-phosphate (S-1-P), to fructose-6-phosphate (F-6-P) (Fig. 5.2).

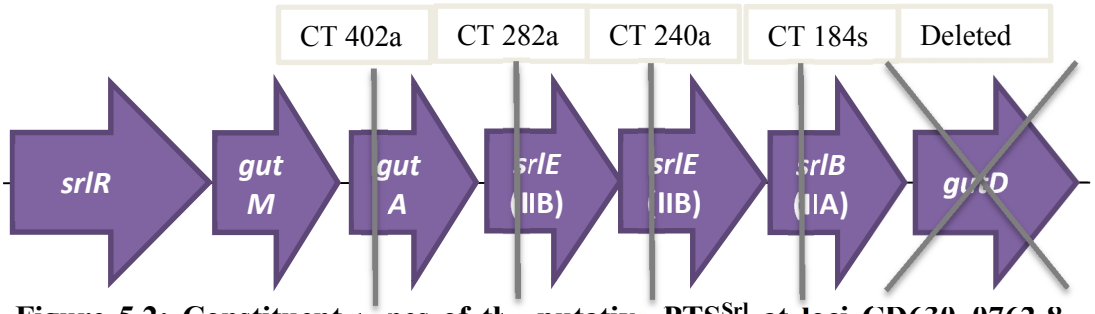

Figure 5.2: Constituent genes of the putative PTS^{Srl} at loci CD630_0762-8, showing genes targeted for CT mutagenesis, indicated by the chosen insertion site, and deletion, marked by a cross (Artemis).
The operon has seven genes apparently encoding six protein products under the control of a single promoter.

5.1.1 SrlR –transcriptional regulator

The *srlR* gene encodes a transcriptional regulatory protein. In *E. coli*, SrlR (GutR) has been suggested to be a repressor (while in *L. casei* it is an activator)[136,139]. However, unlike the sorbitol-specific operon in *E. coli*, which has a separate promoter for the *srlR* and *gutM* genes of the operon, as well as another promoter for the EII domains[136], the *C. difficile* 630 PTS^{Srl} operon at loci CD630_ 0762-8 appears to have a single promoter for the entire system.

5.1.2 GutM – operon activator

gutM has been annotated as encoding an operon activator. It has been speculated that in *L. casei* the ratio of GutR and GutM might determine the extent of expression of the sorbitol operon[136]. To date, nothing is known about the function of GutM in *C. difficile*.

5.1.3 GutA –IIC domain

gutA is annotated as encoding a sorbitol-specific IIC, apparently responsible for facilitating the passage of sorbitol across the bacterial cell membrane (Artemis).

5.1.4 SrlE –IIB domain

srlE encodes a sorbitol IIB domain, which is encoded, unusually, by two genes, at locus CD630_0765 and locus CD630_0766, respectively encoding the N- and C-terminus of the IIB protein (Fig. 5.3).

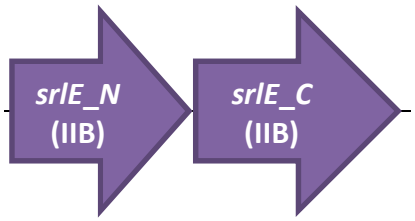

Figure 5.3: CD630_0765-6 encoding the N-terminus (0765) and the C-terminus (0766) of the IIB domain of PTS^{Srl} at loci CD630_0762-8.
Two genes (0765-6), seemingly, encode a single protein product. The genes encoding the entire protein were sequenced in order to clarify that two genes separately encode the N and C termini of SrlE.

To date, this encoding of the N and C termini by separate genes has generally not been observed in PTS. To clarify that this is not an error made during the sequencing and annotation of the *C. difficile* 630 genome, primers encompassing the region encoding the entire protein (CD630_0765-6) were designed, and the resulting PCR fragment was sequenced. Complete homology was found between the sequenced DNA and the annotated data on NCBI, indicating that the structure of CD630 IIB PTS^{Srl} at loci 0765-6 is, indeed, unique (Fig. 5.4).



Figure 5.4: Alignment of sequenced CD630_*srlE* fragment with the sequences of *srlE_N* and *srlE_C* available on GenBank.
Primers, CD_0765-6 F and R, were used to amplify and sequence *srlE*. Complete homology was found between the sequenced fragment and the publicly available *srlE* sequence.

5.1.5 SrlB –IIA domain

SrlB is an apparent IIA domain protein encoded at locus CD630_0767 that is potentially responsible for the phosphorylation of the putative PTS^{Srl} IIB at loci CD630_0765-6.

5.1.6 GutD –Sorbitol Phosphate Dehydrogenase

Encoded by a 0.77 kb gene, GutD has been speculated to be responsible for the conversion of phosphorylated sorbitol to F-6-P (NCBI), and appears to be the only gene present in the genome annotated as having this function.

5.2 Growth, sugar uptake, cytotoxicity, and motility of wild-type (WT) and parental strains

The parental strain, 630Δ*ermΔpyrE*, from which each mutant was to be constructed, was compared with 630 wild-type (WT) to confirm that there were no phenotypic differences in growth and toxicity resulting from the deletion of *C. difficile* 630 *ermB* and *pyrE*[117], which could be mistakenly attributed to those PTS genes which were being targeted for inactivation or deletion.

5.2.1 Growth of 630WT vs. 630Δ*ermΔpyrE* on DM agar

630WT and 630Δ*ermΔpyrE* (used as the parental strain from which the mutants were created) were grown (in triplicates) on DM agar plates with no sugar (not

shown) and with sorbitol. Strong growth was exhibited by both strains on DM and DMS (Fig. 5.5).

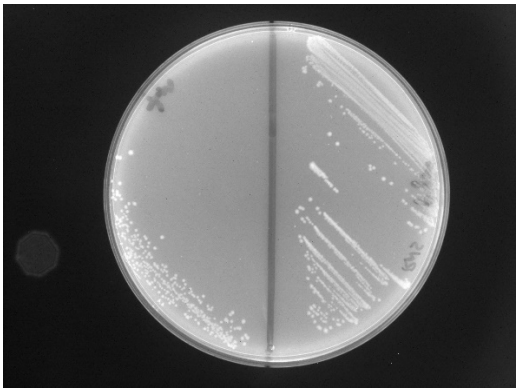

Figure 5.5: Representative image showing growth of WT (left) and parent (right) on DMS agar.
Strains (in triplicates) were streaked on plates of DM agar containing 0.6% w/v sorbitol and incubated at 37°C for 16 h to see if it was possible to observe a growth phenotype. Strong growth was observed with both strains. Differences in the ability to metabolise sorbitol by 630WT and 630Δ*ermΔpyrE* (parent) could not be discerned, as both strains grew well on DM (negative control –not shown) and on DMS.

5.2.2 Growth of 630WT vs. 630Δ*ermΔpyrE* in DM, DMS, and DMG broth

WT and parental (630Δ*ermΔpyrE*) strains in defined conditions both exhibited an increase in OD_{600} levels in sorbitol and glucose compared to when in DM alone. But, 630WT, from 2 h incubation, showed a more rapid increase in OD_{600} in each condition in comparison to 630Δ*ermΔpyrE* at the same time points. 630WT slope of the curve 0-8 h in DMS = 1.64, in DMG = 1.76 (Fig. 5.6).

630Δ*ermΔpyrE* was almost capable of reaching the same level of growth as 630WT, but at a delayed rate. For example, peak OD_{600} for 630WT in DMS was at 8 h (0.82) and in DMG was at 6 h (0.92); while peak OD_{600} for 630Δ*ermΔpyrE* in DMS occurred at 24 h (0.81) and in DMG at 10 h (0.88) (Fig. 5.6). 630Δ*ermΔpyrE* slope of the curve 0-8 h in DMS = 0.73, in DMG = 1.00.

630WT in DMS (peak growth) vs. 630Δ*ermΔpyrE* in DMS (peak growth) ** P < 0.0012.

630WT in DMG (peak growth) vs. 630Δ*ermΔpyrE* in DMG (peak growth) ** P < 0.008.

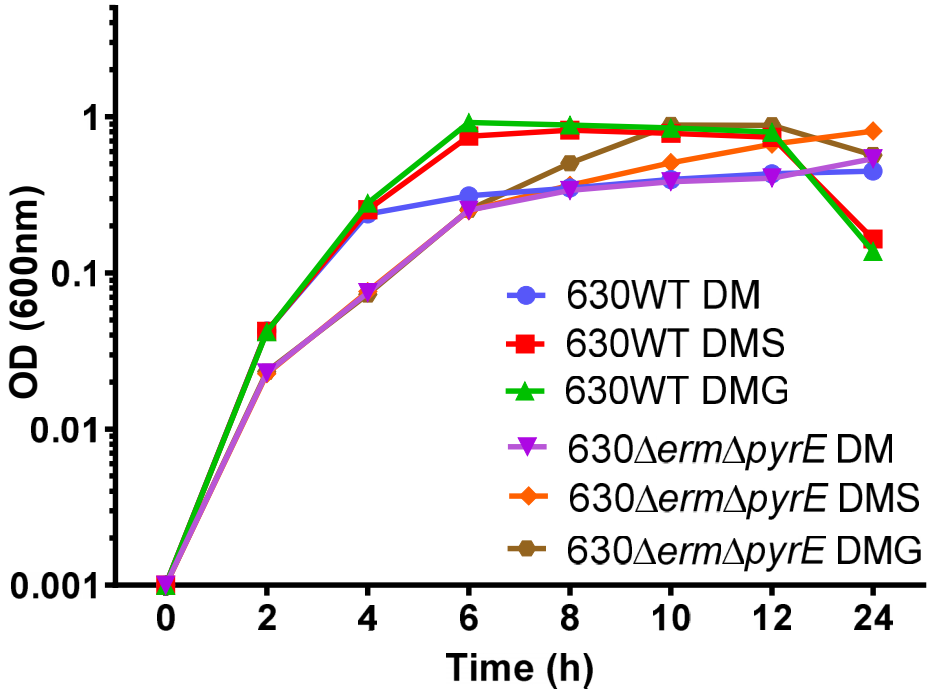

Figure 5.6: Growth of 630WT vs. 630Δ*ermΔpyrE* (parental strain) in DM.
WT and parental strains were incubated for 24 h at 37°C. 1mL extracts (triplicates) were taken at regular time points and the OD_{600} measured.
No differences in growth patterns were seen between the WT and the parental strain, 630Δ*ermΔpyrE*, with both strains exhibiting a significant increase in growth in glucose (from 8 h) and in sorbitol (from 10 h), and hence, no overall differences in growth levels were observed.
630WT slope of the curve 0-8 h in DMS = 1.64, in DMG = 1.76.
630Δ*ermΔpyrE* slope of the curve 0-8 h in DMS = 0.73, in DMG = 1.00.
One-way ANOVA was used to determine statistical significance.
630WT in DMS (peak growth) vs. 630Δ*ermΔpyrE* in DMS (peak growth)
** P < 0.0012.
630WT in DMG (peak growth) vs. 630Δ*ermΔpyrE* in DMG (peak growth)
** P < 0.008.

5.2.3 HPLC evaluation of sorbitol/glucose consumption in DM

630WT and 630Δ*ermΔpyrE* both gradually consumed the available sorbitol until it was completely used by both strains by 24 h, although consumption of the sugar by the parental strain (630Δ*ermΔpyrE*) lagged noticeably behind that of the WT throughout the assay. To cite a single very noticeable example, at 12 h, there was only an average of 0.95mM sorbitol left in the WT samples (8-12 h, slope = 3.18), while the parental strain samples still had 4.39mM sorbitol (8-12 h, slope = 1.59) (WT vs. parent at 12 h * $P < 0.02$) (Fig. 5.7).

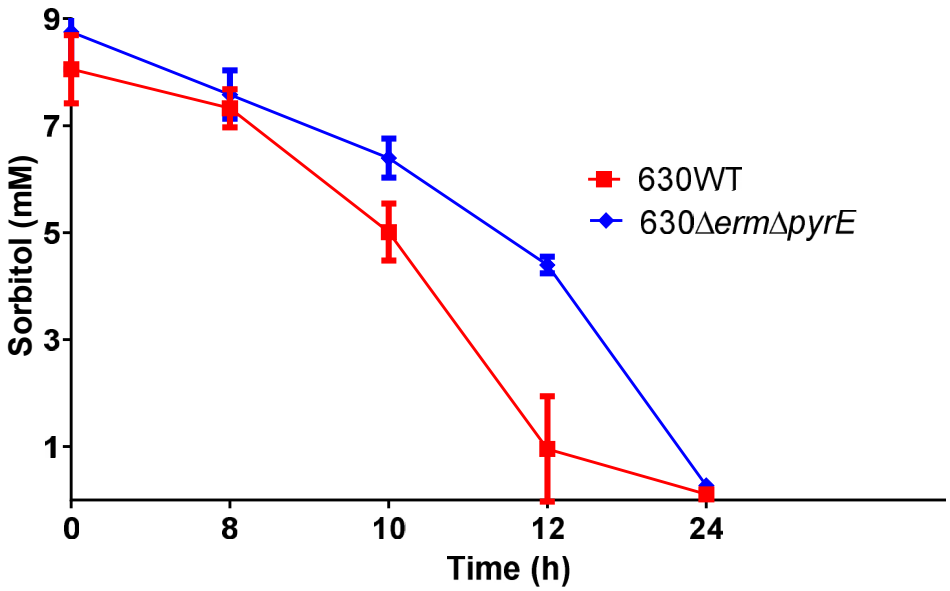

Figure 5.7: HPLC evaluation of sorbitol uptake in DM by 630WT and 630Δ*ermΔpyrE* (parental strain).
Extracts (triplicates) from the growth assay in DM were used to determine by HPLC the exact amount of the sugar remaining in the medium at each time point. The sorbitol in the 630WT and parental strains samples was completely depleted by the 24 h time point.
630WT 8-12 h, slope = 3.18. 630Δ*ermΔpyrE* 8-12 h, slope = 1.59.
One-way ANOVA was used to determine statistical significance.
630WT vs. 630Δ*ermΔpyrE* at 12 h * $P < 0.02$.

Glucose levels in both strains were depleted, as was expected, between 0 h and 24 h (**** $P < 0.0001$). No differences in glucose uptake emerged between the

strains, indicating that the absence of *ermB* and *pyrE* genes is not affecting the glucose metabolising abilities of the parental strain (Fig. 5.8).

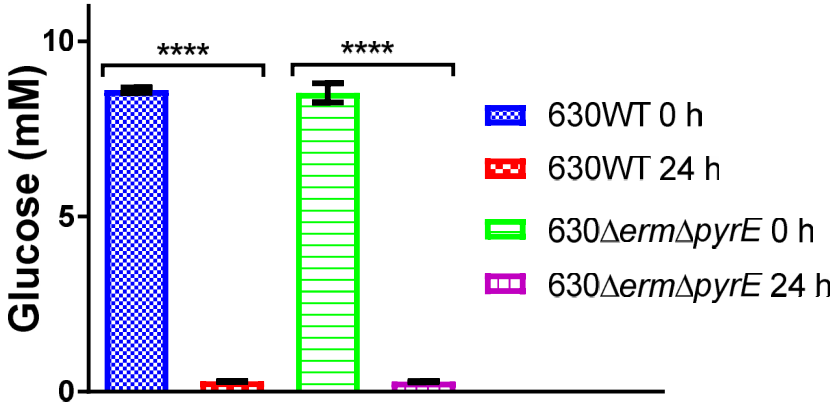

Figure 5.8: HPLC evaluation of glucose uptake in DM by 630WT and 630Δ*erm*Δ*pyrE* (parental strain).
Extracts (triplicates) from the growth assay in DM were used to determine by HPLC the exact amount of the sugar remaining in the medium at both time points. The glucose that was in medium at the start of assay at 0 h was depleted by 630WT and the parental strain by 24 h (**** $P < 0.0001$).
One-way ANOVA was used to determine statistical significance.

5.2.4 Growth of 630WT vs. 630Δ*erm*Δ*pyrE* in TY, TYS, and TYG

No major differences with regard to growth levels were observed between 630WT and 630Δ*erm*Δ*pyrE* (parental strain) in enriched medium. Growth levels of 630WT in TY and TYS were slightly lower than that of the parent, but the growth patterns remain almost the same (Fig. 5.9). OD_{600} levels for both strains in TYS peaked at 24 h, and exhibited a much more gradual decline at 96 h and 120 h than those grown in TY. In TYG, growth for both strains, reached a peak at 12 h (Fig. 5.9).

Growing the WT and parental strains in enriched medium (TY) caused the growth of the WT and parental strains to lag when in the presence of sorbitol compared to

when in TY alone. Growth of the WT in TY peaked at 24 h (OD_{600} = 0.884) and also at 24 h in TYS (OD_{600} = 0.771).

The parental strain, meanwhile (at 24 h), peaked at an OD_{600} of 1.02 in TY and at an OD_{600} of 0.94 in TYS. Overall, from 24-120 h in TYS OD_{600} values of 630Δ*ermΔpyrE* declined more gradually than 630WT, but when calculating for 24-72 h, 630WT decline was marginally slower (OD_{600} for both strains at 96 h and 120 h had much variance) (Fig. 5.9).

In glucose, however, WT growth was slightly quicker than the parental strain with growth peaking at 12 h (OD_{600} 1.15), while the parental strain peaked at 24 h (OD_{600} 1.05) (Fig. 5.9).

630WT slope of curve 2-24 h in TY = 1.47, in TYS = 1.28, in TYG = 1.68, in TYS (downward) 24-72 h = 0.72, in TYS (downward) 24-120 h = 0.47.

630Δ*ermΔpyrE* slope of the curve 2-24 h in TY = 1.7, in TYS = 1.56, in TYG = 1.75, in TYS (downward) 24-72 h = 0.8, in TYS (downward) 24-120 h = 0.40.

630WT vs. 630Δ*ermΔpyrE* in TYS at 24 h (peak growth) * $P < 0.04$.

630WT (peak growth at 12 h) vs. 630Δ*ermΔpyrE* (peak growth at 24 h) in TYG

* $P < 0.02$.

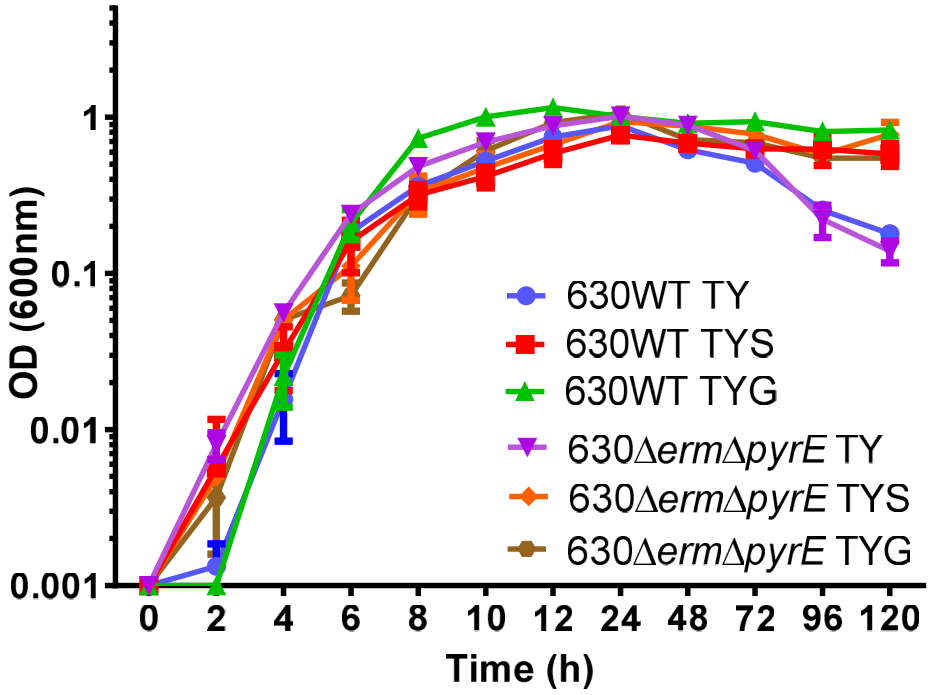

Figure 5.9: Growth of 630WT vs. 630Δ*erm*Δ*pyrE* (parental strain) in TY.
WT and parental strains were incubated for 120 h at 37°C. 1mL extracts (triplicates) were taken at regular time points and the OD_{600} measured.
No differences in growth patterns were seen between the WT and the parental strain, 630Δ*erm*Δ*pyrE*, with both strains exhibiting a significant increase in growth in glucose, and a very gradual decline in sorbitol, and hence, no differences in growth levels were observed.
630WT slope of curve: in TY 2-24 h = 1.47, in TYS = 1.28, in TYG = 1.68, in TYS (downward) 24-72 h = 0.72, in TYS (downward) 24-120 h = 0.47.
630Δ*erm*Δ*pyrE* slope of the curve: in TY 2-24 h = 1.7, in TYS = 1.56, in TYG = 1.75, in TYS (downward) 24-72 h = 0.8, in TYS (downward) 24-120 h = 0.40.
One-way ANOVA was used to determine statistical significance.
630WT vs. 630Δ*erm*Δ*pyrE* in TYS at 24 h (peak growth) * $P < 0.04$.
630WT (peak growth at 12 h) vs. 630Δ*erm*Δ*pyrE* (peak growth at 24 h) in TYG * $P < 0.02$.

5.2.5 Cytotoxicity of 630WT and 630Δ*erm*Δ*pyrE*

In TYS, 630WT showed a decrease in toxin production at 72 h going from a toxin titre of 1.9 x 10^4 in TY to slightly over 1.5 x 10^4 in TYS (* $P < 0.013$) (Fig. 5.10).

Toxin production was also suppressed by sorbitol in 630Δ*erm*Δ*pyrE* with toxin titres of 1.6 x 10^5 in TY to 1.2 x 10^5 in TYS (* $P < 0.02$) (Fig. 5.10).

630WT toxin production in TY was significantly lower than 630Δ*ermΔpyrE* in TY (*** P < 0.00015). 630WT toxin production in TYS was significantly lower than 630Δ*ermΔpyrE* in TYS (**** P < 0.0001) (Fig. 5.10).

630WT (**** P < 0.0001) and 630Δ*ermΔpyrE* (**** P < 0.0001) both suppressed cytotoxicity in TYG (Fig. 5.10).

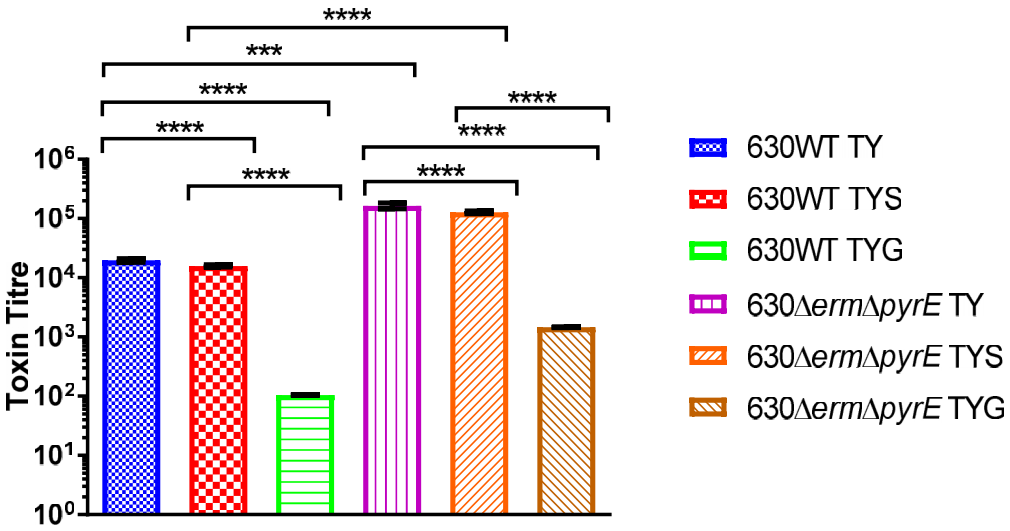

Figure 5.10: Cytotoxicity of 630WT and 630Δ*ermΔpyrE* (parental strain) at 72 h in TY.
Cytotoxicity of 630WT and 630Δ*ermΔpyrE* at 72 h. Serial dilutions of bacterial supernatants (triplicates) were applied to Vero cell monolayers (p34) to determine the toxin titre of the WT and the parental strain (630Δ*ermΔpyrE*).
630WT showed a small toxin decrease in TYS (* P < 0.013), while 630Δ*ermΔpyrE* also significantly (* P < 0.02) suppressed cytotoxicity in TYS. 630WT and 630Δ*ermΔpyrE* both suppressed cytotoxicity in TYG (**** P < 0.0001).
One-way ANOVA was used to determine statistical significance.
630WT TY vs. TYS * P < 0.013.
630WT TY vs. 630Δ*ermΔpyrE* TY *** P < 0.00015
630WT TYS vs. 630Δ*ermΔpyrE* TYS **** P < 0.0001.
630Δ*ermΔpyrE* TY vs. 630Δ*ermΔpyrE* TYS * P < 0.02.

At 96 h, sorbitol suppressed toxin production in 630WT, going from a toxin titre of 3.9 x 10^4 in TY to 1.6 x 10^4 (** P < 0.002) (Fig. 5.11).

In TYS, 630Δ*ermΔpyrE* was seen to significantly (*** P < 0.0002) increase cytotoxicity, going from a toxin titre of 4.7 x 10^5 (with minor variance) in TY to 1.7 x 10^6 in TYS (Fig. 5.11).

630WT toxin production in TY was significantly lower than 630Δ*ermΔpyrE* in TY (** P < 0.004). 630WT toxin production in TYS was significantly lower than 630Δ*ermΔpyrE* in TY (**** P < 0.0001) (Fig. 5.11).

630WT (**** P < 0.0001) and 630Δ*ermΔpyrE* (**** P < 0.0001) cytotoxicity in TYG (Fig. 5.11) was suppressed for both.

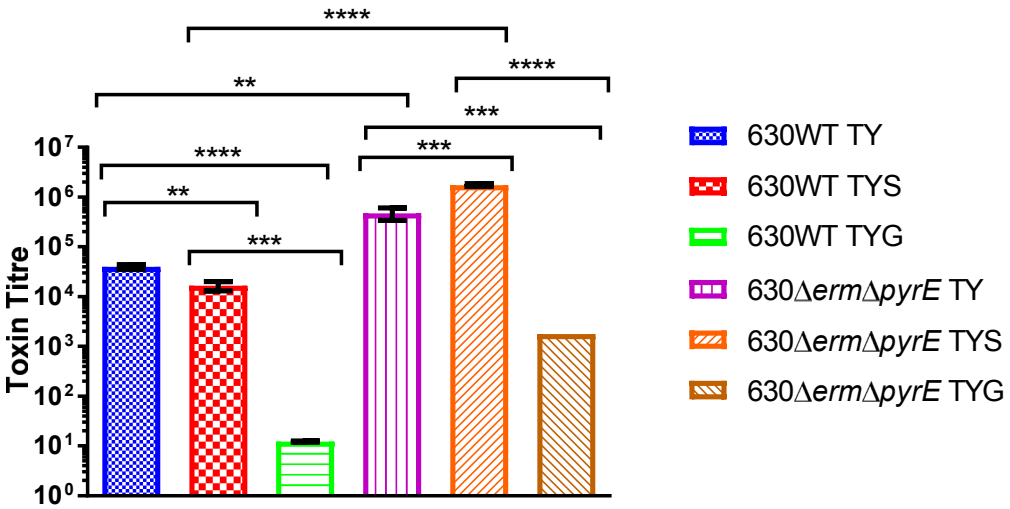

Figure 5.11: Cytotoxicity of 630WT and 630Δ*ermΔpyrE* (parental strain) at 96 h in TY.
Cytotoxicity of 630WT and 630Δ*ermΔpyrE* at 96 h. Serial dilutions of bacterial supernatants (triplicates) were applied to Vero cell monolayers (p34) to determine the toxin titre of the WT and the parental strain (630Δ*ermΔpyrE*).
630WT showed a toxin decrease in TYS (** P < 0.002), while 630Δ*ermΔpyrE* significantly (*** P < 0.0002) increased cytotoxicity in TYS. 630WT and 630Δ*ermΔpyrE* both suppressed cytotoxicity in TYG (**** P < 0.0001).
One-way ANOVA was used to determine statistical significance.
630WT TY vs. TYS ** P < 0.002.
630WT TY vs. 630Δ*ermΔpyrE* TY ** P < 0.004.
630WT TYS vs. 630Δ*ermΔpyrE* TYS **** P < 0.0001.
630Δ*ermΔpyrE* TY vs. 630Δ*ermΔpyrE* TYS *** P < 0.0002.

At 120 h, sorbitol suppressed toxin production in 630WT, going from a toxin titre of 1.9 x 10^4 in TY to 1.5 x 10^4 (* P < 0.013) (Fig. 5.12).

In TYS, cytotoxicity of 630Δ*ermΔpyrE* was seen to significantly (* P < 0.02) decrease, going from a toxin titre of 1.6 x 10^5 in TY to 1.2 x 10^5 in TYS (Fig. 5.12).

630WT toxin production in TY was significantly lower than 630Δ*ermΔpyrE* in TY (*** P < 0.0015). 630WT toxin production in TYS was significantly lower than 630Δ*ermΔpyrE* in TYS (*** P < 0.00013) (Fig. 5.12).

630WT (**** P < 0.0001) and 630Δ*ermΔpyrE* (**** P < 0.0001) both showed suppressed cytotoxicity in TYG (Fig. 5.12).

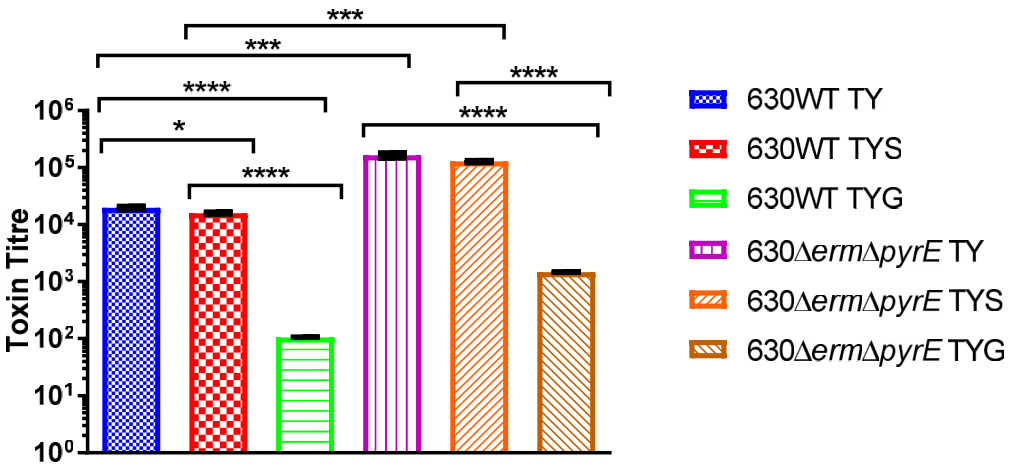

Figure 5.12: Cytotoxicity of 630WT and 630Δ*ermΔpyrE* (parental strain) at 120 h in TY.
Cytotoxicity of 630WT and 630Δ*ermΔpyrE* at 120 h. Serial dilutions of bacterial supernatants (triplicates) were applied to Vero cell monolayers (p34) to determine the toxin titre of the WT and the parental strain (630Δ*ermΔpyrE*).
630WT showed a toxin decrease (* P < 0.013) in TYS, while 630Δ*ermΔpyrE* also significantly (* P < 0.02) decreased cytotoxicity in TYS. 630WT and 630Δ*ermΔpyrE* both suppressed cytotoxicity in TYG (**** P < 0.0001).
One-way ANOVA was used to determine statistical significance.
630WT TY vs. TYS * P < 0.013.
630WT TY vs. 630Δ*ermΔpyrE* TY *** P < 0.0015.
630WT TYS vs. 630Δ*ermΔpyrE* TYS *** P < 0.00013.
630Δ*ermΔpyrE* TY vs. 630Δ*ermΔpyrE* TYS * P < 0.02.

5.2.6 Motility assays

Four variant motility assays were used to examine the potential differences in motility between 630WT and 630Δ*ermΔpyrE*. *C. difficile* M120 and 630Δ*erm*_CT*fliC* were used as negative controls.

5.2.6.1 Motility assays on YT +glucose

630WT and 630Δ*ermΔpyrE* were tested on YT agar +glucose in order to observe the motility of each.

No differences in motility could be seen (0.8cm zone diameter with the wild-type; 0.8cm zone diameter with the parental strain). M120 was used as the negative control, and exhibited reduced motility (0.6cm zone diameter) in comparison to the wild-type and the parent (Fig. 5.13).

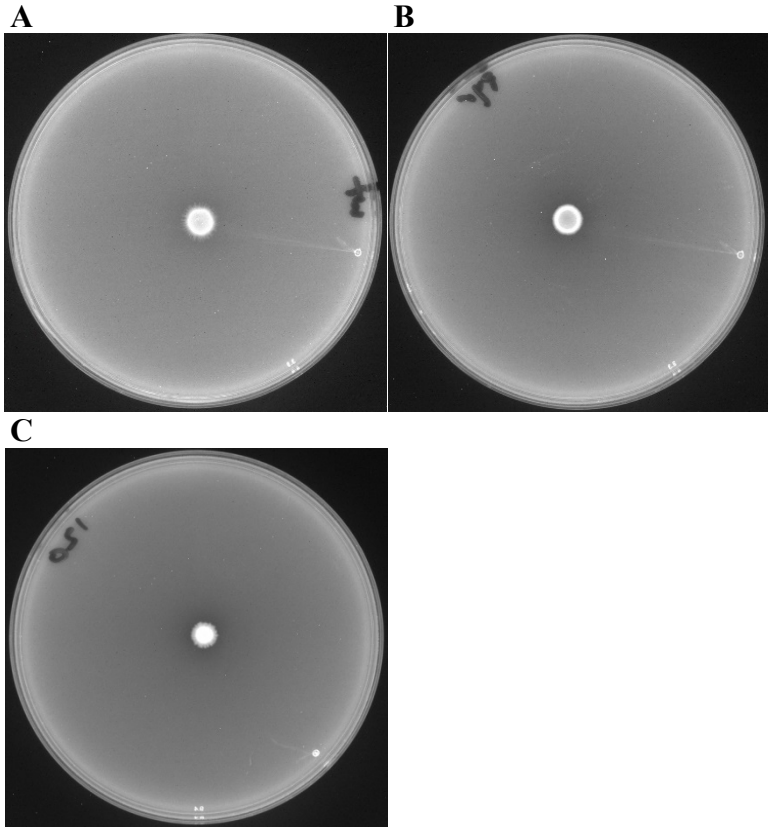

Figure 5.13: Representative images of motility assays showing 630WT (A), parental strain (B), and negative control, M120 (C), on YTG.
2µL of overnight culture of each strain (in triplicates) was spotted onto plates of YTG agar containing 1% w/v glucose and incubated at 37°C for 48 h to see if it was possible to observe a difference in motility.
No differences in motility behaviour could be observed. Similar motility was observed with 630WT and the parental strain (630Δ*erm*Δ*pyrE*).

5.2.6.2 Motility assays on YT +sorbitol

Performing motility assays on YT +sorbitol did not reveal major differences in motility between 630WT and 630Δ*erm*Δ*pyrE*. However, a larger zone of motility was observed with 630WT (1.7cm zone diameter) than what was seen with the parental strain (1.3cm zone diameter). 630Δ*erm*_CT*fliC* was used as the negative control, and exhibited reduced motility (0.9cm zone diameter) in comparison to the wild-type and the parent (Fig. 5.14).

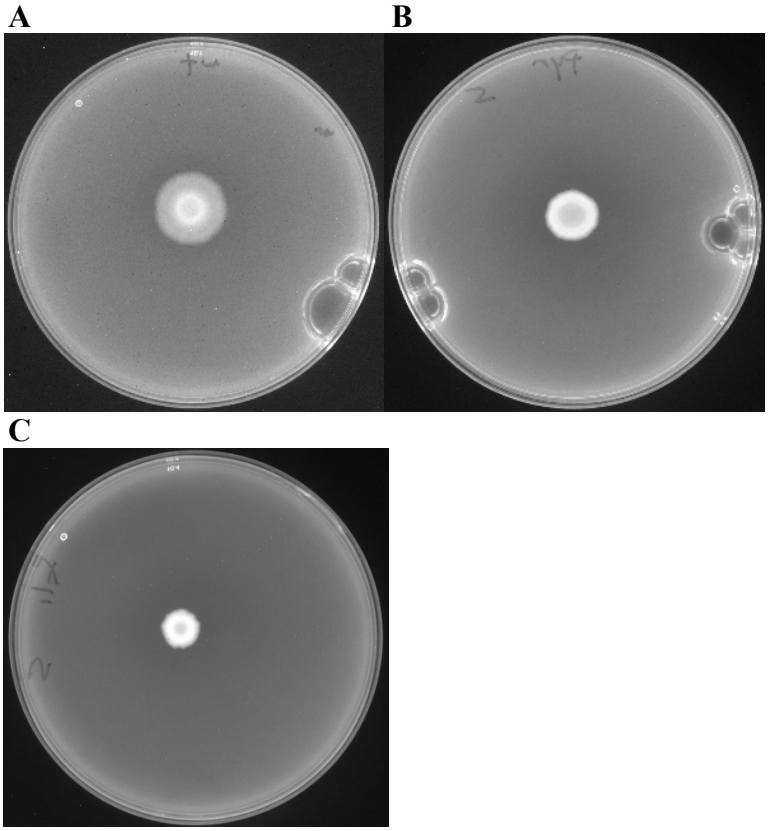

Figure 5.14: Representative images of motility assays showing 630WT (A), parental strain (B), and negative control, CT*fliC*, on YTS.
2µL of overnight culture of each strain (in triplicates) was spotted onto plates of YTS agar containing 1% w/v sorbitol and incubated at 37°C for 48 h to see if it was possible to observe a difference in motility.
No major differences in motility behaviour could be observed. Nonetheless, a larger zone of motility was observed with 630WT than was seen with the parental strain (630Δ*erm*Δ*pyrE*).

5.2.6.3 Motility assays on BHIS +top agar

BHIS +top agar was used to determine potential differences in motility between 630WT and 630Δ*erm*Δ*pyrE*.

No differences were observed with similar zones of motility on the plates observed with both strains (0.7cm zone diameter with the wild-type; 0.7cm zone diameter with the parental strain). CT*fliC* was used as the negative control, and exhibited reduced motility (0.5cm zone diameter) on the plates in comparison to the wild-type and the parent (Fig. 5.15).

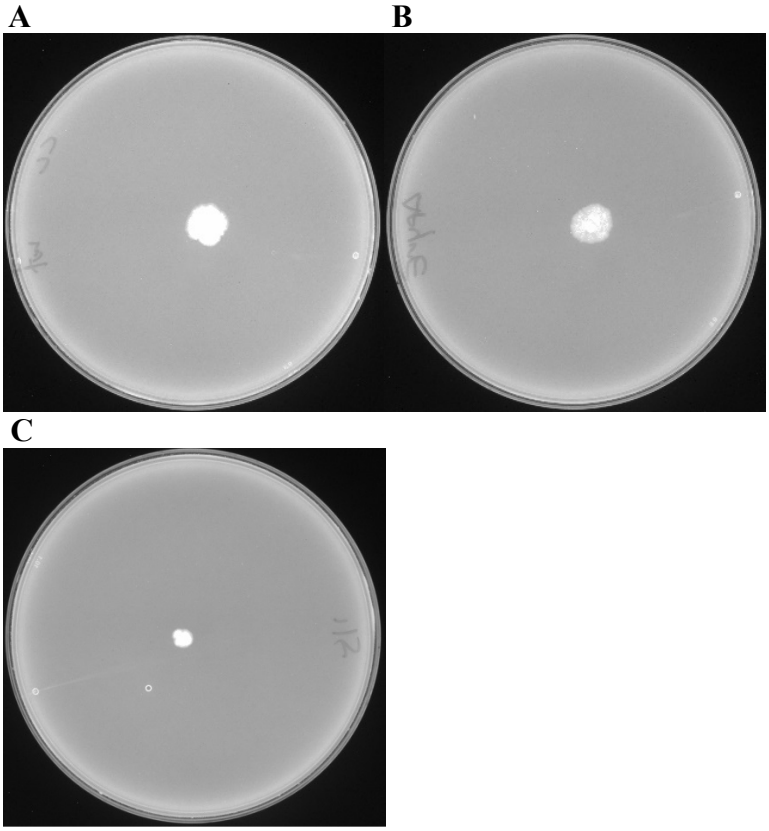

Figure 5.15: Representative images of motility assays on BHIS +top agar showing 630WT (A), parental strain (B), and negative control, CT*fliC* (C).
The surface of the top agar was pierced with a single colony of each strain (in triplicates) and incubated at 37°C for 48 h to see if it was possible to observe a difference in motility.
No differences were observed between 630WT and the parental strain (630Δ*erm*Δ*pyrE*) with similar motility seen with both strains.

5.2.6.4 Motility assays in tubes

Motility assays in glass tubes were prepared using the same medium as was used for the top layer on the BHIS +top layer agar plates (see section 5.2.6.3). 630WT and 630Δ*erm*Δ*pyrE* both showed good turbidity and migrated 11cm from the point of inoculation to the base of the tubes. *C. difficile* M120, which was used as the negative control, showed growth at the very top of the tubes, but did not show any turbidity nor migrate any distance through the agar (Fig. 5.16).



Figure 5.16: Representative images of motility assays showing migration of 630WT (A) and the parental strain (B), through the agar in the tubes. The negative control, M120 (C), did not migrate.
The surface of the agar was pierced with a single colony of each strain (in triplicates) and incubated at 37°C for 24 h to see if it was possible to observe a difference in motility.
630WT and the parental strain (630Δ*erm*Δ*pyrE*) both exhibited good turbidity and migrated to the base of the tubes (11cm), while the negative control (M120) did not migrate any distance.

5.3 Investigation and Characterisation of PTS^{Srl} IIB -GutA

To investigate the role of the putative IIC domain, GutA, in the uptake of sorbitol, a CT mutant, CT*gutA*, made from targeting this potential IIC^{Srl}, was tested.

5.3.1 Characterisation of 630Δ*erm*Δ*pyrE*_CT*gutA* (CD_0764)

gutA was targeted for CT mutagenesis (Fig. 5.17) as it was speculated that inactivating this putative PTS^{Srl} IIC protein would result in a mutant growth phenotype. CT inactivation was initially confirmed by screening 630Δ*erm*Δ*pyrE* erythromycin-resistant colonies (potential CT*gutA* mutants) by PCR (using

primers specific to the insertion) and comparing the fragment sizes with those from 630Δ*ermΔpyrE* on 1% w/v agarose gel (Fig. 5.18).

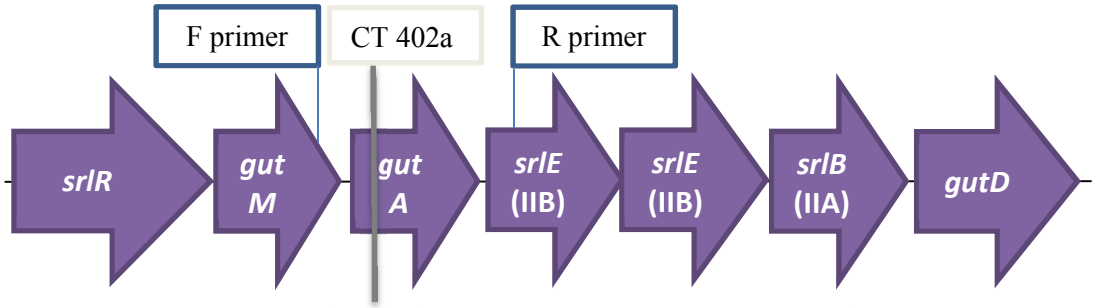

Figure 5.17: PCR screening for deletion of *gutA*.
Position, within the CD630_0762-8 sorbitol-specific operon, of the primers (F and R) designed for the regions outside of *gutA*, used to amplify DNA isolated from selected colonies growing on BHIS +Erm plates.

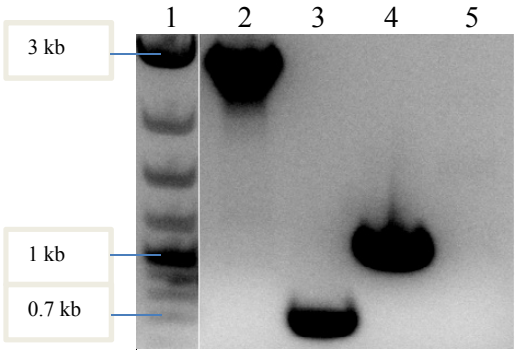

Figure 5.18: CT insertion in *gutA* (CD630_0764), shown by PCR.
Agarose gel (1% w/v) was used to show the CT insertion. Primers specific to outside of the predicted insertion site were designed and used to amplify the desired region in both the parent and the mutant. BHIS +Erm plates (wells 2 & 3); and also, DNA isolated from the parental strain, 630Δ*ermΔpyrE* (wells 4 & 5). Table 5.1 below shows the lane order.

Table 5.1: Content of each well showing by PCR CT insertion in CT*gutA* mutant vs. parent.

Well	Content	Product (kb)
1	Marker	
2	CT*gutA*, F + R primer	2.8
3	CT*gutA*, R + EBS primer	0.6
4	630Δ*ermΔpyrE*, F + R primer	1.0
5	630Δ*ermΔpyrE*, EBS + R primer	-

5.3.1.1 Growth on DM agar

Growing the parent (630Δ*ermΔpyrE*) and the mutant (CT*gutA*) on DMS agar did not reveal differences in the ability to subsist on sorbitol on this type of medium. Strong growth was exhibited by both strains on DM (not shown) and DMS (Fig. 5.19).

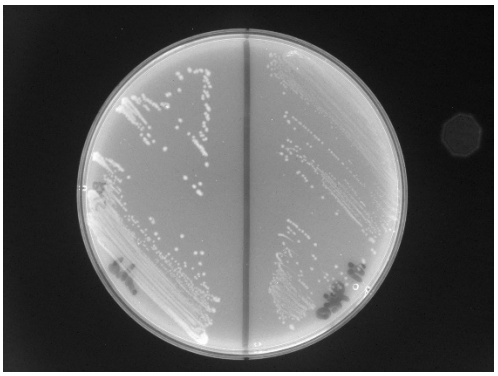

Figure 5.19: Representative image showing growth of 630Δ*ermΔpyrE* -parent (left) and CT*gutA* -mutant (right) on DMS agar.
Strains (in triplicates) were streaked on plates of DMS agar containing 0.6% w/v sorbitol and incubated at 37°C for 24 h to see if it was possible to observe a growth phenotype.
Both strains grew well on DMS. Differences in the ability to metabolise sorbitol could not be determined by this assay as strong growth was also observed on the negative control (DM –not shown).

5.3.1.2 Growth in DM, DMS, and DMG broth

The addition of sorbitol to the medium permitted the parental strain, 630Δ*ermΔpyrE*, to exhibit a higher level of growth in comparison to when it was grown in DM alone. From 10 h incubation onwards, growth in DMS was above growth in DM. For example, at 24 h, which was peak growth in DM and DMS, the OD_{600} level in DM was 0.53, while in DMS it was 0.83 (**** $P < 0.0001$). Slope of the curve in DMS 2-12 h = 1.22 (Fig. 5.20).

An increase in growth levels in the presence of sorbitol was not observed with the mutant, CT*gutA*. Mutant growth in sorbitol was near identical to growth without

the sugar. For example, at peak growth, which was 24 h in DM and DMS, OD_{600} in DM was 0.53, while in DMS it was 0.46. This slight difference in OD_{600} at 24 h was the only time point in which there was any divergence in OD_{600} levels between CT*gutA* in the two conditions. Slope of the curve in DMS 2-12 h = 0.8 (Fig. 5.20).

630Δ*ermΔpyrE* in DMS vs. CT*gutA* in DMS at 24 h **** P < 0.0001.

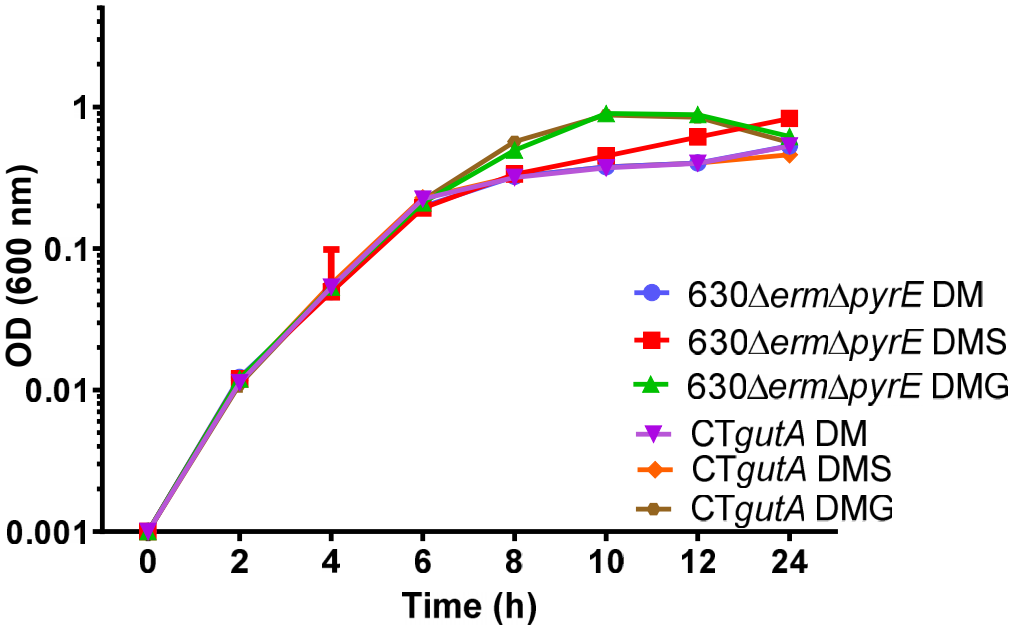

Figure 5.20: Role of *gutA* in *C difficile* 630Δ*ermΔpyrE* growth in DM.
630Δ*ermΔpyrE* (parent) and CT*gutA* (mutant) were incubated for 24 h at 37°C. 1mL extracts (triplicates) were taken at regular time points and the OD_{600} measured.
Growth of CT*gutA* in sorbitol from 10 h onwards was significantly less (P < 0.05) than that of the parent, 630Δ*ermΔpyrE*. Growth of the mutant in DMS was the same as it was in DM, thus exhibiting none of the significant increase seen with the parent in DMS.
630Δ*ermΔpyrE* slope of the curve in DMS 2-12 h = 1.22.
CT*gutA* slope of the curve in DMS 2-12 h = 0.8.
One-way ANOVA was used to determine statistical significance.
630Δ*ermΔpyrE* at 24 h in DM vs. DMS **** P < 0.0001.
630Δ*ermΔpyrE* in DMS vs. CT*gutA* in DMS at 24 h **** P < 0.0001.

5.3.1.3 HPLC evaluation of sorbitol/glucose consumption in DM

HPLC evaluation of sorbitol uptake by both strains revealed that the sugar was steadily consumed by the parent (630Δ*ermΔpyrE*) from 10 h until it was fully depleted by 24 h. 630Δ*ermΔpyrE* slope of the curve from 0-12 h = 1.86 (Fig 5.21).

The mutant (CT*gutA*) failed to utilise any of the available sorbitol. At 24 h, 8.3mM of sorbitol remained (630Δ*ermΔpyrE* vs. CT*gutA* at 24 h **** P < 0.0001). CT*gutA* slope of the curve from 0-12 h = 0 (Fig. 5.21).

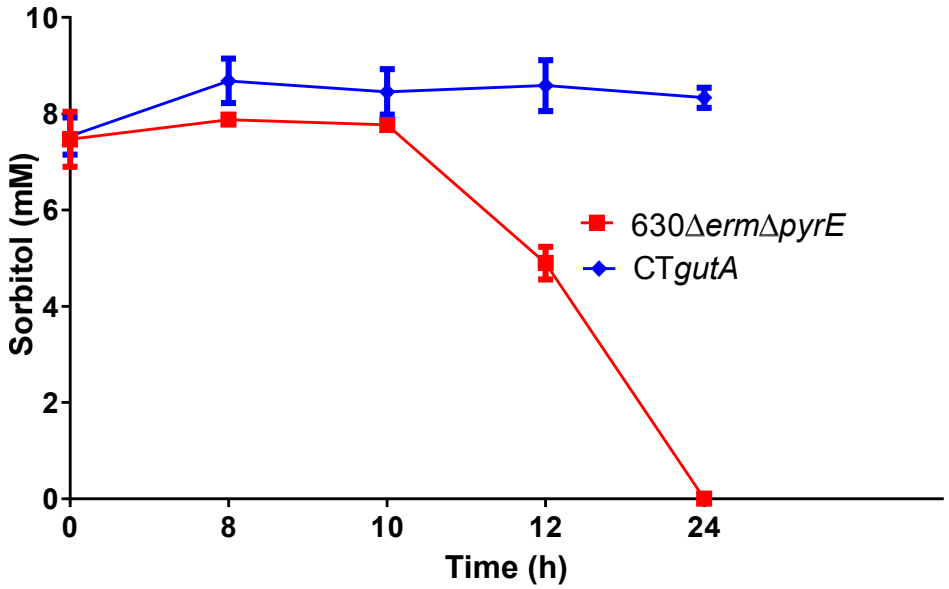

Figure 5.21: HPLC evaluation of sorbitol uptake in DM by 630Δ*ermΔpyrE* (parental strain) and CT*gutA* (mutant).
Extracts (triplicates) from the growth assay were used to determine by HPLC the exact amount of sugar remaining in the medium at each time point. The amount of sorbitol left in the parental strain (630Δ*ermΔpyrE*) and the mutant (CT*gutA*) medium from 12-24 h was significantly different (**** P < 0.0001).
630Δ*ermΔpyrE* slope of the curve in 0-12 h = 1.86.
CT*gutA* slope of the curve in 0-12 h = 0.
One-way ANOVA was used to determine statistical significance.
630Δ*ermΔpyrE* vs. CT*gutA* at 24 h **** P < 0.0001.

Glucose levels in both strains were depleted, as was expected, between 0 h and 24 h (**** $P < 0.0001$). No differences were observed, indicating that interrupting *gutA* produced no effect on glucose metabolism (Fig. 5.22).

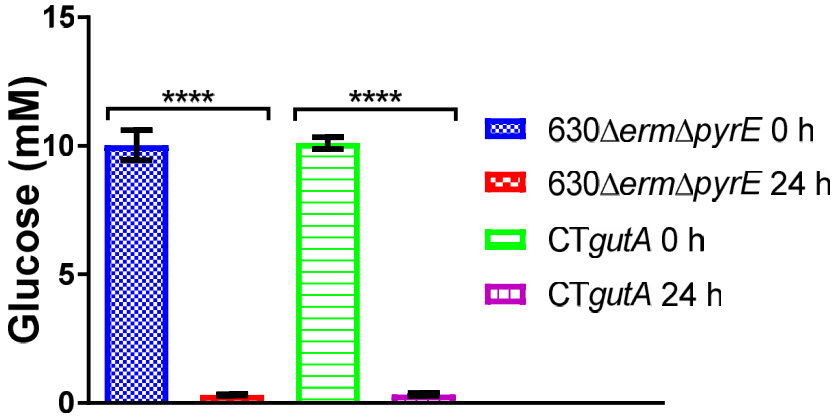

Figure 5.22: HPLC evaluation of glucose uptake by 630Δ*erm*Δ*pyrE* (parental strain) and CT*gutA* (mutant) in DM.
Extracts (triplicates) from the growth assays in DM were used to determine by HPLC the exact amount of sugar remaining in the medium at the start and end of the assay.
Glucose utilisation by each strain was the same with a depletion of glucose between 0 h and 24 h (**** $P < 0.0001$).
One-way ANOVA was used to determine statistical significance.

5.3.1.4 Growth in TY, TYS, and TYG

630Δ*erm*Δ*pyrE* growth in TY medium supplemented with sorbitol showed, from 48 h, an increase in OD_{600} levels in comparison to when it was grown in TY alone. Peak OD_{600} in both conditions occurred at 24 h (in TY it was 0.95, in TYS it was 0.94), but unlike in TY, OD_{600} levels in TYS declined at a much slower rate. The disparity in OD_{600} decline reached significant levels from 72 h onwards. An example at 120 h, when the OD_{600} of the parent in TY had plummeted to 0.3 (a 68.5% decrease from peak OD_{600} at 24 h, slope 24-120 h = 1.62), and in TYS it

was 0.7 (a 25.4% decrease from peak OD_{600} at 24 h, slope 24-120 h = 0.6) (630Δ*ermΔpyrE* TY vs. TYS at 120 h ** P < 0.017) (Fig. 5.23).

In complete contrast to the parent, the mutant, CT*gutA*, exhibited no increases in OD_{600} in sorbitol. Growth of CT*gutA* in both conditions (TY and TYS) remained near identical throughout the assay. Unlike 630Δ*ermΔpyrE* from 48 h onwards, with CT*gutA*, the presence of sorbitol caused no effect on the OD_{600} patterns of the mutant. The mutant behaved as if there was no sorbitol in the medium. To cite an example, mutant OD_{600} at 120 h was 0.21 in both TY and TYS (Fig. 5.23).

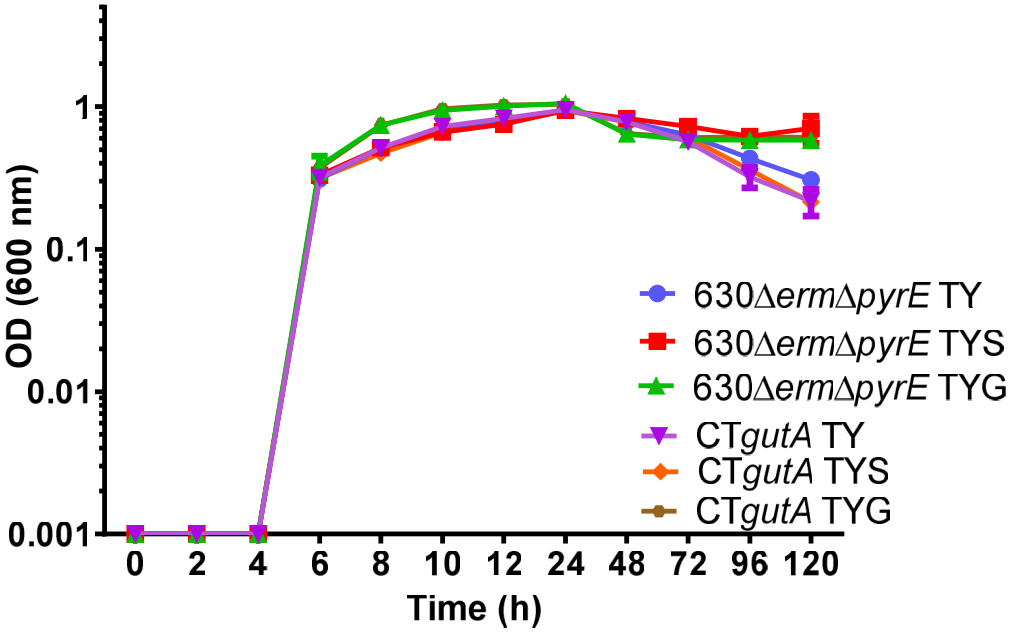

Figure 5.23: Role of CT*gutA* in *C difficile* 630Δ*ermΔpyrE* growth in TY.
630Δ*ermΔpyrE* (parent) and CT*gutA* (mutant) were incubated for 120 h at 37°C. 1mL extracts (triplicates) were taken at regular time points and the OD_{600} measured.
Growth of CT*gutA* in sorbitol from 48 h onwards was significantly less (P < 0.05) than that of the parent, 630Δ*ermΔpyrE*. Growth of the mutant in TYS was the same as it was in TY.
630Δ*ermΔpyrE* slope 24-120 h (downward) = 1.62. CT*gutA* slope 24-120 h (downward) = 0.6.
One-way ANOVA was used to determine statistical significance.
630Δ*ermΔpyrE* TY vs. TYS at 120 h ** P < 0.017.
630Δ*ermΔpyrE* in TYS vs. CT*gutA* in TYS at 120 h * P < 0.0.

5.3.1.5 Cytotoxicity of 630Δ*erm*Δ*pyrE* and 630Δ*erm*Δ*pyrE*_CT*gutA*

At 72 h incubation, in the presence of sorbitol, 630Δ*erm*Δ*pyrE* (parent), exhibited higher cytotoxicity than in TY alone. Toxin levels increased from a toxin titre of 1.5 x 10^2 in TY to 1.3 x 10^3 in TYS (**** P < 0.0001) (Fig. 5.24).

An increase in toxin production in TYS was not observed with the mutant, CT*gutA*. Toxin levels remained at a toxin titre of 1.7 x 10^2 in TY and and 1.6 x 10^2 in TYS. The mutant produced substantially less toxin in TYS than the parent (**** P < 0.0001) (Fig. 5.24).

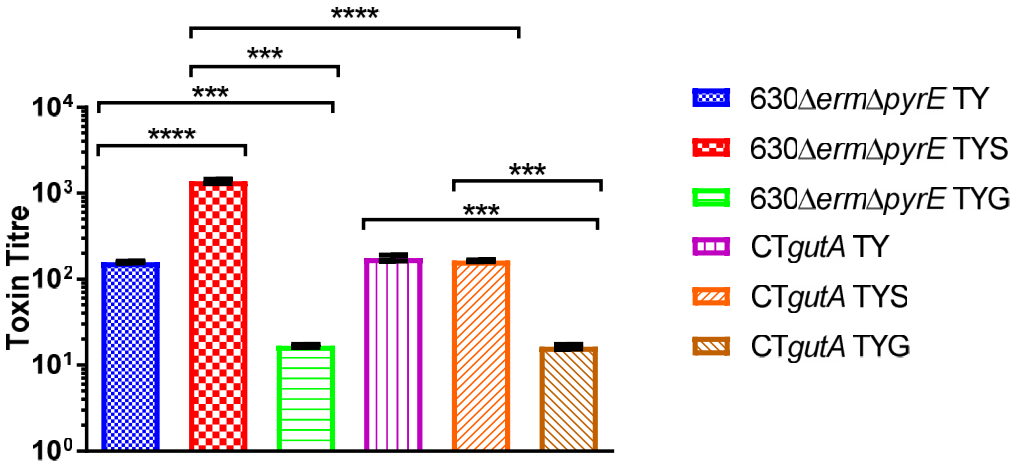

Figure 5.24: Role of CT*gutA* in *C. difficile* 630Δ*erm*Δ*pyrE* toxin expression at 72 h in TY.
Cytotoxicity of CT*gutA* at 72 h. Serial dilutions (10^0-10^{-9}) of bacterial supernatants (triplicates) were applied to Vero cell monolayers (p34) to determine the toxin titre of the parent and the mutant.
The parent (630Δ*erm*Δ*pyrE*) produced significantly higher amounts (**** P < 0.0001) of toxin in TYS compared to when in TY. No change in toxin levels was observed with the mutant (CT*gutA*) when comparing cytotoxicity in TY and TYS.
One-way ANOVA was used to determine statistical significance.
630Δ*erm*Δ*pyrE* in TY vs. TYS **** P < 0.0001.
630Δ*erm*Δ*pyrE* in TYS vs. CT*gutA* TYS **** P < 0.0001.

At 96 h, toxin production by the parent in TYS showed a suppressive trend, with toxin levels going from a toxin titre of 2.3.1 x 10^3 in TY to 1.1 x 10^3 in TYS (with a lot of variance –not significant) (Fig. 5.25).

This was not seen with the mutant as toxin levels in TY (minor variance) and TYS remained at a titre of 3.1 x 10^3 in TY and 2.7 x 10^3 in TYS. Parent and mutant toxin levels differed significantly in TYS (* P < 0.02) (Fig. 5.25).

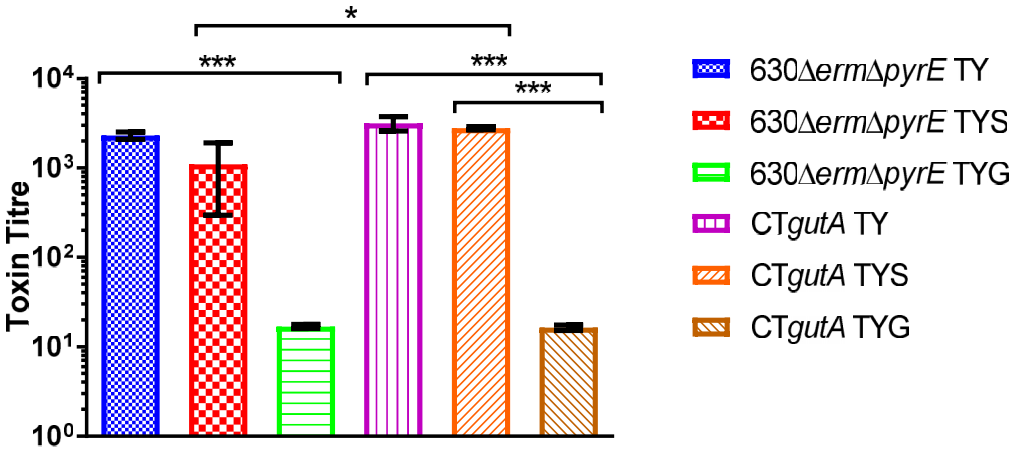

Figure 5.25: Role of CT*gutA* in *C. difficile* 630Δ*erm*Δ*pyrE* toxin expression at 96 h in TY.
Cytotoxicity of CT*gutA* at 96 h. Serial dilutions (10^0-10^{-9}) of bacterial supernatants (triplicates) were applied to Vero cell monolayers (p34) to determine the toxin titre of the parent and the mutant.
The parent (630Δ*erm*Δ*pyrE*) showed a trend towards producing slightly lower amounts of toxin in TYS compared to when in TY. No changes in toxin levels were observed with the mutant (CT*gutA*) when comparing cytotoxicity in TY and TYS.
One-way ANOVA was used to determine statistical significance.
630Δ*erm*Δ*pyrE* in TYS vs. CT*gutA* TYS * P < 0.02.

At 120 h, there was a trend towards toxin suppression by the parent in the presence of sorbitol with toxin levels dropping from a toxin titre of 3.2 x 10^3 in TY to 1.1 x 10^3 in TYS (with much variance) (* P < 0.019) (Fig. 5.26).

Incubating the mutant with sorbitol in the medium produced no tangible effect, with toxin levels staying almost the same in both TY and TYS at a titre of 4.7 x 10^3 in TY and 4.6 x 10^3 in TYS. The mutant produced significantly more toxin in TYS than the parent at this time point (** P < 0.002) (Fig. 5.26).

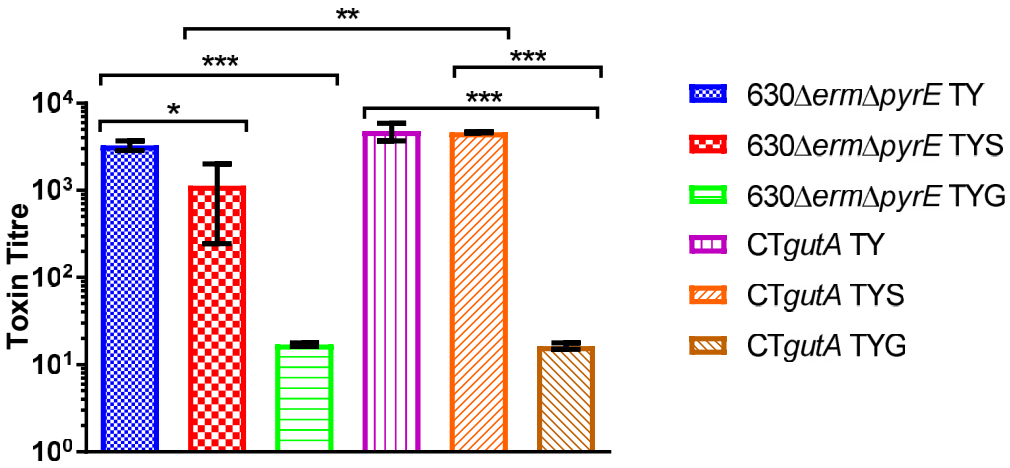

Figure 5.26: Role of CT*gutA* in *C. difficile* 630Δ*erm*Δ*pyrE* toxin expression at 120 h.
Cytotoxicity of CT*gutA* at 120 h. Serial dilutions (10^0-10^{-9}) of bacterial supernatants (triplicates) were applied to Vero cell monolayers (p34) to determine the toxin titre of the parent and the mutant.
The parent (630Δ*erm*Δ*pyrE*) showed a trend towards producing lower amounts of toxin in TYS compared to when in TY (* P < 0.019). No change in toxin levels was observed in the mutant (CT*gutA*) when comparing cytotoxicity in TY and TYS, but mutant toxin levels in TYS were significantly above those of the parent in TYS (** P < 0.002).
One-way ANOVA was used to determine statistical significance.
630Δ*erm*Δ*pyrE* in TY vs. TYS * P < 0.019.
630Δ*erm*Δ*pyrE* in TYS vs. CT*gutA* TYS ** P < 0.002.

5.3.1.6 Motility assays

Four variant motility assays were used to examine the potential differences in motility between 630Δ*erm*Δ*pyrE* and CT*gutA*. The mutant was tested alongside 630Δ*erm*Δ*pyrE*, *C. difficile*Δ*erm*_CT*fliC*, and *C. difficile* M120.

5.3.1.6.1 Motility assays on YT +glucose

Strains were tested on YT medium +glucose in order to observe the motility of each.

No differences were observed between 630Δ*ermΔpyrE* (0.8cm zone diameter) and CT*gutA* (0.8cm zone diameter). M120 was used as the negative control, and exhibited reduced motility (0.6cm zone diameter) in comparison to the parent and the mutant (Fig. 5.27).

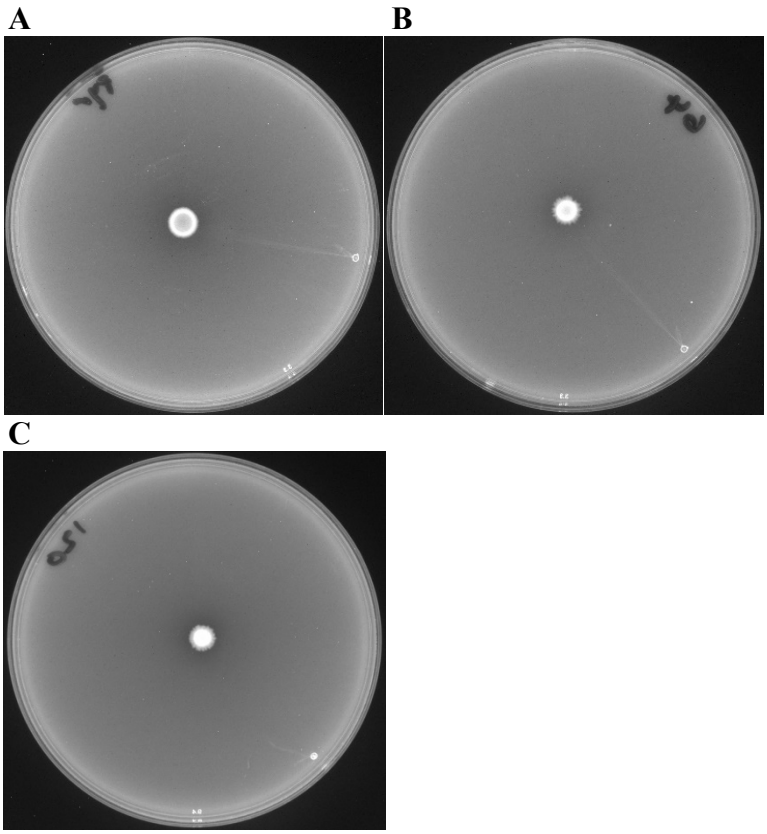

Figure 5.27: Representative images showing motility assays with parental strain (A), mutant (B), and negative control, M120 (C), on YTG.
2µL of overnight culture of each strain (in triplicates) was spotted onto plates of YTG agar containing 1% w/v glucose and incubated at 37°C for 48 h to see if it was possible to observe a difference in motility.
No major differences in motility behaviour could be observed. Similar zones of motility were observed with the parental strain (630Δ*ermΔpyrE*) and the mutant (CT*gutA*).

5.3.1.6.2 Motility assays on YT +sorbitol

Motility assay on YT +sorbitol was undertaken to determine potential differences in motility between 630Δ*ermΔpyrE* and CT*gutA*.

A slightly larger zone of motility was observed with the parental strain (3.9cm diameter) than was observed with the mutant (1.1cm zone diameter). CT*fliC* was used as the negative control, and exhibited reduced motility (0.9cm zone diameter) in comparison to the parent and the mutant (Fig. 5.28).

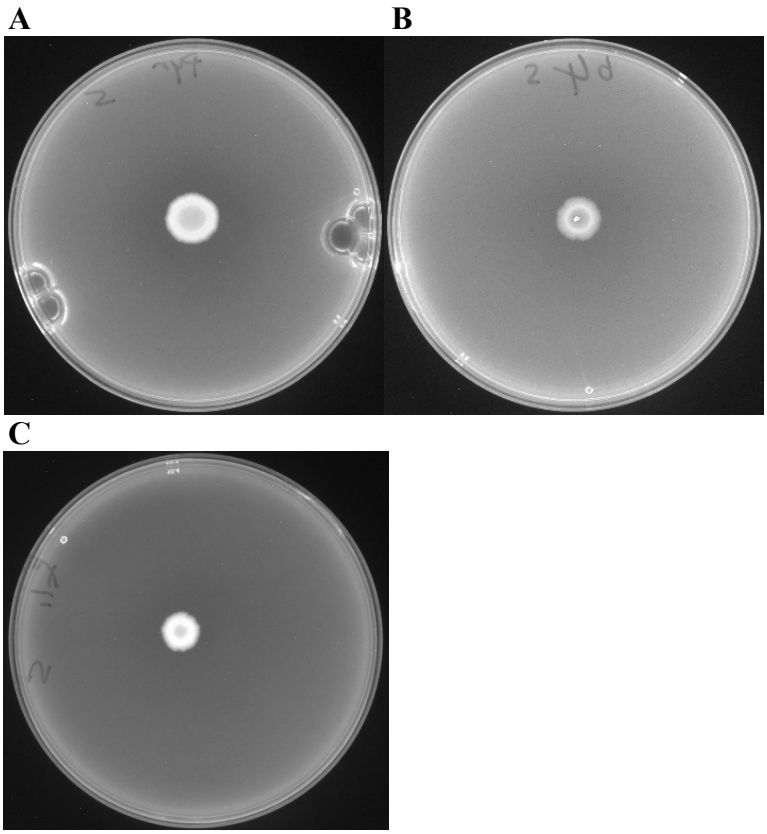

Figure 5.28: Representative images showing motility assays with parental strain (A), mutant (B), and negative control, CT*fliC* (C), on YTS.
2µL of overnight culture of each strain (in triplicates) was spotted onto plates of YTS agar containing 1% w/v sorbitol and incubated at 37°C for 48 h to see if it was possible to observe a difference in motility.
A larger zone of motility on the plates was observed with the parental strain (630Δ*ermΔpyrE*) compared to the mutant (CT*gutA*).

5.3.1.6.3 Motility assays on BHIS +top agar

BHIS +top agar was used to determine potential differences in motility between 630Δ*ermΔpyrE* and CT*gutA*.

No differences were observed, with similar zones of motility on the plates seen with both strains (both having a zone diameter of 0.7cm). CT*fliC* was used as the negative control, and exhibited a reduced zone of motility (0.5cm zone diameter) in comparison to 630Δ*ermΔpyrE* and CT*gutA* (Fig. 5.29).

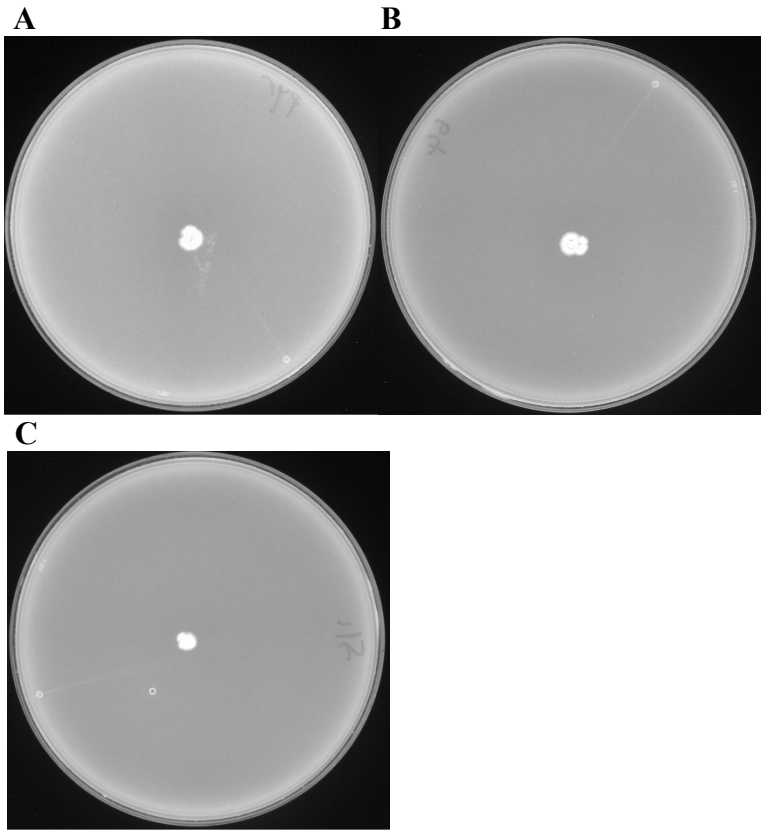

Figure 5.29: Representative images showing motility assays with parental strain (A), mutant (B), and negative control, CT*fliC* (C).
The surface of the top agar was pierced with a single colony of each strain (in triplicates) and incubated at 37°C for 48 h to see if it was possible to observe a difference in motility.
No differences were observed between the parental strain (630Δ*ermΔpyrE*) and the mutant (CT*gutA*) with similar motility on the plates seen with both strains.

5.3.1.6.4 Motility assays in tubes

The same medium which comprised the top layer on the BHIS +top agar motility assay plates was used in tubes to determine potential differences in motility between 630Δ*erm*Δ*pyrE* and CT*gutA*.

No differences were observed, with both strains showing good turbidity and migrating to 11cm from the point of inoculation to the base of the tubes. *C. difficile* M120 was used as the negative control, showed growth at the very top of the tubes, but did not exhibit any turbidity nor migrate any distance through the agar (Fig. 5.30).

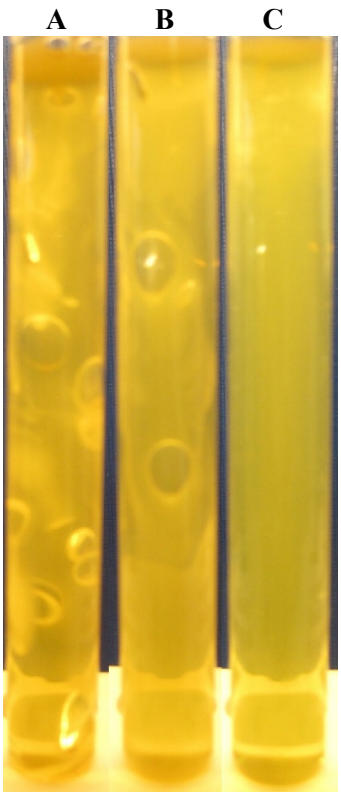

Figure 5.30: Representative images showing motility assays indicating the migration of control strain (A) and mutant (B) through the agar in the tubes. The negative control, M120 (C), did not migrate.
The surface of the agar was pierced using a sterile cocktail stick to inoculate a single colony of each strain (in triplicates) into the medium and incubated at 37°C for 24 h to see if it was possible to observe a difference in motility.
The control strain (630Δ*erm*Δ*pyrE*) and the mutant (CT*gutA*) both exhibited good turbidity and migrated to the base of the tubes (11cm), while the negative control (M120) did not migrate any distance.

5.4 Investigation and Characterisation of PTS^{Srl} IIB –SrlE

To investigate the role of the putative IIB, SrlE, in the uptake of sorbitol, CT mutants, CT*srlE_N* and CT*srlE_C*, made from targeting this potential IIB^{Srl}, were tested. This involved targeting the N and C termini of the protein encoded by CD630_0765 and CD630_0766 respectively.

5.4.1 Characterisation of 630Δ*erm*Δ*pyrE*_CT*srlE_N* (CD_0765)

srlE_N was targeted for CT mutagenesis as it was speculated that inactivating this section of the putative PTS^{Srl} IIB protein would result in a mutant growth phenotype (Fig. 5.31). CT inactivation was initially confirmed by screening 630Δ*erm*Δ*pyrE* erythromycin-resistant colonies (potential CT*srlE_N* mutants) by PCR (using primers specific to the CT insertion) and comparing the fragment sizes with those from 630Δ*erm*Δ*pyrE* on 1% w/v agarose gel (Fig. 5.32). Southern blotting confirmed that the CT insertion occurred in a single location (Fig. 5.33).

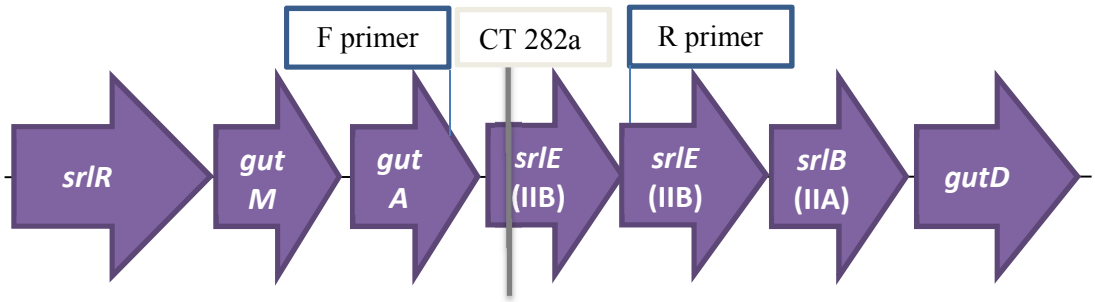

Figure 5.31: Primers used for PCR screening for CT mutagenesis of *srlE_N*. Position, within the CD630_0762-8 putative PTS^{Srl} operon, of the primers (F and R) designed for the regions immediately outside of *srlE_N*, used to amplify DNA isolated from selected colonies growing on BHIS +Erm plates.

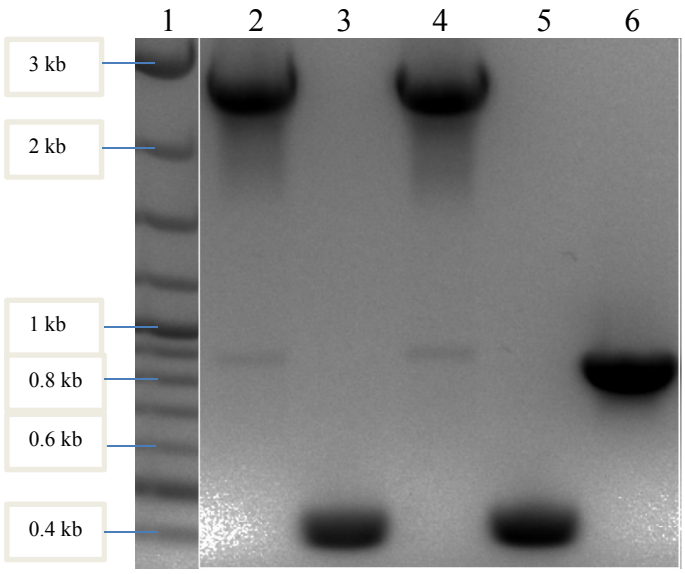

Figure 5.32: CT insertion in *srlE_N* (CD630_0765) mutants A and B shown by PCR.
Agarose gel (1% w/v) was used to show the CT insertion. Primers specific to outside of the predicted insertion site were designed and used to amplify the desired region in both the parent and the mutant. BHIS plates +Erm (wells 2-5); and also, DNA isolated from the parental strain, 630Δ*ermΔpyrE* (well 6). Table 5.2 below shows the lane order.

Table 5.2: Content of each well showing by PCR CT insertion in CT*srlE_N* mutant vs. parent.

Well	Content	Product (kb)
1	Marker	
2	CT*srlE_N* mut. A, F + R primer	2.61
3	CT*srlE_N* mut. A, R + EBS primer	0.44
4	CT*srlE_N* mut. B, F + R primer	2.61
5	CT*srlE_N* mut. B, R + EBS primer	0.44
6	630Δ*ermΔpyrE*, F + R primer	0.82

Following initial screening, by PCR, of *C. difficile* 630Δ*ermΔpyrE* erythromycin-resistant colonies for the presence of the CT insertion (as described in Materials and Methods, section 2.4.8), Southern blotting was performed in order to verify a single CT insertion in *C. difficile* 630Δ*ermΔpyrE* (Fig. 5.33, Table 5.3).

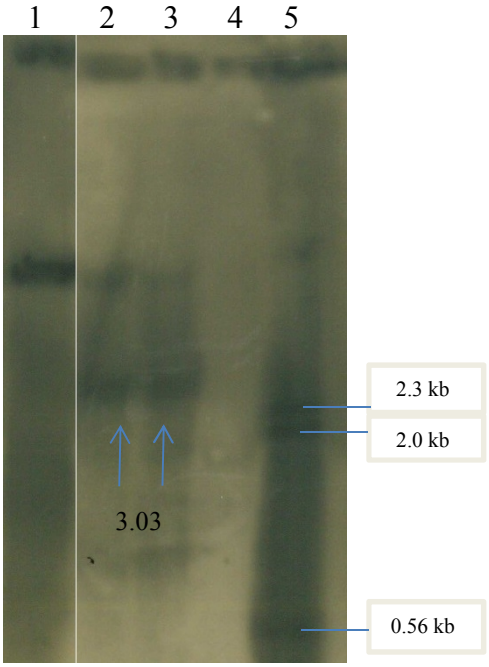

Figure 5.33: Southern blot showing CT insertion in CT*srlE_N*.
Chromosomal genomic DNA was cut with *Hind*III. Arrows show the group II intron insertion fragment of the expected size. Mutant samples indicating a successful insertion were loaded twice (mutants A and B). Table 5.3 below shows the lane order.

Table 5.3: Southern blot confirmation of CT insertion.

Well	**Content**	**Size (kb)**
1	CT plasmid -positive control	8.9
2	CT*srlE_N* mut. A	3.03
3	CT*srlE_N* mut. B	3.03
4	630Δ*ermΔpyrE* -negative control	-
5	λ *Hind*III marker	

5.4.1.1 Growth on DM agar

Growing the parent (630Δ*ermΔpyrE*) and the mutant (CT*srlE_N*) on DMS agar did not reveal differences in the ability to subsist on sorbitol on this type of

medium. Strong growth was exhibited by both strains on DM (negative control - not shown) and DMS (Fig. 5.34).

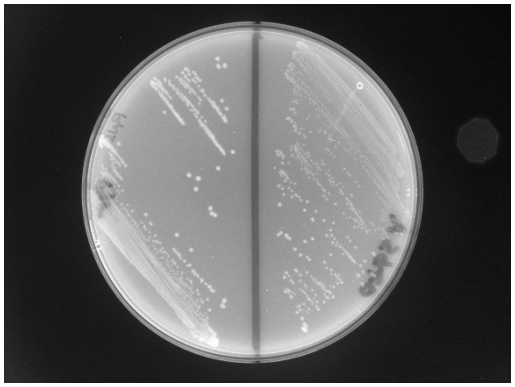

Figure 5.34: Representative image showing growth of 630Δ*erm*Δ*pyrE* -parent (left) and CT*srlE_N* -mutant (right) on DMS agar.
Strains (in triplicates) were streaked on plates of DM agar containing 0.6% w/v sorbitol and incubated at 37°C for 16 h to see if it was possible to observe a growth phenotype.
Differences in the ability to metabolise sorbitol could not be determined by this assay as both strains exhibited good growth on DM (not shown) and DMS.

5.4.1.2 Growth in DM, DMS, and DMG broth

The presence of sorbitol induced an increase in growth of the parent (630Δ*erm*Δ*pyrE*) from 10 h with OD_{600} levels increasing significantly in comparison to parental growth in DM alone. At 24 h, which was peak growth in DM and DMS, OD_{600} was 0.56 in DM, and in DMS it was 0.82 (**** $P < 0.0001$). Slope of the curve in DMS 0-24 h = 1.18 (Fig. 5.35).

The presence of sorbitol did not induce such an increase in CT*srlE_N* (mutant), as the OD_{600} of the mutant in DMS was not above that in plain DM. For example, at peak growth (24 h), OD_{600} was 0.56 in DM, and 0.47 in DMS. Slope of the curve in DMS 0-24 h = 0.68 (Fig. 5.35).

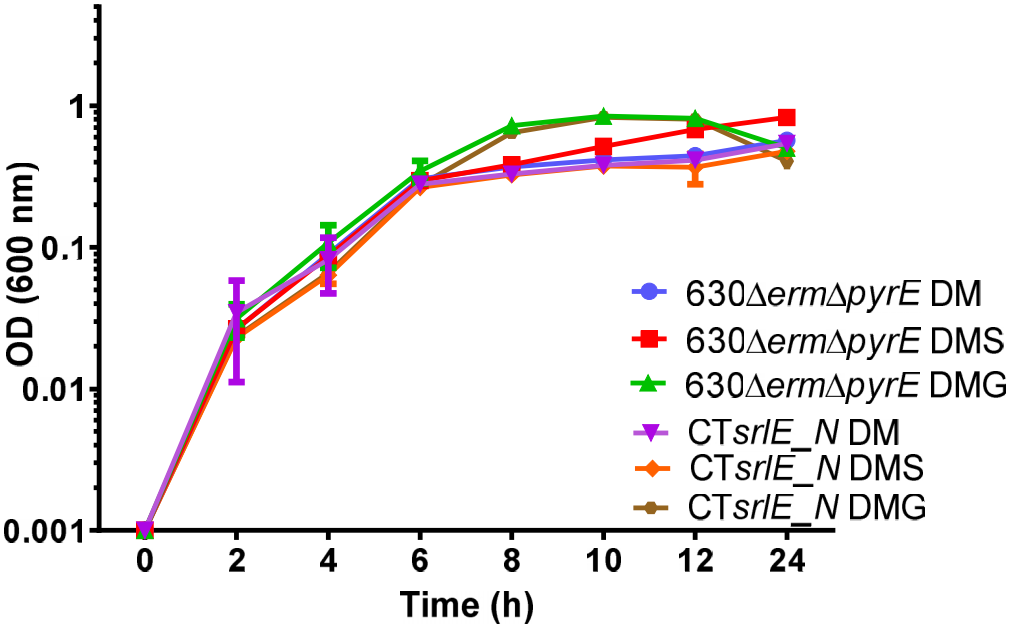

Figure 5.35: Role of *srlE_N* in *C difficile* 630Δ*erm*Δ*pyrE* growth in DM.
630Δ*erm*Δ*pyrE* (parent) and CT*srlE_N* (mutant) were incubated for 24 h at 37°C. 1mL extracts (triplicates) were taken at regular time points and the OD_{600} measured.
Growth of CT*srlE_N* in sorbitol from 10 h onwards was significantly less (**** P < 0.0001) than that of the parent, 630Δ*erm*Δ*pyrE*. Growth of the mutant in DMS was the similar to that in DM.
630Δ*erm*Δ*pyrE* slope of the curve in DMS 0-24 h = 1.18.
CT*srlE_N* slope of the curve in DMS 0-24 h = 0.68.
One-way ANOVA was used to determine statistical significance.
630Δ*erm*Δ*pyrE* at 24 h (peak growth) in DM vs. in DMS **** P < 0.0001.
CT*srlE_N* in DMS vs. 630Δ*erm*Δ*pyrE* in DMS at 24 h (peak growth) **** P < 0.0001.

5.4.1.3 HPLC evaulation of sorbitol/glucose consumption in DM

HPLC analysis was undertaken to determine the exact level of sugar uptake by the parent (630Δ*erm*Δ*pyrE*) and by the mutant (CT*srlE_N*). The analysis indicated at 24 h that there was 0.007mM sorbitol remaining in the parent culture medium, and 8.54mM in the mutant samples. Starting from 8 h, there was an observable downward trend in the amount of sorbitol in medium of the parental strain (unlike the mutant), a difference which reached significance by 10 h (** P < 0.0022). By 24 h, almost of the sorbitol in the parent samples had been depleted, while sugar

levels remained stable in the mutant cultures throughout the entire assay. 630Δ*ermΔpyrE* slope of the curve 0-24 h = 2.24. CT*srlE_N* slope of the curve 0-24 h = 0 (Fig. 5.36).

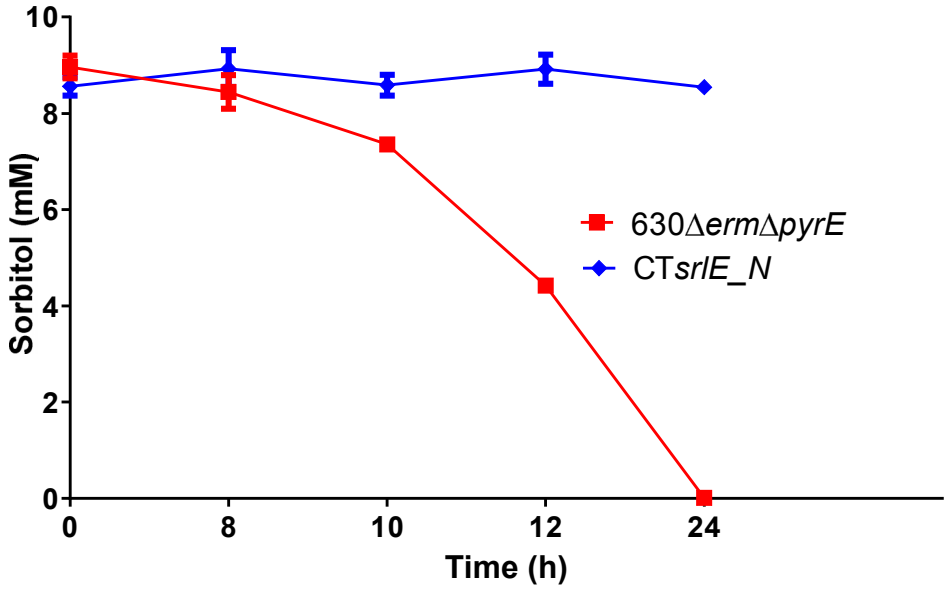

Figure 5.36: HPLC evaluation of sorbitol uptake in DM by 630Δ*ermΔpyrE* (parent) and CT*srlE_N* (mutant).
Extracts (triplicates) from the growth assay were used to determine by HPLC the exact amount of sugar remaining in the medium at each time point.
The sorbitol in the parental medium was spent by 24 h, while sorbitol levels in mutant cultures remain unchanged.
630Δ*ermΔpyrE* slope of the curve 0-24 h = 2.24. CT*srlE_N* slope of the curve 0-24 h = 0.
One-way ANOVA was used to determine statistical significance.
630Δ*ermΔpyrE* vs. CT*srlE_N* at 10 h ** $P < 0.0022$.

Glucose was consumed by 630Δ*ermΔpyrE* and CT*srlE_N* between 0 h and 24 h with glucose levels dropping from 8.65mM and 8.66 respectively at 0 h to 0.27mM and 0.29mM respectively at 24 h (**** $P < 0.0001$) (Fig. 5.37), indicating that interrupting *srlE_N* is not effecting glucose uptake.

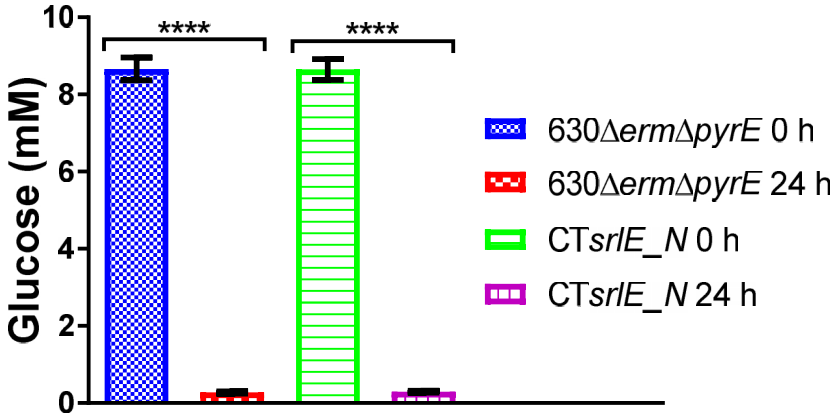

Figure 5.37: HPLC evaluation of glucose uptake in DM by 630Δ*erm*Δ*pyrE* (parent) and CT*srlE_N* (mutant).
Extracts (triplicates) from the growth assay were used to determine by HPLC the exact amount of the sugar remaining in the medium at both time points.
The glucose that was in the parental and mutant cultures at 0 h was depleted by the 24 h time point (**** $P < 0.0001$).
One-way ANOVA was used to determine statistical significance.

5.4.1.4 Growth in TY, TYS, and TYG

Mutant (CT*srlE_N*) OD_{600} in sorbitol from 24-120 h was significantly reduced in comparison to the parental strain (630Δ*erm*Δ*pyrE*) (Fig. 5.38). The average OD_{600} value for the mutant in sorbitol at 24 h (peak growth) was 0.66, without sorbitol it was 0.67 (no significant difference); while the parent OD_{600} at 24 h was 0.69 and 0.84 with and without sorbitol respectively (**** $P < 0.0001$). 630Δ*erm*Δ*pyrE* and CT*srlE_N* OD_{600} at 24 h in TYS significantly differed (**** $P < 0.0001$). This indicated an inability of the mutant to make use of the available sorbitol. Slope of curve 24-120 h in TYS (downward): 630Δ*erm*Δ*pyrE* = 1.25, CT*srlE_N* = 1.35 (Fig. 5.38).

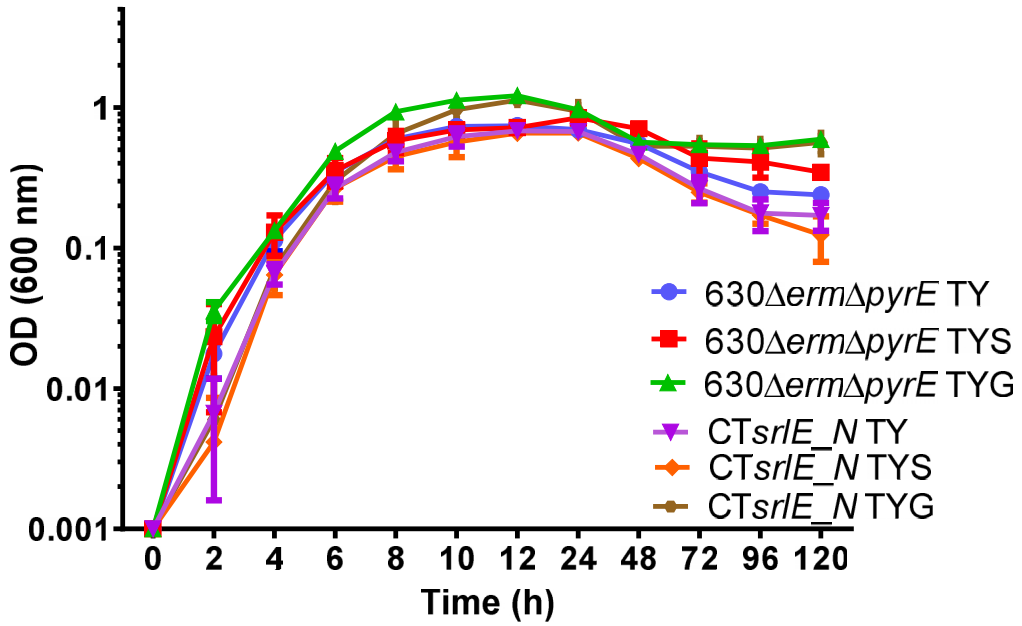

Figure 5.38: Role of *srlE_N* in *C difficile* 630Δ*erm*Δ*pyrE* growth in TY.
630Δ*erm*Δ*pyrE* (parent) and CT*srlE_N* (mutant) were incubated for 120 h at 37°C. 1mL extracts (triplicates) were taken at regular time points and the OD_{600} measured.
Growth of CT*srlE_N* in sorbitol from 24 h onwards was significantly less (**** P < 0.0001) than that of the parent, 630Δ*erm*Δ*pyrE*. Growth of the mutant in TYS was the same as it was in TY.
Slope of curve (downward) 24-120 h in TYS: 630Δ*erm*Δ*pyrE* = 1.25, CT*srlE_N* = 1.35.
One-way ANOVA was used to determine statistical significance.
630Δ*erm*Δ*pyrE* at 24 h in TY vs. in TYS **** P < 0.0001.
630Δ*erm*Δ*pyrE* vs. CT*srlE_N* at 24 h in TYS **** P < 0.0001.

5.4.1.5 Cytotoxicity of 630Δ*erm*Δ*pyrE* and 630Δ*erm*Δ*pyrE*_CT*srlE_N*

At each time point (72, 96, and 120 h), cytotoxicity levels of the mutants in TYS remained similar as the mutant cultures grown in TY alone (Fig. 5.39-5.41). Unlike the cultures grown in TYG (which showed toxin reduction), there was no sorbitol-induced reduction in toxin levels. However, the parent overall displayed a significantly higher level (120 h, not significant) of toxin activity in TYS than the mutant.

At 72 h, 630Δ*ermΔpyrE* in TYS produced more toxin than in TY, going from a toxin titre of 2.8 x 10^4 to 1.7 x 10^6 (with high variance) (Fig. 5.39).

This was not seen with CT*srlE_N*. No significant increase in toxicity in TYS was observed (1.2 x 10^5 in TY (with high variance) and 4.1 x 10^4 in TYS); and the toxin produced in TYS by the mutant was below that of the parent in TYS (* P < 0.02) (Fig. 5.39).

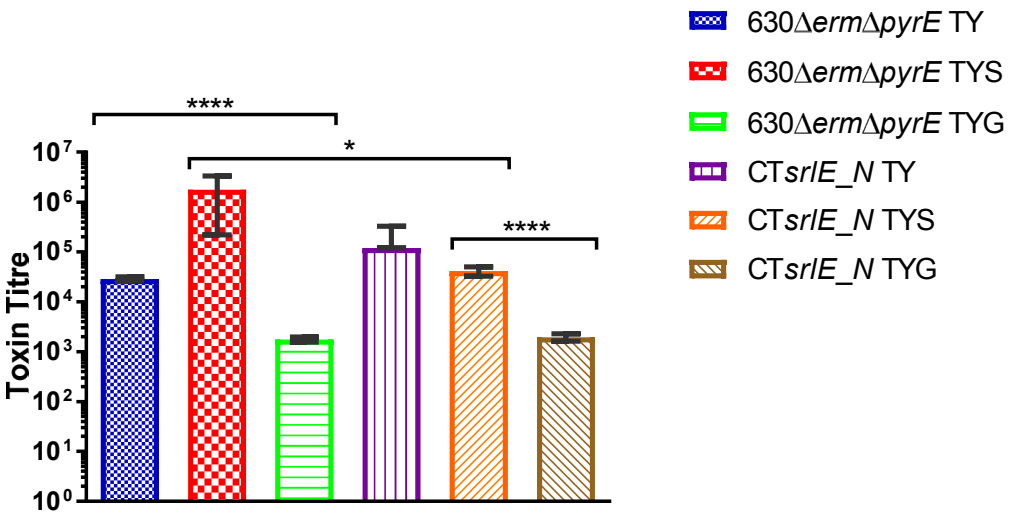

Figure 5.39: Role of *srlE_N* in *C. difficile* 630Δ*ermΔpyrE* toxin production at 72 h in TY.
Cytotoxicity of CT*srlE_N* at 72 h. Serial dilutions (10^0-10^{-9}) of bacterial supernatants (triplicates) of 630Δ*ermΔpyrE* and CT*srlE_N* mutants A and B (pooled) (as two mutants had been generated by the time the assays were performed) were applied to Vero cell monolayers (p29) to determine the toxin titre of the parent and the mutant.
The parent (630Δ*ermΔpyrE*) produced higher amounts of toxin in TYS compared to when it was in TY (not significant). No overall change in toxin levels was observed with the mutant (CT*srlE_N*) when comparing cytotoxicity in TY and TYS.
One-way ANOVA was used to determine statistical significance.
630Δ*ermΔpyrE* TYS vs. CT*srlE_N* TYS * P < 0.02.

At 96 h incubation, the same general trend that was observed at 72 h was seen again (but with greater significance) with the parent producing more toxin in TYS (2.5×10^7) than in TY (3.9×10^4) (** $P < 0.002$) (Fig. 5.40).

The mutant failed to increase toxicity in TYS (2.2×10^5 in TY (with minor variance) and 6.0×10^5 in TYS) and remaining significantly below the toxicity of the parent in TYS (**** $P < 0.0001$) (Fig. 5.40).

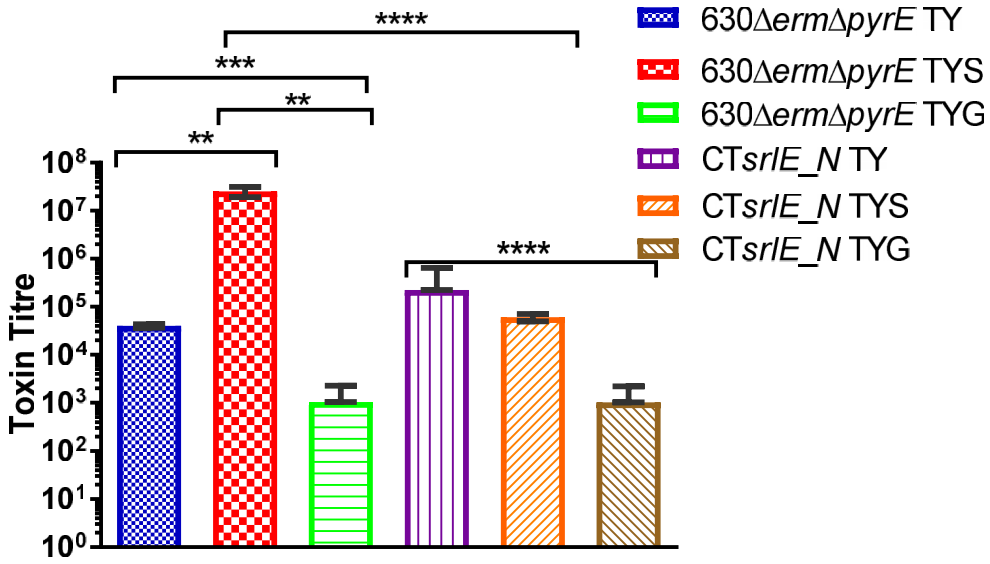

Figure 5.40: Role of *srlE_N* in *C. difficile* 630Δ*erm*Δ*pyrE* toxin expression at 96 h in TY.
Cytotoxicity of CT*srlE_N* at 96 h. Serial dilutions (10^0-10^{-9}) of bacterial supernatants (triplicates) of 630Δ*erm*Δ*pyrE*, and CT*srlE_N* mutants A and B (pooled) were applied to Vero cell monolayers (p29) to determine the toxin titre of the parent and the mutant.
The parent (630Δ*erm*Δ*pyrE*) produced significantly higher amounts (** $P < 0.002$) of toxin in TYS compared to when it was in TY. No change in toxin levels was observed in the mutant (CT*srlE_N*) when comparing cytotoxicity in TY and TYS.
One-way ANOVA was used to determine statistical significance.
630Δ*erm*Δ*pyrE* TY vs. TYS ** $P < 0.002$.
630Δ*erm*Δ*pyrE* TYS vs. CT*srlE_N* TYS **** $P < 0.0001$.

At 120 h, 630Δ*ermΔpyrE* produced more toxin in TYS than in TY, going from a toxin titre of 4.1 x 10^4 in TY to 1.6 x 10^7 in TYS (with variance, not considered significant) (Fig. 5.41).

CT*srlE_N* toxin levels remained almost the same in TY and TYS with a titre of 6.2 x 10^4 in TY and 9.7 x 10^4 in TYS. Again, there was a trend towards the parent producing more toxin in TYS than the mutant (not significant) (Fig. 5.41).

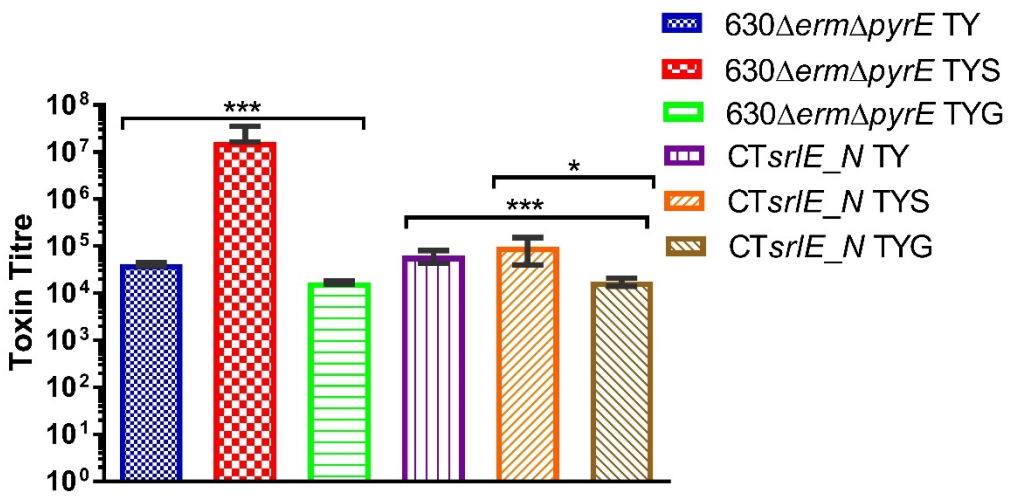

Figure 5.41: Role of *srlE_N* in *C. difficile* 630Δ*ermΔpyrE* toxin expression at 120 h in TY.
Cytotoxicity of CT*srlE_N* at 120 h. Serial dilutions (10^0-10^{-9}) of bacterial supernatants (triplicates) of 630Δ*ermΔpyrE* and CT*srlE_N* mutants A and B (pooled) were applied to Vero cell monolayers (p29) to determine the toxin titre of the parent and the mutant.
As previously observed at 72 h and 96 h (Fig. 5.39 and 5.40), the parent (630Δ*ermΔpyrE*) produced higher amounts of toxin (not significant) in TYS compared to when in TY.
No overall change in toxin levels was observed with the mutant (CT*srlE_N*) when comparing cytotoxicity in TY and TYS.
One-way ANOVA was used to determine statistical significance.

5.4.1.6 Motility assays

Four variant motility assays were used to examine the potential differences in motility between 630Δ*ermΔpyrE* and CT*srlE_N*. *C. difficile* 630Δ*erm*_ CT*fliC* and *C. difficile* M120 were used as the negative controls.

5.4.1.6.1 Motility assays on YT +glucose

Strains were tested on YT medium +glucose in order to observe motility of each. No differences were seen between 630Δ*ermΔpyrE* (0.8cm zone diameter) and CT*srlE_N* (0.8cm diameter). M120 was used as the negative control, exhibiting reduced motility (0.6cm diameter) in comparison to parent and mutant (Fig. 5.42).

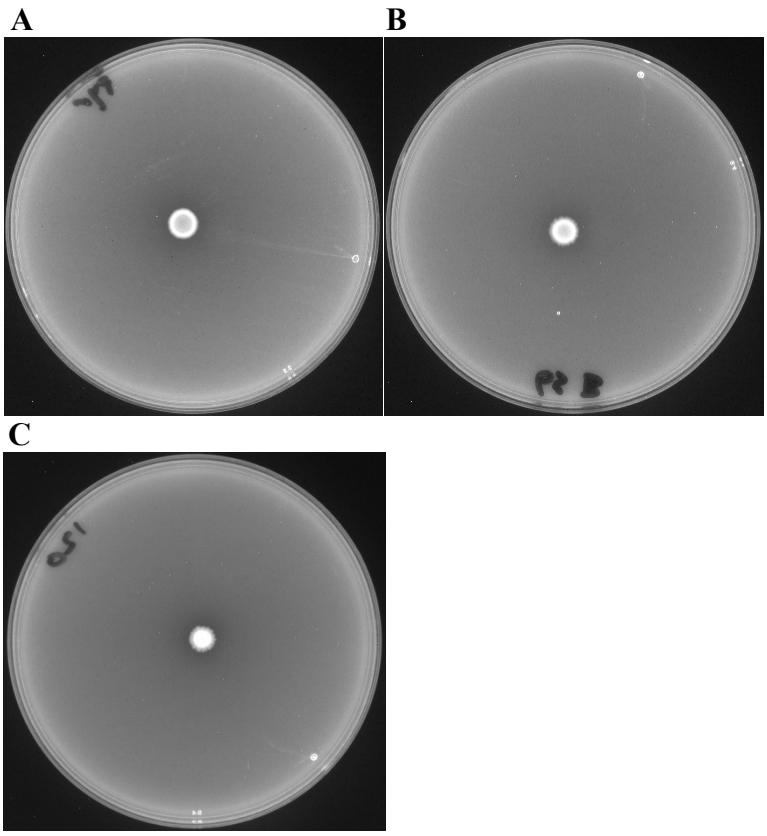

Figure 5.42: Representative images showing motility assays with parental strain (A), mutant (B), and negative control, CT*fliC* (C), on YTG.
2µL of overnight culture of each strain (in triplicates) was spotted on plates of YTG agar containing 1% w/v glucose and incubated at 37°C for 48 h to see if it was possible to observe a difference in motility.
Similar zones of motility were observed with the parental strain (630Δ*ermΔpyrE*) and the mutant (CT*srlE_N*).

5.4.1.6.2 Motility assays on YT +sorbitol

Motility assays on YTS agar were performed in order to determine potential differences in motility between 630Δ*erm*Δ*pyrE* and CT*srlE_N*. A larger zone of motility was observed with the parental strain (1.3cm zone diameter) than what was seen with the mutant (1cm zone diameter), indicating that the mutant had reduced motility on YTS. CT*fliC* was used as the negative control, and exhibited reduced motility (0.9cm zone diameter) in comparison to the parent and the mutant (Fig. 5.43).

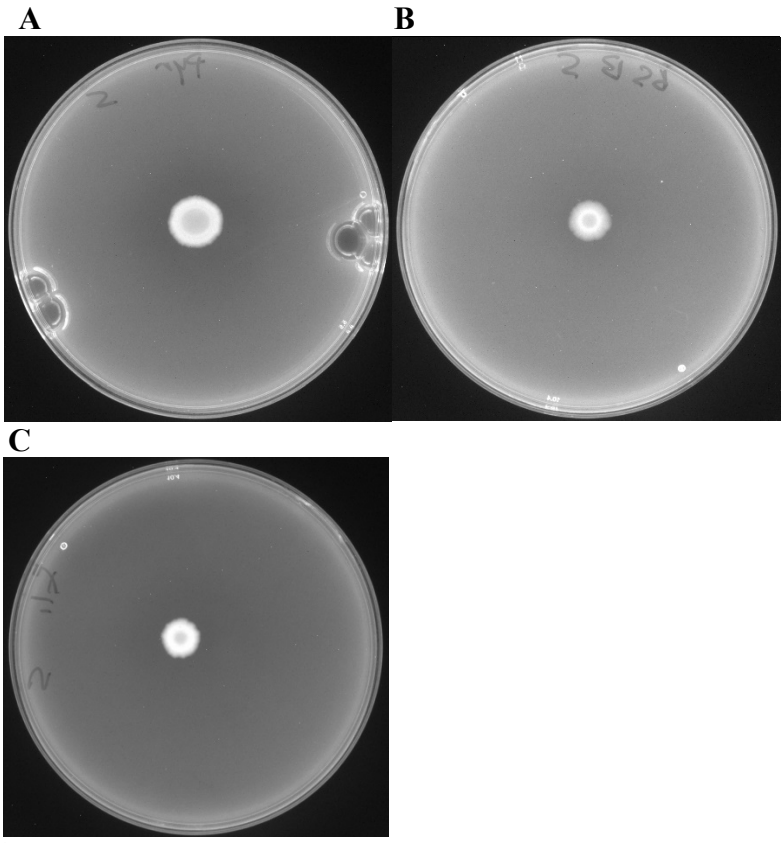

Figure 5.43: Representative images showing motility assays with parental strain (A), mutant (B), and negative control, CT*fliC* (C), on YTS.
2µL of overnight culture of each strain (in triplicates) was spotted on plates of YTS agar containing 1% w/v sorbitol and incubated at 37°C for 48 h to see if it was possible to observe a difference in motility.
A large motility zone was observed with the parental strain (630Δ*erm*Δ*pyrE*), while less motility was seen with the mutant (CT*srlE_N*).

5.4.1.6.3 Motility assays on BHIS +top agar

BHIS +top agar was used to determine potential differences in motility between 630Δ*ermΔpyrE* and CT*srlE_N*.

No differences were observed with similar motility on the plates observed with both strains (0.6cm zone diameter with the parent; 0.6cm zone diameter with the mutant). CT*fliC* was used as the negative control, and exhibited reduced motility (0.5cm zone diameter) in comparison to 630Δ*ermΔpyrE* and CT*srlE_N* (Fig. 5.44).

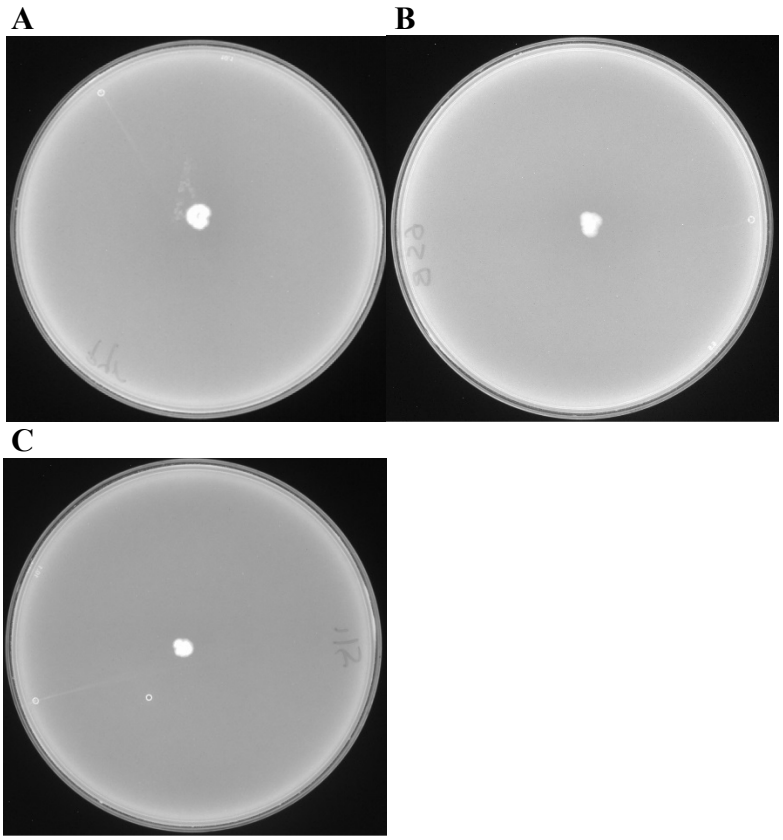

Figure 5.44: Representative images showing motility assays on top agar with control strain (A), mutant (B), and negative control, CT*fliC* (C).
The surface of the top agar was pierced with a single colony of each strain (in triplicates) and incubated at 37°C for 48 h to see if it was possible to observe a difference in motility.
No differences were observed between the parental strain (630Δ*ermΔpyrE*) and the mutant (CT*srlE_N*) with similar motility on the plates seen with both strains.

5.4.1.6.4 Motility assays in tubes

The same agar that was used as the top layer in the BHIS + top layer motility assay was utilised in tubes to determine possible differences in motility between 630Δ*ermΔpyrE* and CT*srlE_N*.

No differences were observed with both strains exhibiting good turbidity observed and migrated 11cm from the point of inoculation to the bottom of the tubes. M120 was used as the negative control, showed growth at the very top of the tubes, but didn't exhibit turbidity nor migrate through the agar (Fig. 5.45).

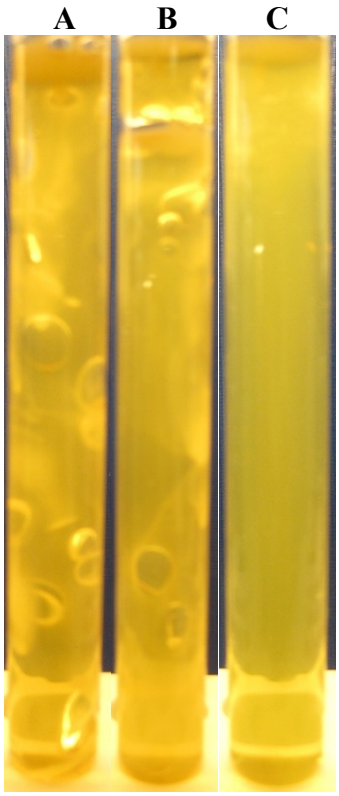

Figure 5.45: Representative images showing motility assays with the migration of control strain (A), mutant (B), and negative control (C) through the agar in the tubes. The negative control, M120 (C), did not migrate.
The surface of the agar was pierced using a sterile cocktail stick to inoculate a single colony of each strain (in triplicates) into the medium and incubated at 37°C for 24 h to see if it was possible to observe a difference in motility.
The control strain (630Δ*ermΔpyrE*) and the mutant (CT*srlE_N*) both exhibited good turbidity growth and migrated to the base of the tubes (11cm), while the negative control (M120) did not migrate any distance.

5.4.2 Characterisation of 630Δ*erm*Δ*pyrE*_CT*srlE_C* (CD630_0766)

CT inactivation was determined by screening 630Δ*erm*Δ*pyrE* erythromycin-resistant colonies (potential CT*srlE_C* mutants) by PCR (using primers outside of the CT insertion –Fig. 5.46) and comparing the fragment sizes with those from 630Δ*erm*Δ*pyrE* on 1% w/v agarose gel (Fig. 5.47).

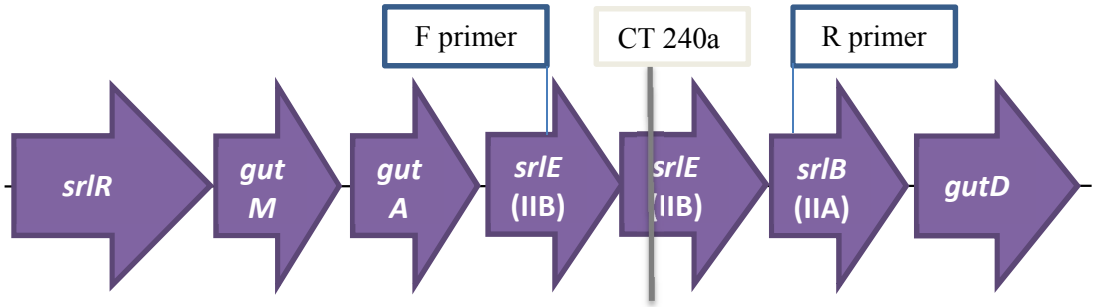

Figure 5.46: Primers used for PCR screening for CT mutagenesis of *srlE_C*. Position, within the sorbitol-specific operon at loci CD630_0762-8, of the primers (F and R) designed for the regions outside of *srlE_C*, which were used to amplify DNA isolated from selected colonies growing BHIS +Erm plates.

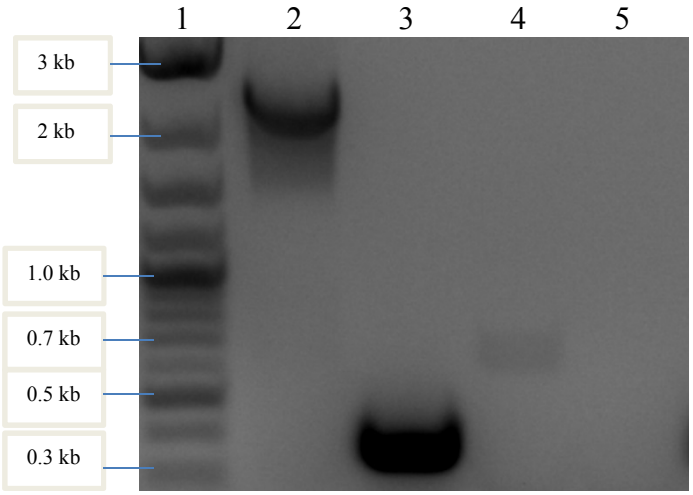

Figure 5.47: CT insertion in *srlE_C* (CD630_0766), shown by PCR. Agarose gel (1% w/v) was used to show the CT insertion. Primers were designed specific to outside of the predicted insertion site were designed and used to amplify the desired region in both parent and mutant. Table 5.4 below shows the lane order.

Table 5.4: Content of each well showing by PCR the CT insertion in CT*srlE_C* mutant vs. parent.

Well	Content	Size (kb)
1	Marker	
2	CT*srlE_C*, F + R primer	2.53
3	CT*srlE_C*, R + EBS primer	0.4
4	630Δ*ermΔpyrE*, F + R primer	0.73
5	630Δ*ermΔpyrE*, R + EBS primer	-

5.4.2.1 Growth on DM agar

Growing the parent (630Δ*ermΔpyrE*) and the mutant (CT*srlE_C*) on DMS agar did not reveal differences in the ability to subsist on sorbitol on this type of agar. Strong growth was exhibited by both strains (Fig. 5.48), but also on the negative control containing no sugar (DM) (not shown here).

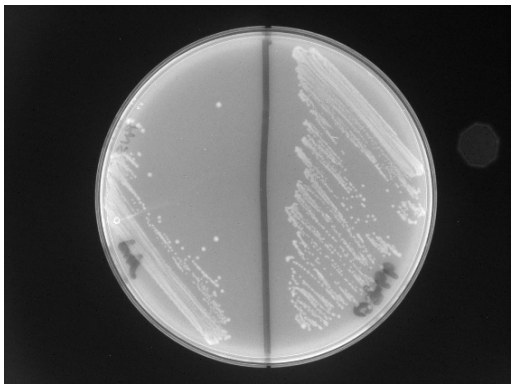

Figure 5.48: Representative image showing growth of 630Δ*ermΔpyrE* -parent (left) and CT*srlE_C* -mutant (right) on DMS agar.
Strains (in triplicates) were streaked on plates of DMS agar containing 0.6% w/v sorbitol and incubated at 37°C for 16 h to see if it was possible to observe a growth phenotype.
Differences in the ability to metabolise sorbitol could not be determined by this assay as strong growth was also observed on the negative control plates (not shown).

5.4.2.2 Growth in DM, DMS, and DMG broth

Parent (630Δ*ermΔpyrE*) growth from 10 h in DMS saw an increase in OD_{600} levels compared to when in DM alone, which was significant at 24 h (peak growth in both conditions) when growth of the parent was 0.53 in DM and 0.83 in DMS (**** $P < 0.0001$). Slope of curve 0-24 h in DMS = 1.18 (Fig. 5.49).

This sorbitol-induced increase was not observed with CT*srlE_C* as there was no significant difference in the OD_{600} levels of the mutant in DM and DMS. An example being at 24 h, which was also peak growth for CT*srlE_C* in these conditions, when OD_{600} in DM was 0.5, and was 0.46 in DMS. Slope of curve 0-24 h in DMS = 0.65 (Fig. 5.49).

630Δ*ermΔpyrE* in DMS vs. CT*srlE_C* in DMS at 24 h **** $P < 0.0001$.

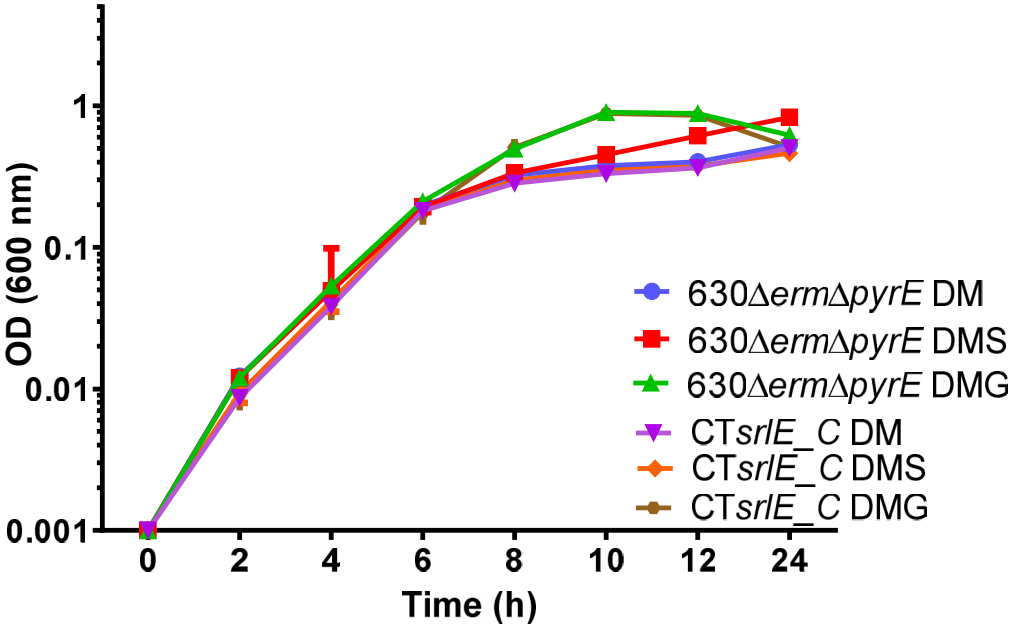

Figure 5.49: Role of *srlE_C* in *C difficile* 630Δ*erm*Δ*pyrE* growth in DM.
630Δ*erm*Δ*pyrE* (parent) and CT*srlE_C* (mutant) were incubated for 24 h at 37°C. 1mL extracts (triplicates) were taken at regular time points and the OD_{600} measured.
Growth of CT*srlE_C* in sorbitol from 10 h onwards was less (at 24 h **** P < 0.0001) than that of the parent, 630Δ*erm*Δ*pyrE* sorbitol. Growth of the mutant in DMS was similar to what it was in plain DM.
630Δ*erm*Δ*pyrE* slope of curve 0-24 h in DMS = 1.18.
CT*srlE_C* slope of curve 0-24 h in DMS = 0.65.
One-way ANOVA was used to determine statistical significance.
630Δ*erm*Δ*pyrE* at 24 h in DM vs. in DMS **** P < 0.0001.
630Δ*erm*Δ*pyrE* in DMS vs. CT*srlE_C* in DMS at 24 h **** P < 0.0001.

5.4.2.3 HPLC evaluation of sorbitol/glucose consumption in DM

630Δ*erm*Δ*pyrE* (parental strain) sorbitol levels declined from 7.47mM at 0 h to 0mM at 24 h. 630Δ*erm*Δ*pyrE* slope of curve 0-24 h in DMS = 1.86 (Fig. 5.50).

Mutant sorbitol levels remained roughly the same with 7.47mM at 0 h and 7.96mM detected at the end point of the assay (24 h). The divergence in sorbitol uptake between the parent and the mutant had reached significant levels by 12 h (** P < 0.0023). CT*srlE_C* slope of curve 0-24 h in DMS = 0 (Fig. 5.50).

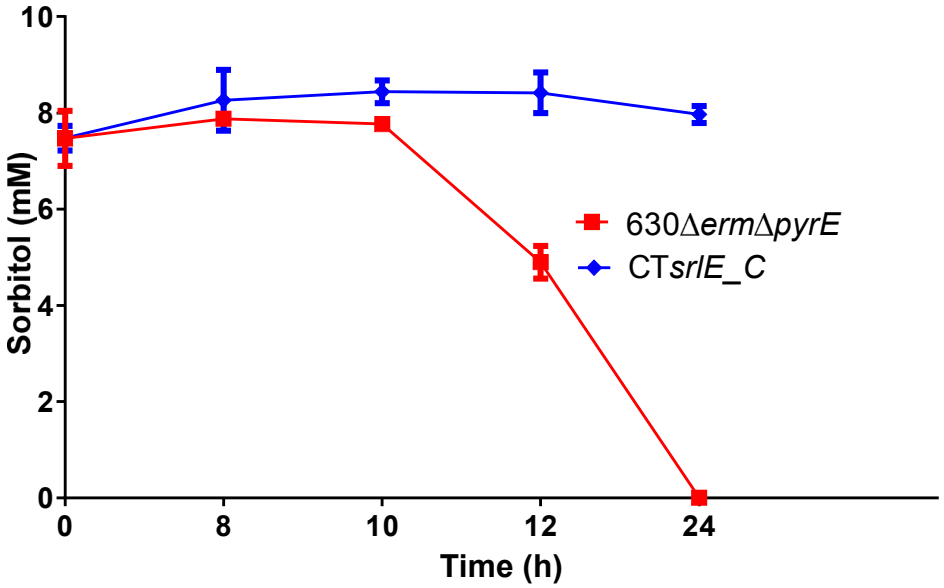

Figure 5.50: HPLC evaluation of sorbitol uptake in DM by 630Δ*ermΔpyrE* (parent) and CT*srlE_C* (mutant).
Extracts (triplicates) from the growth assay in DM were used to determine by HPLC the exact amount of sugar remaining in the medium at each time point.
The sorbitol in the parental medium was completely spent by 24 h. The mutant was unable to use any of the available sorbitol.
630Δ*ermΔpyrE* slope of curve 0-24 h = 1.86.
CT*srlE_C* slope of curve 0-24 h = 0.
One-way ANOVA was used to determine statistical significance.
630Δ*ermΔpyrE* vs. CT*srlE_C* at 12 h ** $P < 0.0023$.

Glucose was consumed by 630Δ*ermΔpyrE* and CT*srlE_C* between 0 h and 24 h (**** $P < 0.0001$) with glucose levels dropping from 8.65mM and 8.66mM respectively at 0 h, to 0.27mM and 0.29mM respectively at 24 h (Fig. 5.51).

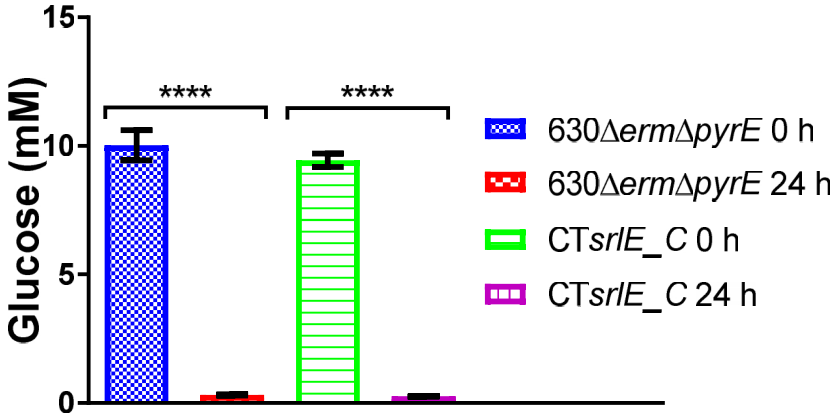

Figure 5.51: HPLC evaluation of glucose uptake in DM by 630Δ*erm*Δ*pyrE* (parent) and CT*srlE_C* (mutant).
Extracts (triplicates) from the growth assay in DM were used to determine by HPLC the exact amount of glucose remaining in the medium at end of the assay. The glucose in the medium was depleted by both strains by the 24 h time point (**** $P < 0.0001$).
One-way ANOVA was used to determine statistical significance.

5.4.2.4 Growth in TY, TYS, and TYG

Growth of the mutant, CT*srlE_C*, in sorbitol, like CT*srlE_N*, lagged behind that of the parent in sorbitol. Growth behaviour of the mutant in sorbitol mirrored that of the parent in TY alone (Fig. 5.52). From 24 h, the presence of sorbitol permitted the parental strain in TYS to exhibit a higher OD_{600} than when in plain TY, a trend not observed at any point with the mutant. At 48 h, when growth of the parent in TYS peaked at an OD_{600} of 0.8, and in TY it was 0.55 (**** $P < 0.0001$); while the OD_{600} for CT*srlE_C* in both TY and TYS was 0.52 (no significant difference when compared with the parent in TY) (Fig. 5.52). Slope of the curve 24-120 h in TYS (downward): 630Δ*ermΔpyrE* = 1.05, CT*srlE_C* = 1.1.

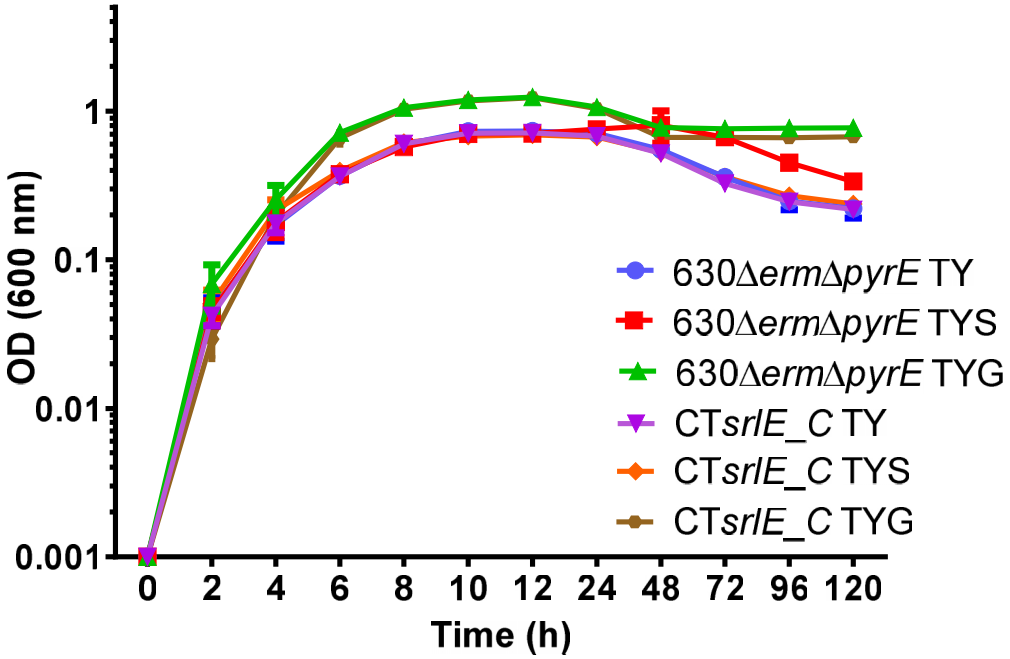

Figure 5.52: Role of *srlE_C* in *C. difficile* 630Δ*erm*Δ*pyrE* growth in TY.
630Δ*erm*Δ*pyrE* (parent) and CT*srlE_C* (mutant) were incubated for 120 h at 37°C. 1mL extracts (triplicates) were taken at regular time points and the OD_{600} measured.
From 24 h onwards, CT*srlE_C* in TYS growth was significantly (** $P < 0.01$) attenuated in comparison to 630Δ*erm*Δ*pyrE* in the same conditions. Slope of the curve 24-120 h in TYS (downward): 630Δ*erm*Δ*pyrE* = 1.05, CT*srlE_C* = 1.1.
One-way ANOVA was used to determine statistical significance.
630Δ*erm*Δ*pyrE* at 48 h (peak growth) in TY vs. TYS **** $P < 0.0001$.
630Δ*erm*Δ*pyrE* at 48 h (peak growth) in TYS vs. CT*srlE_C* at 12 h (peak growth) in TYS ** $P < 0.01$.

5.4.2.5 Cytotoxicity of 630Δ*erm*Δ*pyrE* and 630Δ*erm*Δ*pyrE*_CT*srlE_C*

With the cytotoxicity assays, when comparing TY and TYS, no substantial differences were observed in toxin levels in either parent or mutant (Fig. 5.53-5.55). But, at each time point, there was an observable trend towards a minor increase in parental strain toxin levels, as was seen in TYS in comparison to toxin levels in TY.

At the 72 h time point, toxicity rose slightly, but not significantly, in the parent in TYS from 2.8 x 10^5 in TY to 7.9 x 10^6 (with a high degree of variance); while

mutant toxin levels remained near the same level, at 3.0 x 10^5 in TY and 2.7 x 10^5 in TYS (Fig. 5.53).

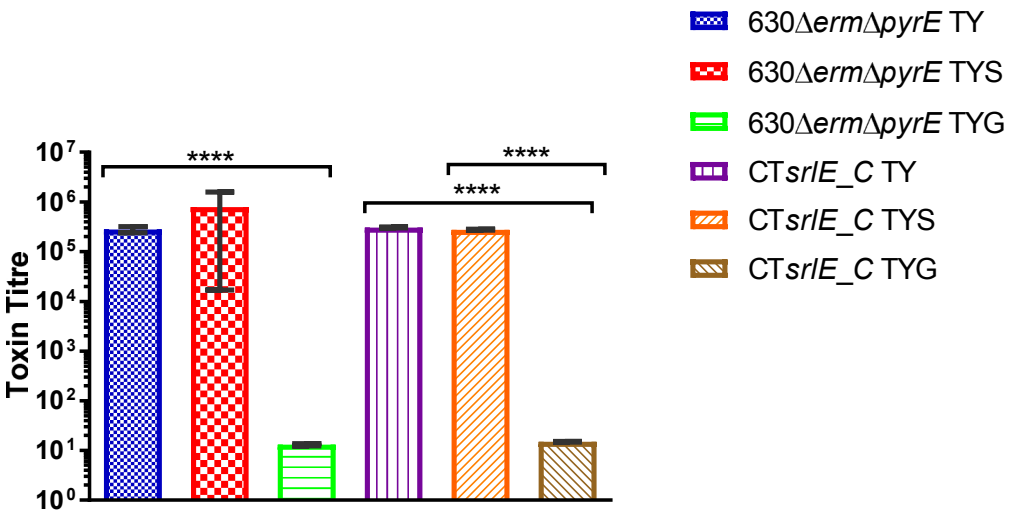

Figure 5.53: Role of *srlE_C* in *C. difficile* 630Δ*erm*Δ*pyrE* toxin production at 72 h in TY.
Cytotoxicity of CT*srlE_C* at 72 h. Serial dilutions (10^0-10^{-9}) of bacterial supernatants (triplicates) were applied to Vero cell monolayers (p31) to determine the toxin titre of the parent (630Δ*erm*Δ*pyrE*) and the mutant (CT*srlE_C*).
With the parent, there was a minor trend towards toxin levels rising slightly in TYS. No differences in toxin levels were observed with the mutant when comparing cytotoxicity in TY and TYS.
One-way ANOVA was used to determine statistical significance.

At 96 h, with the parent, a minor increase in toxin titre was observed. Toxin production went from 4.9 x 10^4 in TY to 4.8 x 10^5 in TYS (with a large variance) (Fig. 5.54).

Mutant toxin levels appear to have risen in TY and TYS in comparison to the parental strain levels in these conditions (in TY **** $P < 0.0001$, in TYS * $P < 0.02$), and remained almost the same in TY and TYS, with respective toxin titres of 4.0 x 10^5 and 3.6 x 10^5 (Fig. 5.54).

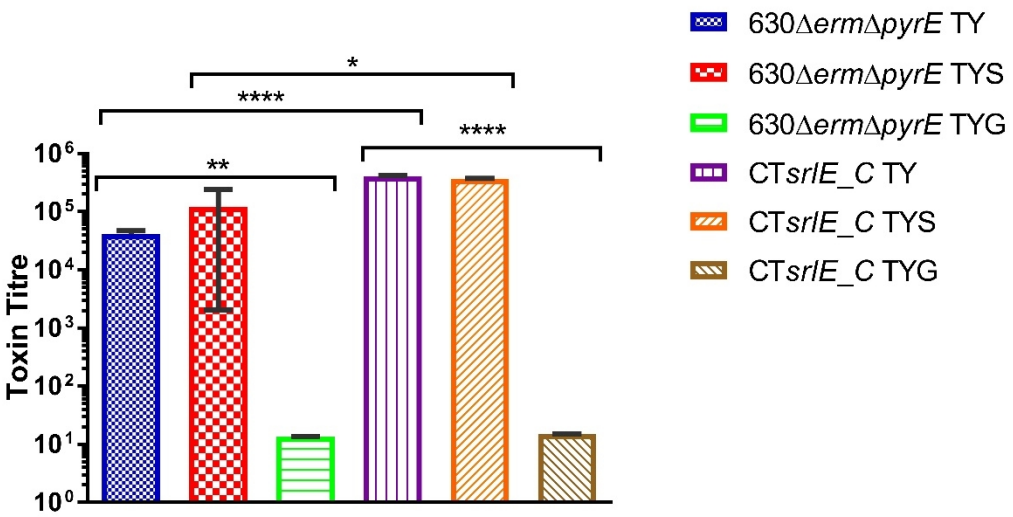

Figure 5.54: Role of *srlE_C* in *C. difficile* 630Δ*erm*Δ*pyrE* toxin production at 96 h in TY.
Cytotoxicity of CT*srlE_C* at 96 h. Serial dilutions (10^{0}-10^{-9}) of bacterial supernatants (triplicates) were applied to Vero cell monolayers (p31) to determine the toxin titre of the parent (630Δ*erm*Δ*pyrE*) and the mutant (CT*srlE_C*).
There was a trend towards toxin levels rising slightly in the parent in TYS. No changes in toxin levels were observed with the mutant when comparing cytotoxicity in TY and TYS. Mutant toxin levels in TY were significantly above those of the parent in TY (**** $P < 0.0001$).
One-way ANOVA was used to determine statistical significance.
630Δ*erm*Δ*pyrE* in TY vs. CT*srlE_C* TY **** $P < 0.0001$.
630Δ*erm*Δ*pyrE* in TYS vs. CT*srlE_C* TYS * $P < 0.02$.

At 120 h, toxin production by the parent, rose slightly (with much variance) in TYS in comparison to when it was in TY (going from 4.5 x 10^5 in TY to 1.5 x 10^6 in TYS) (Fig. 5.55).

Mutant toxin levels remained at almost the same level in TY and TYS at 4.5 x 10^5 and 4.1 x 10^5 respectively (Fig. 5.55).

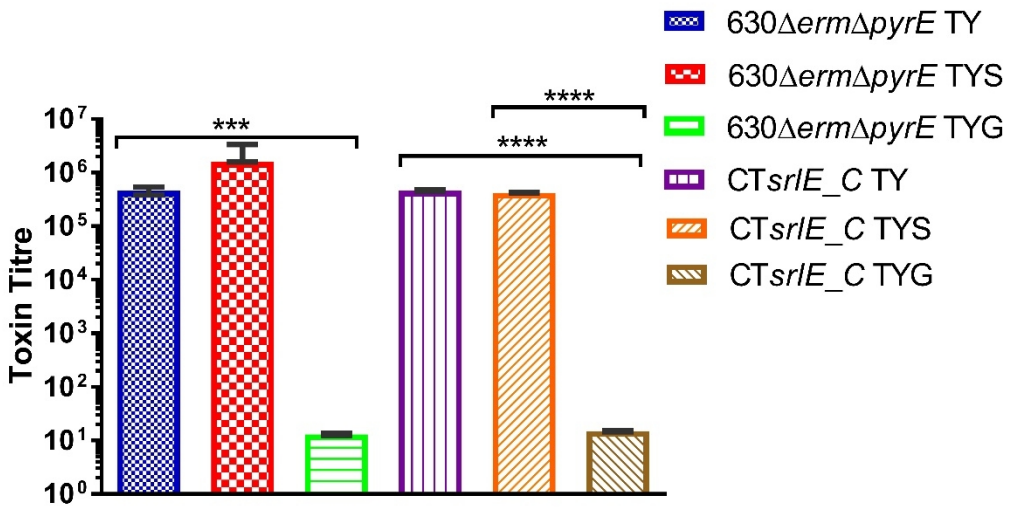

Figure 5.55: Role of *srlE_C* in *C. difficile* 630Δ*erm*Δ*pyrE* toxin production at 120 h in TY.
Cytotoxicity of CT*srlE_C* at 120 h. Serial dilutions (10^{0}-10^{-9}) of the bacterial supernatants (triplicates) were applied to Vero cell monolayers (p31) in order to determine the toxin titre of the parent (630Δ*erm*Δ*pyrE*) and the mutant (CT*srlE_C*).
Toxin levels rose slightly in the parent in TYS. No differences in toxin levels were observed with the mutant when comparing cytotoxicity in TY and TYS.
One-way ANOVA was used to determine statistical significance.

5.4.2.6 Motility assays

Motility was tested using four variant motility assays. The mutant was tested alongside 630Δ*erm*Δ*pyrE*, *C. difficile* 630Δ*erm*_CT*fliC*, and *C. difficile* M120.

5.4.2.6.1 Motility assays on YT +glucose

Motility assays on YTG revealed no differences between the parental strain (630Δ*erm*Δ*pyrE*) and the mutant (CT*srlE_C*) with similar zones of motility seen with both strains (0.8cm with the parent; 0.8cm with the mutant). M120 was used as the negative control, and exhibited reduced motility (0.6cm zone diameter) in comparison to the parent and the mutant (Fig. 5.56).

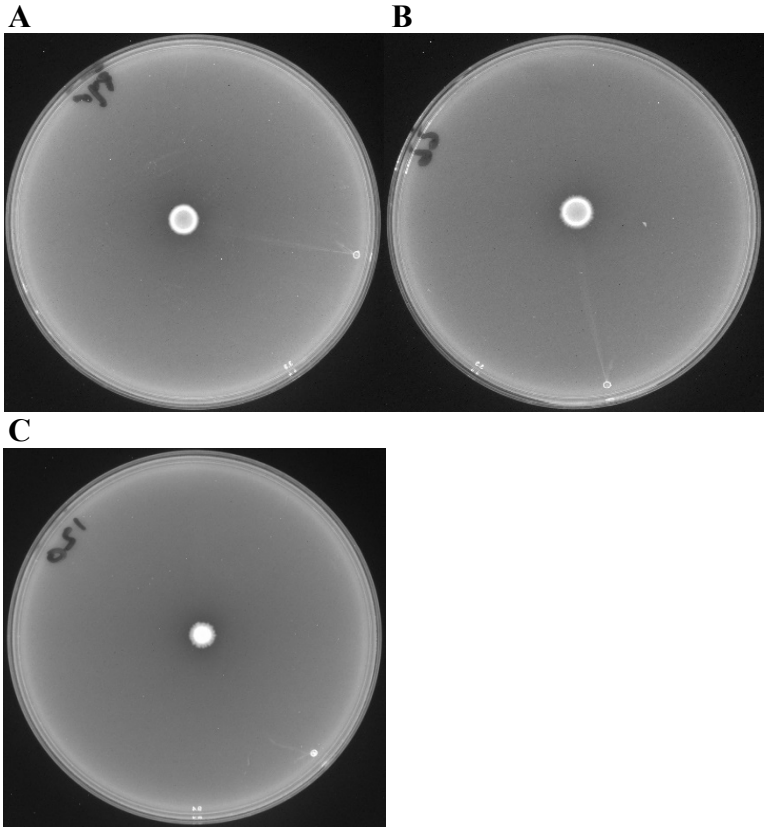

Figure 5.56: Representative images showing motility assays with parental strain (A), mutant (B), and negative control, CT*fliC* (C), on YTG.
2µL of overnight culture of each strain (in triplicates) was spotted on plates of YTS agar containing 1% w/v glucose and incubated at 37°C for 48 h to see if it was possible to observe a difference in motility.
No differences in motility behaviour could be observed. Similar motility was observed with the parental strain (630Δ*ermΔpyrE*) and the mutant (CT*srlE_C*).

5.4.2.6.2 Motility assays on YT +sorbitol

Motility assays on YTS agar revealed no differences between the parental strain (630Δ*ermΔpyrE*) and the mutant (CT*srlE_C*) in terms of motility, but a slightly larger zone of motility was seen with the parent (1.3cm zone diameter) than was seen with the mutant (1cm zone diameter), indicating that CT*srlE_C* is less efficiently utilising the sorbitol in the agar. CT*fliC* was used as the negative control, and exhibited reduced motility (0.9cm zone diameter) in comparison to the parent and the mutant (Fig. 5.57).

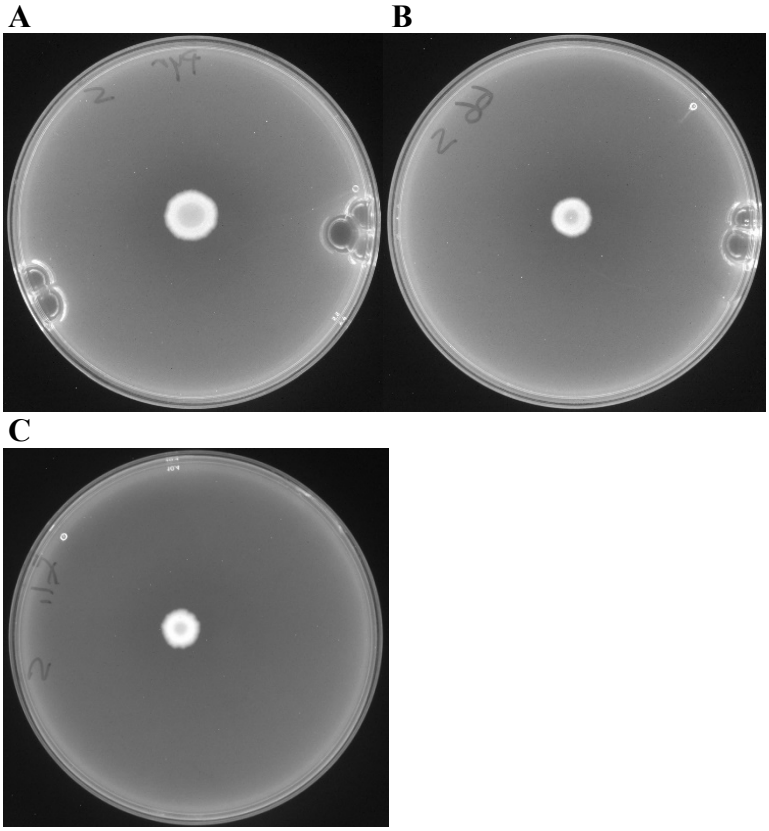

Figure 5.57: Representative images showing motility assays with parental strain (A), mutant (B), and negative control, CT*fliC* (C), on YTS.
2µL of overnight culture of each strain (in triplicates) was spotted on plates of YTS agar containing 1% w/v sorbitol and incubated at 37°C for 48 h to see if it was possible to observe a difference in motility.
No major differences in motility behaviour could be observed. Notwithstanding, a wider zone of motility on the plates was observed with the parental strain (630Δ*erm*Δ*pyrE*). Reduced motility was observed with the mutant (CT*srlE_C*).

5.4.2.6.3 Motility assays on BHIS +top agar

BHIS +top agar was used to determine possible differences in motility between 630Δ*erm*Δ*pyrE* and CT*srlE_C*. No differences were observed with both strains exhibiting similar motility on the plates (0.6cm zone diameter with the parent; 0.6cm zone diameter with the mutant). CT*fliC* was used as the negative control, and exhibited reduced motility (0.5cm zone diameter) in comparison to 630Δ*erm*Δ*pyrE* and CT*srlE_C* (Fig. 5.58).

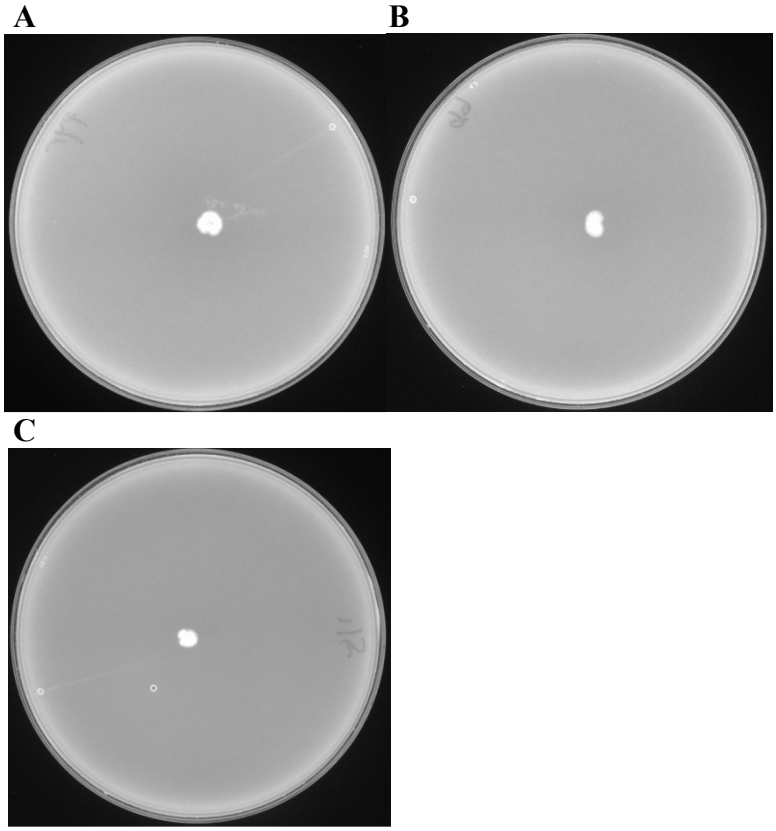

Figure 5.58: Representative images showing motility assays on top agar showing control strain (A), mutant (B), and negative control, CT*fliC* (C).
The surface of the top agar was pierced with a single colony of each strain (in triplicates) and incubated at 37°C for 48 h to see if it was possible to observe a difference in motility.
No differences were observed between the parental strain (630Δ*ermΔpyrE*) and the mutant (CT*srlE_C*) with similar motility on the plates seen with both strains.

5.4.2.6.4 Motility assays in tubes

The same type of agar that was used as the top layer in the BHIS +top agar motility assay plates was aliquoted into tubes and used to determine potential differences in motility between 630Δ*ermΔpyrE* and CT*srlE_C*.

No differences were observed with both strains exhibiting robust turbidity and migrating 11cm from the point of inoculation to the bottom of the tubes. *C. difficile* M120 was used as the negative control, showed growth at the very top of the tubes, but did not exhibit any turbidity nor migrate any distance through the agar (Fig. 5.59).



Figure 5.59: Representative images of motility assays showing migration of control strain (A) and mutant (B) through the agar in the tubes. The negative control, M120 (C), did not migrate.
The surface of the agar was pierced using a sterile cocktail stick with a single colony of each strain (in triplicates) and incubated at 37°C for 24 h to see if it was possible to observe a difference in motility.
The control strain (630Δ*erm*Δ*pyrE*) and the mutant (CT*srlE_C*) both exhibited good turbidity and migrated (11cm) to the base of the tubes, while the negative control (M120) did not migrate any distance.

5.5 Investigation and Characterisation of PTS^{Srl} IIC -SrlB

srlB putatively encodes a IIA for PTS^{Srl} at locus CD630_0767, and was targeted for inactivation by CT mutagenesis (Fig. 5.60).

5.5.1 Characterisation of 630Δ*erm*Δ*pyrE*_CT*srlB* (CD630_0767)

CT inactivation of *srlB* was determined by screening 630Δ*erm*Δ*pyrE* erythromycin-resistant colonies (potential CT*srlE_N* mutants) by PCR (with primers outside the CT insertion) and comparing the fragment sizes with those

from 630Δ*ermΔpyrE* on 1% w/v agarose gel (Fig. 5.61). Predicted fragment sizes (Table 5.4) indicated the presence of a CT_*srlB* mutant.

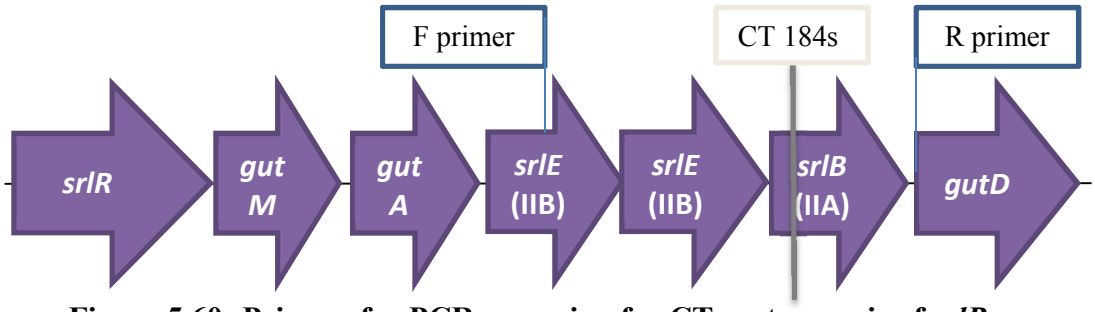

Figure 5.60: Primers for PCR screening for CT mutagenesis of *srlB*. Position, within the CD630_0762-8 sorbitol-specific operon, of the primers (F and R) designed for the regions outside of *srlB*, which were used to amplify DNA isolated from selected colonies growing on BHIS +Erm plates.

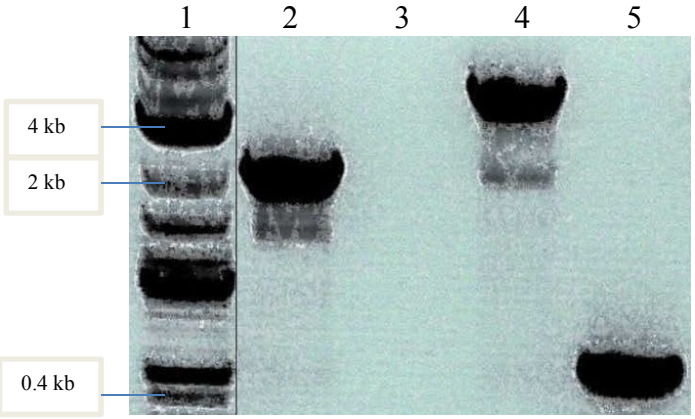

Figure 5.61: CT insertion shown by PCR in *srlB* (CD630_0767). Agarose gel (1% w/v) was used to show the CT insertion in *srlB*. Primers specific to outside of the predicted insertion site were designed and used to amplify the desired region in both parent and mutant. Table 5.5 below shows the lane order.

Table 5.5: Content of each well when showing by PCR the CT insertion in CT*srlB* mutant vs. parent.

Well	Content	Size (kb)
1	Marker	
2	630Δ*ermΔpyrE*, F + R primer	2.3
3	630Δ*ermΔpyrE*, R + EBS primer	-
4	CT*srlB*, F + R primer	4.1
5	CT*srlB*, R + EBS primer	0.5

5.5.1.1 Growth on DM agar

Growing the parent (630Δ*ermΔpyrE*) and the mutant (CT*srlB*) on DMS agar did not reveal differences in the ability to subsist on sorbitol on this type of medium. Strong growth was exhibited by both strains on DM (not shown) and on DMS (Fig. 5.62).

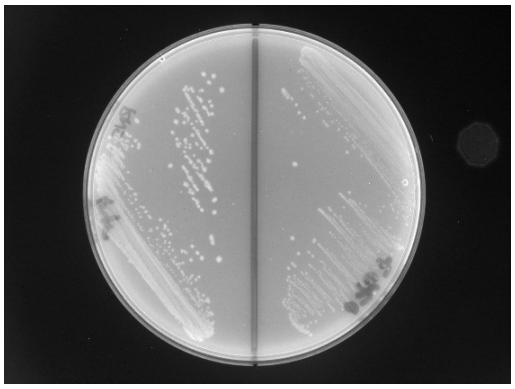

Figure 5.62: Representative image showing growth of 630Δ*ermΔpyrE* -parent (left) and CT*srlB* -mutant (right) on DMS agar.
Strains (in triplicates) were streaked on plates of DMS agar containing 0.6% w/v sorbitol and incubated at 37°C for 16 h to see if it was possible to observe a growth phenotype.
Differences in the ability to metabolise sorbitol could not be determined by this assay as both strains grew well on DM (not shown) and DMS agar.

5.5.1.2 Growth in DM, DMS, and DMG broth

The presence of sorbitol induced an increase in the growth of the parent (630Δ*ermΔpyrE*). From 10 h of incubation sorbitol allowed OD_{600} levels to increase significantly (*** $P < 0.00017$) above the OD_{600} levels in DM alone. At peak growth, at 24 h, OD_{600} in DM was 0.57, and in DMS was 0.84 (**** $P < 0.0001$). 630Δ*ermΔpyrE* slope of the curve in DMS 0-24h = 1.2 (Fig. 5.63).

Mutant growth in sorbitol exhibited no increase in OD_{600} levels above those in DM alone. CT*srlB* OD_{600} in DM was 0.53 and in DMS was 0.52. CT*srlB* slope of the curve in DMS 0-24 h = 0.75 (Fig. 5.63).

630Δ*ermΔpyrE* vs. CT*srlB* at 10 h in DMS *** P < 0.0003; at 24 h **** P < 0.0001.

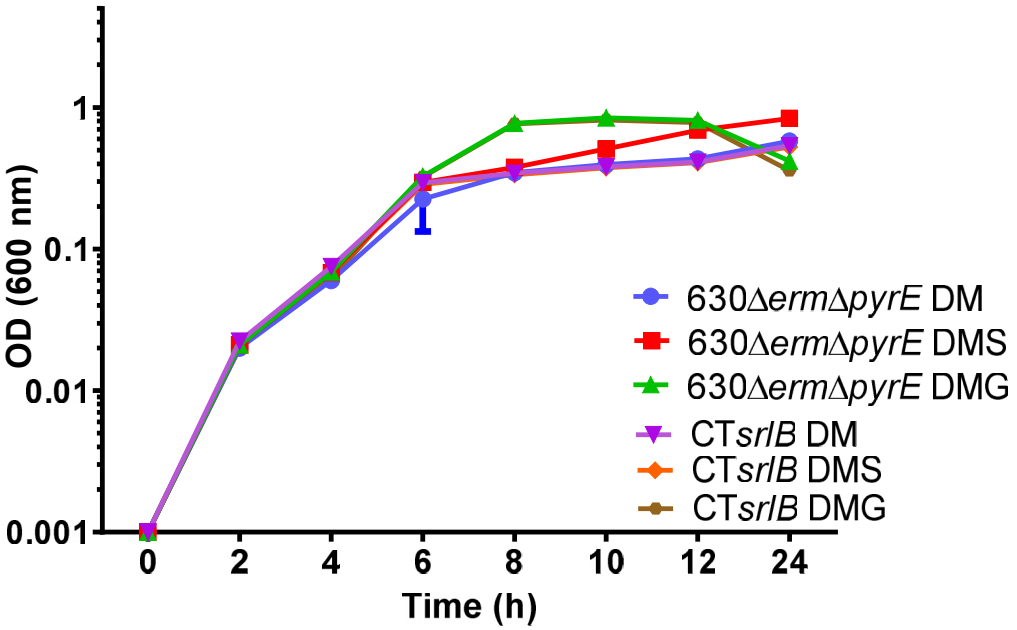

Figure 5.63: Role of *srlB* in *C difficile* 630Δ*ermΔpyrE* growth in DM.
630Δ*ermΔpyrE* (parent) and CT*srlB* (mutant) were incubated for 24 h at 37°C.
1 mL extracts (triplicates) were taken at regular timepoints.
Growth of CT*srlB* in sorbitol from 10 h onwards was significantly less (*** P < 0.0003) than that of the parent, 630Δ*ermΔpyrE*. Growth of the mutant in DMS was the same as it was in DM.
630Δ*ermΔpyrE* slope of the curve in DMS 0-24h = 1.2.
CT*srlB* slope of the curve in DMS 0-24 h = 0.75.
One-way ANOVA was used to determine statistical significance.
630Δ*ermΔpyrE* vs. CT*srlB* at 10 h in DMS *** P < 0.0003; at 24 h **** P < 0.0001.
630Δ*ermΔpyrE* in DM vs. DMS at 10 h *** P < 0.0017; at 24 h **** P < 0.0001.

5.5.1.3 HPLC evaluation of sorbitol/glucose consumption in DM

With the HPLC analysis to determine sorbitol uptake, from 10 h there was a rapid usage of sorbitol by the parent, 630Δ*ermΔpyrE*, which was not at all seen with the mutant, CT*srlB* (**** P < 0.0001). At 24 h, there was no sorbitol remaining in the 630Δ*ermΔpyrE* medium, while CT*srlB* cultures had an average of 9.5mM,

indicating no sorbitol uptake by the mutant (Fig. 5.64). 630Δ*ermΔpyrE* slope of the curve 0-24 h = 2.1. CT*srlB* slope of the curve 0-24 h = 0.

630Δ*ermΔpyrE* vs. CT*srlB* at 10 h **** P < 0.0001.

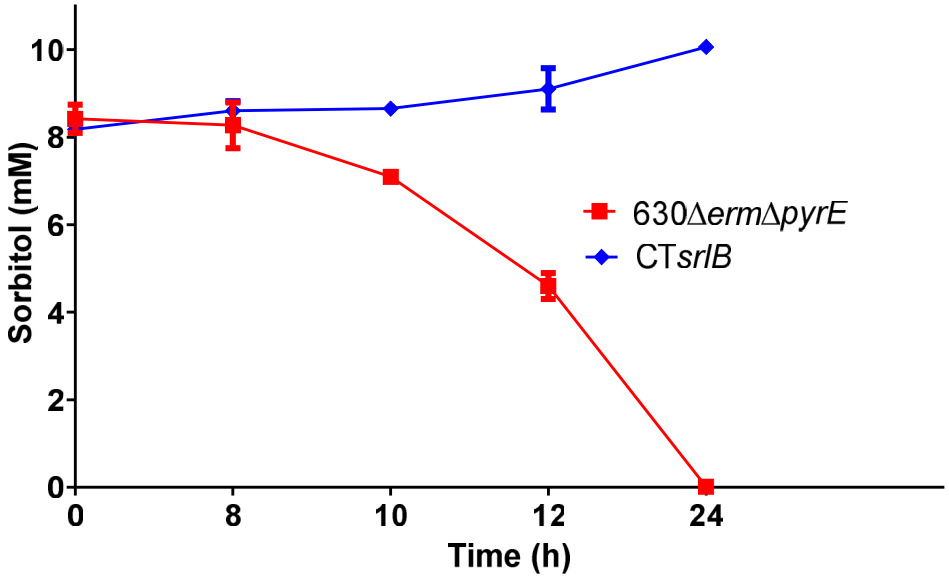

Figure 5.64: HPLC evaluation of sorbitol uptake in DM by 630Δ*ermΔpyrE* (parent) and CT*srlB* (mutant).
Extracts (triplicates) from the growth assay in DM were used to determine by HPLC the exact amount of sugar remaining in the medium at each time point.
The parent utilised all of the available sorbitol, while mutant sorbitol levels were, overall, unchanged.
630Δ*ermΔpyrE* slope of the curve 0-24 h = 2.1. CT*srlB* slope of the curve in 0-24 h = 0.
One-way ANOVA was used to determine statistical significance.
630Δ*ermΔpyrE* vs. CT*srlB* at 10 h **** P < 0.0001.

Glucose was consumed by 630Δ*ermΔpyrE* and CT*srlB* between 0 h and 24 h (**** P < 0.0001) with glucose levels dropping from 8.65mM and 8.66 respectively at 0 h to 0.27mM and 0.29mM respectively at 24 h (Fig. 5.65).

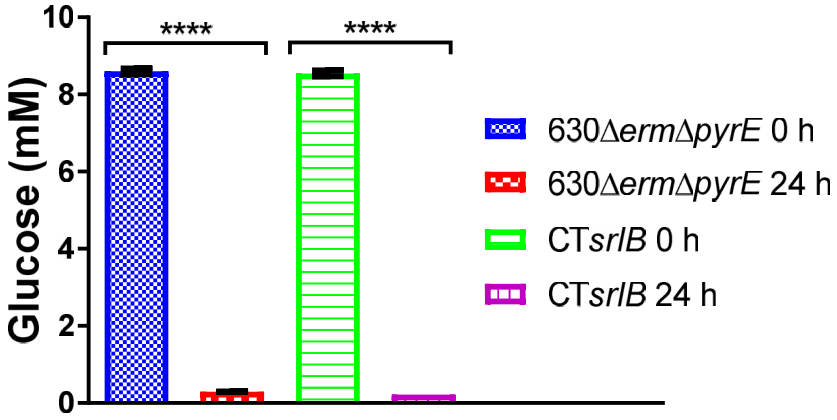

Figure 5.65: HPLC evaluation of glucose uptake in DM by 630Δ*erm*Δ*pyrE* (parent) and CT*srlB* (mutant).
Extracts (triplicates) from the growth assay in DM were used to determine by HPLC the exact amount of the sugar remaining in the medium at both time points. Glucose was spent by the parental strain and the mutant by 24 h (**** P < 0.0001).
One-way ANOVA was used to determine statistical significance.

5.5.1.4 Growth in TY, TYS, and TYG

From 72 h, the presence of sorbitol allowed the parental strain, 630Δ*erm*Δ*pyrE*, to exhibit an increase in OD_{600} levels above those cultures that were in TY alone at the later time points of the assay (72-120 h). The OD_{600} values in TYS declined at a much more gradual rate than those in TY (TY 48-120 h, slope (downward) = 1.31; TYS 48-120 h, slope = 0.63). For example, at 96 h (peak OD_{600} in TYS), OD_{600} in TY was 0.28, but was 0.74 in TYS (*** P < 0.0002) (Fig. 5.66).

Mutant OD_{600} levels exhibited no increase in sorbitol supplemented cultures in comparison to when in TY alone. At the later time points (72-120 h), mutant decline in TYS occurred at the same rate as in TY. An example being at 96 h, OD_{600} in TY was 0.33, and in TYS it was 0.36. 630Δ*erm*Δ*pyrE* and CT*srlB* at 96 h in TYS differed significantly (** P < 0.001). Slope of curve 24-120 h in TYS (downward): 630Δ*erm*Δ*pyrE* = 0.75, CT*srlB* = 1.07 (Fig. 5.66).

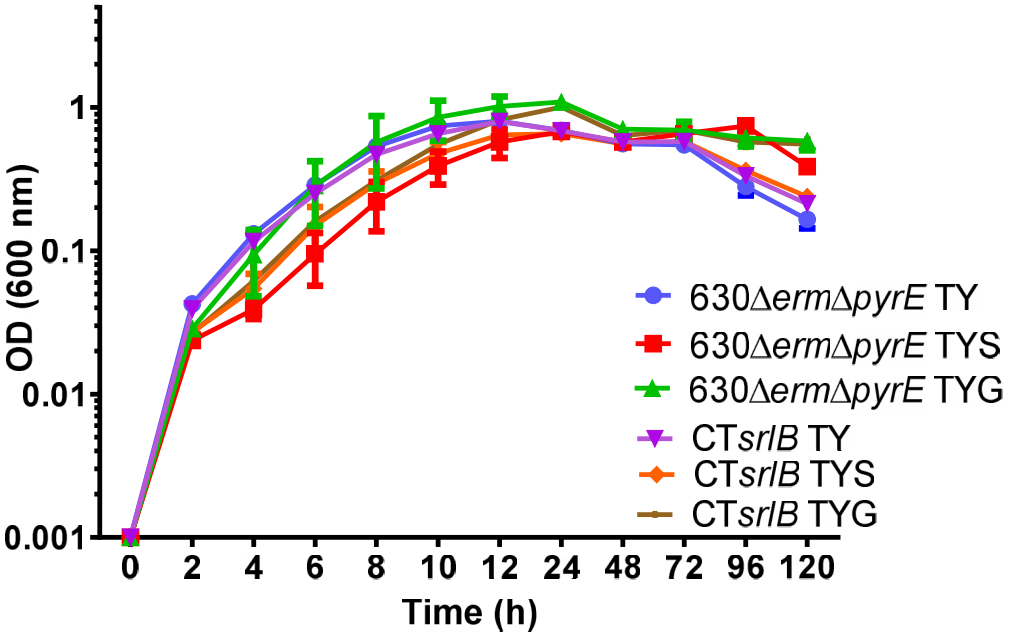

Figure 5.66: Role of *srlB* in *C. difficile* 630Δ*erm*Δ*pyrE* growth in TY.
630Δ*erm*Δ*pyrE* (parent) and CT*srlB* (mutant) were incubated for 120 h at 37°C. Decline of the mutant, CT*srlB*, in TYS from 24 h (mutant peak growth) onwards did not mimic the very gradual decline of the parent, 630Δ*erm*Δ*pyrE*, in TYS, indicating that sorbitol was not being utilised by the mutant.
Slope of curve 24-120 h in TYS (downward): 630Δ*erm*Δ*pyrE* = 0.75,
CT*srlB* = 1.07.
One-way ANOVA was used to determine statistical significance.
630Δ*erm*Δ*pyrE* in TY vs. in TYS at 96 h ** $P < 0.001$.
630Δ*erm*Δ*pyrE* in TYS vs. CT*srlB* in TYS at 96 h *** $P < 0.0002$.

5.5.1.5 Cytotoxicity of 630Δ*erm*Δ*pyrE* and 630Δ*erm*Δ*pyrE*_CT*srlB*

At 72 h, the parental strain showed an increase in toxicity in TYS compared to when in TY going from a toxin titre of 1.8 x 10^2 in TY to 1.5 x 10^3 in TYS (**** $P < 0.0001$) (Fig. 5.67).

The toxin levels of the mutant remained unchanged with a toxin titre of 1.7 x 10^2 in TY and 1.7 x 10^2 in TYS (Fig. 5.67).

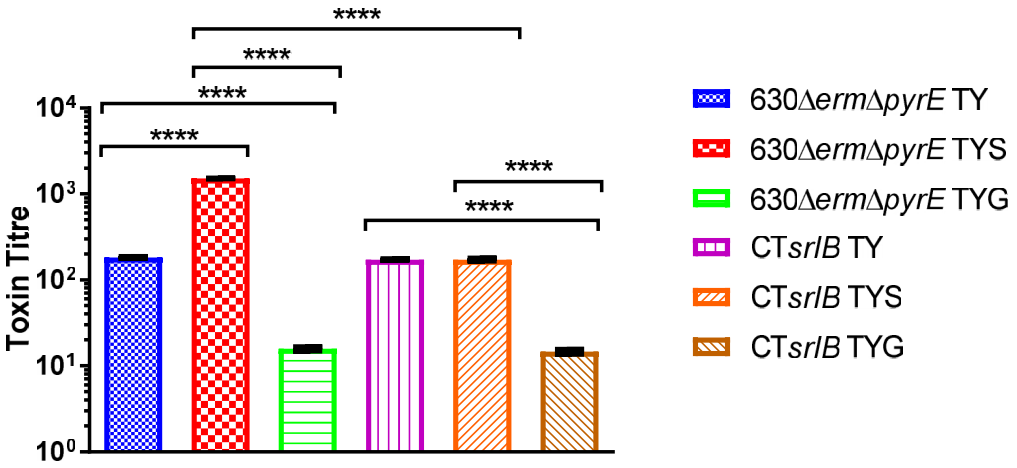

Figure 5.67: Role of *srlB* in *C. difficile* 630Δ*erm*Δ*pyrE* toxin production at 72 h in TY.

Cytotoxicity of CT*srlB* at 72 h. Serial dilutions (10^{0}-10^{-9}) of the bacterial supernatants (triplicates) were applied to Vero cell monolayers (p35) in order to determine the toxin titre of the parent (630Δ*erm*Δ*pyrE*) and the mutant (CT*srlB*). The parent produced significantly more toxin in TYS than in TY (**** $P < 0.0001$), which was not seen with the mutant.
One-way ANOVA was used to determine statistical significance.
630Δ*erm*Δ*pyrE* in TY vs. in TYS **** $P < 0.0001$.
630Δ*erm*Δ*pyrE* in TYS vs. CT*srlB* in TYS **** $P < 0.0001$.

At 96 h, the parental strain showed a trend towards toxin increase in TYS compared to when in TY, going from a toxin titre of 3.6 x 10^2 in TY (with minor variance) to 9.6 x 10^2 in TYS (with a lot of variance) (Fig. 5.68).

The toxin levels of the mutant remained almost unchanged with a toxin titre of 2.9 x 10^2 in TY and 2.7 x 10^2 in TYS (Fig. 5.68).

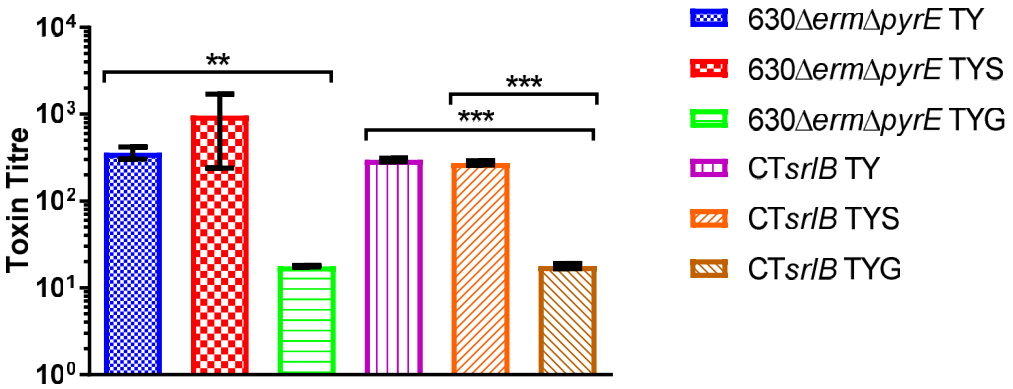

Figure 5.68: Role of *srlB* in *C. difficile* 630Δ*erm*Δ*pyrE* toxin production at 96 h in TY.

Cytotoxicity of CT*srlB* at 96 h. Serial dilutions (10^0-10^{-9}) of the bacterial supernatants (triplicates) were applied to Vero cell monolayers (p35) in order to determine the toxin titre of the parent and the mutant.

The parent, 630Δ*erm*Δ*pyrE*, exhibited a minor trend towards increasing toxin levels in TYS, which was not seen with the mutant.

One-way ANOVA was used to determine statistical significance.

At 120 h, the parental strain showed a trend towards toxin reduction in TYS compared to when in TY, going from toxin titre of 6.1 x 10^3 in TY (with minor variance) to 1.7 x 10^3 in TYS (with much variance) (** $P < 0.01$) (Fig. 5.69).

The toxin levels of the mutant remained unchanged with a toxin titre of 4696 x 10^3 in TY and in TYS (Fig. 5.69).

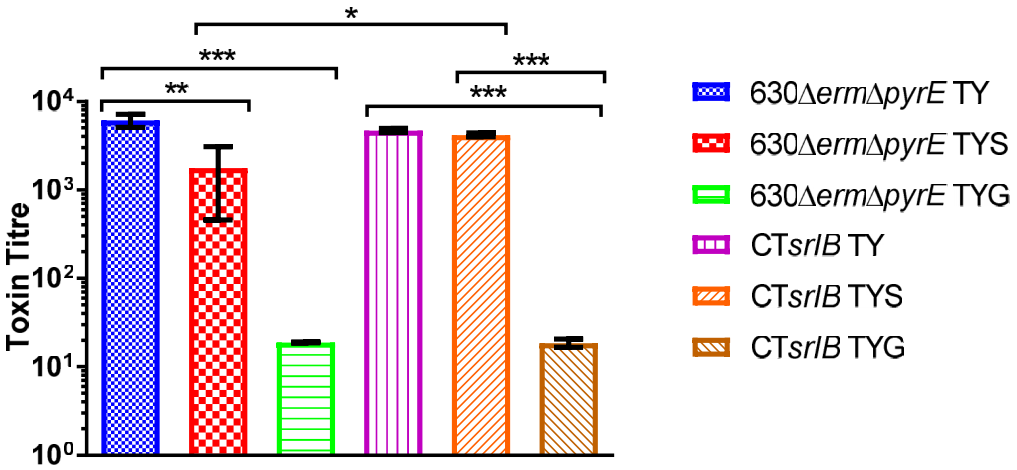

Figure 5.69: Role of *srlB* in *C. difficile* 630Δ*erm*Δ*pyrE* toxin production at 120 h in TY.

Cytotoxicity of CT*srlB* at 120 h. Serial dilutions (10^{0}-10^{-9}) of the bacterial supernatants (triplicates) were applied to Vero cell monolayers (p35) in order to determine the toxin titre of the parent and the mutant.

The parent, 630Δ*erm*Δ*pyrE*, significantly suppressed toxin levels in TYS (** $P < 0.01$). No changes in toxin levels were observed with the mutant, CT*srlB*, when comparing its cytotoxicity in TY and TYS.

One-way ANOVA was used to determine statistical significance.

630Δ*erm*Δ*pyrE* in TY vs. in TYS ** $P < 0.01$.

630Δ*erm*Δ*pyrE* in TYS vs. CT*srlB* in TYS * $P < 0.03$.

5.5.1.6 Motility assays

Motility was tested using four variant motility assays. The mutant was tested alongside 630Δ*erm*Δ*pyrE*, *C. difficile* 630Δ*erm*_CT*fliC*, and *C. difficile* M120.

5.5.1.6.1 Motility assays on YT +glucose

Motility assays on YTG revealed no differences between the parental strain (630Δ*erm*Δ*pyrE*) (0.8cm zone diameter) and the mutant (CT*srlB*) (0.8cm zone diameter) with a similar zone of motility seen with both strains. M120 was used as the negative control, and exhibited reduced motility (0.6cm zone diameter) in comparison to the parent and the mutant (Fig. 5.70).

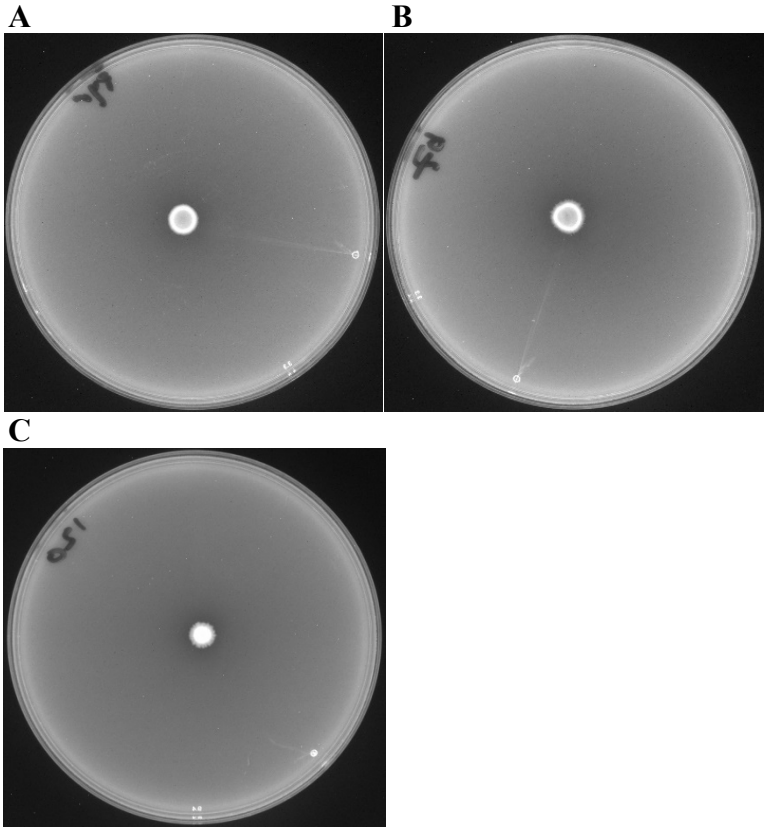

Figure 5.70: Representative images of motility assays showing parental strain (A), mutant (B), and negative control, M120 (C) on YTG.
2µL of overnight culture of each strain (in triplicates) was spotted onto plates of YTG agar containing 1% w/v glucose and incubated at 37°C for 48 h to see if it was possible to observe a difference in motility.
No differences in motility behaviour were observed. Similar zones of motility were observed with the parental strain (630Δ*erm*Δ*pyrE*) and the mutant (CT*srlB*).

5.5.1.6.2 Motility assays on YT +sorbitol

Motility assays on YTS agar revealed no differences between the parental strain (630Δ*erm*Δ*pyrE*) and the mutant (CT*srlB*) in terms of motility, but a larger zone of motility was seen with parent (1.3cm zone diameter) than was seen with the mutant (not shown), indicating that CT*srlB* was less efficiently utilising the sorbitol in the agar (not shown). CT*fliC* was used as the negative control, and exhibited reduced motility in comparison to the parent and the mutant (not shown).

5.5.1.6.3 Motility assays on BHIS +top agar

BHIS +top agar was used to determine potential differences in motility between 630Δ*ermΔpyrE* and CT*srlB*.

No differences were observed with similar motility on the plates observed with both strains (0.6cm zone diameter for both strains). CT*fliC* was used as the negative control, and exhibited reduced motility (0.5cm zone diameter) in comparison to 630Δ*ermΔpyrE* and CT*srlB* (Fig. 5.71).

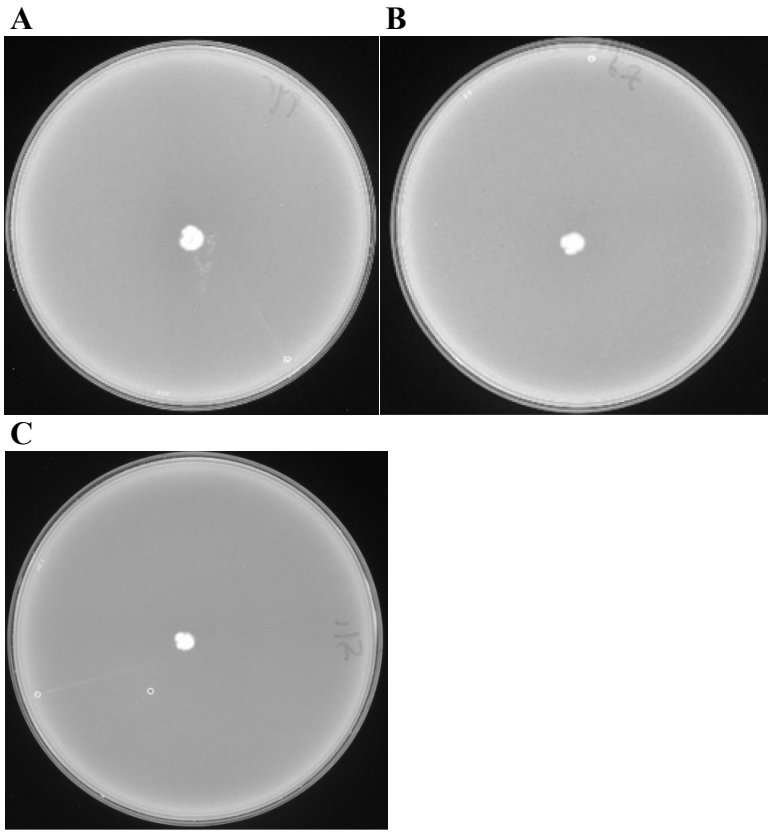

Figure 5.71: Representative images of motility assays on BHIS +top agar showing control strain (A), mutant (B), and negative control, CT*fliC* (C).
The surface of the top agar was pierced with a single colony of each strain (in triplicates) and incubated at 37°C for 48 h to see if it was possible to observe a difference in motility.
No differences were observed between the parental strain (630Δ*ermΔpyrE*) and the mutant (CT*srlB*) with the same degree of motility seen with both strains.

5.5.1.6.4 Motility assays in tubes

Agar which comprised the top layer in the BHIS +top agar motility assays was used in tubes to determine possible differences in motility between 630Δ*erm*Δ*pyrE* and CT*srlB*.

No differences were observed with both strains exhibiting robust turbidity and migrating (11cm) from the point of inoculation to the base of the tubes. *C. difficile* M120 was used as the negative control, showed growth at the very top of the tubes, but did not exhibit any turbidity nor migrate any distance through the agar (Fig. 5.72).



Figure 5.72: Representative images of motility assays showing migration of control strain (A) mutant (B) through the agar in the tubes. The negative control, M120 (C), did not migrate.
The surface of the agar was pierced using a sterile cocktail stick with a single colony of each strain (in triplicates) and incubated at 37°C for 24 h to see if it was possible to observe a difference in motility.
The control strain (630Δ*erm*Δ*pyrE*) and the mutant (CT*srlB*) both exhibited robustturbidity and migrated to the base of the tubes (11cm), while the negative control (M120) did not migrate any distance.

5.6 Investigation and Characterisation of PTS^{Srl} Phosphate Dehydrogenase -GutD

gutD (Fig. 5.73) was selected for deletion in order to investigate its role, and to determine whether it is truly the only gene apparently responsible for conversion of phosphorylated sorbitol to F-6-P. This was achieved by allele-coupled exchange (ACE) using the Δ*pyrE* system as described by Ng *et al.* 2013[117].

5.6.1 Characterisation of 630Δ*erm*Δ*pyrE*Δ*gutD* (CD630_0768)

Deletion of *gutD* (Fig. 5.73) was initially determined by screening colonies growing on MM plates +FOA with primers specific for the region immediately

outside of the LHA and RHA of *gutD* and running the PCR products on a 1% w/v agarose gel (Fig. 5.74). Predicted fragment sizes of the parent and the mutant revealed a Δ*gutD* strain (Table 5.6). Following this, the 1.7kb fragment (Δ*gutD*) was sequenced with the same primers, confirming deletion of *gutD* (data not shown).

To determine if the mutant, Δ*gutD*, exhibited any effects, of *gutD* being deleted, growth, sorbitol uptake, cytotoxicity, and motility assays were performed using the parent and the mutant.

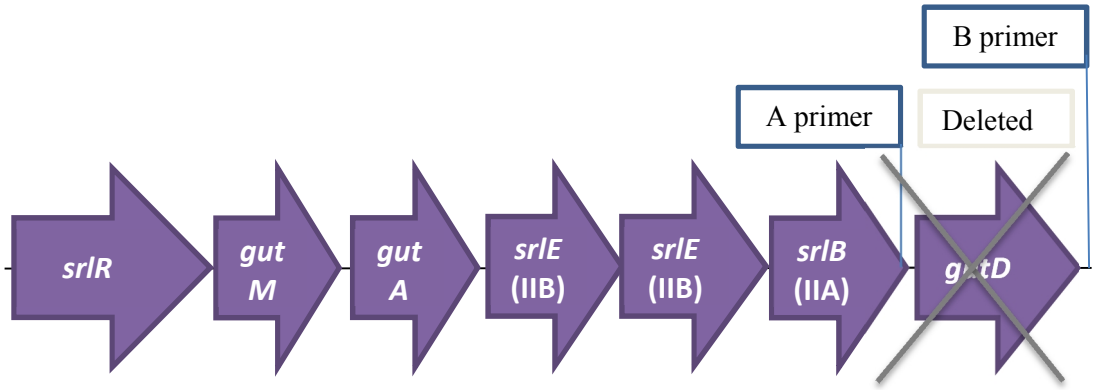

Figure 5.73: Primers for PCR screening for deletion of *gutD*.
Position, within the CD630_0762-8 sorbitol-specific operon, of the primers (A and B) designed for the regions immediately outside of the LHA and RHA of *gutD*, which were used to amplify DNA isolated from selected colonies growing on MM plates +FOA.

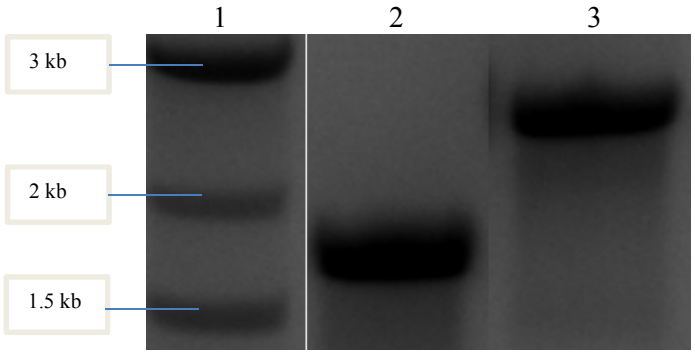

Figure 5.74: PCR screening for deletion of *gutD*.
Primers (A and B), specific for the regions immediately outside of the LHA and RHA, were used to amplify DNA isolated from selected colonies growing on MM plates +FOA (well 2); and also, DNA isolated from the parental strain, 630Δ*ermΔpyrE* (well 3). Table 5.6 below shows the lane order.

Table 5.6: Contents of each well when showing by PCR the deletion of *gutD*.

Well	Content	Size (kb)
1	Marker	
2	630Δ*ermΔpyrEΔgutD*	1.70 (2.47-0.77)
3	630Δ*ermΔpyrE*	2.47

5.6.1.1 Growth on DM Agar

Growing the parent (630Δ*ermΔpyrE*) and the mutant (Δ*gutD*) on DMS agar did not reveal differences in the ability to subsist on sorbitol on this type of medium. Strong growth was exhibited by both strains on DM (negative control -not shown) and DMS (Fig. 5.75).

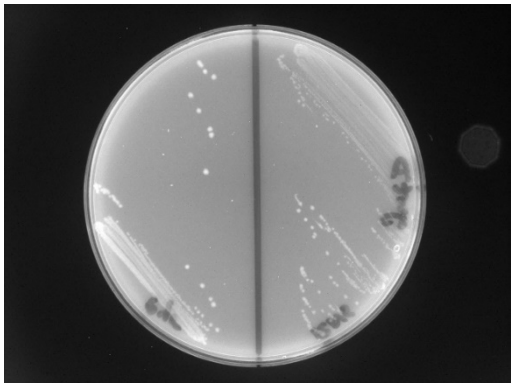

Figure 5.75: Representative image showing growth of 630Δ*ermΔpyrE* -parent (left) and Δ*gutD* -mutant (right) on DMS agar.
Strains (in triplicates) were streaked on plates of DMS agar containing 0.6% w/v sorbitol and incubated at 37°C for 16 h to see if it was possible to observe a growth phenotype.
Differences in the ability to metabolise sorbitol could not be determined by this assay as strong growth was exhibited by both strains on DM (not shown) and DMS agar.

5.6.1.2 Growth in DM, DMS, and DMG broth

The addition of sorbitol induced a significant increase in the growth of the parental strain, 630Δ*ermΔpyrE*, from 10 h. At peak growth in DM and DMS (24 h), OD_{600} without sorbitol was 0.57, while in sorbitol it was 0.84 (**** $P < 0.0001$). Slope of the curve in DMS 0-24 h = 1.2 (Fig. 5.76).

Growth of the mutant (Δ*gutD*) in sorbitol showed no increase above that of the mutant in DM alone. At 24 h, which was peak growth in DM and DMS, OD_{600} was 0.53 in DM, and in DMS was 0.49. Slope of the curve in DMS 0-24 h = 0.7 (Fig. 5.76).

630Δ*ermΔpyrE* vs. Δ*gutD* at 10 h *** $P < 0.0003$, at 24 h **** $P < 0.0001$.

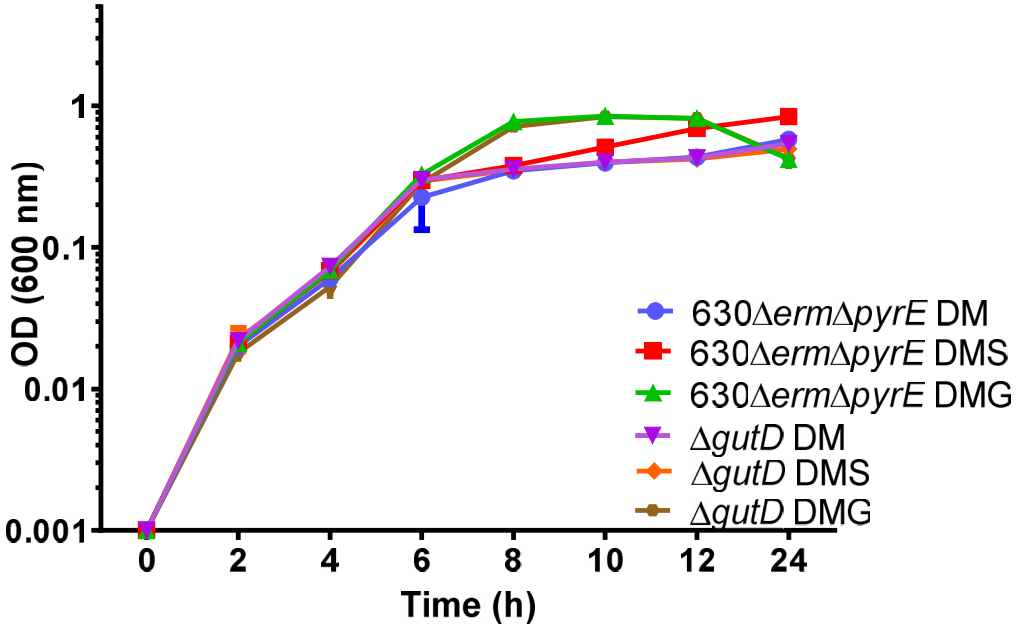

Figure 5.76: Role of *gutD* in *C difficile* 630Δ*erm*Δ*pyrE* growth in DM.
630Δ*erm*Δ*pyrE* (parent) and Δ*gutD* (mutant) were incubated for 24 h at 37°C. 1ml extracts (triplicates) were taken at regular time points and OD_{600} measured. Growth of Δ*gutD* in sorbitol from 10 h onwards was significantly less (*** $P < 0.0003$) than that of the parent, 630Δ*erm*Δ*pyrE*, in the same conditions. Growth of the mutant in DMS was the same as it was in DM.
630Δ*erm*Δ*pyrE* slope of the curve in DMS 0-24 h = 1.2.
Δ*gutD* slope of the curve in DMS 0-24 h = 0.7.
One-way ANOVA was used to determine statistical significance.
630Δ*erm*Δ*pyrE* at 24 h in DM vs. DMS **** $P < 0.0001$.
630Δ*erm*Δ*pyrE* vs. Δ*gutD* at 10 h *** $P < 0.0003$, at 24 h **** $P < 0.0001$.

5.6.1.3 HPLC evaluation of sorbitol/glucose in DM

Sorbitol consumption by 630Δ*erm*Δ*pyrE* (parental strain) was observed after 8 h of incubation, reaching a significant level of sugar uptake at 10 h (** $P < 0.0022$) with 4.6mM of the sugar remaining (from 8.41mM at 0 h). By 24 h, all of the available sorbitol had been spent. Slope of the curve 0-24 h = 1.2 (Fig. 5.77).

630Δ*erm*Δ*pyrE* 0 h vs. 10 h ** $P < 0.0022$.

There was no uptake of sorbitol by the mutant (Δ*gutD*). At 0 h, there was 7.8mM sorbitol in the Δ*gutD* samples. By 24 h, 9.04mM sorbitol was present. Slope of the curve 0-24 h = 0 (Fig. 5.77).

630Δ*ermΔpyrE* 10 h vs. Δ*gutD* 10 h *** P < 0.0003.

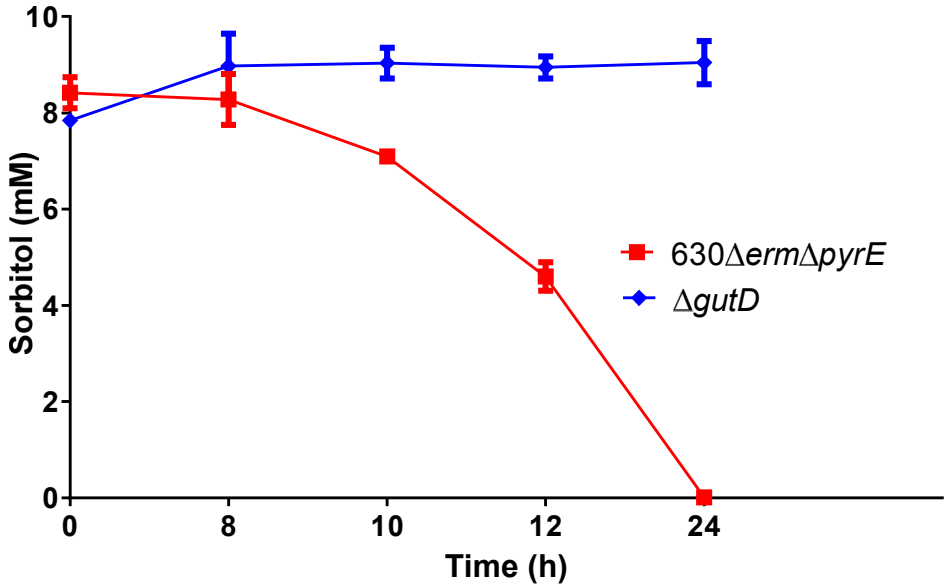

Figure 5.77: HPLC evaluation of sorbitol uptake in DM by 630Δ*ermΔpyrE* (parent) and Δ*gutD* (mutant).
Extracts (triplicates) from the growth assay in DM were used to determine by HPLC the exact amount of sugar remaining in the medium at each time point.
The parent utilised all of the available sorbitol, while the mutant sorbitol levels showed no decrease.
630Δ*ermΔpyrE* slope of the curve 0-24 h = 1.2.
Δ*gutD* slope of the curve 0-24 h = 0.
One-way ANOVA was used to determine statistical significance.
630Δ*ermΔpyrE* 0 h vs. 10 h ** P < 0.0022.
630Δ*ermΔpyrE* 10 h vs. Δ*gutD* 10 h *** P < 0.0003.

Glucose was consumed by 630Δ*ermΔpyrE* and Δ*gutD* between 0 h and 24 h with glucose levels dropping from 8.65mM and 8.66mM respectively at 0 h, to 0.27mM and 0.29mM respectively at 24 h (**** P < 0.0001) (Fig. 5.78).

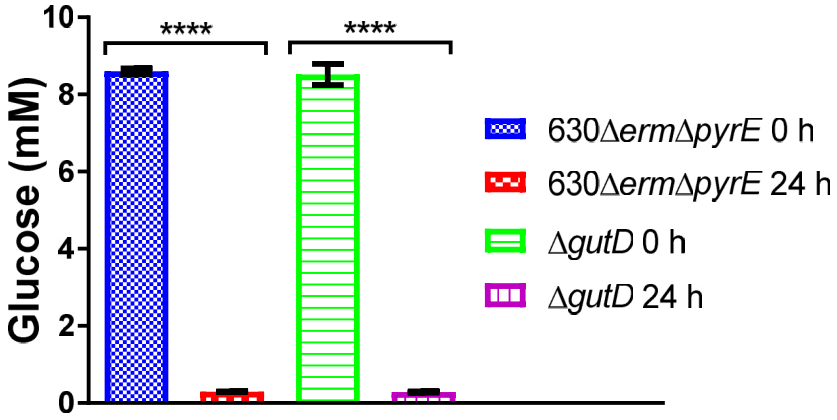

Figure 5.78 HPLC evaluation of glucose uptake in DM by 630Δ*erm*Δ*pyrE* (parent) and Δ*gutD* (mutant).
Extracts (triplicates) from the growth assay in DM were used to determine by HPLC the exact amount of the sugar remaining in the medium at both time points. The glucose in the parent and mutant medium was depleted by the 24 h time point (**** $P < 0.0001$).
One-way ANOVA was used to determine statistical significance.

5.6.1.4 Growth in TY, TYS, and TYG

Deletion of *gutD* inhibited the ability of the mutant (Δ*gutD*) to utilise sorbitol (Fig. 5.79). From 24 h, when the parent appeared to start making use of the sorbitol in the medium, the OD_{600} level of the mutant in TYS declined (OD_{600} 0.69), while the OD_{600} level (OD_{600} 0.74) of the parent in TYS remained steady (*** $P < 0.0005$) (Fig. 5.79).

At 72 h, when the greatest difference in OD_{600} value between the parent in TY (OD_{600} 0.21) and TYS (OD_{600} 0.69) were observed (**** $P < 0.0001$), growth levels of Δ*gutD* showed an OD_{600} of 0.3 and 0.31 in TY and TYS respectively (no significant difference). Parent vs. mutant OD_{600} in TYS at this time point (72 h) differed significantly (**** $P < 0.0001$) (Fig. 5.79).

At the later time points of 96 and 120 h, decline of the parent in TYS was much less (OD_{600} 0.3 and 0.29 at 96 h and 120 h respectively) than that of the mutant

(OD_{600} 0.17 and 0.16 at 96 h and 120 h respectively), indicating much reduced or no sorbitol uptake by the mutant (24-120 h in TYS slope (downward): 630Δ*ermΔpyrE* = 0.9; Δ*gutD* = 1.06) (Fig. 5.79).

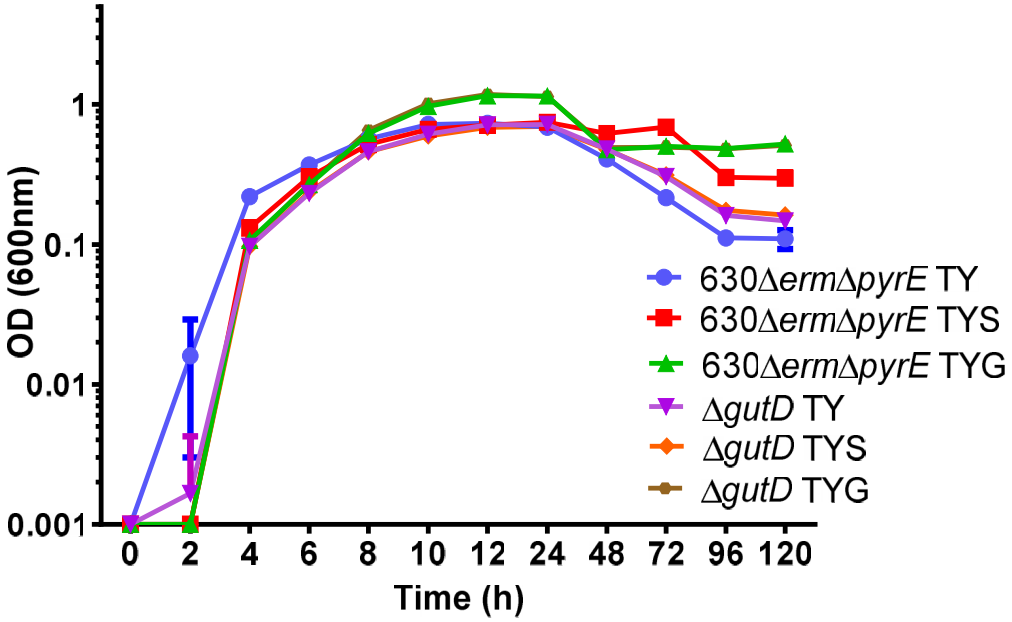

Figure 5.79: Role of *gutD* in *C. difficile* 630Δ*ermΔpyrE* growth in TY.
630Δ*ermΔpyrE* (parent) and Δ*gutD* (mutant) were incubated for 120 h at 37°C. 1mL extracts were taken a regular time points and the OD_{600} measured.
Unlike the parent in TYS (which showed a much more gradual decline), Δ*gutD* in TYS exhibited a decline which was comparable to the samples in plain TY.
Slope (downward) 24-120 h in TYS: 630Δ*ermΔpyrE* = 0.9; Δ*gutD* = 1.06.
One-way ANOVA was used to determine statistical significance.
630Δ*ermΔpyrE* in TY vs. in TYS at 24 h *** $P < 0.0005$, at 72 h **** $P < 0.0001$.
630Δ*ermΔpyrE* vs. Δ*gutD* in TYS at 72 h **** $P < 0.0001$.

5.6.1.5 Cytotoxicity of 630Δ*ermΔpyrE* and 630Δ*ermΔpyrEΔgutD.*

At 72 h, the parent, 630Δ*ermΔpyrE*, toxin levels were suppressed going from 4.6 x 10^5 in TY to 1.4 x 10^5 in TYS (*** $P < 0.0002$); while no change in toxin levels was observed with the mutant, Δ*gutD*, with toxin levels almost remaining at 3.2 x 10^5 in TY and 3.1 x 10^5 in TYS. In TY, the parent also produced significantly

more toxin than the mutant in TY (*** P < 0.001); but, the mutant produced more toxin in TYS **** P < 0.0001) (Fig. 5.80).

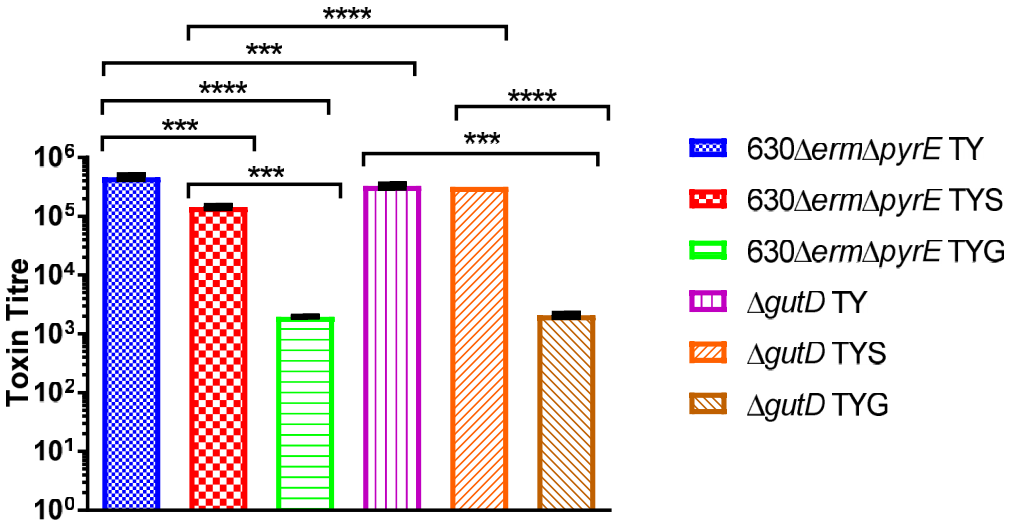

Figure 5.80: Role of *gutD* in *C. difficile* 630Δ*erm*Δ*pyrE* toxin production at 72 h in TY.
Cytotoxicity of Δ*gutD* at 72 h. Serial dilutions (10^{0}-10^{-9}) of the bacterial supernatants (triplicates) were applied to Vero cell monolayers (p32) in order to determine the toxin titre of the parent and the mutant.
The parent, 630Δ*erm*Δ*pyrE*, significantly suppressed toxin levels in TYS (*** P < 0.002). No differences in toxin levels were observed with the mutant, Δ*gutD*, when comparing cytotoxicity in TY and TYS.
One-way ANOVA was used to determine statistical significance.
630Δ*erm*Δ*pyrE* in TY vs. in TYS *** P < 0.0002.
630Δ*erm*Δ*pyrE* vs. Δ*gutD* in TY *** P < 0.0001.
630Δ*erm*Δ*pyrE* vs. Δ*gutD* in TYS **** P < 0.0001.

Cytotoxicity of the parental strain at 96 h showed an increase in sorbitol, going from 9.0 x 10^5 in TY to 3.3 x 10^6 in TYS (**** P < 0.0001) (Fig. 5.81).

Mutant cytotoxicity [which was substantially lower than the parent in TY (** P < 0.005) and TYS (**** P < 0.0001)] stayed almost the same in TY and TYS at 6.2 x 10^5 and 5.7 x 10^5 respectively (Fig. 5.81).

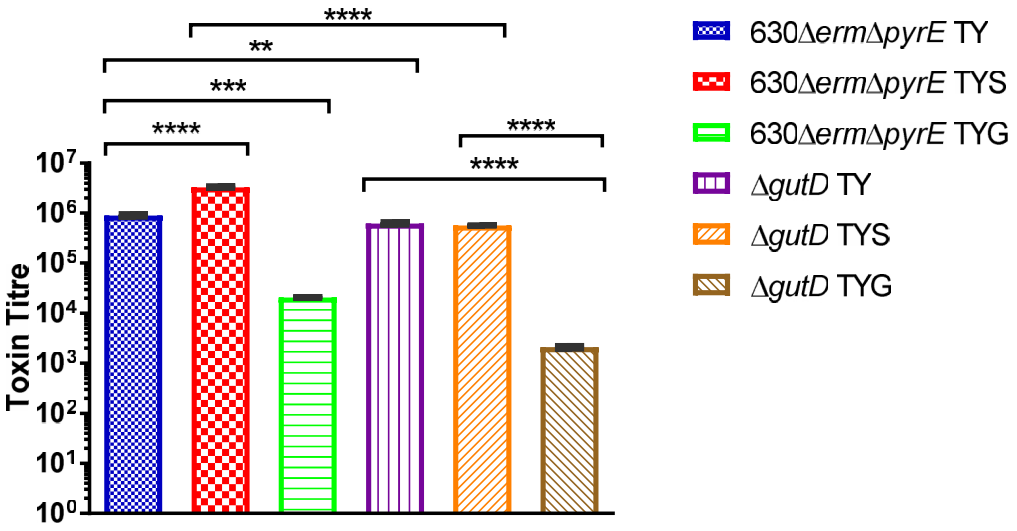

Figure 5.81: Role of *gutD* in *C. difficile* 630Δ*erm*Δ*pyrE* toxin production at 96 h in TY.

Cytotoxicity of Δ*gutD* at 96 h. Serial dilutions (10^{0}-10^{-9}) of the bacterial supernatants (triplicates) were applied to Vero cell monolayers (p32) in order to determine the toxin titre of the parent and the mutant.

The parent, 630Δ*erm*Δ*pyrE*, significantly increased toxin levels in TYS (**** $P < 0.0001$). No differences in toxin levels were observed with the mutant, Δ*gutD*, when comparing cytotoxicity in TY and TYS.

One-way ANOVA was used to determine statistical significance.

630Δ*erm*Δ*pyrE* in TY vs. in TYS **** $P < 0.0001$.

630Δ*erm*Δ*pyrE* vs. Δ*gutD* in TY ** $P < 0.005$.

630Δ*erm*Δ*pyrE* vs. Δ*gutD* in TYS **** $P < 0.0001$.

At 120 h (Fig. 5.82), there was a significant increase in toxin release by the parental strain in sorbitol, going from a toxin titre of 9.3 x 10^5 in TY to 3.3 x 10^6 in TYS (**** $P < 0.0001$) (Fig. 5.82).

Mutant toxin levels were much lower than the parent (in TY **** $P < 0.0001$; in TYS **** $P < 0.0001$) with toxin levels the almost the same in TY and TYS at 6.8 x 10^4 and 6.1 x 10^4 respectively (Fig. 5.82).

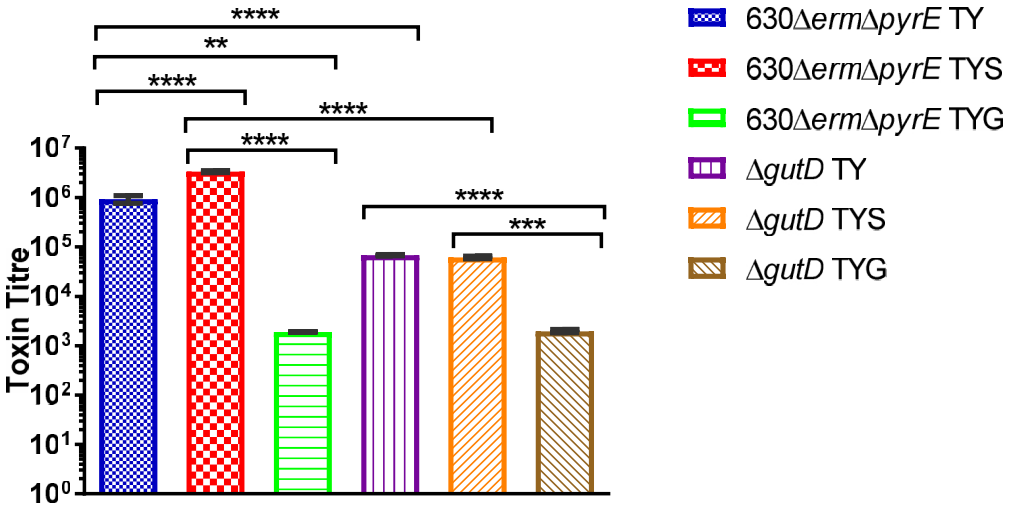

Figure 5.82: Role of *gutD* in *C. difficile* 630Δ*erm*Δ*pyrE* toxin production at 120 h in TY.

Cytotoxicity of Δ*gutD* at 120 h Serial dilutions (10^0-10^{-9}) of the bacterial supernatants (triplicates) were applied to Vero cell monolayers (p32) in order to determine the toxin titre of the parent and the mutant.

The parent, 630Δ*erm*Δ*pyrE*, significantly increased toxin levels in TYS (**** $P < 0.0001$). No changes in toxin levels were observed with the mutant, Δ*gutD*, when comparing its cytotoxicity in TY and TYS.

One-way ANOVA was used to determine statistical significance.

630Δ*erm*Δ*pyrE* in TY vs. in TYS **** $P < 0.0001$.

630Δ*erm*Δ*pyrE* vs. Δ*gutD* in TY **** $P < 0.0001$.

630Δ*erm*Δ*pyrE* vs. Δ*gutD* in TYS **** $P < 0.0001$.

5.6.1.6 Motility assays

Motility was tested using four variant motility assays. The mutant was tested alongside 630Δ*erm*Δ*pyrE*, *C. difficile* 630Δ*erm*_CT*fliC*, and *C. difficile* M120.

5.6.1.6.1 Motility assays on YT +glucose

Motility assays on YTG revealed no major differences between the parental strain (630Δ*erm*Δ*pyrE*) (0.8cm zone diameter) and the mutant (Δ*gutD*) (0.9cm diameter) with a similar zone of motility seen with both strains. M120 was used the negative control, and exhibited reduced motility (0.6cm zone diameter) in comparison to the parent and the mutant (Fig. 5.83).

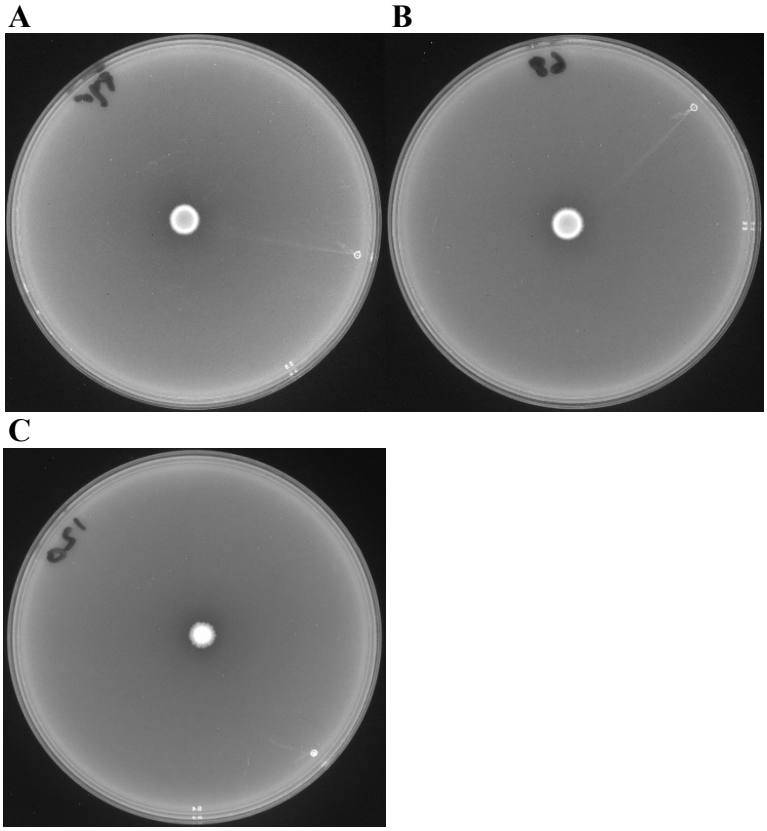

Figure 5.83: Representative images of motility assays showing parental strain (A), mutant (B), and negative control, M120 (C), on YTG.
2µL of overnight culture of each strain (in triplicates) was spotted onto plates of YTG agar containing 1% w/v glucose and incubated at 37°C for 48 h to see if it was possible to observe a difference in motility.
No differences in motility behaviour could be observed. Similar motility was observed with the parental strain (630Δ*erm*Δ*pyrE*) and the mutant (Δ*gutD*).

5.6.1.6.2 Motility assays on YT +sorbitol

Motility assays on YTS agar revealed a divergence between the parental strain (630Δ*erm*Δ*pyrE*) and the mutant (Δ*gutD*) in terms of the size of the zones of motility by each strain. A slightly larger zone was seen with the parent (1.3cm zone diameter) than what was seen with the mutant (1.2cm zone diameter), indicating that Δ*gutD* was less efficiently utilising the sorbitol in the agar. CT*fliC* was used as the negative control, and exhibited reduced motility (0.9cm zone diameter) in comparison to the parent and the mutant (Fig. 5.84).

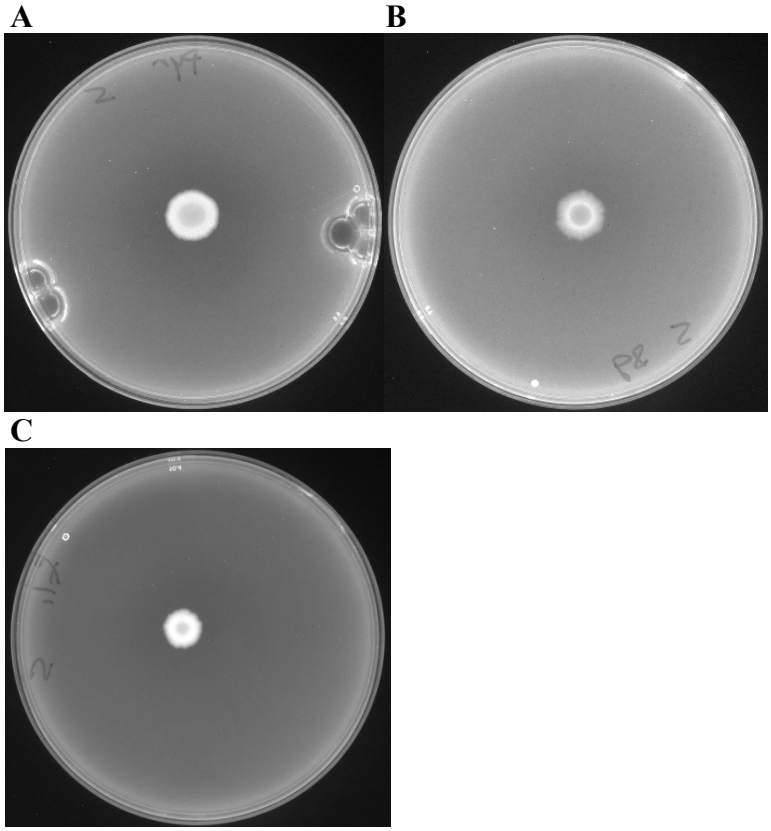

Figure 5.84: Representative images of motility assays showing parental strain (A), mutant (B), and negative control, CT*fliC* (C) on YTS.
2µL of overnight culture of each strain (in triplicates) was spotted onto plates of YTS agar containing 1% w/v sorbitol and incubated at 37°C for 48 h to see if it was possible to observe a difference in motility.
Great motility was observed on the plates with the parental strain (630Δ*erm*Δ*pyrE*). Reduced zones of motility were observed with the mutant (Δ*gutD*).

5.6.1.6.3 Motility assays on BHIS +top agar

BHIS +top agar was used to determine possible differences in motility between 630Δ*erm*Δ*pyrE* and Δ*gutD*.

No major differences were observed with both strains exhibiting similar motility, although the mutant exhibited a slightly reduced zone of motility (0.6cm zone diameter) in comparison to the parent (0.7cm zone diameter). CT*fliC* was used as the negative control, and exhibited reduced motility (0.5cm zone diameter) in comparison to 630Δ*erm*Δ*pyrE* and Δ*gutD* (Fig. 5.85).

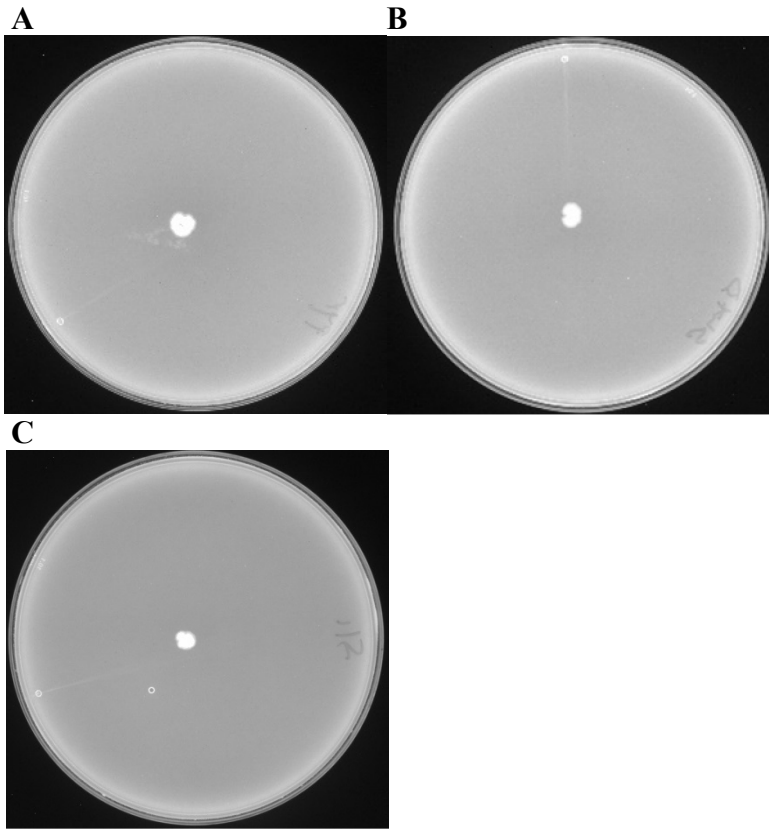

Figure 5.85: Representative images showing motility assays on BHIS +top agar showing control strain (A), mutant (B), and negative control, CT*fliC* (C).
The surface of the top agar was pierced with a single colony of each strain (in triplicates) and incubated at 37°C for 48 h to see if it was possible to observe a difference in motility.
No major differences were observed between the parental strain (630Δ*erm*Δ*pyrE*) and the mutant (Δ*gutD*) with similar motility seen with both strains.

5.6.1.6.4 Motility assays in tubes

Agar which comprised the top layer in the BHIS +top agar motility assays was used in tubes to determine potential differences in motility between 630Δ*erm*Δ*pyrE* and Δ*gutD*.

No differences were observed with both strains exhibiting robust turbidity and migrating (11cm) from the point of inoculation to the base of the tubes. *C. difficile* M120 was used as the negative control, showed growth at the very top of

the tubes, but did not exhibit any turbidity nor migrate any distance through the agar (Fig. 5.86).

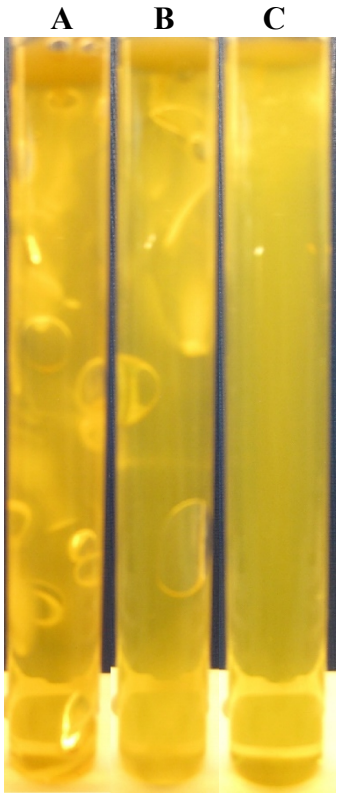

Figure 5.86: Representative images of motility assays showing migration of control strain (A), mutant (B) through the agar in the tubes. The negative control, M120 (C), did not migrate.
The surface of the agar was pierced using a sterile cocktail stick to inoculate the medium with a single colony of each strain (in triplicates) and incubated at 37°C for 24 h to see if it was possible to observe a difference in motility. The control strain (630Δ*erm*Δ*pyrE*) and the mutant (Δ*gutD*) both exhibited robust turbidity and migrated to the base of the tubes (11cm), while the negative control (M120) did not migrate any distance.

5.7 Discussion

The genome of *C. difficile* 630 encodes two potential sorbitol-specific PTS (Artemis), and has been shown to be capable of fermenting sorbitol as a sole carbonhydrate source (Fig. 3.1). The putative PTS^{Srl} at loci CD630_0762-8 was speculated to be the primary sorbitol PTS, mainly due to the presence of an

apparent SPDH in the operon, and so, its constituent genes were targeted for inactivation and deletion.

630Δ*ermΔpyrE* growth, in general, lagged behind that of 630WT. This was consistently seen in defined as well as in enriched conditions (Fig. 5.7 & 5.10). This is further supported by the HPLC results which showed a slightly more rapid rate of sorbitol uptake by the WT (Fig. 5.8). Growth of the parental strain reached the levels of the WT, but slightly later. As mentioned, *pyrE* has been deleted from the parental strain, so it is possible that the removal of *pyrE* is exerting an additional effect (although not an extreme one) not solely related to uracil production. Another possible reason may be that over the course of time successive manipulation of *C. difficile* 630 (from 630WT to 630Δ*erm* to 630Δ*ermΔpyrE*) has led to an accumulation of a large amount of single nucleotide polymorphisms (SNPs) which are cumulatively responsible for the differences in growth rates, especially in enriched conditions, and the consequent effect on toxin production (630WT producing more toxin earlier than 630Δ*ermΔpyrE*).

The TY assay also revealed that with 630WT, when testing in enriched conditions, the presence of sorbitol at the early stages of the assay (up to 24 h) induced a lower level of growth than was seen than without sorbitol. This was only observed with 630WT, and can possibly be only attributable to the genetic differences between the two strains (Δ*pyrE* and SNPs)[130].

From 96 h to 120 h, overall toxin levels of 630Δ*ermΔpyrE* were above those of 630WT. Unlike 630WT at any the time point, at 96 h, 630Δ*ermΔpyrE* up-regulated toxin synthesis in sorbitol (Fig. 5.11-5.12). Both strains suppressed toxin in TYG.

CT mutagenesis of *gutA* prevented uptake of sorbitol by the mutant. CT*gutA* growth in defined medium up to 24 h, unlike the parental strain, exhibited no increase in OD_{600} in the presence of sorbitol (Fig. 5.20). Reflecting this, the HPLC results obtained using the supernatants taken during the assays in defined medium, showed that the mutant was totally unable to utilise any of the available sorbitol (Fig. 5.21). Also, mutant zones of motility on YTS plates were noticeably reduced in comparison to the parent (Fig. 5.28).

The presence of sorbitol in TY media allowed the parental strain to maintain levels of growth above that of the bacteria in plain TY indicating usage of sorbitol (Fig. 5.23). It has been consistently observed in enriched conditions that when cultured in the presence of sorbitol *C. difficile* will not grow rapidly in the early stages of the growth assay (up to 12 h) as seen when in glucose, and mannitol. But, that sorbitol in the medium will allow the bacterial growth to remain steady from 24 h, or decline at a much reduced rate than when there is no sorbitol present, as seen, for example, in TY medium. This appears to be a clear example of CCR, where up to 24 h there are other carbon sources contained in the medium such as tryptose, which are being preferentially utilised instead of sorbitol, but, as these are spent, usually between 12-24 h, the bacteria will then make use of the available sorbitol. Sorbitol is considered a secondary carbon source[22]. Studies have found that the genes of the PTS^{Srl} at loci CD630_0764-8, although repressed by the presence of glucose, are not under the control of CcpA[22]. In *C. beirinkijii*, *gut* genes are expressed only when glucose (if present in the media) has been depleted[122].

In enriched medium, the presence of sorbitol exerted an effect after 24 h on the OD_{600} levels of the parent with an increase in TYS compared to when in TY. Peak

growth of the parent had occurred by 24 h of incubation in TY (0.95) and TYS (0.94). However, at 48 h, OD_{600} was noticeably higher in TYS as the presence of sorbitol induced a slower decline than was seen in TY (Fig. 5.23). This was not seen with the mutant, CT*gutA*, as OD_{600} levels declined at the same level and rate in TY and TYS, indicating that mutant is not making use of the sugar in enriched medium (Fig. 5.23).

Relatedly, at 72 h, the cytotoxicity of the parental strain showed a strong up-regulation in TYS compared to its cytotoxicity when in TY alone. Toxin levels increased very significantly in TYS. Such an increase was not observed with the mutant as similar toxin levels were seen in both TY and TYS (Fig. 5.24). At 96 h, there was a slight reduction in toxin production by the parental strain in TYS (not significant) compared to when in TY. This was not observed with the mutant as the toxin titre remained unchanged in TY and TYS (Fig. 5.25). Similarly, at 120 h, toxin levels of the parental strain again dropped slightly in TYS, a change which was not observed with CT*gutA*, as toxin levels again stayed the same in TY and TYS (Fig. 5.26).

The results, showing sorbitol uptake by the parental strain and indicating a change seen in toxin levels when sorbitol is present in the medium, establish a link between sorbitol and the alteration of toxin production (whether up or down). Since sorbitol was not being utilised by the mutant as evidenced by the growth curves and HPLC results, the effects on toxin production were, as a consequence, not observed.

gutA hypothetically encodes an IIC, which would mean that it's role is designated as sensing sorbitol and facilitating the passage of the sugar across the bacterial

cell membrane, which would then allow the sugar to be phosphorylated by the IIB domain of the PTS, assumedly SrlE. Inactivating *gutA* most likely prevents the available sugar (in this case sorbitol) in the medium from being detected by the organism, as this is a role IICs are also known to play[101,102,105]. CT inactivation of *gutA* appears to have not resulted in a change in motility of the organism (Fig. 5.27-5.30) (see further discussion below).

CT inactivation of *srlE_N*, the N-terminus of the putative IIB^{Srl} at locus CD630_0765, rendered the mutant incapable of fermenting sorbitol (Fig. 5.35). In defined conditions, CT*srlE_N* in sorbitol exhibited none of the increases observed by the parent in the same conditions from 10-24 h. The mutant behaved as if it was completely unable to metabolise sorbitol (Fig. 5.35). This was also seen in the HPLC results, which were obtained from analysing the same samples of cultures from the same assay in defined medium to determine the exact level of sugar uptake, as sorbitol concentrations were rapidly depleted between 8 h and 24 h in the parent samples, but remained almost unchanged in those of the mutant (Fig. 5.36). Additionally, mutant growth on YTS plates was reduced in comparison to the parent on YTS (Fig. 5.43).

In enriched broth, the presence of sorbitol in the medium permitted the parental strain to decline at a more gradual rate than when it was in plain TY, indicating uptake of sorbitol. Mutant growth in sorbitol, from 24 h until the final time point at 120 h, declined in the same way as the parent and the mutant in TY alone, indicating that the sorbitol could not be used (Fig. 5.38).

It was hypothesised that inactivation of the IIB component of the PTS would inhibit sorbitol utilisation by preventing the phosphorylation of the incoming

sorbitol molecule. With the IIB no longer functional, it was to be assumed that the IIA component of the system would remain phosphorylated, potentially resulting in an accumulation of phosphate in the IIA domain (SrlB).

Cytotoxicity of the organism in sorbitol does not follow the same clear, consistent, repressive pattern, as seen with fermentable primary sugars like glucose and mannitol[28]. In the assays testing the cytotoxicity of CT*srlE_N*, toxin levels for the parental strain at 72-120 h showed an increase in sorbitol, which is a direct contrast to what is commonly observed with a fermentable sugar[28]. Mutant toxin levels did not exhibit this increase at all. Mutant toxin levels were significantly below those of the parent in sorbitol indicating that the increase in toxin levels induced by the presence of sorbitol is not occurring with the mutant (Fig. 5.39-5.41). This seems to be connected to the mutant's inability to ferment sorbitol. As it is known that toxin repression, when a fermentable carbon source is being utilised, occurs via the regulator, CcpA[23], it would be assumed that this protein would perhaps have a role in inducing the increase in toxin levels seen in TYS. However, *srlE* has been demonstrated as not being under the control of CcpA[22,23], so CcpA cannot be involved in regulating the increase in toxin levels seen when in sorbitol.

CT inactivation of *srlE_N* did not result in a change in motility of the organism (Fig. 5.42-5.45) (see further discussion below).

CT mutagenesis of *srlE_C*, the C-terminus of the putative IIB^{Srl} at locus CD630_0766, rendered the mutant incapable of utilising sorbitol. As observed with CT*srlE_N* in defined conditions, CT *srlE_C* also failed to utilise the available sorbitol (Fig. 5.49). Indeed, CT *srlE_C* was wholly unable to make use

of any of the sorbitol, which was proved by the HPLC results (Fig. 5.50). On YTS, CT *srlE_C* growth was much reduced in comparison to the parent on the same medium (Fig. 5.57).

Like CT*srlE_N*, from 24 h, CT*srl_C* in TYS exhibited a much steeper decline in OD_{600} than the parent in TYS (Fig. 5.52). This decline mirrored that of the parent and mutant in TY alone. In contrast to the parent samples used during the CT*srlE_N* growth assay, in this assay there was no significant increase in parent toxin levels in sorbitol. Nevertheless, at each time point there was a trend towards a minor increase in toxin release by the parent. This was not seen with the mutant, with toxin release staying the same in TY and TYS (Fig. 5.53-5.55). At 96 h, there was significantly more toxin being produced by the mutant in TY and TYS compared to the parent in those same conditions (Fig 5.54).

CT inactivation of *srlE_C* appeared not to have resulted in a change in motility of the organism (Fig. 5.56-5.59) (see further discussion below).

The results indicate that SrlE is a probable site of sorbitol phosphorylation in *C. difficile*, and that it is the primary IIB responsible for phosphorylation of sorbitol, and not the second putative sorbitol-specific IIB encoded at locus CD630_2417. That is not to rule out a role for CD_2417, say, as an auxiliary IIB to SrlE, or to work in tandem with SrlE. CD_2417 shows a large degree of homology to SrlE (55% identity), so it is very possible that it has a role sorbitol uptake. But, the very clear phenotype achieved by targeting *srlE* for knock-out would indicate that SrlE encoded within the operon at loci CD630_0762-8 is the main site of IIB phosphorylation of incoming sorbitol, and imperative to sorbitol uptake and utilisation. Due to the nature of the CT, it is possible that the phenotype exhibited

by CT*srlE* is the result of a 'polar effect'. This is when the CT insertion has an effect on a neighbouring transcript in the operon (due to a read-through from the *ermB* promoter or the CT blocking access to a common promoter used by genes in the operon), perhaps producing a phenotypic difference which is resulting from the different gene in the operon being inactivated instead of the desired one[40,140,141]. Notwithstanding this, it can be stated with confidence that targeting this operon has prevented growth in sorbitol and that this operon is indispensable in the phosphorylation and use of sorbitol.

The differences (significant and small), in cytotoxicity observed between parent and the *srlE* mutants, would appear not to be due to an effect exerted by a regulatory gene involved in toxin modulation like *ccpA*, due to the toxin suppressor (when in the presence of a fermentable sugar), CcpA, not controlling any of IIA, IIB, IIC genes of PTS^{Srl} at 0764-8[22]. It seems more likely that the differences observed are stress effects arising from the organism having to rely on a less preferred secondary sugar as a carbon source, and so, producing more toxin. *C difficile* increases toxin production in response to environmental stresses such as exposure to sub-minimum inhibitory concentrations (MIC) of antibiotics[133], and prolonged subsistence on sorbitol may, therefore, cause the organism to produce more toxin.

Targeting the putative IIA domain of the operon, SrlB, also prevented increased growth in sorbitol. CT*srlB* exhibited, in defined medium, a very clear lack of sorbitol-induced increase in growth that was seen with the parent (Fig. 5.63). HPLC analysis of samples taken from this assay supported this, showing a steady decline of parental sorbitol concentrations, while the mutant's sugar levels remained unchanged overall (Fig. 5.64). On plates of YTS, CT*srlB* exhibited

much less motility in comparison to 630Δ*erm*Δ*pyrE* on the same medium (Fig. 5.70).

In enriched broth, CT*srlB* OD_{600} levels in TYS declined to similar readings and at a similar rate as CT*srlB* in TY alone. From 48 h onwards, when it appeared that the sugar was starting to be used by the parent, 630Δ*erm*Δ*pyrE*, leading to a significant disparity between parent OD_{600} levels in TY and TYS at 96 h, CT*srlB* OD_{600} levels were virtually the same from 24-120 h (Fig. 5.66). The toxicity of the mutant showed no change in TYS, unlike the parent, which up-regulated and down-regulated toxin levels at 72 h and 120 h respectively (Fig. 5.67-9).

The results in this chapter (in combination with the bioinformatics results from Chapter 3) indicate that SrlB is the primary sorbitol IIA of *C. difficile* 630, and it is likely to be the protein which is phosphorylating the IIB^{Srl}. This could result in phosphoryl build-up in HPr as without a functioning IIA domain to receive and to later donate the phosphate group[101,102,105], it is to be assumed it will accumulate in HPr.

CT inactivation of *srlB* did not result in a change in the motility of the organism (Fig. 5.70-5.72) (see further discussion below).

gutD, the SPDH, was successfully deleted from *C. difficile* 630Δ*erm*Δ*pyrE* using ACE (Fig. 5.74). The mutant, Δ*gutD*, failed to utilise sorbitol in defined and enriched conditions (Fig. 5.76 & 5.79). As mentioned, Δ*gutD* growth in DMS was similar to that of Δ*gutD* (and the parent) in DM alone, a complete contrast to the growth of the parent in DMS, indicating a total inability to utilise the sugar under tight, defined conditions (Fig. 5.76). This was confirmed by the HPLC results which showed absolutely no uptake of the sugar (Fig. 5.77). Also, Δ*gutD* growth

on plates of YTS exhibited noticeably reduced motility in comparison to 630Δ*ermΔpyrE* on the same medium (Fig. 5.84).

Correspondingly, in TY, growth of the mutant in sorbitol mimicked that of the parent and mutant in TY alone with the OD_{600} of these cultures declining at a similar rate, in contrast to the parental samples in sorbitol which experienced a far more gradual decline in OD_{600} (for example, OD_{600} level of the parent in TYS at 24 h was 0.74, at 72 h it was 0.69; while the mutant was 0.69 at 24 h and 0.31 at 72 h), thus indicating a lack of sorbitol utilisation by the mutant (Fig. 5.79). With the cytotoxicity assays, the parent had significantly suppressed toxin levels in TYS at 72 h (Fig. 5.80), and significantly increased toxin levels in TYS at 96 h (Fig. 5.81) and 120 h (Fig. 5.82); while mutant toxin levels in TYS did not increase or decrease in TYS. Perhaps the increase in toxin levels at 96 h and 120 h is connected to the parent experiencing a steep decline in OD_{600} at these time points (and also, sorbitol uptake), whereas at 72 h, a decrease in toxicity does correspond with the bacteria maintaining a steady OD_{600} in TYS. Again, it would seem likely that such an increase in toxicity (which is not seen with the mutant) may be merely due to a stress effect[133] of the organism having to rely upon a less preferred sugar such as sorbitol (see further discussion below).

Deletion of *gutD* seems not to have resulted in a change in the motility of the organism (Fig. 5.83-5.86) (see further discussion below).

The deletion of the SPDH, *gutD*, resulted in a complete inability of the mutant to utilise sorbitol. The mutant behaved as if there was no sorbitol in the medium (Fig. 5.76-5.77, 5.79, & 5.84). Deletion of *gutD* would assumedly leave IIA, IIB, and IIC intact to sense, transport, and phosphorylate sorbitol, but no SPDH to

subsequently oxidise S-6-P to F-6-P. It can be assumed that the IIB domain would have phosphorylated the incoming sugar, and that since S-1-P is not being converted, that there must be a build-up of phosphorylated sorbitol in the cells.

The presence of sorbitol always (18 times) induced a change in the toxin levels of the parental strain, 630Δ*erm*Δ*pyrE*. On most occasions (13/18 times), the addition of sorbitol to the medium caused an increase (7/13 times, significantly) in the cytotoxicity of the parent. However, this was not consistently seen, as sometimes (5/18 times, 3/5 of which were significant) the presence of sorbitolresulted in suppression. Overall, toxin increase in sorbitol occurred more often than not, and enough times for there to be an observable trend.

The cytotoxicity of each mutant did not reflect the cytotoxic pattern of the parent it was tested alongside, indicating that deletion/inactivation of the gene of interest prevented the increase/decrease induced by the presence of sorbitol (due to the inability of each mutant to use sorbitol) seen in the parental strain. To summarise, with regards to cytotoxicity, it appeared that the uptake of sorbitol would induce an increase or decrease (usually an increase) in the parent, which was not seen in the mutant. But, sorbitol appears to have no direct role in toxin production as seen with primary sugars like glucose, fructose, and mannitol, which always suppress toxin synthesis[28].

Testing the role that the genes of the operon have in the motility of the bacterium did not reveal an apparent link between PTS^{Srl} at loci CD630_0764-8 and *C. difficile* 630 motility. The motility of the parent and each mutant it was tested alongside was the same on YTG (Fig. 5.83), BHIS +top agar (Fig. 5.85), and when using top agar in tubes (Fig. 5.86). Differences observed on YTS cannot be

considered a difference in motility as it is near certain that the phenotype observed on those plates was more related to the differences in the ability of each strain to use sorbitol (Fig. 5.84).

Although there are several published links between the PTS and bacterial motility[142,115], the relationship between the two is, mostly, under-researched. As yet, there appears to be no established link between the PTS and *C. difficle* motility. The *C. difficile* 630 genome encodes a single putative MCP (CD630_0539) (whose function has not yet been confirmed) and the lack of proof of its role in motility of *C. difficile* 630 is perhaps connected to the lack of a clear motility phenotype observed with any of the PTS^{Srl} mutants.

6.0 Final Discussion

The aim of this study was to investigate and characterise the *C. difficile* 630 PTS hypothesised to be involved in the fermentation of mannitol and sorbitol, and to study their possible roles in toxin production and motility.

Targeting each gene in the putative PTS^{Mtl} at loci CD630_2331-4 produced a growth and a cytotoxicity phenotype (Table 6.1).

Table 6.1: Mutants created indicating the presence of a phenotype following assays.
'Yes' denotes that a phenotypic difference was observed (following the creation of a mutant) when assaying for growth, sugar uptake, cytotoxicity, and motility; 'No' denotes that a phenotypic difference was not observed.

Strain Name	**Growth**	**Sugar Uptake**	**Toxin Titre**	**Motility**
CT*gutA* (0764, IIC)	Yes	Yes	No	No
CT*srlE_N* (0765, IIB) mut. A	Yes	Yes	No	No
CT*srlE_N* (0765, IIB) mut. B	Yes	Yes	No	No
CT*srlE_C* (0766, IIB)	Yes	Yes	No	No
CT*srlB* (0767, IIA)	Yes	Yes	No	No
Δ*gutD* (0768)	Yes	Yes	No	No
Δ*mtlD* (2331)	Yes	Yes	Yes	No?
CT*mtlF* (2332, IIA)	Yes	Yes	Yes	No
CT*mtlR* (2333)	Yes	Yes	Yes	No
Δ*mtlA* (2334, IIBC)	Yes	Yes	Yes	No

Δ*mtlD*, created by deleting the putative mannitol-1-phosphate dehydrogenase (MPDH) of the operon, exhibited differences in growth not merely connected to growth in mannitol. Deletion of *mtlD* completely blocked the ability of the

organism to utilise mannitol, but it also strongly attenuated the general level of growth in DM/TY, as well as in DMG/TYG (Fig. 4.15-4.16, & 4.18-4.20).

Restoration of *mtlD* allowed the complemented mutants to once again proliferate, and utilise mannitol and glucose (Fig. 4.17 & 4.21). But, although a high level of restoration was seen with the mutant complemented with *mtlD* at the regular gene dosage, overexpression of *mtlD* was necessary to return mannitol uptake to control strain levels.

Similarly, cytotoxicity assays of the mutant showed restored toxin production in the presence of mannitol, but also revealed a strain with an altered cytotoxicity, with toxin levels significantly increasing in mannitol (Fig. 4.22, 4.24, & 4.26). Complementation proved successful, restoring suppression of cytotoxicity in TYM (Fig. 4.23, 4.25, & 4.27), due to the restored mannitol-uptake ability.

It is possible that *mtlD* may have a role in motility. The motility assays on glucose (YTG) showed slightly larger zones of motility on the plates of the control strain and the complemented mutants (*mtlD* comp and *mtlD* overex) than was seen with the mutant, Δ*mtlD* (Fig. 4.28). Nonetheless, this could be the imperfect ability of Δ*mtlD* to utilise glucose affecting this assay (as well as the general growth defect observed of this strain throughout all the other assays).

The motility assays on BHIS +top agar (Fig. 4.30) and, more noticeably, in tubes, indicated marginally weaker motility (Fig. 4.31). However, again this may not be related to actual motility, but to a generally weakened *mtlD*-negative strain (Δ*mtlD* migrated the full distance in the motility assay tubes).

The findings prove that *mtlD* is involved in the utilisation of mannitol by *C. difficile* 630. When the results are considered in combination with the MtlD sequence which shows homology with MtlD of other bacteria, the organisation of the protein, and the annotation, MtlD most probably catalyses the conversion of phosphorylated mannitol, mannitol-1-phosphate (M-1-P) to fructose-6-phosphate (F-6-P). Also, there is very possibly a greater role for *mtlD* in the growth and virulence of the organism as evidenced by the reduced and unpredictable growth and cytotoxicity levels of Δ*mtlD*. Although it may be unlikely, considering that *mtlD* may have multiple roles, a role in motility cannot be completely excluded as much reduced motility was observed in the motility assays (Fig. 4.28-4.31), a reduction likely due to the organism being effected (in terms of survival and proliferation) by the removal of the gene, but which may also have reduced the mobility as well as the general growth of the bacterium. Timelapse microscopy examining the flagella could be a potential way to test for this in the future.

mtlF, the apparent IIA of the system, appears to be involved in *C. difficile* 630 uptake of mannitol. CT (ClosTron) inactivation of *mtlF* inhibited growth in mannitol in defined medium up to 24 h (Fig. 4.37), and in enriched medium, inhibited the uptake of the sugar up to 24 h (Fig. 4.41), and inhibited the suppression of cytotoxicity (especially at 72h) (Fig. 4.43, 4.45. & 4.47).

Notwithstanding, at 24 h (in defined medium) and at 48-72 h (enriched medium), mannitol was being utilised by CT*mtlF* (Fig. 4.37, 4.39, & 4.41) indicating that some of the sugar was somehow getting through to the bacteria. There are several possibilities. First, since the CT system does not remove the gene targeted for mutagenesis, but inactivates it by insertion of a group II intron[118,120,135], a minor portion of the gene potentially remains intact and transcribed. In the case of *mtlF*,

the CT insertion was at position 64sense (s) (in a gene of 423bp giving a 140AA protein) possibly leaving the first 15% of gene intact, and perhaps, transcribed. However, the phosphorylation site of *mtlF* is at a histidine residue (Fig. 6.1), as IIA phosphorylation will occur at the histidine residues[95,144], at AA position 63 (45% of the protein) (one of only two histidines in the entire MtlF protein; the other is at AA position 106). This would appear to eliminate the possibility of CT*mtlF* still retaining enough activity (to be phosphorylated) despite the CT insertion.

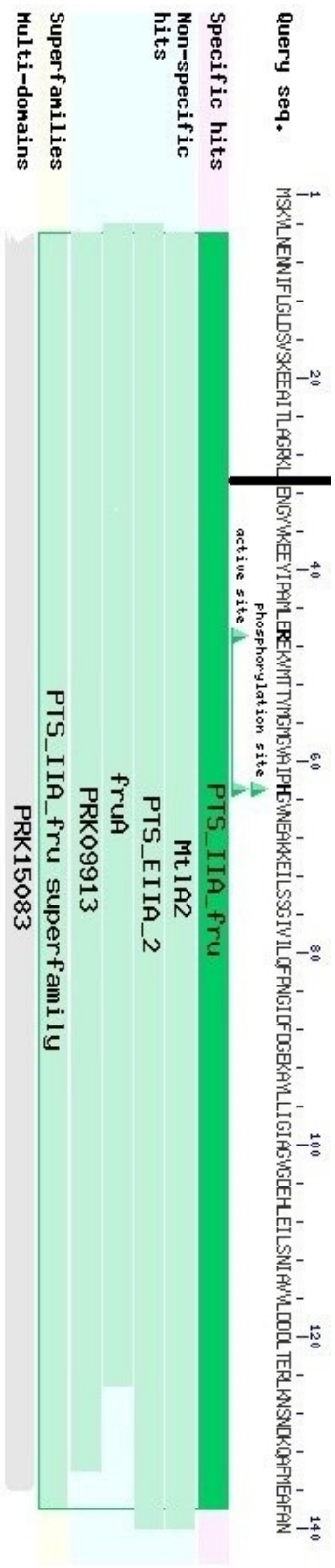

Figure 6.1: Diagram of MtlF showing the presence of histidine residues at AA positions 63 and 106 (NCBI).

IIAs are phosphorylated at the histidine residues[102], which are at AA postions 63 and 106 in *mtlF*. CT insertion was at the region which encodes AA position 31 (valine), indicated by the black marker.

A second possibility is that another compatible IIA is responsible for the belated mannitol uptake by CT*mtlF* (Fig. 4.37, 4.39, & 4.41). As discussed before (4.6 Discussion), there are five other putative IIAs annotated as belonging to the fructose-mannitol family of IIAs, one of which, CD_0206, has 29% homology with *mtlF*, and is possibly compatible with mannitol uptake, and has a role in phosphorylating the PTS^{Mtl} IIB, after itself being phosphorylated by HPr, and therefore, is resulting in the delayed mannitol utilisation that was consistently seen at 24-72 h (Fig. 4.41).

Complementing CT*mtlF* using the native promoter (*Pmtl*) and using the *fdx* promoter partially and imperfectedly restored some mannitol uptake and cytotoxicity. This incomplete restoration which exhibited itself was either due to the presence of another, 'auxliary' IIA, or possibly it was because the phenotypes achieved with CT*mtlF* were the result of a CT polar effect. Perhaps a neighbouring transcript (such as was likely seen with CT*mtlF*) was inactivated and this produced the phenotype observed.

Determining from the sequences, the protein arrangement (NCBI), and the annotation (Artemis), as well as the apparent successful creation of an *mtlF* CT mutant (and if not considering the possibility of a polar effect resulting from the CT), it appears likely that *mtlF* is an IIA^{Mtl}. However, final tests (phosphorylation assays and CD630_0206 inactivation –see 7.0 Future Work) will be necessary to eliminate any doubts about the exact role of *mtlF* in mannitol uptake and mannitol-related cytotoxicity (as expanded in 7.0 Future Work below).

CT*mtlR*, made from targeting the apparent regulator of the operon, completely failed to utilise mannitol (Fig. 4.57, 4.59, & Fig. 4.61), and also restored

cytotoxicity levels in mannitol (Fig. 4.62, 4.64, & 4.66). Complementation successfully re-established mannitol uptake and consequent suppression of toxin expression. Therefore, it is certain that *mtlR* is involved in the utilisation of mannitol in *C. difficile* 630. The results indicate, in agreement with the publicly available MtlR sequences (NCBI) and annotation (Artemis), that the role of *mtlR* appears to be that of a transcriptional regulator. Unlike *mtlF* and *mtlA*, there appears to be no other gene in the *C. difficile* 630 genome capable of playing (or even part playing) the role of a mannitol PTS transcriptional regulator. Targeting *mtlF* and *mtlA* still allowed the organism to use small, yet noticeable, amounts of mannitol at later time points (Fig. 4.37, 4.39, & 4.41, 24-72 h; Fig. 4.77, 4.79, & 4.81, 24-72 h). This was not seen with CT*mtlR* (Fig. 4.57, 4.59, & 4.61), which was unable to make use of the available mannitol. As indicated, this is probably because there is no other gene available to act as a PTS^{Mtl} antiterminator. Antiterminators will become dephosphorylated, and hence, activated as mannitol is being taken up by the IIC^{Mtl}. Turning off this activation will presumedly result in MtlR remaining phosphorylated, and thus, being unable to mediate for the efficient uptake of mannitol in the organism.

Deletion of *mtlA*, the putative $IICB^{Mtl}$, produced different phenotypes in mannitol, in growth and cytotoxicity, from those seen with the control strain, 630Δ*erm* (Fig. 4.77, 4.79, 4.81, 4.83, 4.85, & 4.87). Use of mannitol was completely blocked in defined medium (up to 24 h) (Fig. 4.78), in enriched medium (Fig. 4.82), and toxin levels in mannitol were restored (Fig. 4.84, 4.86, & 4.88).

Notwithstanding this, like CT*mtlF* (Fig. 4.37, 4.39, & 4.41), Δ*mtlA* in defined medium was able to use much (24.6%) of the available mannitol by 24 h, as evidenced by the HPLC evaluation of sugar uptake (Fig. 4.80).

Judging from the *C. difficile* 630 MtlA sequence showing homologues with MtlAs in other bacteria (NCBI), the protein organisation indicating it to be a IIBC (NCBI) (Fig. 6.2), and the annotation (Artemis) of MtlA, it seems highly likely that MtlA is a $IICB^{Mtl}$, which transports mannitol across the *C. difficile* cell membrane and phosphorylates it to M-1-P, permitting it to be converted to F-6-P by MtlD. Although there are no homologues of *mtlA* amongst them, there are five other PTS annotated as part of the fructose-mannitol family which contain IIB/Cs. It is possible that one or more of these proteins is responsible for the minor degree of mannitol uptake by Δ*mtlA*. Nonetheless, *mtlA* is very likely the primary route of mannitol transportation into the bacterial cell, and also, via its IIB domain, phosphorylates the sugar, permitting the MPDH (MtlD) to catalyse its conversion to F-6-P.

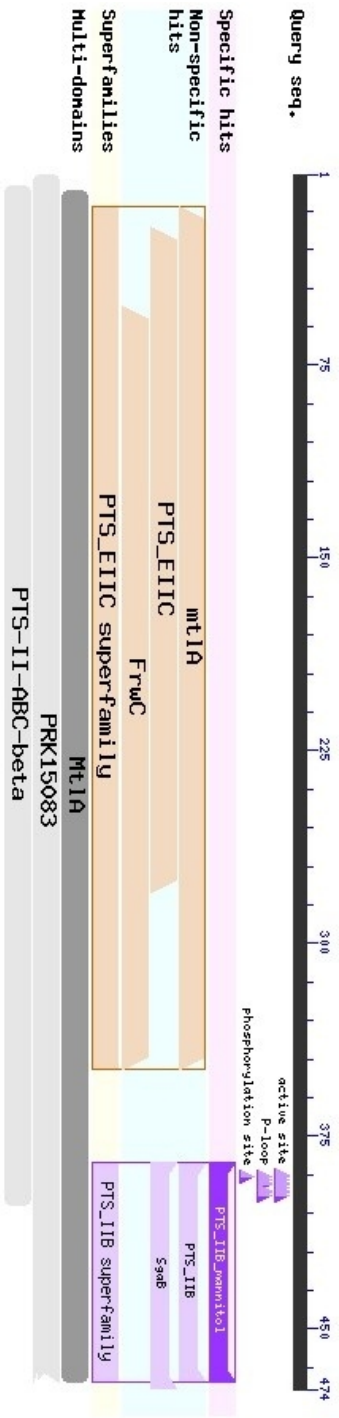

Figure 6.2: Illustration of *C. difficile* 630 MtlA encoded at locus CD630_2334 showing the IIB and IIC domains of the protein (NCBI).
No homologues of *mtlA* have been found in the *C. difficile* 630 genome. However, there are five potential PTS^{Fru} which may be compatible with mannitol uptake and play a partial role of a mannitol IIB/C.

Regarding the role that PTS^{Mtl} at loci CD630_2331-4 plays in the motility of the bacterium, it seems that, with the possible exception of *mtlD*, the genes of this

operon have no clear or direct role in the motility of this organism *in vitro*. Testing the mutants (and the complements) alongside 630WT, 630Δ*erm*, CT*fliC*, and the non-motile strain, M120, did not reveal differences in motility using four variant motility assays.

A possible reason for seeing a lack of a motility phenotype is that there is only one putative MCP encoded in *C. difficile* 630 (contrasting with, for example, *E. coli* K12 MCP, whose function is confirmed and shown to interact with the PTS[142]). The single, unconfirmed MCP that is putatively encoded at CD630_0539 (CheA) possibly does not interact directly with PTS^{Mtl}.

The role of PTS^{Mtl} in *C. difficile* 630 spore formation cannot be stated with any certainty or even probability. But, the early indications in this unresearched area are that two of the key components of this PTS (*mtlR* and *mtlA*) have no role, and by default, it seems unlikely (but not impossible) that the operon is involved in sporulation.

To summarise, molecular characterisation via gene inactivation has proved that the operon at loci CD630_2331-4 is the main transport system responsible for mannitol utilisation in *C. difficile* 630. It seems to be at the very least, with regard to the IIA, IIB, and IIC domains, the primary route of mannitol uptake and phosphorylation. Even considering the possibility of other PTS compatible with mannitol transport and phosphorylation facilitating uptake of the sugar, with the IIA, IIB, and IIC encoded by *mtlF* and *mtlA* at loci CD630_2332-4, mannitol utilisation is, for the most part, not possible. The PTS^{Mtl} appears to completely depend on the phosphate dehydrogenase, and especially, the regulator component of the operon, respectively encoded by *mtlD* and *mtlR*. Without these genes and

their transcribed proteins, mannitol uptake and utilisation seems near impossible. Taken all together, the operon at loci CD630_2331-4 is certainly the *C. difficile* 630 PTS^{Mtl}, and its presence is fundamental to the import and use of mannitol by the organism, the use of which will influence the toxicity of the bacterium.

The uptake mechanisms of sorbitol, a fermentable carbon source for *C. difficile*, were examined in order to determine the role of the PTS hypothesised to be responsible for the uptake of this sugar.

CT inactivation of *gutA* (IIC at CD630_0764), *srlE* (IIB at CD630_0765-6), and *srlB* (IIA at CD630_0767) completely prevented growth in sorbitol (Fig. 5.21, Fig. 5.35, Fig. 5.49, and Fig. 5.63). Complementation of CT*gutA*, CT*srlE*, and CT*srlB* would indicate whether the growth phenotypes observed are the result of CT polar effects. The inability of CT*gutA* (Fig. 5.21 and Fig. 5.24) to subsist on sorbitol probably stems from the likelihood that disabling GutA prevents sorbitol from being detected by the bacterium and then being facilitated across the bacterial membrane, and so, the sugar will be neither taken up nor phosphorylated.

Inactivation of SrlE assumedly prevented phosphorylation of sorbitol as it entered the cells. The growth phenotypes achieved (Fig. 5.35 and Fig. 5.49), by separately targeting the N terminus and the C terminus of SrlE, would indicate that both of these regions are required for receipt (from IIA) and donation (to the incoming sorbitol molecule) of phosphate. Four cysteine residues (generally the sites of IIB phosphorylation[123,143]; very occasionally, histidine residues are the sites of IIB phosphorylation –mannose PTS[102]) are encoded in *srlE_N* (369bp gene), but only two cysteine residues (and a single histidine) are encoded in the larger (567bp

gene) *srlE_C*, indicating that perhaps SrlE_N is more likely to be the part of the protein being phosphorylated by IIA^{Srl}. These findings along with the growth phenotypes achieved from inactivating each terminus separately would, therefore, suggest that the N-terminus may possibly be the phosphate recipient, and raises the possibility that perhaps the C-terminus may have a role in the donation of the received phosphate.

The inability of CT*srlB*, the putative IIA of the system to grow in sorbitol (Fig. 5.63), and the SrlB sequence which is homologous to SrlB in other bacteria (NCBI), as well as the annotation describing SrlB as an IIA^{Srl} (Artemis), indicates, once the possibility of a CT polar effect is ruled out, that its role is that of a phosphate donor to IIB^{Srl}, which is most likely SrlE (CD_0765-6).

Deletion of *gutD* prevented growth in sorbitol (Fig. 5.76). No uptake of the sugar was observed, indicating that without *gutD* (probably to catalyse the conversion of phosphorylated sorbitol, S-6-P, to F-6-P following its probable phosphorylation by SrlE), *C. difficile* 630 fermentation of the sugar is not possible.

It seems that the genes of PTS^{Srl} at CD630_0764-8 have no obvious role in the motility of the organism. Testing the motility of each mutant did not reveal a phenotype. Only two genes of this operon remain untested (CD630_0762-3), and unless the proteins transcribed from those genes (SrlR –putative regulator and GutM –operon activator) go against the trend exhibited by the other proteins of this system, it appears that PTS^{Srl} plays no role in *C. difficile* 630 *in vitro* motility.

Due to the inconsistency of increased toxin release observed in the presence of sorbitol (see 5.8 Discussion), and also, to the fact that the genes at loci CD630_0764-8 do not fall under the control of $CcpA^{22}$, it seems highly

improbable that sorbitol itself (in a sort of inverse imitation of glucose and other primary sugars) is directly inducing this effect, but it is, rather, a stress response by the bacteria of having to subsist on sorbitol alone, a situation the organism is probably not used to, judging from the small number of potential PTS^{Srl} (2), in comparison to the number of potential glucose (6), fructose (5), and mannitol (1 + 5 possible PTS^{Fru})-specific systems, encoded in the bacterial genome. *C. difficile* has been shown to increase toxin production in response to environmental stress[133]. Dependency only on sorbitol, a less-preferred secondary sugar[22], for long periods (72-120 h) could be considered as an environmental stress as the bacteria are being starved of their principal sources of carbon. Also supporting this is the fact that whenever *C. difficile* 630Δ*erm*Δ*pyrE* was grown in the presence of sorbitol, the addition of the sugar never induced the rapid increase (from 6 h in DM/TY) in OD_{600} levels which was always observed with mannitol and glucose. The ability of sorbitol to increase OD_{600} was only observable from 10 h in DM, or, in TY, it merely permitted the bacteria to maintain the OD_{600} they had already reached. To sum up, *C. difficile* 630 appears not to increase (or decrease) toxin production because of a direct influence of sorbitol (as seen, for example, with mannitol and glucose), but likely because the organism is stressed due to having to subsist completely on a secondary sugar, and is responding by producing higher amounts of toxin. It is possible that the production of higher amounts of toxin would mimic an effort by the organism to destroy more host cells to release primary sugars[43].

Targeting the operon encoded at loci CD630_0762-8, specifically the apparent IIA, IIB, IIC, and phosphate dehydrogenase portions, has resulted in an inability of *C. difficile* 630 to use sorbitol, and therefore, indicates, that without this

particular system, uptake of the sugar is mostly impossible. This does not completely exclude the second potential PTS^{Srl} at loci CD630_2414-8 from being involved in sorbitol utilisation (as without targeting the genes it cannot be said with certainty –see Future Work 7.0), but since the SPDH (the mutant of which, Δ*gutD*, completely failed to grow in sorbitol) is encoded within the CD630_0762-8 operon, as well as the inability of each mutant to subsist on the sugar, it would appear that CD630_0762-8 is primarily responsible for the uptake of sorbitol.

The predicted PTS^{Srl} at loci CD630_0762-8 may be vital in permitting the survival of *C. difficile*, when other available carbon sources have been expended by the bacteria, allowing the organism not to thrive, but at least to maintain a level of growth so as to enable it to survive for an extended period, or possibly, to survive until more suitable environmental conditions provide access to other, more readily fermentable, carbon sources.

The ability to utilise available PTS sugars, such as those found in the human diet like mannitol[129] and sorbitol[136-138] (and as a possible consequence, the human gut), is of prime importance to the survival, proliferation, and virulence of *C. difficile*. The PTS appears to be one of the main ways the organism optimises its ability to survive and to proliferate in such environments, and the efficient use of mannitol and sorbitol via the PTS demonstrates the importance of the system to *C. difficile* growth and pathogenesis. This study has demonstrated *in vitro* the role of the *C. difficile* PTS in carbohydrate uptake and utilisation, and relatedly, its connection to the cytotoxicity of the organism by researching two PTS involved in the fermentation of mannitol and sorbitol, two sugars proven to allow the bacteria to survive and grow, and thereby, increasing the pathogenesis of organism. Therefore, the PTS appears (when the results of this study are

considered in combination with those of previous studies)[22,23], specifically in the case of mannitol and sorbitol, to be of great importance in the survival, growth, and regulation of the pathogenesis of *C. difficile* when in the presence of sugars which may be found in the gut.

7.0 Future Work

7.1 Complementation of Mutants – CT*srlE_N*, CT*srlB*, and CT*mtlF*

Work has already commenced on complementing CT*srlE_N* and CT*srlB*, which aims to restore the inactivated genes with, firstly, the native promoter [apparently located immediately upstream of CD630_0762 (*srlR*)] in order to restore growth and cytotoxicity to that of the control strain, 630Δ*erm*; and secondly, using the *fdx* (ferredoxin) overexpression promoter, so as to observe the effects of having the restored gene under the influence of a strong, constitutive promoter. If successful, this will remove any remaining doubts about the roles of *srlE/srlB* in sorbitol uptake and cytotoxicity at the protein level. The complemented strains will be subjected to the same growth, sugar uptake, cytotoxicity, and motility assays used in this study.

Complementation of CT*mtlF* with *mtlD* (or *mtlR*) may be considered in order to investigate if *mtlD* was in any way inactivated by the CT instead of *mtlF*.

7.2 Targeting mannitol-specific IIA domains

It is of interest to determine exactly how the small amount of mannitol being used by CT*mtlF* at 48-72 h is getting through to the organism. The putative fructose-specific IIA at locus CD630_0206 which has homology (29%) with *mtlF*, is an interesting potential target for CT inactivation. Due to its homology, CD_0206 is probably the best choice of the five potential fructose/mannitol IIAs encoded in the *C. difficile* 630 genome. Also, targeting CD_0206 for deletion, but using CT*mtlF* as the parental strain could be considered, and could potentially completely prevent the tardy mannitol uptake observed with CT*mtlF*. The resulting double mutant would then be subjected to growth, cytotoxicity, and motility assays alongside CT*mtlF* (its parent) and 630Δ*erm*.

7.3 Overexpressing the mannitol-specific PTS IIB and IIC domains

Δ*mtlA* will also later be overexpressed using the above mentioned method. Difficulties were encountered when attempting to overexpress *mtlA* during this work. It was not possible to insert the gene beside the *fdx* promoter in pMTL-YN1X. Overexpression of the IIB and IIC domains will separately be attempted, which will hopefully clarify the role of *mtlA* (as well as maybe revealing which domain of this transmembrane protein was causing the difficulties in putting the gene into the pMTL-YN1X vector) and also disclose if the small level of mannitol uptake seen with Δ*mtlA* (Fig. 4.79) is primarily due to the IIB or to the IIC domain (or not at all).

7.4 Investigation and Characterisation of PTS^{Srl} Regulator (CD630_0762)

The putative regulator of the PTS^{Srl} at loci CD630_0762-8, *SrlR*, has been successfully targeted for CT mutagenesis, and will now be tested for differences in growth, sugar uptake, cytotoxicity, and motility (following the methods used in this study).

7.5 Investigation of Sorbitol IIB (CD630_2417)

SrlE at locus CD630_2417, forming part of the putative second sorbitol-specific PTS at loci CD630_2414-8 is being targeted for CT inactivation, and will be subjected to the growth, sugar uptake, cytotoxicity, and motility assays described in this study in order to determine its possible relationship (if any) to sorbitol uptake and utilisation.

7.6 Phosphorylation assays

All the mutants and complements created in this study (and any future ones created), as well as the WT, and the control and parental strains, will be subjected to assays to determine the level of phosphorylation of each mutant, and its PTS protein domains of interest. Briefly, this will be by identification of phosphor-labelled proteins by making protein extracts from each strain using methods from Peri *et al.* (1984)[144]. Mutant extracts should show EI and HPr phosphorylated, but should differ for those domains that were targeted. For example, CT*mtlF* (IIA inactivated) should show no radiolabelled IIA or IIB, and Δ*mtlA* (IIBC deleted) should show a labelled IIA, but no labelled IIB, while WT, control, and parental strains should indicate labelling of all domains.

7.7 Spore assays

The observed increase in toxin production by *C. difficile* 630 when in sorbitol is probably a symptom of environmental stress (see 6.0 Final Discussion). It is possible that such environmental conditions will also affect the rate of sporulation of the organism. Sporulation assays, according to Burns *et al.* (2010)[46,145], will be performed (using those CT PTS^{Srl} mutants exhibiting a growth phenotype), comparing the sporulation rates over 120 h of 630Δ*erm*Δ*pyrE*, CT*gutA*, CT*srlE_N*, CT*srlE_C*, CT*srlB*, and Δ*gutD* [and possibly CT*srlR* and CT*srlE* (CD_2417)] with and without sorbitol.

Future research into the *C. difficile* PTS will potentially look deeper into the role of the PTS in growth and the virulence factors such as toxin production and motility, possibly leading to a more developed approach to patient treatment. Increased understanding of the *C. difficile* PTS and it's role in virulence could

allow future researchers and carers to apply more nuanced methods of tackling the pathogenesis of the bacterium, permitting a more effective response to infection involving dietary alterations, such as limiting patient access to certain PTS sugars (on which the organism can thrive) in the diet (and providing suitable alternative carbohydrates which are not readily fermentable by *C. difficile*) in combination with probiotics (to promote growth of beneficial species –e.g. *Sacchromyces boulardii* or *Lactobacillus acidophilus*)[146,147] during the infection period. The continued study of the *C. difficile* PTS can only permit an expansion of the treatment and prevention strategies in understanding and combatting CDI.

8.0 Acknowledgements

Dr. Sarah Kuehne, Professor Nigel Minton, Dr. Mark Collery, Dr. Emma Stevenson, Dr. Carolyn Meaney, Dr. Anne Henstra, Dr. Stephen Cartman, Dr. Rachel Ng, Michelle Kelly, Nurul Hj Morni, Cara Wray, Jacqueline Minton, Leanne Mitchell, and Professor Ian MacDonald (all University of Nottingham) for their guidance, help, and assistance.

I thank Professor Wilfrid Mitchell (Heriot-Watt University, Edinburgh) for his generous advice and guidance with this work.

I would like to acknowledge Marie Curie Actions and the University of Nottingham for kindly funding this study.

Many thanks go to my family, relatives, friends, collaborators, and close colleagues (past and present) for their support during the research.

9.0 Additional Sources

Artemis

Clostridia Research Group (CRG) 'Protocols for Clostridial Gene Knockout: ClosTron Technology and Allelic Exchange' University of Nottingham, Marie Curie Actions Workshop, December 2010

clostron.com

Clustal programme -European Bioinformatics Institute (EBI)

Clustal X

DNASTAR

dna20.com (DNA2.0)

Graphpad Prism

insilico.ehu.es

Invitrogen –thermofisher.com

Mitchell W. J. 'Phylogenetic tree of phosphotransferase systems found in the *Clostridium difficile* 630 genome' (2012), unpublished; Heriot-Watt University, Edinburgh, UK

National Center for Biotechnology Information (NCBI) Basic Local Alignment Search Tool (BLAST)

NCBI Genbank

NCBI PubChem

NCBI Pubmed

Notepad++

SnapGene

Tcoffee

vassarstats.net/anova1u.html

10.0 References

1 Durre, P. Fermentative butanol production: bulk chemical and biofuel. *Annals of the New York Academy of Sciences* **1125**, 353-362, doi:10.1196/annals.1419.009 (2008).
2 Wen, Z. *et al.* Artificial symbiosis for acetone-butanol-ethanol (ABE) fermentation from alkali extracted deshelled corn cobs by co-culture of Clostridium beijerinckii and Clostridium cellulovorans. *Microbiology Cell Facts* **13**, 92, doi:10.1186/s12934-014-0092-5 (2014).
3 Kopke, M., Held, C., Hujer, S., Liesegang, H., Wiezer, A.,Wollherr, A., Ehrenreich, A., Liebl, W., Gottschalk, G. & Durre, P. Clostridium ljungdahlii represents a microbial production platform based on syngas. *Proceedings of the National Academy of Sciences of the United States of America* **107**, 13087-13092, doi:10.1073/pnas.1004716107 (2010).
4 Kopke, M., Mihalcea C., Liew, F., Tizard, T.H., Ali, M.S., Conolly, J.J., Al-Sinawi, B. & Simpson, S.D. 2,3-butanediol production by acetogenic bacteria, an alternative route to chemical synthesis, using industrial waste gas. *Applied and Environmental Microbiology* **77**, 5467-5475, doi:10.1128/AEM.00355-11 (2011).
5 Heap, J. T., Theys, J, Ehsaan, M., Kubiak, A.M., Dubois, L., Paesmans, K., Mellaert, L.V., Knox, R., Kuehne, S.A., Lambin, P. & Minton, N.P. Spores of Clostridium engineered for clinical efficacy and safety cause regression and cure of tumors in vivo. *Oncotarget* **5**, 1761-1769 (2014).
6 Staedtke, V., Bai, R., Sun, W., Huang, J., Kibler, K.K., Tyler, B.M., Gallia, G.L., Kinzler, K., Vogelstein, B., Zhou, S. & Riggins, G.J. Clostridium novyi-NT can cause regression of orthotopically implanted glioblastomas in rats. *Oncotarget* **6**, 5536-5546 (2015).
7 Samul, D., Worsztynowicz, P., Leja, K. & Grajek, W. Beneficial and harmful roles of bacteria from the Clostridium genus. *Acta Biochim Pol* **60**, 515-521 (2013).
8 Uzal, F. A., Freedman J.C., Shrestha, A., Theoret, J.R., Garcia, J., Awad, M.M., Adams, V., Moore, R.J., Rood, J.I. & McClane, B.A. Towards an understanding of the role of Clostridium perfringens toxins in human and animal disease. *Future Microbiology* **9**, 361-377, doi:10.2217/fmb.13.168 (2014).
9 Cartman, S. T., Heap, J. T., Kuehne, S. A., Cockayne, A. & Minton, N. P. The emergence of 'hypervirulence' in Clostridium difficile. *International Journal of Medical Microbiology : IJMM* **300**, 387-395, doi:10.1016/journal.ijmm.2010.04.008 (2010).
10 Aldape, M. J., Bryant, A. E. & Stevens, D. L. Clostridium sordellii infection: epidemiology, clinical findings, and current perspectives on diagnosis and treatment. *Clinical Infectious Diseases : An Official Publication of the Infectious Diseases Society of America* **43**, 1436-1446, doi:10.1086/508866 (2006).
11 Stevens, D. L., Aldape, M. J. & Bryant, A. E. Life-threatening clostridial infections. *Anaerobe* **18**, 254-259, doi:10.1016/journal.anaerobe.2011.11.001 (2012).
12 Aronoff, D. M. Clostridium novyi, sordellii, and tetani: mechanisms of disease. *Anaerobe* **24**, 98-101, doi:10.1016/journal.anaerobe.2013.08.009 (2013).
13 Buffie, C. G., Bucci, V., Stein, R.R., McKenney, P.T., Ling, L., Gobourne, A., No, D., Liu, H., Kinnebrew, M., Viale, A., Littman, E., van

der Brink, M.R., Jeng, R.R., Taur, Y., Sander, C., Cross, J.R., Toussaint, N.C., Xavier, J.B. & Pamer, E.G. Precision microbiome reconstitution restores bile acid mediated resistance to Clostridium difficile. *Nature* **517**, 205-208, doi:10.1038/nature13828 (2015).

14 Kuehne, S. A., Cartman, S.T., Heap, J.T., Kelly M.L., Cockayne, A. & Minton, N. The role of toxin A and toxin B in Clostridium difficile infection. *Nature* **467**, 711-713, doi:10.1038/nature09397 (2010).

15 Poutanen, S. M. & Simor, A. E. Clostridium difficile-associated diarrhea in adults. *Cmaj* **171**, 51-58 (2004).

16 Elliott, B., Chang, B. J., Golledge, C. L. & Riley, T. V. Clostridium difficile-associated diarrhoea. *Internal Medicine J* **37**, 561-568 (2007).

17 Awad, M. M., Johanesen, P. A., Carter, G. P., Rose, E. & Lyras, D. Clostridium difficile virulence factors: Insights into an anaerobic spore-forming pathogen. *Gut Microbes* **5**, 579-593, doi:10.4161/19490976.2014.969632 (2014).

18 Dineen, S. S., Villapakkam, A. C., Nordman, J. T. & Sonenshein, A. L. Repression of Clostridium difficile toxin gene expression by CodY. *Molecular Microbiology* **66**, 206-219, doi:10.1111/j.1365-2958.2007.05906.x (2007).

19 Wilson, K. H. & Perini, F. Role of competition for nutrients in suppression of Clostridium difficile by the colonic microflora. *Infection and Immunity* **56**, 2610-2614 (1988).

20 Kinross, J. M., Darzi, A. W. & Nicholson, J. K. Gut microbiome-host interactions in health and disease. *Genome Medicine* **3**, 14, doi:10.1186/gm228 (2011).

21 Theriot, C. M. & Young, V. B. Interactions Between the Gastrointestinal Microbiome and Clostridium difficile. *Annual Review of Microbiology* **69**, 445-461, doi:10.1146/annurev-micro-091014-104115 (2015).

22 Antunes, A. *et al.* Global transcriptional control by glucose and carbon regulator CcpA in Clostridium difficile. *Nucleic Acids Research* **40**, 10701-10718, doi:10.1093/nar/gks864 (2012).

23 Antunes, A., Martin-Verstraete, I. & Dupuy, B. CcpA-mediated repression of Clostridium difficile toxin gene expression. *Molecular Microbiology* **79**, 882-899, doi:10.1111/journal.1365-2958.2010.07495.x (2011).

24 Cartman, S. T., Heap, J. T., Kuehne, S. A., Cockayne, A. & Minton, N. P. The emergence of 'hypervirulence' in Clostridium difficile. *International Journal of Medical Microbiology : IJMM* **300**, 387-395, doi:10.1016/journal.ijmm.2010.04.008 (2010).

25 Pultz, N. J. & Donskey, C. J. Effect of antibiotic treatment on growth of and toxin production by Clostridium difficile in the cecal contents of mice. *Antimicrobial Agents and Chemotherapy* **49**, 3529-3532, doi:10.1128/AAC.49.8.3529-3532.2005 (2005).

26 Bouillaut, L., Dubois, T., Sonenshein, A. L. & Dupuy, B. Integration of metabolism and virulence in Clostridium difficile. *Research in Microbiology* **166**, 375-383, doi:10.1016/journal.resmic.2014.10.002 (2015).

27 Karlsson, S., Dupuy, B., Mukherjee, K., Norin, E., Burman, L.G. & Akurland, T. Expression of Clostridium difficile toxins A and B and their sigma factor TcdD is controlled by temperature. *Infection and Immunity* **71**, 1784-1793 (2003).

28 Dupuy, B. & Sonenshein, A. L. Regulated transcription of Clostridium difficile toxin genes. *Molecular Microbiology* **27**, 107-120 (1998).

29 Brouwer, M. S., Warburton, P. J., Roberts, A. P., Mullany, P. & Allan, E. Genetic organisation, mobility and predicted functions of genes on integrated, mobile genetic elements in sequenced strains of Clostridium difficile. *PloS One* **6**, e23014, doi:10.1371/journal.pone.0023014 (2011).

30 Brouwer, M. S., Allan, E., Mullany, P. & Roberts, A. P. Draft genome sequence of the nontoxigenic Clostridium difficile strain CD37. *Journal of Bacteriology* **194**, 2125-2126, doi:10.1128/JB.00122-12 (2012).

31 Brouwer, M. S., Brouwer, A.P.,Hussain, H., Williams, R.J., Allan, E. & Mullany, P. Horizontal gene transfer converts non-toxigenic Clostridium difficile strains into toxin producers. *Nature Communications* **4**, 2601, doi:10.1038/ncomms3601 (2013).

32 von Eichel-Streiber, C., Laufenberg-Feldmann, R., Sartingen, S., Schulze, J. & Sauerborn, M. Comparative sequence analysis of the Clostridium difficile toxins A and B. *Molecular & General Genetics : MGG* **233**, 260-268 (1992).

33 Yuan, P., Zhang, H., Cai, C., Zhu, S., Zhou, Y., Yang, X., He, R., Li, C., Guo, S., Li, S., Huang, T., Perez-Cordon, G., Feng, H. & Wei, W. Chondroitin sulfate proteoglycan 4 functions as the cellular receptor for Clostridium difficile toxin B. *Cell Research* **25**, 157-168, doi:10.1038/cr.2014.169 (2015).

34 LaFrance, M. E., Farrow, M.A., Chandrasekaran, R., Sheng, J., Rubin, D.H. & Borden Lacy, D. Identification of an epithelial cell receptor responsible for Clostridium difficile TcdB-induced cytotoxicity. *Proceedings of the National Academy of Sciences of the United States of America* **112**, 7073-7078, doi:10.1073/pnas.1500791112 (2015).

35 Matamouros, S., England, P. & Dupuy, B. Clostridium difficile toxin expression is inhibited by the novel regulator TcdC. *Molecular Microbiology* **64**, 1274-1288, doi:10.1111/journal.1365-2958.2007.05739.x (2007).

36 Lemee, L., Dhalluin, A., Testelin, S., Mattrat, M.A., Maillard, K., Lemeland, J.F. & Pons, J.L. Multiplex PCR targeting tpi (triose phosphate isomerase), tcdA (Toxin A), and tcdB (Toxin B) genes for toxigenic culture of Clostridium difficile. *Journal of Clinical Microbiology* **42**, 5710-5714, doi:10.1128/JCM.42.12.5710-5714.2004 (2004).

37 Mani, N. & Dupuy, B. Regulation of toxin synthesis in Clostridium difficile by an alternative RNA polymerase sigma factor. *Proceedings of the National Academy of Sciences of the United States of America* **98**, 5844-5849, doi:10.1073/pnas.101126598 (2001).

38 Mani, N. *et al.* Environmental response and autoregulation of Clostridium difficile TxeR, a sigma factor for toxin gene expression. *Journal of Bacteriology* **184**, 5971-5978 (2002).

39 Carter, G. P., Douce, G.R., Govind, R., Howarth, P.M., Mackin, K.E., Spencer, J., Buckley, A.M., Antunes, A., Kotsanas, D., Jenkin, G.A., Dupuy, B., Rood, J.I. & Lyras, D. The anti-sigma factor TcdC modulates hypervirulence in an epidemic BI/NAP1/027 clinical isolate of Clostridium difficile. *PLoS Pathogens* **7**, e1002317, doi:10.1371/journal.ppat.1002317 (2011).

40 Cartman S.T., K. M. L., Heeg D., Heap J.T., Minton N.P. . Precise manipulation of the Clostridium difficile chromosome reveals a lack of association between tcdC genotype and toxin production. *Applied Environmental Microbiology 2012* **20** (2012).

41 Bakker, D., Smits, W. K., Kuijper, E. J. & Corver, J. TcdC does not significantly repress toxin expression in Clostridium difficile 630DeltaErm. *PloS One* **7**, e43247, doi:10.1371/journal.pone.0043247 (2012).

42 Govind, R. & Dupuy, B. Secretion of Clostridium difficile toxins A and B requires the holin-like protein TcdE. *PLoS Pathogens* **8**, e1002727, doi:10.1371/journal.ppat.1002727 (2012).

43 Dineen, S. S., McBride, S. M. & Sonenshein, A. L. Integration of metabolism and virulence by Clostridium difficile CodY. *Journal of Bacteriology* **192**, 5350-5362, doi:10.1128/JB.00341-10 (2010).

44 Mallozzi, M., Bozue, J., Giorno, R., Moody, K.S., Slack, A., Cote, C., Qiu, D., Wang, R., McKenney, P., Lai, E.M., Maddock, J.R.,Friedlander, A., Welkos, S., Eichenberger, P. & Driks, A. Characterization of a Bacillus anthracis spore coat-surface protein that influences coat-surface morphology. *FEMS Microbiology Letters* **289**, 110-117, doi:10.1111/journal.1574-6968.2008.01380.x (2008).

45 Giorno, R., Mallozzi, M., Bozue, J., Moody, K.S., Slack, A., Qiu, D., Wang, R., Friedlander, A., Welkos, S. & Driks, A. Localization and assembly of proteins comprising the outer structures of the Bacillus anthracis spore. *Microbiology* **155**, 1133-1145, doi:10.1099/mic.0.023333-0 (2009).

46 Burns, D. A., Heap, J. T. & Minton, N. P. SleC is essential for germination of Clostridium difficile spores in nutrient-rich medium supplemented with the bile salt taurocholate. *Journal of Bacteriology* **192**, 657-664, doi:10.1128/JB.01209-09 (2010).

47 Mackin, K. E., Carter, G. P., Howarth, P., Rood, J. I. & Lyras, D. Spo0A differentially regulates toxin production in evolutionarily diverse strains of Clostridium difficile. *PloS One* **8**, e79666, doi:10.1371/journal.pone.0079666 (2013).

48 Rosenbusch, K. E., Bakker, D., Kuijper, E. J. & Smits, W. K. C. difficile 630Deltaerm Spo0A regulates sporulation, but does not contribute to toxin production, by direct high-affinity binding to target DNA. *PLoS One* **7**, e48608, doi:10.1371/journal.pone.0048608 (2012).

49 Underwood, S., Guan, S., Vijayasubhash, V., Baines, S.D., Graham, L., Lewis, R.J., Wilcox, M.H., & Stephenson, K. Characterization of the sporulation initiation pathway of Clostridium difficile and its role in toxin production. *Journal of Bacteriology* **191**, 7296-7305, doi:10.1128/JB.00882-09 (2009).

50 Antunes, A., Camiade, E., Monot, M., Courtois, E., Barbut, F., Sernova, N.V., Rodionov, D.A., Martin-Verstraete, I. & Dupuy, B. Global transcriptional control by glucose and carbon regulator CcpA in Clostridium difficile. *Nucleic Acids Research*, doi:10.1093/nar/gks864 (2012).

51 Rupnik, M. & Janezic, S. An Update on Clostridium difficile Toxinotyping. *Journal of Clinical Microbiology* **54**, 13-18, doi:10.1128/JCM.02083-15 (2016).

52 Lyras, D. *et al.* Toxin B is essential for virulence of Clostridium difficile. *Nature* **458**, 1176-1179, doi:10.1038/nature07822 (2009).

53 Goncalves, C., Decre, D., Barbut, F., Burghoffer, B. & Petit, J. C. Prevalence and characterization of a binary toxin (actin-specific ADP-ribosyltransferase) from Clostridium difficile. *Journal of Clinical Microbiology* **42**, 1933-1939 (2004).

54 Stabler, R. A., He, M., Dawson, L., Martin, M., Valiente, E., Corton, C., Lawley, T.D., Sebaihia, M., Quail, M.A., Rose, G., Gerding, D.N., Gibert, M., Popoff, M.R., Parkhill, J., Dougan, G. & Wren B.W. Comparative genome and phenotypic analysis of Clostridium difficile 027 strains provides insight into the evolution of a hypervirulent bacterium. *Genome Biology* **10**, R102, doi:10.1186/gb-2009-10-9-r102 (2009).

55 Alonso, R., Martin, A., Pelaez, T., Marin, M., Rodriguez-Creixems, M. & Bouza, E. Toxigenic status of Clostridium difficile in a large Spanish teaching hospital. *Journal of Medical Microbiology* **54**, 159-162, doi:10.1099/jmm.0.45809-0 (2005).

56 Pituch, H. *et al.* Detection of binary-toxin genes (cdtA and cdtB) among Clostridium difficile strains isolated from patients with C. difficile-associated diarrhoea (CDAD) in Poland. *Journal of Medical Microbiology* **54**, 143-147, doi:10.1099/jmm.0.45799-0 (2005).

57 Barbut, F., Decre, D., Lalande, V., Burghoffer, B., Robert, J., Mangeol, A., Branger, C., & Petit, J.C. Clinical features of Clostridium difficile-associated diarrhoea due to binary toxin (actin-specific ADP-ribosyltransferase)-producing strains. *Journal of Medical Microbiology* **54**, 181-185, doi:10.1099/jmm.0.45804-0 (2005).

58 Barbut, F., Decre, D., Lalande, V., Burghoffer, B., Noussair, L., Gigandon, A., Espinasse, F., Raskine, L., Robert, J., Mangeol, A., Branger, C. & Petit, J.C. Clinical features of Clostridium difficile-associated infections and molecular characterization of strains: results of a retrospective study, 2000-2004. *Infection Control and Hospital Epidemiology* **28**, 131-139, doi:10.1086/511794 (2007).

59 McEllistrem, M. C., Carman, R. J., Gerding, D. N., Genheimer, C. W. & Zheng, L. A hospital outbreak of Clostridium difficile disease associated with isolates carrying binary toxin genes. *Clinical Infectious Diseases : An Official Publication of the Infectious Diseases Society of America* **40**, 265-272, doi:10.1086/427113 (2005).

60 Brazier, J. S., Patel, B. & Pearson, A. Distribution of Clostridium difficile PCR ribotype 027 in British hospitals. *Euro surveillance : bulletin Europeen sur les Maladies Transmissibles = European Communicable disease Bulletin* **12**, E070426 070422 (2007).

61 Carter, G. P., Lyras, D., Allen, D.L., Mackin, K.E., Howarth, P.M, O'Connor, J.R. & Rood, J.I. Binary toxin production in Clostridium difficile is regulated by CdtR, a LytTR family response regulator. *Journal of Bacteriology* **189**, 7290-7301, doi:10.1128/JB.00731-07 (2007).

62 Lyon, S. A., Hutton, M. L., Rood, J. I., Cheung, J. K. & Lyras, D. CdtR Regulates TcdA and TcdB Production in Clostridium difficile. *PLoS Pathogens* **12**, e1005758, doi:10.1371/journal.ppat.1005758 (2016).

63 Aktories, K. & Wegner, A. Mechanisms of the cytopathic action of actin-ADP-ribosylating toxins. *Molecular Microbiology* **6**, 2905-2908 (1992).

64 Shen, A. Clostridium difficile toxins: mediators of inflammation. *Journal of Innate Immunity* **4**, 149-158, doi:10.1159/000332946 (2012).

65 Barra-Carrasco, J., Olguin-Araneda, V., Plaza-Garrido, A., Miranda-Cardenas, C., Cofre-Araneda, G., Pizarro-Guajardo, M., Sarker, M.R. & Paredes-Sabja, D. The Clostridium difficile exosporium cysteine (CdeC)-rich protein is required for exosporium morphogenesis and coat assembly. *Journal of Bacteriology* **195**, 3863-3875, doi:10.1128/JB.00369-13 (2013).

66 Pizarro-Guajardo, M., Olgiun-Araneda, V., Barra-Carrasco, J., Brito-Silva, C., Sarker, M.R. & Paredes-Sabja, D. Characterization of the collagen-like exosporium protein, BclA1, of Clostridium difficile spores. *Anaerobe* **25**, 18-30, doi:10.1016/journal.anaerobe.2013.11.003 (2014).

67 Lawley, T. D., Croucher, N.J., Yu, L., Clare, S., Sebaihia, M., Goulding, D., Pickard, D.J., Parkhill, J., Choudhary, J. & Dougan, G. Proteomic and genomic characterization of highly infectious Clostridium difficile 630 spores. *Journal of Bacteriology* **191**, 5377-5386, doi:10.1128/JB.00597-09 (2009).

69 Fimlaid, K. A., Jensen, O., Donnelly, M. L., Siegrist, M. S. & Shen, A. Regulation of Clostridium difficile Spore Formation by the SpoIIQ and SpoIIIA Proteins. *PLoS Genetics* **11**, e1005562, doi:10.1371/journal.pgen.1005562 (2015).

70 Higgins, D. & Dworkin, J. Recent progress in Bacillus subtilis sporulation. *FEMS Microbiology Reviews* **36**, 131-148, doi:10.1111/j.1574-6976.2011.00310.x (2012).

71 Tan, I. S. & Ramamurthi, K. S. Spore formation in Bacillus subtilis. *Environmental Microbiology Reports* **6**, 212-225, doi:10.1111/1758-2229.12130 (2014).

72 Fimlaid, K. A. & Shen, A. Diverse mechanisms regulate sporulation sigma factor activity in the Firmicutes. *Current Opinion in Microbiology* **24**, 88-95, doi:10.1016/journal.mib.2015.01.006 (2015).

73 McKenney, P. T., Driks, A. & Eichenberger, P. The Bacillus subtilis endospore: assembly and functions of the multilayered coat. *Nature Reviews. Microbiology* **11**, 33-44, doi:10.1038/nrmicro2921 (2013).

74 Henriques, A. O. & Moran, C. P., Jr. Structure, assembly, and function of the spore surface layers. *Annual Review of Microbiology* **61**, 555-588, doi:10.1146/annurev.micro.61.080706.093224 (2007).

75 Burns, D. A., Heap, J. T. & Minton, N. P. Clostridium difficile spore germination: an update. *Research in Microbiology* **161**, 730-734, doi:10.1016/j.resmic.2010.09.007 (2010).

76 Paredes-Sabja, D., Shen, A. & Sorg, J. A. Clostridium difficile spore biology: sporulation, germination, and spore structural proteins. *Trends in Microbiology* **22**, 406-416, doi:10.1016/j.tim.2014.04.003 (2014).

77 Francis, M. B., Allen, C. A. & Sorg, J. A. Spore Cortex Hydrolysis Precedes Dipicolinic Acid Release during Clostridium difficile Spore Germination. *Journal of Bacteriology* **197**, 2276-2283, doi:10.1128/JB.02575-14 (2015).

78 Francis, M. B., Allen, C. A., Shrestha, R. & Sorg, J. A. Bile acid recognition by the Clostridium difficile germinant receptor, CspC, is important for establishing infection. *PLoS Pathogens* **9**, e1003356, doi:10.1371/journal.ppat.1003356 (2013).

79 Kevorkian, Y., Shirley, D. J. & Shen, A. Regulation of Clostridium difficile spore germination by the CspA pseudoprotease domain. *Biochimie*, doi:10.1016/journal.biochi.2015.07.023 (2015).

80 Adams, C. M., Eckenroth, B. E., Putnam, E. E., Doublie, S. & Shen, A. Structural and functional analysis of the CspB protease required for Clostridium spore germination. *PLoS Pathogens* **9**, e1003165, doi:10.1371/journal.ppat.1003165 (2013).

81 Tasteyre, A., Barc, M. C., Collignon, A., Boureau, H. & Karjalainen, T. Role of FliC and FliD flagellar proteins of Clostridium difficile in adherence and gut colonization. *Infection and Immunity* **69**, 7937-7940, doi:10.1128/IAI.69.12.7937-7940.2001 (2001).

82 Baban, S. T., Kuehne, S.A., Barketi-Klai, A., Cartman, S.T., Kelly, M.L., Hardie, K.R., Kansau, I., Collignon, A. & Minton, N.P. The role of flagella in Clostridium difficile pathogenesis: comparison between a non-epidemic and an epidemic strain. *PloS One* **8**, e73026, doi:10.1371/journal.pone.0073026 (2013).

83 Aubry, A., Hussack, G., Chen, W., KuoLee, R., Twine, S.M., Fulton, K.M., Foote, S., Carillo, C.D., Tanha, J. & Logan, S.M. Modulation of toxin production by the flagellar regulon in Clostridium difficile. *Infection and Immunity*, doi:doi:10.1128/IAI.00224-12 (2012).

84 Barketi-Klai, A., Monot, M., Hoys, S., Lambert-Bordes, S., Kuehne, S.A., Minton, N., Collignon, A., Dupuy, B. & Kansau I. The flagellin FliC of Clostridium difficile is responsible for pleiotropic gene regulation during in vivo infection. *PloS One* **9**, e96876, doi:10.1371/journal.pone.0096876 (2014).

85 Stevenson, E., Minton, N. P. & Kuehne, S. A. The role of flagella in Clostridium difficile pathogenicity. *Trends in Microbiology* **23**, 275-282, doi:10.1016/journal.tim.2015.01.004 (2015).

86 Deneve, C., Janoir, C., Poilane, I., Fantinato, C. & Collignon, A. New trends in Clostridium difficile virulence and pathogenesis. *International journal of antimicrobial agents* **33 Suppl 1**, S24-28, doi:10.1016/S0924-8579(09)70012-3 (2009).

87 Talay, S. R. Gram-positive adhesins. *Contributions to Microbiology* **12**, 90-113, doi:10.1159/000081691 (2005).

88 Tulli, L. *et al.* CbpA: a novel surface exposed adhesin of Clostridium difficile targeting human collagen. *Cellular Microbiology* **15**, 1674-1687, doi:10.1111/cmi.12139 (2013).

89 Hennequin, C., Janoir, C., Barc, M. C., Collignon, A. & Karjalainen, T. Identification and characterization of a fibronectin-binding protein from Clostridium difficile. *Microbiology* **149**, 2779-2787, doi:10.1099/mic.0.26145-0 (2003).

90 Kovacs-Simon, A., Leuzzi R., Kasendra, M., Minton, N., Titball R.W. & Mitchell, S.L. Lipoprotein CD0873 is a novel adhesin of Clostridium difficile. *The Journal of Infectious Diseases* **210**, 274-284, doi:10.1093/infdis/jiu070 (2014).

91 Dozot, M., Poncet, S., Nicholas, C., Copin, R., Bouraoui, H., Maze, R., Deutscher, J., De Bolle, X. & Letesson, J.J. Functional characterization of the incomplete phosphotransferase system (PTS) of the intracellular pathogen Brucella melitensis. *PloS One* **5**, doi:10.1371/journal.pone.0012679 (2010).

92 Gooderham, W. J. & Hancock, R. E. Regulation of virulence and antibiotic resistance by two-component regulatory systems in Pseudomonas aeruginosa. *FEMS Microbiology Reviews* **33**, 279-294, doi:10.1111/j.1574-6976.2008.00135.x (2009).
93 Davidson, A. L., Dassa, E., Orelle, C. & Chen, J. Structure, function, and evolution of bacterial ATP-binding cassette systems. *Microbiology and Molecular Biology Reviews : MMBR* **72**, 317-364, table of contents, doi:10.1128/MMBR.00031-07 (2008).
94 Pao, S. S., Paulsen, I. T. & Saier, M. H., Jr. Major facilitator superfamily. *Microbiology and Molecular Biology reviews : MMBR* **62**, 1-34 (1998).
95 Behrens, S., Mitchell, W. & Bahl, H. Molecular analysis of the mannitol operon of Clostridium acetobutylicum encoding a phosphotransferase system and a putative PTS-modulated regulator. *Microbiology* **147**, 75-86, doi:10.1099/00221287-147-1-75 (2001).
96 Zhao, Y., Mao, G., Liu, M., Zhang, L., Wang X. & Zhang, X.C. Crystal structure of the E. coli peptide transporter YbgH. *Structure* **22**, 1152-1160, doi:10.1016/j.str.2014.06.008 (2014).
97 Servinsky, M. D., Kiel, J. T., Dupuy, N. F. & Sund, C. J. Transcriptional analysis of differential carbohydrate utilization by Clostridium acetobutylicum. *Microbiology* **156**, 3478-3491, doi:10.1099/mic.0.037085-0 (2010).
98 Rees, D. C., Johnson, E. & Lewinson, O. ABC transporters: the power to change. *Nature reviews. Molecular Cell Biology* **10**, 218-227, doi:10.1038/nrm2646 (2009).
99 Goosen, N. & Moolenaar, G. F. Role of ATP hydrolysis by UvrA and UvrB during nucleotide excision repair. *Research in Microbiology* **152**, 401-409 (2001).
100 Cuthbertson, L., Kimber, M. S. & Whitfield, C. Substrate binding by a bacterial ABC transporter involved in polysaccharide export. *Proceedings of the National Academy of Sciences of the United States of America* **104**, 19529-19534, doi:10.1073/pnas.0705709104 (2007).
101 Barabote, R. D. & Saier, M. H., Jr. Comparative genomic analyses of the bacterial phosphotransferase system. *Microbiology and Molecular Biology Reviews : MMBR* **69**, 608-634, doi:10.1128/MMBR.69.4.608-634.2005 (2005).
102 Saier, M. H. & Shlykov, M. A. Group Translocation - PEP:PTS. doi:10.1002/9780470015902.a0001423.pub2 (2012).
103 Saier, M. H., Hvorup, R. N. & Barabote, R. D. Evolution of the bacterial phosphotransferase system: from carriers and enzymes to group translocators. *Biochemical Society transactions* **33**, 220-224, doi:10.1042/BST0330220 (2005).
104 Sebaihia, M., Wren B.W., Mullany, P., Fairweather, N.F., Minton, N., Stabler, R., Thomson, N.R., Roberts, A.P., Cerdeno-Tarraga, A.M., Wang, H., Holden, M.T.G., Wright, A., Churcer, C., Quail, M.A., Baker, S., Bason, N., Brooks, K., Chillingworth, T., Cronin, A., Davis, P., Dowd, L., Fraser, A., Feltwell, T., Hance, Z., Holroyd, S., Jagels, K., Moule, S., Mungall, K., Price, C., Rabbinowitsch, E., Sharp, S., Simmonds, M., Stevens, K., Unwin, L., Whithead, S., Dupuy, B., Dougan, G., Barrell, B. & Parkhill, J. The multidrug-resistant human pathogen Clostridium

difficile has a highly mobile, mosaic genome. *Nature Genetics* **38**, 779-786, doi:10.1038/ng1830 (2006).

105 Saier, M. H. The bacterial phosphotransferase system. (HorizonScientific ; Springer-Verlag Distributor, 2002).

106 Mitchell, W. J. & Tangney, M. in *Handbook on Clostridia* (ed P. Durre) (Boca Raton: CRC Press, 2005).

107 Postma, P. W. & Lengeler, J. W. Phosphoenolpyruvate:carbohydrate phosphotransferase system of bacteria. *Microbiological Reviews* **49**, 232-269 (1985).

108 McCoy, J. G., Levin, E. J. & Zhou, M. Structural insight into the PTS sugar transporter EIIC. *Biochimica et Biophysica Acta* **1850**, 577-585, doi:10.1016/journal.bbagen.2014.03.013 (2015).

109 Opacic, M., Vos, E. P., Hesp, B. H. & Broos, J. Localization of the substrate-binding site in the homodimeric mannitol transporter, EIImtl, of Escherichia coli. *The Journal of Biological Chemistry* **285**, 25324-25331, doi:10.1074/jbc.M110.122523 (2010).

110 Tangney, M. & Mitchell, W. J. Analysis of a catabolic operon for sucrose transport and metabolism in Clostridium acetobutylicum ATCC 824. *Journal of Molecular Microbiology and Biotechnology* **2**, 71-80 (2000).

111 Saier, M. H., Jr. Beneficial bacteria and bioremediation. *Journal of Molecular Microbiology and Biotechnology* **9**, 63-64, doi:10.1159/000088836 (2005).

112 Shimizu, T. *et al.* Complete genome sequence of Clostridium perfringens, an anaerobic flesh-eater. *Proceedings of the National Academy of Sciences of the United States of America* **99**, 996-1001, doi:10.1073/pnas.022493799 (2002).

113 Shi, Y., Li, Y. X. & Li, Y. Y. Large number of phosphotransferase genes in the Clostridium beijerinckii NCIMB 8052 genome and the study on their evolution. *BMC Bioinformatics* **11 Suppl 11**, S9, doi:10.1186/1471-2105-11-S11-S9 (2010).

114 Neumann, S., Grosse, K. & Sourjik, V. Chemotactic signaling via carbohydrate phosphotransferase systems in Escherichia coli. *Proceedings of the National Academy of Sciences of the United States of America* **109**, 12159-12164, doi:10.1073/pnas.1205307109 (2012).

115 Adler, J. & Epstein, W. Phosphotransferase-system enzymes as chemoreceptors for certain sugars in Escherichia coli chemotaxis. *Proceedings of the National Academy of Sciences of the United States of America* **71**, 2895-2899 (1974).

116 Dembek, M., Stabler, R. A., Witney, A. A., Wren, B. W. & Fairweather, N. F. Transcriptional analysis of temporal gene expression in germinating Clostridium difficile 630 endospores. *PloS One* **8**, e64011, doi:10.1371/journal.pone.0064011 (2013).

117 Ng, Y. K. Ehsaan, M.E., Philip, S., Collery, M.M., Janoir, C., Collignon, A., Cartman, S.T. & Minton, N. P.. Expanding the repertoire of gene tools for precise manipulation of the Clostridium difficile genome: allelic exchange using pyrE alleles. *PloS One* **8**, e56051, doi:10.1371/journal.pone.0056051 (2013).

118 Heap, J. T., Kuehne, S.A., Ehsaan, M., Cartman, S.T., Cooksley, C.M, Scott, J.C. & Minton, N.P. The ClosTron: Mutagenesis in Clostridium

refined and streamlined. *Journal of Microbiological Methods* **80**, 49-55, doi:10.1016/journal.mimet.2009.10.018 (2010).

119 Kuehne, S. A. & Minton, N. P. ClosTron-mediated engineering of Clostridium. *Bioengineered* **3**, 247-254, doi:10.4161/bioe.21004 (2012).

120 Heap, J. T., Cartman, S. T., Kuehne, S. A., Cooksley, C. & Minton, N. P. ClosTron-targeted mutagenesis. *Methods in Molecular Biology* **646**, 165-182, doi:10.1007/978-1-60327-365-7_11 (2010).

121 Valiente, E., Dawson, L. F., Cairns, M. D., Stabler, R. A. & Wren, B. W. Emergence of new PCR ribotypes from the hypervirulent Clostridium difficile 027 lineage. *Journal of Medical Microbiology* **61**, 49-56, doi:10.1099/jmm.0.036194-0 (2012).

122 Tangney, M., Brehm, J. K., Minton, N. P. & Mitchell, W. J. A gene system for glucitol transport and metabolism in Clostridium beijerinckii NCIMB 8052. *Applied and environmental Microbiology* **64**, 1612-1619 (1998).

123 Heravi, K. M. & Altenbuchner, J. Regulation of the Bacillus subtilis mannitol utilization genes: promoter structure and transcriptional activation by the wild-type regulator (MtlR) and its mutants. *Microbiology* **160**, 91-101, doi:10.1099/mic.0.071233-0 (2014).

124 Joyet, P., Bouraoui, H., Ake, F.M.D., Derkaoui, M., Zebre, A.C., Cao, T.N., Ventroux, M., Nessler, S., Noirot-Gros, M.F., Deutscher, J. & Milohanic, E. Transcription regulators controlled by interaction with enzyme IIB components of the phosphoenolpyruvate: sugar phosphotransferase system. *Biochimica et Biophysica Acta* **1834**, 1415-1424, doi:10.1016/journal.bbapap.2013.01.004 (2013).

125 Stulke, J., Arnaud, M., Rapoport, G. & Martin-Verstraete, I. PRD--a protein domain involved in PTS-dependent induction and carbon catabolite repression of catabolic operons in bacteria. *Molecular Microbiology* **28**, 865-874 (1998).

126 Henstra, S. A., Tuinhof, M., Duurkens, R. H. & Robillard, G. T. The Bacillus stearothermophilus mannitol regulator, MtlR, of the phosphotransferase system. A DNA-binding protein, regulated by HPr and iicbmtl-dependent phosphorylation. *The Journal of Biological Chemistry* **274**, 4754-4763 (1999).

127 Otte, S. & Lengeler, J. W. The mtl genes and the mannitol-1-phosphate dehydrogenase from Klebsiella pneumoniae KAY2026. *FEMS Microbiology Letters* **194**, 221-227 (2001).

128 Peng, X., Okai, N., Vertes A.A., Inatomi K., Inui M. & Yakuwa H.. Characterization of the mannitol catabolic operon of Corynebacterium glutamicum. *Applied Microbiology and Biotechnology* **91**, 1375-1387, doi:10.1007/s00253-011-3352-x (2011).

129 Jensen, A. & Haug, A. Geographical and seasonal variation in the chemical composition of Laminaria hyperborea and Laminaria digitata from the Norwegian coast. . 1–8 (Norwegian Institute of Seaweed Research, Akademisk Trykningssentral, Blindern, Oslo. , 1956).

130 Collery, M. M., Kuehne, S.A., McBride, S.M., Kelly, M.L., Monot, M., Cockayne, A., Dupuy, B. & Minton N.P. What's a SNP between friends: The influence of single nucleotide polymorphisms on virulence and phenotypes of Clostridium difficile strain 630 and derivatives. *Virulence*, 1-15, doi:10.1080/21505594.2016.1237333 (2016).

131 Honeyman, A. L. & Curtiss, R., 3rd. Isolation, characterization, and nucleotide sequence of the Streptococcus mutans mannitol-phosphate dehydrogenase gene and the mannitol-specific factor III gene of the phosphoenolpyruvate phosphotransferase system. *Infection and Immunity* **60**, 3369-3375 (1992).
132 Kenny, J. G., Moran J., Kolar, S.L., Ulanov, A., Li, Z., Shaw, L.N., Josefsson, E. & Horsburgh, H.M. Mannitol utilisation is required for protection of Staphylococcus aureus from human skin antimicrobial fatty acids. *PloS One* **8**, e67698, doi:10.1371/journal.pone.0067698 (2013).
133 Onderdonk, A. B., Lowe, B. R. & Bartlett, J. G. Effect of environmental stress on Clostridium difficile toxin levels during continuous cultivation. *Applied and Environmental Microbiology* **38**, 637-641 (1979).
134 Burns, D. A. & Minton, N. P. Sporulation studies in Clostridium difficile. *Journal of Microbiological Methods* **87**, 133-138, doi:10.1016/journal.mimet.2011.07.017 (2011).
135 Heap, J. T., Pennington, O. J., Cartman, S. T., Carter, G. P. & Minton, N. P. The ClosTron: a universal gene knock-out system for the genus Clostridium. *Journal of Microbiological Methods* **70**, 452-464, doi:10.1016/journal.mimet.2007.05.021 (2007).
136 Alcantara, C., Sarmiento-Rubiano, L.A., Monedero, V., Deutscher, J., Perez-Martinez, G. & Yebra, M.J. Regulation of Lactobacillus casei sorbitol utilization genes requires DNA-binding transcriptional activator GutR and the conserved protein GutM. *Applied and Environmental Microbiology* **74**, 5731-5740, doi:10.1128/AEM.00230-08 (2008).
137 Silveira, M. M. & Jonas, R. The biotechnological production of sorbitol. *Applied Microbiology and Biotechnology* **59**, 400-408, doi:10.1007/s00253-002-1046-0 (2002).
138 Wrolstad, R. E. & Shallenberger, R. S. Free sugars and sorbitol in fruits--a complication from the literature. *Journal - Association of Official Analytical Chemists* **64**, 91-103 (1981).
139 Yamada, M. & Saier, M. H., Jr. Positive and negative regulators for glucitol (gut) operon expression in Escherichia coli. *Journal of Molecular Biology* **203**, 569-583 (1988).
140 Heap, J. T., Ehsaan, M.E., Cooksley, C.M., Ng, Y.K., Cartman, S.T., Winzer, K. & Minton, N.P.. Integration of DNA into bacterial chromosomes from plasmids without a counter-selection marker. *Nucleic Acids Research* **40**, e59, doi:10.1093/nar/gkr1321 (2012).
141 Martin, M. J., Clare, S., Goulding, D., Faulds-Pain, A., Barquist, L., Browne, H.P., Pettit, L., Dougan, G., Lawley, T.D. & Wren, B.W. The agr locus regulates virulence and colonization genes in Clostridium difficile 027. *Journal of Bacteriology* **195**, 3672-3681, doi:10.1128/JB.00473-13 (2013).
142 Lux, R., Munasinge, V.R.N, Castellano, F., Lengeler, J.W., Corrie, J.E.T., & Khan, S. Elucidation of a PTS-carbohydrate chemotactic signal pathway in Escherichia coli using a time-resolved behavioral assay. *Molecular Biology of the Cell* **10**, 1133-1146 (1999).
143 Greenberg, D. B., Stulke, J. & Saier, M. H., Jr. Domain analysis of transcriptional regulators bearing PTS regulatory domains. *Research in Microbiology* **153**, 519-526 (2002).

144 Krishna G. Peri, Kornberg, H. L. & Waygood, E. B. Evidence for the phosphorylation of enzyme II glucose of the phosphoenolpyruvate-sugar phosphotransferase system of Escherichia coli and Salmonella typhimurium *FEBS* **170**, 55-58 (1984).

145 Burns, D. A., Heap, J. T. & Minton, N. P. The diverse sporulation characteristics of Clostridium difficile clinical isolates are not associated with type. *Anaerobe* **16**, 618-622, doi:10.1016/journal.anaerobe. 2010.10.001 (2010).

146 Theriot, C. M. & Young, V. B. Microbial and metabolic interactions between the gastrointestinal tract and Clostridium difficile infection. *Gut Microbes* **5**, 86-95, doi:10.4161/gmic.27131 (2014).

147 Tonna, I. & Welsby, P. D. Pathogenesis and treatment of Clostridium difficile infection. *Postgraduate Medical Journal* **81**, 367-369, doi:10.1136/pgmj.2004.028480 (2005).